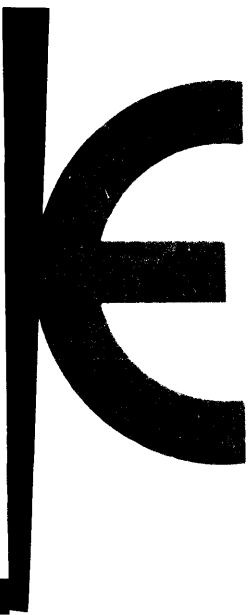


COMMISSION OF THE EUROPEAN COMMUNITIES

**METHODOLOGY FOR EVALUATING
THE RADIOLOGICAL CONSEQUENCES
OF RADIOACTIVE EFFLUENTS
RELEASED IN NORMAL OPERATIONS**

July 1979

**JOINT REPORT BY THE
NATIONAL RADIOLOGICAL PROTECTION BOARD
AND THE
COMMISSARIAT A L'ENERGIE ATOMIQUE**



METHODOLOGY FOR EVALUATING THE RADIOLOGICAL CONSEQUENCES OF RADIOACTIVE EFFLUENTS RELEASED IN NORMAL OPERATIONS

JOINT REPORT BY THE
NATIONAL RADIOLOGICAL PROTECTION BOARD
Harwell, Didcot, United Kingdom
and the
COMMISSARIAT A L'ENERGIE ATOMIQUE
Département de Protection
CEN, Fontenay-aux-Roses, France

M.J. Clark
R.H. Clarke
P.D. Grimwood
J. Hallam

J.A. Jones
G.N. Kelly
G.S. Linsley
K.B. Shaw

J.R. Simmonds
G.A.M. Webb
I.F. White

A. Bouville
R. Coulon
A. Despres
H. Fabre

J.M. Guezengar
J. Le Grand
C. Madelmont
A. Vilquin

July 1979

A Report Prepared Under Contract for the Commission of the
European Communities within its Research and Development
Programme on «Plutonium Recycling in Light Water Reactors»

LEGAL NOTICE

Neither the Commission of the European Communities nor any person acting on behalf of the Commission is responsible for the use which might be made of the following information

P R E F A C E

In the research programme of the Commission of the European Communities on plutonium recycling in light water reactors, the evaluation of the differential radiological impact of radioactive effluents discharged during the nuclear fuel cycle with and without plutonium recycling constitutes a point of major interest.

The present report, prepared by the National Radiological Protection Board, Harwell, UK, and the Commissariat à l'Energie Atomique, Fontenay-aux-Roses, France, presents the methodology and transfer parameters to be used in this evaluation.

However, since the report uses a general approach to evaluating the radiological consequences for man of routine radioactive releases, this methodology can be applied to routine discharges from most types of nuclear installation .

Moreover, the report covers all aspects of the radiological impact of radioactive effluents, from their release to the estimation of health effects within the population of the European Community, taking account of all significant exposure pathways.

For these reasons the Commission believes it appropriate to make the report widely available.

The Commission is grateful to the two organisations who have carried out the work which it believes will prove very useful to all who are concerned with radiological protection.

The International System of Units (SI) has been adopted throughout this report. The relationship between the SI units and previous units are shown in the table below.

Quantity	New named unit and symbol	In other SI units	Old special unit and symbol	Conversion factor
Exposure	-	$C\ kg^{-1}$	röntgen (R)	$1\ C\ kg^{-1} \sim 3876\ R$
Absorbed dose	gray (Gy)	$J\ kg^{-1}$	rad (rad)	$1\ Gy = 100\ rad$
Dose equivalent	sievert (Sv)	$J\ kg^{-1}$	rem (rem)	$1\ Sv = 100\ rem$
Activity	becquerel (Bq)	s^{-1}	curie (Ci)	$1\ Bq \sim 2.7 \times 10^{-11}\ Ci$

ABSTRACT

The aim of this report is to present a methodology for the evaluation of health detriment to the population of the countries of the European Community, from discharges within the community of liquid and gaseous radioactive effluents. This methodology is based on a series of sequential models describing the transfer of radionuclides through the different sectors of the environment, the pathways of exposure of man and the consequential health detriment. The methodology could be applied to evaluate individual exposure, but since health detriment is of interest here, the emphasis in the study has been in the estimation of collective dose and consequent numbers of health effects. The models chosen are of sufficiently general character that the corresponding methodology can find wide application for the evaluation of the radiological consequences of discharges of effluents.

<u>CONTENTS</u>		Page
1.	INTRODUCTION	1
2.	BASIC CONCEPTS, ASSUMPTIONS AND QUANTITIES	5
	References	10
3.	ASSESSMENT OF RADIONUCLIDES RELEASED TO THE ATMOSPHERE	11
3.1	Introduction	11
3.2	Dispersion of radionuclides in the atmosphere	12
3.2.1	Atmospheric dispersion model	12
3.2.2	Gaussian plume diffusion model	14
3.2.2.1	Reflection from the ground and from the top of the mixing layer	
3.2.2.2	Removal processes	
3.2.2.3	External radiation from the plume	
3.2.3	Selection of data used in the model	24
3.2.3.1	Meteorological conditions	
3.2.3.2	Rainfall	
3.2.3.3	Deposition velocity	
3.2.3.4	Release heights	
3.2.4	Summary of selected results from the matrix	27
3.2.5	Site specific application of the matrix of results	28
3.2.6	Global dispersion of radionuclides released to the atmosphere	31
3.3	Transfer of radionuclides through the terrestrial environment	32
3.3.1	Introduction	32
3.3.2	Resuspension of deposited activity	32
3.3.2.1	Review of resuspension data	
3.3.2.2	Resuspension model	
3.3.2.3	Results of the resuspension model	
3.3.3	The transfer of nuclides through the terrestrial environment into food chains	37
3.3.3.1	Introduction	
3.3.3.2	Migration of radionuclides in soil	
3.3.3.3	The transfer of radionuclides to plants	
3.3.3.4	Transfer of radionuclides to animals	
3.3.3.5	Application of the foodchain models and a summary of selected results	
3.3.3.6	The transfer of tritium and carbon-14 in the terrestrial environment	
3.3.4	External irradiation due to surface deposition	54
3.3.4.1	External irradiation due to photons	
3.3.4.2	External irradiation due to electrons	

	Page
3.3.5 Application of the results to a particular site	57
3.3.5.1 External irradiation	
3.3.5.2 Inhalation	
3.3.5.3 Ingestion	
3.3.5.4 Estimation of collective dose equivalent commitments	
3.4 Representation of the distribution of population and agricultural production within the European Community	59
3.4.1 The characteristics of the grid	60
3.4.2 Population grid	60
3.4.2.1 Population data	
3.4.2.2 Geographical Co-ordinates	
3.4.2.3 Derivation of the population grid	
3.4.3 Agricultural grid	61
3.4.3.1 Data collection	
3.4.3.2 Results	
3.4.3.3 Discussion and commentary	
3.4.4 Transformation of the results	64
References	65
4. MODELLING TRANSFERS ASSOCIATED WITH LIQUID DISCHARGES	143
4.1 Introduction	143
4.2 River models	145
4.2.1 Introduction	145
4.2.2 Description of model	146
4.2.2.1 Activity in water	
4.2.2.2 Sediment activity	
4.2.3 Application of the model	148
4.2.3.1 Selection of parameters	
4.2.3.2 Representative results	
4.2.3.3 Sediment activity	
4.3 Estuarine models	152
4.4 Marine models	153
4.4.1 Local model	154
4.4.2 Regional model	157
4.4.2.1 Description of the model used	
4.4.2.2 Results	
References	

	Page
5. GLOBAL CIRCULATION OF RADIONUCLIDES	225
5.1 Introduction	225
5.2 Global circulation models	225
5.2.1 Krypton-85	225
5.2.2 Tritium	226
5.2.3 Iodine-129	226
5.2.4 Carbon-14	226
5.3 Application of the models and selected results	226
5.4 Interface between the regional marine and global models	228
References	230
6. DOSIMETRIC MODELS	239
6.1 Estimation of dose equivalent in the body from unit intakes of radionuclides by ingestion or inhalation	239
6.1.1 Introduction	239
6.1.2 Procedure adopted	240
6.1.3 Committed dose equivalent per unit intake	240
References	242
7. APPLICATION OF THE METHODOLOGY TO ESTABLISH COLLECTIVE AND INDIVIDUAL DOSES	255
7.1 Introduction	255
7.2 Estimation of doses from atmospheric discharges	255
7.2.1 General procedure	255
7.2.1.1 Inhalation and external irradiation pathways	
7.2.1.2 Irradiation by ingestion pathway	
7.2.2 An example of the application of the methodology	259
7.2.2.1 Inhalation of the cloud	
7.2.2.2 External irradiation from the cloud	
7.2.2.3 External irradiation from deposited activity	
7.2.2.4 Inhalation of resuspended activity	
7.2.2.5 Ingestion of contaminated foodstuffs	
7.2.2.6 Summary of the collective dose equivalent commitments from the atmospheric discharge of caesium-137	
7.2.3 Indicative individual exposure	267
7.3 Estimation of doses from discharges to the aquatic environment	270
7.3.1 General procedure	270
7.3.2 An example of the application of the methodology	270

- 7.3.2.1 River environment
- 7.3.2.2 Marine environment
- 7.3.2.3 Summary of collective dose equivalent commitments from the discharge of caesium-137 to the aquatic environment

References

8.	THE ESTIMATION OF HEALTH EFFECTS IN AN EXPOSED POPULATION	281
8.1	Introduction	281
8.2	Estimation of the number of health effects	281
8.2.1	Fatal cancers and hereditary effects in the first two generations	281
8.2.2	Other health effects	282
8.2.3	Procedure	283
	References	285
9.	CONCLUSIONS	287
	GLOSSARY	289

TABLES

- 3.1 The radionuclides considered for release to the atmosphere
- 3.2 Conversion factors to derive dose equivalent in tissue from absorbed dose in air as a function of the initial photon energy
- 3.3 The weighting factors used in calculating the effective dose equivalent from external γ irradiation
- 3.4 β dose rates per unit air concentration
- 3.5 Coefficients given by Hosker to derive the vertical standard deviation of the plume for the various stability categories
- 3.6 Coefficients given by Doury to derive the vertical standard deviation of the plume for various diffusion conditions
- 3.7 Depths of mixing layer assumed for the various dispersion conditions
- 3.8 Air concentrations for a release at height 30m.
- 3.9 Deposition rate for a release at height 30m.
- 3.10 Effective cloud gamma dose rates for a release at height 30m.
- 3.11 External β dose rates in skin for a release at height 30m.
- 3.12 Fraction of long lived nuclide remaining in the plume at various distances downwind
- 3.13 Values of transfer coefficients used in the models for migration in soil
- 3.14 A comparison between the predictions of the model and the experimental results for plutonium migration
- 3.15 Non-element dependent parameters for crops and pasture
- 3.16 Element dependent parameters for crops and pasture
- 3.17 Non-element dependent parameters for animals
- 3.18 Element dependent parameters for cattle
- 3.19 The time integrals of activity transferred to unit mass of various plants
- 3.20 The time integrals of activity in various food products derived from cows grazing contaminated pasture
- 3.21 Time integrals of activity in various food products derived from sheep grazing contaminated pasture
- 3.22 Time integral of activity in animal products derived from cows and sheep inhaling activity at a concentration of 1 Bq m^{-3} in the atmosphere
- 3.23 Time integral of the effective dose equivalent rate (Sv) for external irradiation due to photons from 1 years deposition at a rate of $1 \text{ Bq m}^{-2} \text{ s}^{-1}$.
- 3.24 Definition of the large squares on the European grid
- 3.25 Acquisition of data
- 3.26 Population distribution in Square (7,10)
- 3.27 An example of the quantitative data of agricultural production

- 3.28 Radii used in the transformation of results
- 3.29 Fresh milk production for sectors centred on a site in the Rhone valley
- 4.1 Radionuclides considered in the evaluation of the radiological consequences of aquatic releases
- 4.2 Concentration factors for specified radionuclides
- 4.3 Physical characteristics of the Rhone and Loire
- 4.4 Quantities of water extracted from each section of the Rhone and Loire for drinking purposes
- 4.5 Collective ingestion of strontium-90 and caesium-137 activity in drinking water and fish for each section of the Rhone
- 4.6 Quantities of fish caught in each section of the Rhone and Loire
- 4.7 Quantities of food produced by surface irrigation from the Rhone
- 4.8 Time integral of activity concentration in sediments and truncated collective effective dose equivalent commitments
- 4.9 Classification of radionuclides according to their partition between dissolved and particulate forms in seawater
- 4.10 Site dependent parameters used in local marine model
- 4.11 Results obtained with the local marine model for a discharge into the Gulf of Taranto
- 4.12 Results obtained with the local marine model for a discharge into the Eastern Irish Sea
- 4.13 Assumed values of parameters used to model loss by sedimentation in North European waters
- 4.14 Quantities of fish caught in various regions
- 4.15 Total collective intakes for a release from a local box into the Southern North Sea
- 4.16 Total integrated collective intakes from marine foodstuffs for a release from a local box into four different sea regions
- 4.17 Assumed values of parameters used to model loss by sedimentation in the Mediterranean
- 4.18 Quantities of fish caught in regions of the Mediterranean and other waters
- 4.19 Total integrated collective intake for a release from a local box into the Eastern Mediterranean.
- 4.20 Total integrated collective intake for a release from a local box into the Western Mediterranean.
- 5.1 Time integrals of the activity concentration of each nuclide in various media from their global circulation
- 5.2 Annual intakes of stable materials by reference man
- 5.3 Dose equivalent commitments from external radiation ($\beta \gamma$) per unit time integral of air concentration of krypton-85

VII

- 6.1 Fraction of material reaching body fluids that is transferred to source tissue
- 6.2 Retention parameters
- 6.3 Committed dose equivalents per unit intake by ingestion
- 6.4 Committed dose equivalents per unit intake by inhalation
- 6.5 Inhalation class of the elements in various forms

- 7.1 Radii used to specify annular bands used to characterize the spatial distribution of the agricultural production and radioactivity concentrations
- 7.2 Frequency distribution of dispersion categories assumed for the sector θ_{jj} and airborne concentration, deposition rate and cloud γ dose at 150 km for 1 Bq s^{-1} continuous discharge of caesium-137
- 7.3 Infinite time integral of the concentration of caesium-137 in the various food products, assumed annual yields in the chosen annular segments, mean delay periods between harvest and consumption and individual consumption rates
- 7.4 Summary of the collective dose equivalent commitments in (or from) an annular segment due to an atmospheric discharge of 1 Bq s^{-1} of caesium-137 for 1 year
- 7.5 Collective effective dose equivalent commitment for discharges to the aquatic environment

- 8.1 Application of risk coefficients to evaluate fatal cancers, and hereditary effects

VIII

FIGURES

- 3.1 The variation of air concentration for a non-depositing nuclide with release height and dispersion conditions
- 3.2 Variation in air concentration with distance for noble gases of various half lives
- 3.3 The variation of air concentration and external γ dose rate with release height
- 3.4 The fraction of activity remaining in the plume for the release of various nuclides at 30 m in various dispersion conditions
- 3.5 The variation of the time integrated resuspended air concentration with radioactive half-life
- 3.6 Variation of air concentration during the initial deposition and the subsequent resuspended air concentrations with time
- 3.7 The rate of migration of plutonium-239 and caesium-137 into undisturbed soil as a function of time after initial deposit
- 3.8 The relative importance and time dependence of the important mechanisms for the transfer of plutonium-239 to green vegetables and grain
- 3.9 The relative importance and time dependence of the important mechanisms for the transfer of strontium-90 to green vegetables and grain
- 3.10 The relative importance and time dependence of the important mechanisms for the transfer of plutonium-239 to cow muscle
- 3.11 The relative importance and time dependence of the important mechanisms for the transfer of strontium-90 to cow muscle
- 3.12 Variation of effective dose equivalent with time for external ($X + \gamma$) irradiation from a deposition on the soil of $1 \text{ Bq m}^{-2} \text{ s}^{-1}$ during 1 year
- 3.13 Population density in the European Community
- 3.14 Representation of the squares forming the grid
- 3.15 Production density of fresh milk in the European Community
- 3.16 Production density of potatoes in the European Community
- 3.17 Production density of wheat in the European Community
- 3.18 Cumulative production of fresh milk as a function of distance in three 20° sectors centred on a site in the Rhone valley

- 4.1 Sections of the Rhone and point of discharge
- 4.2 Sections of the Loire and point of discharge
- 4.3 Variation of caesium-137 activity in filtered and non filtered water downstream of a point of discharge on the Rhone
- 4.4 Strontium-90 and caesium-137 sediment activity in the Rhone after 1 year of operation
- 4.5 Variation of strontium-90 and caesium-137 in sediments as a function of time at a point situated at the mouth of the Rhone
- 4.6 Diagram of transfers between river and estuary

- 4.7 Release to sea of strontium-90 originating from a discharge into the Rhone
- 4.8 Release to sea of caesium-137 originating from a discharge into the Rhone
- 4.9 Compartment model of the Northern European Waters
- 4.10 Compartment model of the Mediterranean
- 4.11 Compartments of North European regional model
- 4.12 Compartments of Mediterranean regional model
- 4.13 Effect of suspended sediment load on the depletion of activity from the water phase
- 4.14 Percentage contributions of different marine foodstuffs to the 50 year integrated total collective intake for a discharge to the Southern North Sea
- 4.15 Percentage contribution of different marine foodstuffs to the 50 year integrated total collective intake for a discharge to the Eastern Irish Sea
- 4.16 Percentage contributions of different sea areas to the 50 year integrated total collective intake for a discharge to the Southern North Sea
- 4.17 Integrated total collective intake for a discharge of technetium-99 from a local box in the Southern North Sea
- 4.18 Percentage contributions of different marine foodstuffs to the 50 year integrated total collective intake for a discharge to the upper layer of the Eastern Mediterranean
- 4.19 Percentage contributions of different marine foodstuffs to the 50 year integrated total collective intake for a discharge to the Western Mediterranean
- 4.20 Percentage contributions of different sea areas to the 50 year integrated total collective intake for a discharge to the upper layer of the Eastern Mediterranean
- 4.21 Percentage contributions of different sea areas to the 50 year integrated total collective intake for a discharge into the Western Mediterranean
- 4.22 Integrated total collective intake for a discharge of technetium-99 to the upper layer of the Eastern Mediterranean

- 5.1 Model used for global circulation of krypton-85
- 5.2 Model used for global circulation of tritium and iodine-129
- 5.3 Model used for global circulation of carbon-14
- 5.4 Time variation and time intervals of environmental concentrations of krypton-85 and tritium
- 5.5 Time variation and time intervals of environmental concentration of carbon-14 and iodine-129
- 5.6 The predicted transfer of iodine-129 to the population of the European Community using the regional marine and global models

- 6.1 The lung clearance model and values of parameters used in the model
- 6.2 The model for the gastro-intestinal tract and values of non-element dependent parameters used in the model

- 7.1 Illustration of the scheme of annular segments adopted to represent the spatial distribution of population and radioactivity in various parts of the environment

DIAGRAMS

- 3.1 Schematic diagram of pathways to man considered for atmospheric releases
- 3.2 Model for determining the cloud concentration under conditions of limited vertical mixing
- 3.3 Schematic diagram of well-mixed soil model
- 3.4 Schematic diagram of the model for undisturbed land
- 3.5 Schematic representation of the model to describe the transfer of radionuclides to plants
- 3.6 Schematic representation of the principal mechanisms for the transfer of radionuclides to grazing animals
- 3.7 Schematic representation of the simpler metabolic model
- 3.8 Schematic representation of the more complex metabolic model
- 3.9 Schematic diagram for calculation of external irradiation due to activity deposited on ground

- 4.1 Aquatic pathways to man
- 4.2 Schematic diagram showing interface between local and regional marine models

APPENDICES

- Appendix 3.1 Wind-driven resuspension from urban surfaces
- Appendix 3.2 General form of compartmental model
- Appendix 3.3 Transfer coefficients used in the terrestrial food chain models
- Appendix 3.4 Transformation into sectors of the data contained in the population and agricultural grids
- Appendix 4.1 Mathematical expression for sediment concentration in rivers
- Appendix 4.2 Determination of the rates of transfer between the western and eastern Mediterranean

CHAPTER 1

INTRODUCTION

The methodology which is described in this report has been developed to assess the health detriment in the population of the European Community from the discharge of radioactive effluents. The assessment of health detriment in this context is important in two respects; firstly it provides a quantitative measure of the radiological impact of effluent discharges and secondly it is an essential input to the optimisation procedure for effluent treatment systems. A generalised approach has been adopted with a view to the methodology finding broad application in the assessment of the radiological consequences of routine effluent discharges; it may equally find application in other areas where the potential exists for the releases of activity to the environment. The methodology developed consists of a series of interlinked models which describe the transfer of radionuclides through the various sectors of the environment, the pathways by which man may be irradiated and the health detriment consequent upon this exposure. Although the methodology can be applied equally to the estimation of the exposure of individuals as well as the population as a whole, it is the collective dose which is given greatest consideration in this study since it is a measure of the health detriment in the exposed population.

Radioactive effluents may be discharged to either the atmospheric or the aquatic environment and models have been developed to describe the transfer of radionuclides through the respective parts of the biosphere to man. Radionuclides discharged to the atmosphere are dispersed according to the normal atmospheric mixing processes and as they are transported downwind irradiate the population externally and internally, the latter as a consequence of inhalation of radionuclides from the atmosphere. During their downwind transport radionuclides may deposit from the atmosphere by impaction with the underlying surface or due to washout by rainfall. This transfer onto land surfaces may lead to further irradiation of man by three important routes: external irradiation from deposited activity, internal irradiation from inhalation of resuspended activity and ingestion of contaminated terrestrial foodstuffs. The relative importance of these pathways depends on the radionuclide and the nature of the surface onto which the deposition occurs. The estimated spatial and temporal distribution of radionuclides in the atmosphere and in various materials in the terrestrial environment may be combined with the spatial distributions of population and agricultural production within the European Community with appropriate dosimetric models and dietary habit data, to evaluate the collective dose equivalent from atmospheric discharges. To facilitate this procedure the spatial distributions of the population and agricultural production in the European Community have been established as matrices based on grids having dimensions of approximately 100 km^2 and 10^4 km^2 respectively.

Liquid radioactive effluents may be discharged to a freshwater (principally rivers) or marine environment. Those discharged to rivers are dispersed according to the general water movements and sedimentation processes. The principal routes by which man may be irradiated comprise external irradiation from sediments, ingestion of foodstuffs derived from the river, drinking water taken from the river and water used for irrigation; each pathway has been considered in this report. The subsequent transfer of radionuclides into the ocean or sea via an estuary has also been modelled. The dispersion of radionuclides discharged into the marine environment is determined in the first instance by the local features of the discharge

location, in particular tidal currents and the degree of sedimentation. Subsequent dispersion is influenced by the general water movements and sedimentation processes in the larger ocean masses. Ingestion of marine foodstuffs is the only pathway considered for the purposes of this report for the exposure of man following discharges of effluents to the marine environment. Individual and collective doses can be evaluated from the levels of activity in various materials (eg, fish, water) in the aquatic environment using the appropriate population, food and habit data and dosimetric models. Each of these items is described in this report.

Some radionuclides, owing to their long radioactive half-lives and their behaviour in the environment, may become globally dispersed and act as long term sources of exposure of large populations. Models are described which evaluate the global circulation and transfer to man of such radionuclides as a result of their discharge to either the atmospheric or aquatic environment.

In this report results are presented from the environmental models which have been applied, for a range of radionuclides, to evaluate the temporal and spatial distribution of activity in selected environmental materials for unit release to the atmosphere and to the aquatic environment. The distribution of activity in terrestrial materials is evaluated for unit deposition per unit area of land. The range of nuclides is not exhaustive but was selected to encompass both those usually encountered in effluents from nuclear installations and those known to be of public concern. The matrix of results generated from this application forms a basic data set which can be readily used to assess the collective dose to the population of the European Community for a discharge of defined composition at a particular location. These data may also be applied to calculate representative individual doses. In the case of atmospheric discharges, results are evaluated for a wide range of meteorological conditions and associated parameters; these results can then be applied in a site specific manner to discharges from any location by summation over the various conditions, each weighted according to its frequency of occurrence. A somewhat less general approach is adopted for aquatic discharges where account must be taken, from the outset, of the particular features of the environment into which the discharge is made. The matrix of results which has been established for aquatic discharges comprises data for the discharge of radionuclides from a number of locations into four rivers (the Rhine, Rhone, Loire and Po rivers). In this report results for the Rhone and Loire rivers are presented. In the case of marine discharges the Mediterranean and Northern European waters have been modelled and results are presented for unit discharges at a variety of locations. The collective dose, and its temporal distribution in the population may be determined from these matrices of results, when used with the spatial distribution of the population and its habits, the spatial distribution of the production of terrestrial and marine foodstuffs and the appropriate dosimetric models for external and internal irradiation. The evaluation of the matrices of results and the procedure for the application to estimate collective doses in the population of the European Community are fully described in the report.

The collective dose equivalent is a measure of the health detriment in the exposed population. At the levels of individual dose typically encountered from the discharge of radioactive effluents, only the stochastic effects of radiation need be considered; these comprise both fatal and non-fatal cancers in the exposed population and hereditary effects in its descendants. The relationships between the collective dose equivalent in a population and the incidence of these effects are discussed here and a method-

ology proposed for their assessment. The procedure adopted is conservative in a number of respects, the more important of which are identified. The adoption of a conservative approach has arisen in the interests of simplicity and in the use of widely accepted and already defined dosimetric quantities. The degrees of conservatism however must be recognised and in some situations, particularly in optimisation studies, they should be avoided; indications are given as to how this may be achieved.

The underlying assumptions and concepts utilised in this study are summarised in Chapter 2 together with the dosimetric quantities adopted. The models used to describe the transfer through the environment to man of radionuclides discharged to the atmosphere and the aquatic environment are outlined in Chapters 3 and 4 respectively; the models used to describe the transfer of those nuclides which become globally dispersed are given in Chapter 5. The dosimetric models employed to estimate the irradiation of man from internally incorporated radionuclides are described in Chapter 6. The procedures to estimate collective doses in the population of the European Community from the matrix of results obtained for unit release of each radionuclide, and the consequent health detriment are outlined in Chapters 7 and 8 respectively. The numerical results presented are solely illustrative.

Finally it must be emphasised that this report is concerned with a methodology to be adopted for assessing the radiological impact of effluents. In order to produce illustrative results, particular values for parameters have been chosen which necessarily represent a compromise from within the range of known variability. Thus when the models are applied to specific sites, it may well be necessary to choose alternative values of parameters which better reflect the particular characteristics of interest. The methodology developed here represents a first attempt to assess total health detriment and provides a basis on which to build in future."

CHAPTER 2

BASIC CONCEPTS, ASSUMPTIONS AND QUANTITIES

Before proceeding to describe the environmental models and their application it is pertinent to examine some of the basic concepts and assumptions made in this study and to define the more important radiological quantities evaluated.

At the levels of individual dose equivalent typically encountered from the discharge of radioactive effluents during the normal operation of nuclear installations, consideration can be limited to the incidence of stochastic health effects in the exposed population. Stochastic effects are those for which the probability of occurrence, rather than their severity, is regarded to be a function of dose equivalent, without threshold. Given this assumption and the further assumption that the severity of the effect is independent of the dose equivalent received then according to the International Commission on Radiological Protection [2.17] the detriment to health is proportional to, and may be represented by, the sum of the dose equivalents in the exposed population, i.e., the collective dose equivalent. The stochastic effects which must be taken into account in assessing health detriment are somatic effects in the exposed population and hereditary effects in its descendants; by far the most important somatic effect is the induction of cancer which may or may not prove fatal. The stochastic health effects which need to be considered can thus be divided into three broad categories:

- fatal cancers for which there is no current treatment that is effective.
- non-fatal cancers for which treatment, if needed, is effective in preventing consequential fatality.
- hereditary effects which occur in subsequent generations.

It is assumed in this study that the incidence of these health effects is directly proportional to the collective dose equivalent in the exposed population. This assumption, while conservative, is somewhat of an over-simplification. The delivery of the dose equivalent and the appearance of the consequential effects (if any) are not concurrent and delay periods significantly in excess of a decade are common. The age distribution and life expectancy of the exposed population therefore has a marked influence on the incidence of any health effects as a result of a given collective dose equivalent. This aspect is given further consideration in Chapter 8, and, in a more rigorous analysis, should be taken into account.

No single dosimetric quantity, that has had general application, is sufficient to enable the estimation of the three categories of health effects listed above. Recourse has therefore to be made to the use of several quantities; the number has been kept to the minimum consistent with the evaluation of the total health effects, and with the adoption of generally accepted dosimetric quantities.

The International Commission on Radiological Protection (ICRP) [2.27] has defined the quantity effective dose equivalent, H_E , as

$$H_E = \sum_T w_T H_T \dots\dots\dots(2.1)$$

where H_T is the dose equivalent in tissue T and

w_T is the weighting factor for each tissue and represents the ratio of the stochastic risk from irradiation of tissue, T, to that for the whole body when uniformly irradiated.

The weighting factors have been specified by the ICRP in Publication 26 [2.1] and in their derivation the ICRP chose to consider the risk of fatal cancer in all body organs and tissues, apart from in skin, plus the hereditary effects in the first two generations. The effective dose equivalent may only be used to give a measure of the incidence of these particular health effects; the incidence of the remaining effects must be evaluated from other quantities. The incidence of fatal cancers in skin and of hereditary effects in subsequent generations can be evaluated from a knowledge of the dose equivalents in skin and gonads, H_S and H_G , respectively. The incidence of radiation induced non-fatal cancers maybe most important in the skin and thyroid. This incidence may be calculated from the dose equivalents in these organs, H_S and H_{TH} , respectively. The evaluation of the incidence of the total health effects in an exposed population therefore requires the estimation of both the collective effective dose equivalent and the collective dose equivalents in gonads, skin and thyroid.

The collective effective dose equivalent, S_E , is given by

$$S_E = \int_0^{\infty} H_E N(H_E) dH_E \dots\dots\dots(2.2)$$

where H_E is the effective dose equivalent and $N(H_E)$ is the number of individuals receiving an effective dose equivalent in the range H_E to $H_E + dH_E$

The collective dose equivalent in an organ is obtained by substituting the dose equivalent in that organ for the effective dose equivalent.

Collective effective dose equivalent commitment, S_E^C , is obtained by integrating collective effective dose equivalent rate over all time. When the integration is limited in time the quantity is described as the truncated collective effective dose equivalent commitment. The former quantity is a measure of the total health detriment while the latter is a measure of the detriment over prescribed periods of time.

Collective effective dose equivalent commitment, S_E^C , is given by:

$$S_E^C = \int_0^{\infty} \dot{S}_E(t) dt \dots\dots\dots(2.3)$$

where \dot{S}_E is the collective effective dose equivalent rate.

In evaluating the collective dose equivalent commitment (and other similar quantities) it is convenient to distinguish between external and internal irradiation of the body. For external radiation the integration of equations (2.2), and (2.3) is relatively straight forward. For internal irradiation from radionuclides incorporated in the body the integration is more complex, particularly for those nuclides which have long retention

times in the body; detailed knowledge is required, which is not readily available, of the time variation after intake of the dose equivalent rates in the respective tissues. The integration is more conveniently and readily performed using an alternative representation for S_E^C for internal irradiation:-

$$S_E^C = \bar{H}_E \int_0^{\infty} I \cdot C(t) dt \quad \dots\dots\dots(2.4)$$

where $I \cdot C$ is the collective intake rate by inhalation or ingestion of a nuclide by the population and is a quantity readily evaluated from environmental models

\bar{H}_E is the population averaged effective dose equivalent received from unit intake of the nuclide by inhalation or ingestion, taking into account the age distribution and life expectancy of the population.

\bar{H}_E is given by

$$\bar{H}_E = \int_0^L H_E(L) N(L) dL / \int_0^L N(L) dL \quad \dots\dots\dots(2.5)$$

where $N(L)$ is the number of people with remaining life expectancy L

$H_E(L)$ is the integrated effective dose equivalent received by an individual with a remaining life expectancy L .

$$\text{Thus } H_E(L) = \int_0^L \dot{H}_E(L) dL \quad \dots\dots\dots(2.6)$$

While the estimation of \bar{H}_E for a population of defined age distribution is relatively straightforward using current dosimetric models such calculations have not yet been reported. For the purposes of this study the approximation is made that the quantity \bar{H}_E can be equated to the committed effective dose equivalent, $H_{50,E}$, which is defined as the time integral of the effective dose equivalent rate, $\dot{H}_E(t)$, over a 50 year period following intake.

$$H_{50,E} = \int_0^{50} \dot{H}_E(t) dt \quad \dots\dots\dots(2.7)$$

The committed effective dose equivalent has been introduced by ICRP in the context of occupational exposure to ensure compliance with dose equivalent limits, (50 years being the maximum working lifetime) and it has been estimated for a wide range of radionuclides for intake by inhalation and ingestion [2.37]. For radionuclides whose retention in the body is relatively short (eg, compared with 1 year) the committed and the population averaged effective dose equivalents will be essentially the same and the assumption of equality is well justified. For radionuclides with long

retention times in the body the assumption is likely to overestimate the actual dose equivalent received by the population (owing to the mean life expectancy of the population being less than 50 y); the magnitude of the overestimate has not been quantified and will vary according to the nuclide and population considered. However it is unlikely to exceed a few tens of percent for a population of age distribution typical of the EC.

The representation given in equation (2.4) for the collective effective dose equivalent commitment from internally incorporated radionuclides is adopted in this study while recognising its potential conservatism for radionuclides with long retention times in the body. While not of particular importance in this study, the use of equation (2.4) to evaluate truncated collective effective dose equivalent commitments may result in much greater overestimates for radionuclides with long retention times in the body and where the time of truncation is small compared with the mean life expectancy of the exposed population. In this context equation (2.4) should be used with caution.

Collective effective dose equivalent commitments are therefore evaluated in this study according to the following equation

$$S_E^C = \int_0^{\infty} \dot{S}_{E_{ext}}(t) dt + H_{50,E} \int_0^{\infty} I^C(t) dt \dots\dots\dots(2.8)$$

where the symbols are as previously defined.

In addition to the collective effective dose equivalent commitment the collective dose equivalent commitments in the tissues previously specified (gonads, skin and thyroid) are evaluated by making appropriate substitutions in equation (2.8). The procedure adopted to evaluate the incidence of the various health effects from these collective dose equivalents is described in Chapter 8. Truncated values of the respective collective dose equivalent commitments are also evaluated and the times of truncation chosen are 50, 100 and 500 years following the release of the radionuclide to the environment. These truncated values provide an indication of the temporal distribution of the health detriment in the exposed population and its descendants. While the collective dose equivalent commitments provide a measure of the total detriment over all time temporal distribution of that detriment is particularly important; for example it is apparent that few would regard a particular collective dose equivalent commitment delivered uniformly over, say, one million years as being as significant as the same dose delivered in one year. The levels of individual risk would be very different in the respective cases. The times of truncation are somewhat arbitrary but were selected with two objectives in mind; first to provide a reasonable representation of the temporal distribution of detriment bearing in mind its anticipated behaviour for the majority of situations being investigated in this study; and second to evaluate quantities that could be used to estimate maximum individual dose equivalents from a continuing release of a radionuclide. The estimation of individual dose equivalents is given further consideration later.

In the estimation of collective dose equivalent commitments it is clear that assumptions must be made as to the magnitude and habits of the exposed population and its descendants and the variation of these with time. Current predictions of the population trends could be readily incorporated into the estimates; however the uncertainty of such estimates is considerable

and moreover must increase with time. Bearing in mind the timescales over which integrations are to be performed in this study the additional sophistication of a time varying population is not considered justified. The collective dose equivalent commitments evaluated in this study are based on the assumption that the magnitude and age distribution of the population of the European Community remains constant at its present level over all time. It is further assumed that the habits of the population (eg, dietary intake etc) also remain the same. One further major assumption is made in the estimation of collective dose equivalent commitments; the whole population is assumed to comprise adults for the purposes of estimating doses from the inhalation and ingestion of radionuclides (ie, the whole population is assumed to have the same dietary intake and metabolism). This assumption may, at first sight, seem unreasonable; it has been shown [2.17] however that the variation of dose with age for the intake of radionuclides by inhalation or ingestion is small apart from a very limited age range and for a few radionuclides. Furthermore the adoption of average values of the respective parameters is justified when the quantity being evaluated is the collective dose equivalent in the whole of the population.

The study is concerned almost entirely with a methodology to estimate the health detriment in an exposed population and its descendants, hence this report is largely concerned with collective dose equivalent commitments. The models developed and the quantities evaluated can however be readily applied to the estimation of individual doses. Two such quantities are particularly relevant to the estimation of individual doses consequent on a continuing discharge of a radionuclide; these are the collective dose equivalent commitments truncated at 50 and 500 years. The truncated collective dose equivalent commitment to time, t , for the annual release of a radionuclide can be equated to the annual collective dose equivalent in the year, t , for a release that has been continuous over that time. Thus for discharges that are continuous for 50 years (a conservative estimate of the lifetime of a nuclear installation) or 500 years (a speculative estimate of the continuing use of nuclear energy) annual collective dose equivalents in these years can be readily estimated from the quantities evaluated. From knowledge of the components of the annual collective dose equivalent the annual dose equivalent to individuals in the most exposed group can be estimated after making appropriate provision for their more extreme habits compared to the average values adopted in the assessment of collective doses. The estimation of the individual dose in the most exposed group at the end of a continuing practice is of particular importance in judging the acceptability of an effluent discharge practice.

The estimation of the quantities outlined above, subject to the specified assumptions, are evaluated in the subsequent chapters for the release of radionuclides to the atmosphere and to various parts of the aquatic environments.

REFERENCES

- [2.1] ICRP, Recommendations of the International Commission on Radiological Protection. Oxford, Pergamon Press, ICRP Publication 26. Ann. ICRP, 1, no 3 (1977).
- [2.2] ICRP, Statement from the 1978 Stockholm Meeting of the International Commission on Radiological Protection. Ann. ICRP, 2, no 1 (1978).
- [2.3] Adams, N, Hunt B W and Reissland, J A, Annual limits of intake of radionuclides for workers. Harwell, National Radiological Protection Board, NRPB-R82 (1978). (London, HMSO).
- [2.4] Reactor safety study: An assessment of accident risks in US commercial nuclear power plants. Washington DC, US Nuclear Regulatory Commission, WASH-1400 (NUREG-75/014), App. VI (App. D) (1975).

CHAPTER 3

ASSESSMENT OF RADIONUCLIDES RELEASED TO THE ATMOSPHERE

3.1 Introduction

Radioactive material released to the atmosphere will be transported downwind and dispersed by the normal atmospheric mixing processes. As the radioactive plume travels downwind the exposed population will be irradiated by two principal routes: these comprise external irradiation by electrons and photons from the radioactive decay processes and inhalation of activity in the plume. Radioactive material will be removed from the plume during its transit by deposition processes which occur mainly by impaction of the plume with the underlying surface over which it is travelling. The plume is also depleted by washout caused by rain. This transfer of activity from the plume to the ground results in irradiation of the population by three further important routes: external irradiation by electrons and photons from the deposited activity, the inhalation of activity which is subsequently resuspended into the atmosphere and the transfer of activity through the terrestrial environment to foodstuffs which may be consumed by man.

An assessment of the exposure of the population from the release of radionuclides to the atmosphere must therefore take account of the dispersion of activity in, and its deposition from, the atmosphere as well as the subsequent behaviour of deposited nuclides in the terrestrial environment. The spatial and temporal distribution of nuclides released to the atmospheric and terrestrial environments may be combined with the same distributions of population and agricultural production to calculate the exposure of the population from both external radiation and from the intake of radionuclides by inhalation and ingestion. The main processes and pathways to man that need to be considered in evaluating the exposure of the population are illustrated schematically in Diagram 3.1. Models have been developed to describe the transfer of radionuclides through the different sectors of the environment and these are discussed in the following sections.

Each model is developed and applied generically to obtain a matrix of results that can be used to evaluate the exposure of the population of the EC for a release of radionuclides from any location. This involves the application of the particular parameters appropriate to that location, for example, meteorological conditions, or isotopic composition. In this report the air concentration, deposition rate, and external dose rates are evaluated as a function of distance from the release point for unit release rate of selected nuclides. A range of meteorological and other parameters have been used so that any distribution of meteorological conditions and spectrum of nuclides released from a particular location can be applied for a specific site. The air concentrations and external dose rates may be combined with the spatial distribution of the population of the European Community with respect to the release point, to estimate the collective dose in the population from inhalation of activity and from external radiation from the cloud. In a similar manner the transfer through the terrestrial environment is evaluated for unit deposit of selected nuclides; the time dependent variations of the external dose rates above the surface, the resuspended air concentration and the concentration in a variety of food products are evaluated. These values, when combined with the site specific distributions of population and agricultural production parameters for a particular location can be used to assess the collective doses via the prescribed routes to the population of the European Community.

The nuclides which have been included are shown in Table 3.1. They were selected on the basis either of their potential absolute significance or because they were known to be of public concern; other nuclides can however be readily treated by the models developed. Some of the nuclides considered for releases to the atmosphere are omitted when evaluating the transfer in the terrestrial environment. This is either a consequence of their very short half-lives and hence relatively limited significance in the terrestrial environment, or of their not being deposited from the atmosphere because of their inert behaviour as for example with the noble gases.

The distance over which radionuclides may be transported in the atmosphere depends on many factors such as radioactive half-life, physical and chemical form of the nuclide, meteorological conditions, and deposition processes. In this study the dispersion of activity is modelled over a distance of 3000 km which is in excess of the distance between extreme points in the European Community. In most cases the majority of the released activity is removed from the plume within this distance, either by radioactive decay or by deposition on to the underlying surface. For a limited number of nuclides, either because of their inert behaviour and long radioactive half-life, or rapid exchange between the atmosphere and other sectors of the environment, a significant fraction of activity may be transported beyond this distance. The subsequent global circulation of such nuclides has therefore to be considered as this comprises a further source of exposure of the European Community population. The nuclides which fall into this category have been identified and appropriate models developed.

3.2 Dispersion of radionuclides in the atmosphere

3.2.1 Atmospheric dispersion models

Material released to the atmosphere is transported downwind and dispersed according to the normal atmospheric mixing processes. The estimation of dispersion in the atmosphere is commonly approached by solving the diffusion-transport equation. Several models have been developed for this purpose using a variety of boundary conditions and simplifying assumptions. For example, for releases of very short duration, models (puff models) have been developed which take into account diffusion along three axes corresponding to the directions of the wind and the perpendiculars to this direction in the horizontal and vertical planes; for releases of long duration diffusion in the direction of the wind can be neglected and models using this approach are categorised as plume models.

Most estimates of the dispersion of material released to the atmosphere are based on the Gaussian plume diffusion model initially proposed by Sutton in 1932 [3.1]. Other models [3.2 - 3.4] have been developed which are thought to be more appropriate representations of the physical processes of turbulent diffusion in the atmosphere, but have had only limited application in estimating the dispersion of radioactive material. Furthermore, they have yet to be developed to a state where the user can easily relate the values of the parameters in the model to readily measurable quantities, for example, wind speed, cloud cover, etc. For these reasons such models are given no further consideration in this study for which the Gaussian plume model is adopted.

Isplitzer and Slade [3.5] have reviewed the experimental data on diffusion of effluents in the atmosphere and shown that the Gaussian plume model can be used to describe many practical situations. Pasquill [3.6]

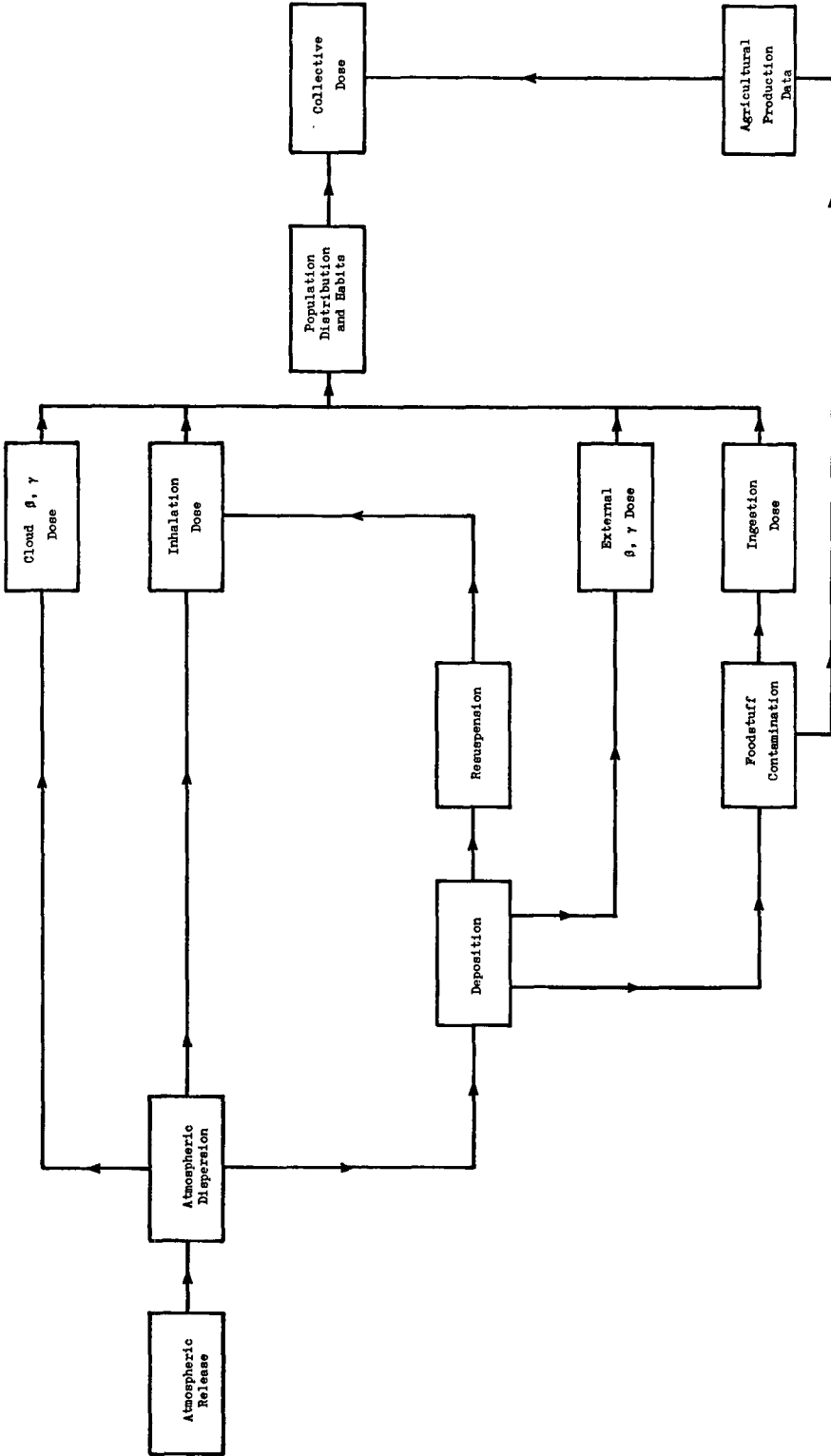


Diagram 3.1 Schematic diagram of pathways to man considered for atmospheric releases

and Elliot [3.7] have also shown that results predicted using Gaussian plume models vary little from predictions of other models and experimental measurements. Most experimental measurements however are limited to down-wind distances of up to several tens of kilometres and predictions of dispersion at greater distances with the Gaussian plume model cannot easily be verified by comparison with experiments; the reliability of the predictions therefore decreases with increasing distance. Other shortcomings in the Gaussian plume model as commonly applied at large distances are the assumptions that the meteorological conditions and direction of the wind remain constant throughout the transit of the plume. To overcome some of these difficulties at longer distances models have recently been developed [3.8, 3.9] which follow the trajectories of masses of air which pass over the release point and take account of changes in meteorological conditions with time. The application of these models requires comprehensive meteorological data, extended both in time and space, is site specific and in addition involves relatively large computational expenditure. The use of such models is considered to be outside the scope of this study which is generic in nature and the objective of which is the assessment of collective dose equivalent in the exposed population. As much of the collective dose equivalent is in general delivered within a few hundred kilometres of the discharge point, the increasing uncertainty with distances in the predictions of the Gaussian plume model is unlikely to be very significant.

3.2.2 Gaussian plume diffusion model

The airborne concentration of a nuclide of long radioactive half-life, $X(x,y,z)$ is given by the Gaussian plume model as:-

$$X(x,y,z) = \frac{Q_0}{2\pi\sigma_y\sigma_z\bar{u}} \exp - \left[\frac{1}{2} \left\{ \frac{y^2}{\sigma_y^2} + \frac{(z-h)^2}{\sigma_z^2} \right\} \right]$$

.....(3.1)

where $X(x,y,z)$ is the airborne concentration at the point (x,y,z) in Bq m^{-3}

x is the downwind distance (m)

y is the cross wind distance from the centre line of the plume (m)

z is the height above the ground of the sampling position (m)

σ_y and σ_z are the standard deviations of the plume, horizontally and vertically (m)

Q_0 is the release rate (Bq s^{-1})

\bar{u} is the mean windspeed (m s^{-1}) and

h is the effective height of release (m)

This equation is derived for a gas and the released aerosol is assumed to behave in a similar manner. The origin of the co-ordinate system is at ground level beneath the discharge point. In the derivation of equation (3.1)

diffusion in the downwind direction is ignored compared with transport by the wind for releases lasting a finite time.

The concentrations obtained from equation (3.1) are applicable to releases which are short compared with the time taken for the direction of the wind to change. For releases of longer duration the horizontal spread of the material is governed by fluctuations in the wind direction. For a continuous release in which the meteorological conditions are assumed to remain constant and the windrose assumed to be uniform, equation (3.1) can be rewritten as [3.10],

$$\bar{X}(x,y,z) = \frac{Q_0}{2\pi x \sqrt{2\pi\sigma_z} \bar{u}} \exp - \left[\frac{(z-h)^2}{2\sigma_z^2} \right] \dots\dots\dots(3.2)$$

where \bar{X} is the mean airborne concentration at the point (x,y,z) in Bq m⁻³.

The dependence in the cross wind direction (y) is removed owing to the assumption of a uniform windrose. In reality of course neither the windrose nor the meteorological conditions will remain constant during a prolonged release of radioactivity. The manner in which equation (3.2) is applied in a practical situation, where the average airborne concentration at any location, (x,y,z) will be a function of both these parameters, is described in section 3.2.5. Equation (3.2), suitably redefined to take account of radioactive decay, wet and dry deposition from the atmosphere and reflections from the ground and the top of the mixing layer, is used in the computer code, ESCLOUD [3.11], which has been developed to evaluate the dispersion, deposition and external doses from the "quasi-continuous" release of activity to the atmosphere. The detailed derivation of the modifications to this equation are given in reference [3.11]; the modifications together with other main features of the code, ESCLOUD, are briefly summarised in the following.

3.2.2.1 Reflection from the ground and from the top of the mixing layer

When material is discharged from an elevated source, the plume will disperse and eventually reach the ground. On reaching the ground the plume is reflected and effectively dispersed back up into the atmosphere. Taking account of reflection of the plume from the ground the mean air concentration is modified from that in equation (3.2) and is given by:

$$\bar{X}(x,z) = \frac{Q_0}{2\pi x \sqrt{2\pi\sigma_z} \bar{u}} \left[\exp - \frac{(z-h)^2}{2\sigma_z^2} + \exp - \frac{(z+h)^2}{2\sigma_z^2} \right] \dots\dots\dots(3.3)$$

Limits to the layer in which mixing takes place in the atmosphere occur at varying heights and arise from changes in temperature gradient. Where a finite mixing layer exists the dispersed material is trapped between the top of this layer and the ground. Reflections in this case occur both on the ground and at the top of the mixing layer as indicated in Diagram 3.2.

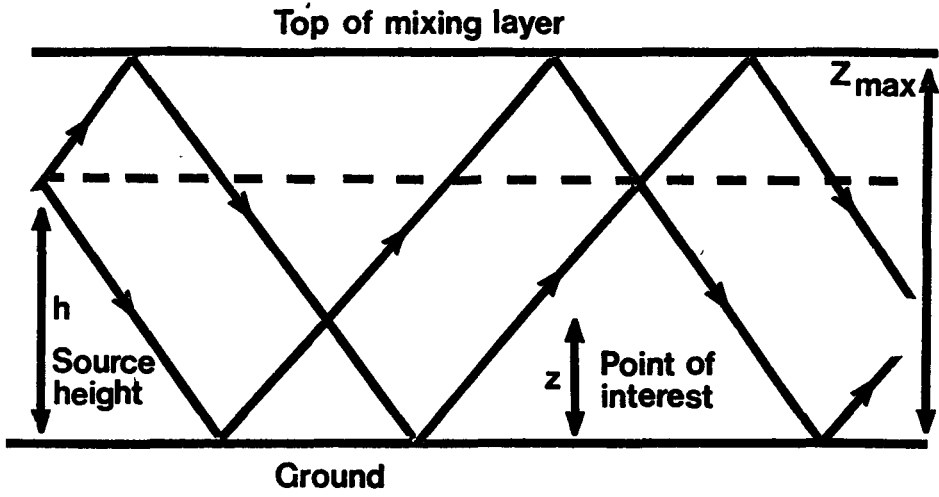


Diagram 3.2 Model for determining the cloud concentration under conditions of limited vertical mixing

Without a finite depth mixing layer the plume would continue to expand in the vertical plane. The effect of introducing reflections is that the airborne concentration is obtained by summation of contributions from many points over the Gaussian. The effect can be simulated by considering virtual sources at a series of heights; from Diagram 3.2 these are:

- a) $-h$ b) $2s z_{\max} + h$

where z_{\max} is the depth of the mixing layer and $s = 1, 2, 3 \dots$

In addition the primary dispersion due to a source at height, h , must be included; this, together with the reflected term from a virtual source at a height, $-h$, corresponds to the terms in equation (3.3) for dispersion including ground reflection. Thus for a finite mixing layer, the mean concentration is given by

$$\bar{X}(x, z) = \frac{Q_0}{2\pi x \sqrt{2\pi} \sigma_z \bar{u}} \sum_{s=0}^{\infty} \exp - \left[\frac{(2s z_{\max} \pm h \pm z)^2}{2\sigma_z^2} \right] \dots\dots\dots(3.4)$$

$s = 0, 1, 2, 3, \dots$ (positive z only when $s = 0$)

In general this series converges rapidly and can be summed to any prescribed accuracy. At large downwind distances, after multiple reflections, the vertical concentration profile of activity essentially becomes uniform between the ground and top of the mixing layer.

3.2.2.2 Removal processes

The concentrations derived from equation (3.4) apply to the dispersion of inert, long lived material (eg, krypton-85) which is not removed significantly from the plume as it travels downwind. A number of processes may act to reduce further the concentrations of discharged activity, in particular radioactive decay and dry and wet deposition. These processes are most readily taken into account by modifying the initial source strength, Q_0 , in equation (3.4) to allow for depletion.

(a) Radioactive decay

Radioactive decay will further reduce the concentrations of a radionuclide as it disperses downwind; the modified concentration can be obtained by substituting a modified source strength, $Q_0 R_p$, into equation (3.4) where

$$R_p = \exp \left[- \lambda_p \frac{x}{\bar{u}} \right] \dots\dots\dots(3.5)$$

where λ_p is the radioactive decay constant of the radionuclide (s^{-1}).

Daughter products will grow into the plume with the decay of the parent radionuclide and the concentration of daughter products can be obtained by substituting $Q_0 R_d$ for Q_0 in equation (3.4) where

$$R_d = \frac{\lambda_d}{\lambda_p - \lambda_d} \left[\exp - \left\{ \lambda_d \frac{x}{u} \right\} - \exp \left\{ \lambda_p \frac{x}{u} \right\} \right] \dots\dots\dots(3.6)$$

where λ_d is the radioactive decay constant of the daughter (s^{-1}).

In ESCLOUD no provision is made for the build up of second or subsequent daughters; where these need to be considered the decay scheme of each nuclide is simplified to a two member chain [3.11].

(b) Wet deposition

Material may be removed from the plume by the action of rain falling through it. Precipitation is intermittent and the true interaction between the plume and rain is very complex. For the purposes of assessing annual average air concentrations or wet deposition rates from the plume for a continuous release a simplified procedure is often followed; the assumption is made that rain is continuous throughout the transit of a fraction of the plume. This fraction is equated to the fraction of the year during which rain is experienced. Removal of material from the plume is determined by the use of a washout coefficient, Λ . In general washout can be assumed to remove material equally throughout the entire vertical extent of the plume. The removal rate at any distance from the source depends therefore only upon the total amount of material reaching that distance and not upon its vertical distribution in the plume. Taking into account washout the air concentration of stable material can be derived by substituting a modified source strength, $Q_0 W$, for Q_0 in equation (3.4) where

$$W = \exp - \left[\frac{\Lambda x}{u} \right] \dots\dots\dots(3.7)$$

and Λ is the washout coefficient (s^{-1})

If there is significant radioactive decay the air concentration of the parent nuclide can be obtained by substituting a modified source strength, $Q_0 W_p$, for Q_0 in equation (3.4) where

$$W_p = \exp - \left[\frac{(\Lambda_p + \lambda_p)x}{u} \right] \dots\dots\dots(3.8)$$

and Λ_p is the washout coefficient of the parent nuclide (s^{-1}).

The air concentration of its daughter product can be derived by substituting $Q_0 W_d$ for Q_0 in equation (3.4) where

$$W_d = \frac{\lambda_d}{(\lambda_p + \Lambda_p) - (\lambda_d + \Lambda_d)} \left[\exp - \left\{ \frac{(\lambda_d + \Lambda_d)x}{\bar{u}} \right\} - \exp - \left\{ \frac{(\lambda_p + \Lambda_p)x}{\bar{u}} \right\} \right] \dots\dots\dots(3.9)$$

and the subscripts p and d refer to parent and daughter respectively. The rate at which the parent radionuclide is deposited from the plume by wet deposition ($Bq\ m^{-2}\ s^{-1}$) is given by

$$\omega_{wp} = \frac{\Lambda_p Q_o W_p}{2\pi x \bar{u}} \dots\dots\dots(3.10)$$

and the deposition rate of the daughter nuclide by

$$\omega_{wd} = \frac{\Lambda_d Q_o W_d}{2\pi x \bar{u}} \dots\dots\dots(3.11)$$

(c) Dry deposition

Dry deposition is the process by which material is removed from the plume by impaction with the underlying surface or obstacles on it, such as vegetation. The rate at which material is deposited from the plume will depend on the nature of the airborne material and the underlying surface and can be estimated using the concept of a deposition velocity, V_g . The deposition velocity is defined as the ratio of the amount of material deposited on the surface per unit area per unit time to the air concentration per unit volume at the surface.

Where the plume is being depleted by dry deposition the air concentration of a stable material can be derived by substituting $Q_o D$, for Q_o in equation (3.4) where

$$D(x) = \exp \left[-\sqrt{\frac{2}{\pi}} \frac{V_g}{\bar{u}} \int_0^x \frac{dx}{\sigma_z} \exp \left\{ -\frac{h^2}{2\sigma_z^2} \right\} \right] \dots\dots\dots(3.12)$$

For a radioactive material the air concentrations of the parent and daughter can be obtained by making the same substitution after appropriate provision is made for radioactive decay as outlined above. For daughter products this procedure is valid only where the deposition velocity of both parent and daughter nuclides is the same. Otherwise a numerical solution is adopted [3.11].

The rate at which material is deposited from the cloud by dry deposition is given by

$$\omega_d = V_g \bar{X}(x, o) (Bq\ m^{-2}\ s^{-1}) \dots\dots\dots(3.13)$$

where $\bar{X}(x, 0)$ is the ground level air concentration of the parent or daughter as appropriate.

(d) Simultaneous depletion of the plume by various mechanisms

When the plume is being depleted simultaneously by a combination of radioactive decay, wet and dry deposition, the source strength Q_0 in equation (3.4) is replaced by the appropriate combination of factors derived above. In the most general case, where all three processes are operative, the air concentration of the parent nuclide in the plume is derived by substituting the following for Q_0 in equation (3.4).

$$Q_0 \exp - \left[\frac{(\lambda_p + \Lambda_p)x}{\bar{u}} \right] \exp - \left[\sqrt{\frac{2}{\pi}} \frac{v_g}{\bar{u}} \int_0^x \frac{dx}{\sigma_z} \exp \left\{ - \frac{h^2}{2\sigma_z^2} \right\} \right]$$

.....(3.14)

The concentration of the daughter nuclide is obtained by replacing Q_0 by:

$$\frac{\lambda_d Q_0}{(\lambda_p + \Lambda_p) - (\lambda_d + \Lambda_d)} \left[\exp - \left\{ \frac{(\lambda_d + \Lambda_d)x}{\bar{u}} \right\} - \exp - \left\{ \frac{(\lambda_p + \Lambda_p)x}{\bar{u}} \right\} \right]$$

$$\cdot \exp - \left[\sqrt{\frac{2}{\pi}} \frac{v_g}{\bar{u}} \int_0^x \frac{dx}{\sigma_z} \exp \left\{ - \frac{h^2}{2\sigma_z^2} \right\} \right]$$

.....(3.15)

Equation (3.15) holds only where the dry deposition velocity of the parent and daughter are the same; otherwise a numerical solution to account for dry deposition is adopted.

3.2.2.3 External radiation from the plume

The estimation of external radiation from a plume is in general carried out in two stages; first the evaluation of the absorbed dose in air followed by the conversion of the absorbed dose in air to dose equivalent in appropriate tissues. Different approaches are adopted depending on the nature of the radiation.

3.2.2.3.1 External irradiation by photons

(a) Absorbed dose in air

Two models are commonly used depending on the dimensions of the plume and the distribution of the activity within it; they are categorised as the semi-infinite and finite cloud models respectively.

Semi-infinite cloud model

The estimation of absorbed dose in air from a plume emitting photons is most simply achieved by use of a semi-infinite cloud model. Implicit in this approach are the assumptions that the air concentration is uniform over the volume of the plume from which photons can reach the point at which the dose is delivered and that the cloud is in radiative equilibrium. The amount of energy absorbed by a given element of cloud is then equal to that released by the same element. The absorbed dose rate in air can be

expressed as:

$$\dot{D}_\gamma = k_1 X \sum_{j=1}^n I_j E_j \dots\dots\dots(3.16)$$

where D_γ is the absorbed dose rate in air ($Gy\ y^{-1}$)

X is the atmospheric concentration of the nuclide ($Bq\ m^{-3}$)

E_j is the initial energy of the photon (MeV)

I_j is the fraction of photons of initial energy E_j emitted per disintegration

n is the number of photons of particular energies emitted per disintegration

$$k_1 = 2.0 \cdot 10^{-6} \text{ (Gy } y^{-1} \text{ per MeV m}^{-3} \text{ s}^{-1}\text{)}$$

Where the concentration distribution in the plume is sufficiently non-uniform to invalidate this approach, a finite cloud model must be used. This latter approach is adopted in ESCLOUD [3.117] for photon energies greater than 20 keV since the use of the semi-infinite cloud model can lead to large errors over a considerable range of downwind distances, particularly for elevated releases. At large distance, when the lateral dimensions of the plume are large compared with the mean free path of the photons considered, the predictions of both models converge. For photons of less than 20 keV energy, a semi-infinite cloud may always be adequate.

Finite cloud model

The finite cloud model involves simulating the plume by a series of small volume sources and integrating over these sources. There are two stages in the calculation, the evaluation of the photon flux at the point of interest and the conversion of the photon flux to absorbed dose in air. In general a number of photons of differing energy and intensity are associated with the decay of a particular nuclide. The procedure for estimating the dose for photons of a discrete decay energy is described; the evaluation of the dose from the decay of any nuclide is obtained by summation over the photon decay energy spectrum.

The photon flux at a distance from a point source has two components, the unscattered and scattered flux. The scattered flux has undergone one or more collisions with air molecules and has a different energy from the unscattered flux; the latter has an energy equal to that of the decay photons. The effective photon flux, F , at a distance, r , from a point source is obtained by using a multiple scattering build-up factor and is given by:

$$F = \frac{q B (E_\gamma, \mu r) e^{-\mu r}}{4 \pi r^2} \dots\dots\dots(3.17)$$

where F is the effective flux ($\gamma \text{ m}^{-2} \text{ s}^{-1}$)

q is the source strength ($\gamma \text{ s}^{-1}$)

r is the distance from the source (m)

μ is the linear attenuation coefficient (m^{-1})

B is the energy deposition build up factor and

E_γ is the initial photon energy (MeV)

The effective flux from a volume element, δV , of a plume with a concentration X per unit volume is obtained by replacing q in equation (3.17) by $X \delta V$. The total effective photon flux, F_c , from the finite cloud is obtained by integrating this modified expression over all space, ie,

$$F_c = \int_V \frac{XB(E_\gamma \mu r) e^{-\mu r}}{4 \pi r^2} dV \dots\dots\dots(3.18)$$

This integral is evaluated numerically in ESCLOUD using spherical polar co-ordinates with the origin at the point for which the dose is to be calculated. The energy deposition build-up factors calculated by Berger and described in reference [3.12] are adopted.

The absorbed dose rate in air is obtained as the product of the effective photon flux and the absorbed dose in air per photon per unit area [3.13], assuming the photon to have an energy equal to the decay energy. The absorbed dose in air per photon per unit area is tabulated in Table 3.2 as a function of the photon energy.

(b) Conversion of absorbed dose in air to dose equivalent in body organs

Dose equivalent rates in various organs can be derived from the absorbed dose rate in air from relationships between these quantities derived from the work of Poston and Snyder [3.14]. The ratios of the dose equivalent rate in the individual organs of interest to the absorbed dose rate in air are given in Table 3.2 for the range of initial photon energies considered by Poston and Snyder; the gonad dose is derived as the mean of the doses in the testes and ovaries. These relationships are applicable to irradiation from a semi-infinite cloud but are assumed equally valid in the case of a finite cloud; this assumption is justifiable at all but the smallest distances from the release point. This is sufficiently accurate in the present work concerned with the calculation of collective doses.

The ratio of the effective dose equivalent rate to the absorbed dose rate in air is also given in Table 3.2 and is evaluated as the weighted sum of the organ dose equivalent rates according to the procedure given in ICRP Publication 26 [3.15]. The weighting factors are summarised in Table 3.3 and the effective dose equivalent rate, \dot{H}_E , obtained as

$$\dot{H}_E = \sum_T w_T \dot{H}_T \dots\dots\dots(3.19)$$

where w_T and \dot{H}_T are the weighting factor for and dose equivalent rate in tissue, T, respectively.

The weighting factor for "remainder tissues" is used in conjunction with the average dose equivalent rate in the five organs, other than the skin and organs with specified weighting factors, with the highest dose equivalents.

The procedure adopted to estimate dose equivalents for particular nuclides is described fully in ESCLOUD [3.11] together with the nuclear data adopted which were taken from references [3.16 - 3.19]. Doses are evaluated at the energies specified in Table 3.2 and values for particular nuclides obtained by interpolation at the energies of interest taking into account the intensity of the emission at each energy.

The dose equivalents evaluated are appropriate to individuals out of doors during the transit of the plume. Doses to people indoors will be significantly lower owing to shielding provided by building structures etc. The reduction will depend on the time spent indoors and the nature of the buildings but a factor of about 2 is probably representative of the degree of overestimation.

3.2.2.3.2 External irradiation by electrons

(a) Absorbed dose in air

The range in air of electrons emitted by the radionuclides of interest is in general small (several metres at most) compared to the dimensions of the plume and an infinite cloud model can be used to estimate the absorbed dose rate. The energy absorbed by a given element of the cloud is equal to that released by the same element and the absorbed dose rate in air can be expressed as

$$\dot{D}_\beta = k_2 X(x,0) \sum_{j=1}^m I_j \bar{E}_j \dots\dots\dots(3.20)$$

where \dot{D}_β is the absorbed dose rate in air (Gy y^{-1})

$X(x,0)$ is the ground level concentration (Bq m^{-3})

\bar{E}_j is the mean energy of the particle or conversion electron (MeV)

I_j is the fraction of electrons of mean energy \bar{E}_j emitted per disintegration

m is the number of β particles and conversion electrons of particular energies per disintegration

$$k_2 = 4 \cdot 10^{-6} \text{ (Gy y}^{-1} \text{ per MeV m}^{-3} \text{s}^{-1}\text{)}$$

In β decay the particles are emitted with a spectrum of energies which is characterised partially by the maximum energy $E_{\beta\text{max}}$. The mean energy of the β particle, \bar{E}_j , is to a good approximation, equal to one third of the maximum energy:

$$\bar{E}_j = \frac{E_{\beta \max j}}{3} \dots\dots\dots(3.21)$$

The nuclear data adopted in the estimation of absorbed dose rates in air were taken from references [3.18] and [3.19]. The absorbed dose rate in air per unit air concentration of each nuclide considered is given in Table 3.4.

(b) Conversion of absorbed dose in air to dose equivalent in body organs

The range of electrons in tissue varies with energy but for electron energies typical of radioactive decay the range rarely exceeds a few millimetres. Consideration can therefore be limited to irradiation of the skin. The radiosensitive cells nearest the skin surface are located at the basal layer of the epidermis at a depth of about 70 μm. The dose equivalent rate in skin is evaluated from the absorbed dose rate in air, allowing for exponential absorption of the electron flux in the 70 μm layer, and is given as

$$\dot{H}_\beta = 0.5 e^{-\mu l} \dot{D}_\beta QF \dots\dots\dots(3.22)$$

where \dot{H}_β is the dose equivalent rate in skin (Sv y⁻¹)

QF is the quality factor for β radiation and taken as unity

μ is the absorption coefficient in tissue and taken as inversely proportional to the range in tissue corresponding to the mean energy of the electron considered (m⁻¹)

l is the thickness of the epidermal layer and taken as 7 10⁻⁵ m
 the coefficient 0.5 is a conversion factor from the infinite geometry since the electrons are unable to penetrate the thickness of the body.

The dose equivalent rate in skin per unit air concentration for each of the nuclides considered is given in Table 3.4.

The imprecise nature of the estimation of the dose in skin from electrons must be stressed. This imprecision arises from theoretical difficulties associated with the estimation of electron absorption in the epidermis which varies in thickness over the body and from practical considerations such as absorption by clothing and other nearby objects eg, seats, etc. To account for such factors is complex and beyond the scope of this study. Nevertheless it must be recognised that because they have not been considered the dose equivalents estimated are overestimates.

3.2.3 Selection of data used in the model

The Gaussian plume model and the procedures for calculating external doses from the cloud are implemented in ESCLOUD which is used to establish the matrix of results. For a release rate of 1 Bq s⁻¹ of each nuclide the air concentration, deposition rate and external dose equivalents from photons

are evaluated as a function of distance for a range of meteorological conditions and range of values of other parameters where appropriate. The ranges analysed are sufficiently wide to enable the resulting matrix of results to be applied in a site specific manner once the values of the appropriate parameters are specified for the particular site. The range of conditions evaluated and the values adopted for the various parameters are outlined.

3.2.3.1 Meteorological conditions

The concentration at any point downwind of a release of radioactivity is a function of the degree of atmospheric diffusion. The relationship between meteorological quantities and atmospheric diffusion is not well understood and several empirically based, qualitative typing schemes have been developed in order to solve practical atmospheric diffusion problems. Most of these schemes have been reviewed by Gifford [3.20]. Within the EC the meteorological data measured at the majority of existing nuclear reactor sites have been categorised into one of two schemes, those due to Pasquill [3.21] and Doury [3.22]. Calculations have been made for each of these schemes and the one selected to calculate the consequences of a release at a specific site is determined by the form of the meteorological data available.

(a) Pasquill/Smith/Hosker scheme

Pasquill [3.21] recommended a procedure for the calculation of the horizontal and vertical dispersion of a plume based on experimental observations of smoke clouds. He defined six weather categories, A-F, in order of increasing atmospheric stability, and for each of these he specified values for the wind speed and the vertical and horizontal standard deviations of the plume as functions of the downwind distance from the source. Smith, [3.23] in his scheme, took account of further experimental data but instead of discrete categories of atmospheric stability he defined stability in terms of a continuous variable, P. Values for P of 0.5, 1.5, 2.5, 3.6, 4.5 and 5.5 are taken to correspond to Pasquill's categories A-F respectively. Smith solved the diffusion equation numerically over a range of atmospheric conditions and windspeeds, matching the value of σ_z to the data. This allowed a further parameter to be introduced into the calculations, the ground roughness length. The roughness length is a measure of the mechanical turbulence introduced into the atmosphere by the roughness of the underlying surface; its value varies from less than 1 cm for water to in excess of 1 m for urban areas. In this study an intermediate value of the surface roughness length of 10 cm, typical of a rural area, is assumed. To facilitate numerical analysis Hosker [3.24] fitted equations to Smith's results which were presented graphically out to distances of 100 km. For a roughness length of 10 cm the equation has the form

$$\sigma_z = \frac{a x^b}{1 + c x^d} \dots\dots\dots(3.23)$$

Values for the coefficients a, b, c, d are given in Table 3.5. This representation for σ_z is used in this study and assumed to apply over all distances considered.

(b) Doury scheme

From a review of experimental data Doury [3.22] derived a relationship between the vertical standard deviation of the plume, σ_z , and the time of travel t , (x/\bar{u}) . The relationship has the form

$$\sigma_z = (At)^k \dots\dots\dots(3.24)$$

Two variations of σ_z with time are considered and categorised as normal and poor diffusion; combining these with different windspeeds a range of dispersion conditions may be accommodated. The values of A and k for a variety of travel times in each diffusion category are given in Table 3.6. These values are assumed to be valid over all times and distances of interest in this study. For each diffusion category three different wind speeds are considered (see Table 3.6).

A further parameter which may have a considerable influence on the degree of dispersion is the depth of the mixing layer; vertical turbulent mixing virtually ceases at the top of this layer. The depth of the mixing layer varies with the prevailing meteorological conditions; there is variation from one atmospheric stability category to another as well as within individual categories. Representative values of the depth of the mixing layer have been adopted in this study and they are summarised in Table 3.7 for the respective stability categories; it is recognised however that in reality there may be significant variation about these values.

3.2.3.2 Rainfall

Rain is only considered possible in Pasquill's categories C and D and under Doury's normal diffusion conditions. In these conditions when it is raining the value of the washout coefficient, Λ , is taken as 10^{-4}s^{-1} for all radionuclides except the noble gases, which are assumed not to be washed out. Carbon-14 and tritium are assumed to be returned to the atmosphere after washout in a timescale short compared with their half-lives; in estimating the downwind airborne concentrations of these nuclides no allowance is therefore made for washout. The washout coefficient varies considerably with, for example, the form and intensity of the precipitation, and the chemical and physical properties of the radioactive particulate [3.25]. The value adopted is appropriate to small particulate material and a rainfall rate of a few millimetres per hour, which is typical of rainfall rates in Western Europe.

The estimation of dispersion under Pasquill categories C and D and under Doury normal conditions must therefore be evaluated with and without rainfall. The implication is that five of the twelve dispersion conditions identified in Section 3.2.3.1 must be evaluated in these two modes.

3.2.3.3 Deposition Velocity

The deposition velocity is variable over several orders of magnitude, (eg, see Slimm [3.25]), and depends on the size of the particle or the reactivity of the gas, the nature of the underlying surface and the meteorological conditions. A single representative value of $5 \cdot 10^{-3} \text{m s}^{-1}$ is used for all radionuclides considered in this study except for the noble gases, which are assumed not to deposit, and for the organic forms of iodine. The value is typical of particles of aerodynamic diameter of

several microns depositing on a wide variety of surfaces. The representative nature of this value, chosen for use in this generic assessment, must be recognised; if attention were to be given to a particular radionuclide having a well defined physico-chemical form an alternative value may be more appropriate.

The estimation of the deposition of iodine is particularly complex [3.26] and a relatively simple approach is adopted in this study. The deposition velocity of iodine varies considerably with its chemical form which may also change as the material is dispersed. For inorganic forms of iodine a deposition velocity of $5 \cdot 10^{-3} \text{ m s}^{-1}$ is reasonably representative; the deposition velocity of organic forms is however much lower, a value of $5 \cdot 10^{-5} \text{ m s}^{-1}$ being typical. As both inorganic and organic forms of iodine are commonly encountered in effluents from nuclear installations the deposition of iodine in the respective forms is evaluated. In estimating the deposition the iodine is assumed to remain in the form in which it is released while recognising that, in reality some changes would occur which could significantly alter the spatial pattern of deposition.

For the reasons expounded in Section 3.2.3.2 no allowance is made for the dry deposition of carbon-14 and tritium in estimating the downwind air concentrations.

3.2.3.4 Release heights

The height of release may significantly affect the air concentration of a nuclide downwind of the release point, particularly close to the release. Two heights of release are investigated in this assessment, 30 m and 100 m, and they were chosen as typical of the range of heights at which effluents are released from various types of nuclear installation in the European Community. At some installations even greater heights of release may be experienced; in such cases the use of the data derived for the release heights specified would be conservative. No account is taken in this study of the possible further elevation of the plume due to its momentum and buoyancy at the time of release or of any subsequent self heating due to radioactive decay or chemical changes within the plume.

3.2.4 Summary of selected results from the matrix

The air concentration, deposition rate, and dose equivalents from external radiation from the plume have been evaluated as a function of distance for a release rate of 1 Bq s^{-1} of each nuclide, assuming a uniform windrose. Results have been obtained for releases in each of the meteorological conditions considered and for releases at effective heights of 30 m and 100 m. A small selection of the matrix of results generated is illustrated in Tables 3.8 - 3.11; air concentration, deposition rate, effective dose equivalent from photons and dose equivalent in skin from electrons are tabulated, respectively, for some nuclides at selected distances. The results correspond to a release from an effective stack height of 30 m in Pasquill category D conditions; similar results for each of the other meteorological conditions and release heights, for all of the radionuclides considered, are contained in the matrix at a considerably greater number of distances.

Some of the more important features of the results are illustrated in Figures 3.1 to 3.4. The variation of air concentration assuming a uniform windrose of a long lived non-depositing radionuclide released at different heights in various meteorological conditions is shown in Figure 3.1. Two features are apparent. The peak air concentration for a release in a

particular weather category decreases with increasing height of release and it also occurs further downwind. The air concentration is seen to vary significantly with meteorological conditions and the variation, at greater distances where the height of release no longer has an influence, is typically more than an order of magnitude.

The air concentration as a function of distance, for unit release of several noble gases of various radioactive half-lives, are shown in Figure 3.2. The concentrations correspond to releases from an effective stack height of 100 m in Pasquill category A conditions. The influence of radioactive decay in reducing the concentrations of the shorter lived nuclides at long distances is clearly illustrated. The different pattern of variation of air concentration with distance of a daughter nuclide is also shown, the less rapid rate of decrease in its concentration with distance, at intermediate distances, is a consequence of its accumulation in the plume owing to decay of its parent.

The variation with distance of the air concentration and effective dose equivalent rate from external γ radiation from the cloud for unit release of krypton-85 at different release heights is shown in Figure 3.3. Although there are very large differences in ground level air concentrations at short distances for releases at different heights (several orders of magnitude), the difference in the effective dose equivalent rates from external γ radiation is small (within a factor of about 2). The marked difference in air concentration is a consequence of the plume not having reached the ground in the case of the more elevated release; the effect on the dose from external γ radiation, however, is much smaller owing to the mean free path of the γ rays being comparable with the elevation of the respective plumes.

The removal of activity from the plume as it travels downwind is illustrated in Figure 3.4. The relative importance of dry deposition processes for releases in various dispersion conditions is indicated for plutonium-239 as an example, for which radioactive decay is negligible. The much greater fraction of organic forms of iodine-129 remaining in the plume is also shown, a consequence of the much lower dry deposition velocity assumed for these forms, which illustrates the dependence of these curves on the value of deposition velocity chosen. The influence of radioactive decay can be ascertained by contrasting the remaining fractions of plutonium-239 and xenon-133m for release in the same dispersion conditions.

3.2.5 Site specific application of the matrix of results

The matrix of results derived assuming a uniform windrose and for a range of meteorological conditions can be used to evaluate annual average air concentrations, deposition rates, and external doses as a function of distance and direction from the release of a spectrum of radionuclides from any site subject to the specification of appropriate site parameters; these parameters include the height of release, the windrose, the spectrum of meteorological conditions and the nuclides released. In effect the procedure comprises the evaluation of weighted mean air concentrations (and other appropriate parameters, eg, cloud γ dose, ground deposition rate etc) in particular sectors and as a function of distance with respect to the discharge location; the weighting is applied according to the frequency with which the wind blows into that sector and the associated spectrum of meteorological conditions appropriate to the discharge location. This procedure is approximate in a number of respects, in particular in the assumptions that the direction and meteorological conditions experienced by the plume remain constant throughout its transit. In addition, implicit in the approach adopted to estimate cloud γ doses, is the assumption

that the wind frequency and spectrum of meteorological conditions in neighbouring sectors are identical to those in the sector under consideration. The imprecision introduced by these approximations is not however considered significant in the context of the overall uncertainty involved in the dose estimation.

(a) Annual average air concentration

The annual average air concentration of a nuclide, i , and, in polar co-ordinates, at a distance, d , and in a sector in the direction θ is evaluated as

$$C(i,d,\theta) = N Q_o(i) \sum_c \bar{X}_o(i,c,d) f(\theta,c) \quad (\text{Bq m}^{-3})$$

.....(3.25)

where $Q_o(i)$ is the release rate of nuclide, i , (Bq s^{-1})

$\bar{X}_o(i,c,d)$ is the air concentration per unit release rate of nuclide, i , in a dispersion condition, c , and assuming a uniform windrose (Bq m^{-3} per Bq s^{-1})

$f(\theta,c)$ is the fraction of time a particular dispersion condition, c , exists with the wind in the sector of direction θ and of width $360^\circ/N$

where N is the number of sectors in the windrose

(b) Annual average intake by inhalation

The annual average intake by inhalation of nuclide, i , at (d,θ) can be evaluated from the air concentration as

$$I_{inh}(i,d,\theta) = C(i,d,\theta) R \quad (\text{Bq y}^{-1})$$

.....(3.26)

where R is the mean adult annual breathing rate and is equal to

$$8030\text{m}^3 \text{ per y } \sqrt{3.27}$$

The committed effective dose equivalent together with the doses in various organs can be derived from this annual intake as

$$H_{E,50}(i,d,\theta) = I_{inh}(i,d,\theta) H_{inh}(i) \quad (\text{Sv from intakes in a year})$$

.....(3.27)

where $H_{inh}(i)$ is the committed effective dose equivalent from intake of nuclide, i , by inhalation (Sv per Bq).

The evaluation of H_{inh} for the nuclides of interest is described in Chapter 6.

For the release of a spectrum of nuclides the committed effective dose equivalent from the annual intake of all nuclides is obtained as

$$H_{E,50}(d, \theta) = \sum_i I_{inh}(i, d, \theta) H_{inh}(i) \quad (\text{Sv from intakes in a year})$$

.....(3.28)

(c) Annual deposition rate and external doses

In the same manner, the average deposition rate (ω), cloud γ effective (and organ) dose equivalent rates (\dot{H}_γ), and cloud β dose equivalent rates in skin (\dot{H}_β) can be derived at (d, θ) for the release of nuclide, i . They can be expressed as

$$\omega(i, d, \theta) = N Q_o(i) \sum_c G(i, c, d) f(\theta, c) \quad (\text{Bq m}^{-2} \text{ s}^{-1})$$

.....(3.29)

$$\dot{H}_\gamma(i, d, \theta) = N Q_o(i) \sum_c \dot{HG}(i, c, d) f(\theta, c) \quad (\text{Sv y}^{-1})$$

.....(3.30)

$$\dot{H}_\beta(i, d, \theta) = N Q_o(i) \sum_c \dot{HB}(i, c, d) f(\theta, c) \quad (\text{Sv y}^{-1})$$

.....(3.31)

where $G(i, c, d)$, $\dot{HG}(i, c, d)$ and $\dot{HB}(i, c, d)$ are the deposition rate ($\text{Bq m}^{-2} \text{ s}^{-1}$ per Bq s^{-1}), cloud γ effective dose equivalent rate (Sv y^{-1}) and cloud β dose equivalent rate in skin (Sv y^{-1}), respectively, for unit release of nuclide, i , in dispersion condition, c , assuming a uniform windrose.

The cloud γ effective dose equivalent and cloud β dose equivalent in skin for the total release can be obtained by summation over the spectrum of nuclides.

3.2.6. Global dispersion of radionuclides released to the atmosphere

The atmospheric dispersion models previously described apply to the first pass of the activity as it disperses downwind. Activity remaining in the plume after it has travelled beyond the boundaries of the EC will, if not subsequently deposited, continue to disperse throughout the troposphere and if sufficiently long-lived become globally distributed, thus leading to further exposure of the EC population.

The fraction of a stable, or long-lived, nuclide remaining in the plume at a range of downwind distances is shown in Table 3.12 for releases in selected dispersion conditions. For nuclides whose deposition velocity is assumed to be $5 \cdot 10^{-3} \text{ m s}^{-1}$ the fractions remaining in the plume beyond the boundaries of the European Community are small and will not have any significant global impact. For a deposition velocity of $5 \cdot 10^{-5} \text{ m s}^{-1}$ (chosen to characterise the deposition of organic forms of iodine) the removal from the plume is much less. The subsequent dispersion of long-lived iodine radionuclide released in the organic form must be considered; in reality however changes in chemical form as organic iodine is transported downwind may result in greater removal from the plume than indicated in Table 3.12. The noble gases do not deposit from the atmosphere to any significant extent and if sufficiently long-lived will become globally dispersed; of the noble gases only krypton-85 has a half-life long enough for it to be considered in a global context.

Some radionuclides are very mobile in the environment and even if deposited from the atmosphere may be recirculated in a timescale short compared with their radioactive half-lives. Tritium and carbon-14 are particular examples of radionuclides of this type; their involvement in many physical and biological processes leads to fairly rapid and widespread dispersion and ultimately to global circulation.

The only other nuclide which needs to be considered in a global context is iodine-129 owing to its extremely long radioactive half-life ($1.57 \cdot 10^7 \text{ y}$) and relative mobility, which however is somewhat less than that for tritium or carbon-14. By far the majority of iodine-129, irrespective of its chemical form will be deposited in its first pass over the earth's surface; however, owing to the above factors it may subsequently become generally dispersed throughout the global iodine pool in a time short compared with its radioactive half-life.

The models adopted to evaluate the global dispersion and subsequent exposure of the population of the European Community after the first pass of activity released to the atmosphere, are described in Chapter 5.

3.3 Transfer of radionuclides through the terrestrial environment

3.3.1 Introduction

Radioactive material deposited from the atmosphere onto land surfaces will be transferred through the terrestrial environment and may lead to irradiation of man by three main routes; inhalation of resuspended activity, external irradiation and ingestion of contaminated foodstuffs. Models have been developed which describe the transfer of activity from the atmosphere to land surfaces, its subsequent transfer through the terrestrial environment and the pathways by which man may be exposed.

Each model is described in the following sections and they are applied to evaluate the time integrals of resuspended air concentration, of external dose and of activity transferred to selected food products as a function of time after the continuous deposition on unit area of land of each radionuclide for a year at unit rate. The matrix of results obtained, when combined with the results from application of the atmospheric dispersion model and the spatial distributions of population and agricultural yields, can be used to assess the exposure of the population via the terrestrial environment following the release of activity to the atmosphere.

3.3.2 Resuspension of deposited activity

In the resuspension process surface particles become airborne due to physical disturbances. In the out-door environment, surface disturbances are usually created by the action of wind or rain or by human or animal activities. The magnitude and time dependence of the process varies depending on the type of surface and the nature of the disturbance. The resuspension of radioactive particles from surfaces can continue long after their initial deposition and so the mechanism is usually of most significance for long-lived radionuclides, especially those which are less readily transferred through foodchains, for example plutonium.

Resuspension mechanisms can be broadly subdivided into man-made and wind-driven disturbances. Resuspension caused by man-made disturbances such as vehicular traffic, digging and farming activities is usually localised. Its magnitude is variable depending on the nature of the disturbance and evaluation of the irradiation of individuals due to localised resuspension requires habit surveys in which occupational factors must be identified. While localised resuspension could be an important exposure pathway for particular individuals, in terms of collective dose in populations the wind-driven mechanism is likely to be more important. This study is concerned particularly with the assessment of detriment to the exposed population; localised resuspension is not considered further.

The process of wind-driven resuspension is complex and resuspension models tend to describe experimental observations of airborne levels above a contaminated surface rather than mechanisms. The availability of material for resuspension varies with surface type and resuspension from undisturbed and ploughed soils as well as from urban surfaces is considered. Compared with undisturbed surfaces, ploughing and cultivation of land on which deposition has occurred is expected to reduce the initial wind-driven resuspended air concentration because of dilution of the contaminant surface layer. At long times, however, ploughing may enhance the resuspended air concentration by returning

activity to the soil surface. Wind-driven resuspension from urban surfaces has received little attention. The mechanisms involved in the removal of deposits from urban surfaces are different from those from agricultural land but no quantitative data are available.

3.3.2.1 Review of resuspension data

The majority of experimental observations of resuspension in the outdoors environment has been made of plutonium from undisturbed surfaces at nuclear weapons test sites in semi-arid conditions [3.28]. The resuspended air concentration is observed to decline with time after the material is first deposited. The decline is due to the surface deposit becoming progressively less available for resuspension as a result of chemical and physical changes. For example, soil analyses have shown plutonium particles to become attached to larger less mobile soil particles [3.29]. Some decline in surface availability due to penetration processes and to losses due to resuspension and subsequent dispersion also occurs but these processes alone are insufficient to account for the magnitude of the observed decline in air concentration within a few months (or years) of the initial deposition (reduction factors of 10^3 to 10^5). After a few years when deposits on undisturbed surfaces have 'aged' the resuspended air concentration appears to reach an essentially constant level, at least over the period while observations have been made, typically 20 years.

Observations of the relationship between surface and resuspended air contamination have been related by means of the resuspension factor, K

$$\text{where } K(\text{m}^{-1}) = \frac{\text{Resuspended air concentration (Bq m}^{-3}\text{)}}{\text{Surface deposit (Bq m}^{-2}\text{)}} \dots (3.32)$$

The use of this factor is a convenient way of expressing the observed relationship between surface and air contamination but its physical significance is limited. In the absence of an adequate model to describe the physical processes of resuspension the factor is used in this study to assess resuspended air concentrations. Data on resuspension have recently been reviewed by Linsley [3.28]. Most of the measurements relate to the resuspension of plutonium from undisturbed surfaces in semi-arid environments. These measurements indicate that K declines from values in the range 10^{-4} to 10^{-6} m^{-1} shortly after deposition to 10^{-8} - 10^{-9} m^{-1} after a few years. The time taken for the decline in resuspension factor to occur has been variously assumed to be in the range 2 to 17 years. The initial values of resuspension factor apply to the whole of the deposit which is present as a thin surface layer shortly after deposition. For aged deposits the reported values variously relate to the whole of the deposit, even if it is distributed to a depth of 20 cm, or the amount present in the top 1 cm soil layer. In the model developed in the next section, the convention is adopted that the values for K correspond to the whole of the deposit.

The applicability of the above values and their time dependence to European conditions, where soils tend to be more moist and where there is greater vegetative cover, is uncertain. There is, however, some support for their validity from measurements over deposits of uranium in soils [3.30] in the UK which suggest that 10^{-9} m^{-1} may be an appropriate, if conservative value of K for aged deposits. The lower end of the range of time period reported (2 to 17 years) for the decline of resuspension factor from its initial levels to values of the order of 10^{-9} m^{-1} is

considered to be most appropriate to European conditions, where the effects of rainfall and vegetative cover might be expected to inhibit resuspension.

Measurements over aged deposits give values of resuspension factor in the region of 10^{-9} m^{-1} at up to 20 years (the extent of the measurements) after the deposition event. At longer times it seems likely that resuspension over undisturbed soils will decline still further as a result of the gradual removal of the resuspendible contaminant by further penetration and consolidation; for ploughed surfaces while the initial decline is likely to be more rapid it may be slower in the longer term due to the regular return of activity to the surface.

The observations of time dependent changes of resuspended air concentrations reported above in terms of resuspension factors, relate to average wind conditions. While such averaged values are appropriate for use in assessing, for example annual average resuspended air concentrations, the instantaneous values of air concentration will vary considerably with meteorological conditions, particularly wind velocity.

Few data are available on the resuspension of elements other than plutonium and the model developed in this study for plutonium is assumed for all nuclides.

3.3.2.2. Resuspension model

The model used in this study is based on a time-dependent resuspension factor. The value of the resuspension factor immediately after deposition is uncertain and a value intermediate in the reported range is adopted ($K = 10^{-5} \text{ m}^{-1}$) while recognising that this may be an overestimate for some of the damper European climates. In particular, the value is considered to be over-conservative for situations where surface deposition is occurring by washout (ie, wet deposition). Under these conditions the contaminant is likely to become associated with soil particles more rapidly than in dry deposition and some penetration into the soil surface may occur.

The resuspension factor is assumed to decline exponentially from the initial value to one typical of an aged deposit (10^{-9} m^{-1}) within a 2 year period. This reduction is consistent with a half-life of about 0.15 years.

Observations of the time dependence of resuspension are limited to follow-up periods of about 20 years after deposition. The processes governing the subsequent decline in the rate of resuspension are complex; changes in physico-chemical form, variation in the nature of the surface, and rate of downwards migration all have an influence. The insufficiencies in the data in this area are such that any estimate of the subsequent rate of decline must be speculative. From consideration of the migration data for plutonium, strontium and caesium (see Section 3.3.3.2) a half-life of 100 years is adopted in this study for the longer term rate of decline of the resuspension factor. The speculative nature of this estimate must however be recognised. This half-life is assumed applicable to the resuspension of all elements. For those elements which migrate through soil somewhat faster than plutonium (eg, iodine) their resuspension is likely to be overestimated as a consequence of this assumption.

The data on resuspension are considered insufficiently precise to warrant a distinction being made between undisturbed and ploughed land. The same model is therefore adopted for resuspension from all land surfaces.

The resuspension model is based on the relationship:

$$K = 10^{-5} \exp(-(\lambda_1 + \lambda_2 + \lambda)t) + 10^{-9} \exp(-(\lambda_2 + \lambda)t) \dots\dots\dots(3.33)$$

- where K is the resuspension factor, (m⁻¹)
- t is the time after the initial deposition, (s)
- λ₁ is the decay constant for the initial decline in the resuspension factor (s⁻¹)
- λ₂ is the decay constant for the longer term decline in the resuspension factor (s⁻¹)
- λ is the radioactive decay constant of the nuclide of interest (s⁻¹).

The values of λ₁ and λ₂ are 1.46 x 10⁻⁷ s⁻¹ and 2.2 x 10⁻¹⁰ s⁻¹ and correspond to half-lives of 0.15 years and 100 years respectively.

The integrated resuspended air concentration, I_R, to time t₂ resulting from the deposition of a radionuclide continuously for 1 year at a rate of 1 Bq s⁻¹ m⁻² can be expressed as

$$I_R = \sum_{t_1 = 1}^{3.15 \times 10^7} \int_0^{t_2 - t_1} K(t) dt \dots\dots\dots(3.34)$$

where t is in seconds.

For t₂ → ∞, the integral can be written explicitly as

$$I_R = 3.15 \times 10^7 \int_0^{\infty} K(t) dt \dots\dots\dots(3.35)$$

The integrated resuspended air concentrations of daughter products, where they are important, can be evaluated in a similar manner.

The relationship developed in equation (3.25) is based entirely on data related to undisturbed surfaces in rural environments. The initial value of the resuspension factor from urban surfaces may be of the same order as observed in rural conditions but the mechanisms determining the subsequent behaviour of material on the respective surfaces may be very different. The magnitude of resuspension from the respective surfaces is contrasted in Appendix 3.1; in the case of urban surfaces rainfall and subsequent wash-off is assumed the sole mechanism for reducing resuspension. The integrated resuspended air concentration above rural surfaces is shown in Appendix 3.1 to be greater than that above urban surfaces. Bearing in mind the uncertainties involved in the comparison the conservative assumption is made that the

model for resuspension above rural surfaces is also applicable to urban surfaces.

3.3.2.3. Results of the resuspension model

A matrix of results has been evaluated comprising the time integral (to various times) of the resuspended air concentration of each nuclide above a surface on which the nuclide has been deposited at a rate of $1 \text{ Bq m}^{-2} \text{ s}^{-1}$ for a year. The resuspension factor adopted is independent of the deposited element and variation in the integrated air concentration from one nuclide to another is solely a function of radioactive half-life. The variation of the integrated resuspended air concentration with radioactive half-life is illustrated in Figure 3.5. For half-lives in excess of about 1 year the integrated resuspended air concentration reaches a constant level determined primarily by the initial rate at which the resuspension factor declines. Integrals of resuspended air concentration to different times show that by far the largest contribution comes in the first year, and even for long-lived radionuclides the integral to infinity only increases by a further 35% over that at the end of the first year.

The integrated air concentration above the surface during the deposition process (assuming dry deposition only) is contrasted with the resuspended air concentration in Figure 3.5. The former is inversely proportional to the deposition velocity assumed for dry deposition and the value in Figure 3.5 is derived for a deposition velocity of $5 \cdot 10^{-3} \text{ m s}^{-1}$. For this value of deposition velocity the time integrals of resuspended air concentration are always smaller than the integrated air concentration during the dry deposition; for long lived nuclides the ratio between these two quantities is 0.36. The resuspended air concentration would only become comparable with that during dry deposition for deposition velocities in excess of 10^{-2} m s^{-1} . Thus, while the uncertainties in estimating resuspension are considerable, they are unlikely to have a significant effect on the overall detriment under conditions of dry deposition.

In addition to dry deposition, activity may be deposited by washout. Depending on its magnitude the latter may influence the relative importance of the integrated air concentrations during deposition and subsequent resuspension. It is difficult to generalise on this matter since much depends on the meteorological conditions considered. However the potential exists for the relative importance of the respective concentrations to be altered from that indicated above. It should be noted however that the same resuspension factor is assumed to apply to activity deposited under dry and wet conditions and that this will overestimate the significance of the latter.

The time dependence of the initial and resuspended air concentrations and their time integrals are shown for two nuclides plutonium-239 and ruthenium-103, with significantly different radioactive half-lives in Figure 3.6; their half-lives are $2.44 \cdot 10^4 \text{ y}$ and 0.108 y respectively. Within 1 year of deposition ceasing, the resuspended air concentration of ruthenium-103 has declined by five orders of magnitude compared with that of plutonium-239 which declines by two orders of magnitude. In subsequent years the resuspended air concentration of the relatively short-lived ruthenium nuclide continues to decline rapidly whereas the resuspended air concentration of plutonium-239 levels off after another year. The longer term decline of the resuspended air concentration of plutonium-239 is associated with the predicted reduction in availability of material for resuspension due to consolidation and penetration processes.

3.3.3 The transfer of nuclides through the terrestrial environment into food chains

3.3.3.1 Introduction

The transfer of radionuclides through the terrestrial environment into foodstuffs is complex; many processes are involved and much depends on the nature of the nuclide, the environment and the contaminating mechanism being considered. The more important processes include migration into soil and the transfer of activity from soil to plants and from plants to animals, all by several mechanisms. In modelling the movement of activity through the terrestrial environment a modular approach [3.31] is adopted owing to the multiplicity of pathways and processes that must be considered. Each module is concerned with a particular process for which there may be more than one module; the development of more than one module per process may reflect the need for models of differing complexity or for models tailored to accommodate the available environmental data which may be in varied forms. The modules [3.31] can be combined in various ways to describe the movement of activity through the terrestrial environment in a manner most appropriate to the prevailing circumstances. While they were developed in the context of land contamination from activity deposited from the atmosphere the models are general in nature and can be applied equally to other modes of deposition - for example, irrigation, with appropriate choice of parameters.

In the past most models developed to evaluate the irradiation of man from the transfer of activity to foodstuffs have been based on the assumption of "quasi-equilibrium" between the respective parts of the environment. Under such conditions the amounts of activity in different parts of the environment can be related by simple concentration factors. An example of this approach is the derivation of a relationship between the concentration of iodine-131 in cows' milk and the deposition rate of iodine-131 on pasture assuming the process to be continuous [3.32]. For long-lived nuclides or releases of relatively short duration the assumption of "quasi-equilibrium" between all parts of the foodchain may not be valid and account must be taken of the time dependence of particular processes. The models [3.31] utilised in this study are dynamic in nature and enable the important time dependent processes to be evaluated where appropriate.

Early laboratory and field studies established that the radionuclides of strontium, caesium and iodine are the most important for transfer into foodchains following releases to atmosphere of mixed fission products, particularly in the case of fall-out from the atmospheric testing of nuclear weapons. Consequently the movement of these elements through the foodchains to man have been the most comprehensively studied. In general the transfer of other nuclides which may be contained in airborne effluents from nuclear installations is relatively less well understood, although in recent years further data have been accumulated for several potentially important nuclides, particularly for those of the transuranium elements. In many cases the reliability that can be ascribed to the transfer data is very variable. This may be due to the paucity of data or to the real variation in the value of a transfer parameter with different plant species or soil composition. One of the greatest areas of uncertainty in assessing the long-term transfer of activity to foodstuffs is the prediction of the migration of nuclides down through soil and of any physical or biochemical processes that modify their availability for uptake into plants with time. Similarly only limited data are available on the intake and transfer of many elements in grazing animals and the quality of these data determine to some extent the nature of the models used in this study

for particular parts of the foodchain. For example, two models of varying complexity are used to assess the metabolism of activity taken in by grazing animals.

The transfer through the terrestrial environment to foodchains of radionuclides listed in Table 3.1, with the exception of tritium and carbon-14 is modelled using the general methodology described in the following sections. The exchange processes between atmosphere, vegetation and soil for tritium and carbon-14 differ from those of the other nuclides in several respects. For tritium and carbon-14 a simplified procedure, comprising the use of a specific activity approach [3.33] has been adopted.

The number of foodstuffs consumed by man is considerable. With the exception of a few nuclides, data on the transfer processes of radionuclides in a wide range of different plant types are limited. For this study therefore the various foodstuffs have been grouped into a number of categories; these were selected from consideration of the components of the average diet in the European Community and by distinguishing the crop types for which the same contamination mechanisms are important. The categories selected comprise grain products, green vegetables, root vegetables, meat, liver and milk products. Few transfer data are available for fruit crops and these are categorised with green vegetables in this study. The data on the transfer of radionuclides to animal produce (meat, liver and milk) are limited and consideration is limited to cattle and sheep. The transfer of radionuclides to produce from other animals is estimated where appropriate by analogy with the transfer to sheep or cattle.

It is recognized that products derived from other animals contribute significantly to man's diet, in particular, products derived from pigs and chickens. However the intake of activity by these animals is variable depending on feeding practices especially when they are reared in an indoor environment; further, little information exists on the metabolism of the elements being considered in these animals. In view of these considerations such animals have been omitted from consideration in this methodology although their potential importance is recognised.

The modules developed to describe the three principle processes that influence the transfer of radionuclides through foodchains to man are outlined in the following sections; the three processes comprise migration of radionuclides in soil, transfer to plants and transfer to animals. The technique of compartmental analysis is adopted to model the transfer of activity through each system. The technique in its most general form is summarised in Appendix 3.2 and in essence involves the representation of the system being considered by a series of compartments. Activity can be transferred between compartments according to prescribed transfer rates and within each compartment uniform mixing is assumed.

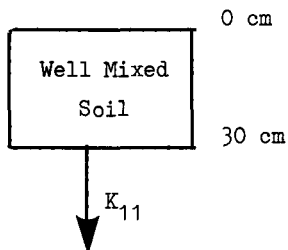
3.3.3.2 Migration of radionuclides in soil

Migration into soil, together with radioactive decay, are the principal mechanisms which determine the time dependence of the uptake of radionuclides into plants and animal products following the deposition of activity onto land. For some elements, however, changes in chemical form affect their availability for uptake by roots. Many parameters influence the rate of migration, particularly the nature of the element and its chemical form, soil composition, climate and rainfall. Agricultural land can be categorised into one of two types for the purposes of modelling migration: undisturbed land (eg, permanent pasture) or land where the soil is kept well mixed by frequent ploughing or cultivation. Two models have been developed to represent

migration in the respective conditions and their main features are outlined.

(a) Model for well mixed soil

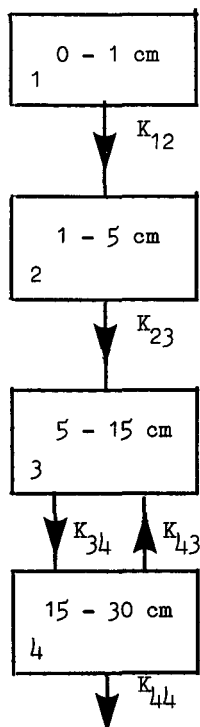
Diagram 3.3 Schematic diagram of well-mixed soil model



The model, shown schematically above, is intended to represent land which is ploughed or cultivated annually or more frequently. The contaminant is assumed to be uniformly mixed and equally available through the top 30 cm of soil; the choice of a depth of 30 cm encompasses the variation in depth of the root zones of most plants. Implicit in this approach is the assumption that the uniform profile is not significantly altered by migration in the intervening period between ploughing or cultivation; this assumption is in general valid for the nuclides considered in this study. Loss from the root zone occurs by downwards penetration processes of which diffusion and transport along with general water movement are the most important; the rate of loss is determined by the transfer coefficient, K_{11} .

(b) Model for undisturbed land

Diagram 3.4 Schematic diagram of the model for undisturbed land



The model, shown schematically above, is intended to represent migration through undisturbed agricultural land of which permanent pasture is an example. The movement of the contaminant through the soil column is represented by a series of transfers between compartments of varying depth; within each compartment the contaminant is assumed to be uniformly mixed. The rates of transfer are determined by the transfer coefficients $K_{12} - K_{44}$. The selection of compartments is a compromise between ensuring an adequate representation of the migration processes and including those that have physical significance for other parts of the terrestrial model. For example, resuspension of the contaminant onto plant surfaces is assumed to be derived solely from the top 1 cm of soil, that is, the surface compartment. Soil which is consumed inadvertently by animals is also assumed to be derived from the top 1 cm layer. The root zone of pasture grass is considered to extend to 15 cm in depth and the contaminant present in each of the upper three compartments is available for root uptake.

Migration into soils has only been studied for a limited number of elements mainly those long-lived radionuclides which are present in nuclear weapons fall-out, in particular nuclides of caesium, strontium and plutonium. In addition there are some migration data available, particularly for plutonium, from single deposits on the ground following tests and accidents with nuclear devices [3.34, 3.35] and leakage of radioactive material at a nuclear facility [3.36]. The rate of movement into the soil for caesium, strontium and plutonium is slow, although there is significant variation between the results of the various observations due to differences in soil composition and annual rainfall. None of the observations extends beyond 30 years after the deposition event.

In view of the limited data on soil migration the transfer coefficients used in the model in this assessment are based on the soil migration data for plutonium and are assumed applicable to all other elements. This approach is considered realistic for elements such as caesium and strontium which appear to migrate at a similar rate to plutonium, but for more mobile elements such as iodine [3.37] the approach is conservative. The transfer coefficients have been derived from experimental measurements of the migration of single deposits of plutonium in various soils [3.34 - 3.36] and are summarised in Table 3.13. The observed rates of migration show considerable variation with soil type and the transfer coefficients adopted are those which give the best overall fit. The precision of the fit is indicated in Table 3.14 where the predictions of the model are contrasted with the experimental measurements.

Observations of the migration of plutonium in soils have only been made for periods extending to about 30 years after the initial deposition. Any estimate of the rate of migration at greater times must therefore be speculative. From a review and extrapolation of the migration data for plutonium, strontium and caesium a judgement has been made that a half-life of 100 years can be taken as representative of the rate of removal of activity from the top 30cm of soil (or a half-life of 50 years for removal from the 15 - 30 cm zone in the undisturbed model). The speculative nature of this estimate must however be recognised. The transfer coefficients K_{11} and K_{44} in the well mixed and undisturbed soil models, respectively, are consistent with the above half-lives. The transfer coefficients given in Table 3.13 relate to the migration of a stable nuclide; radioactive decay, or ingrowth of daughter products, is incorporated separately into the model with additional transfer coefficients from each of the compartments.

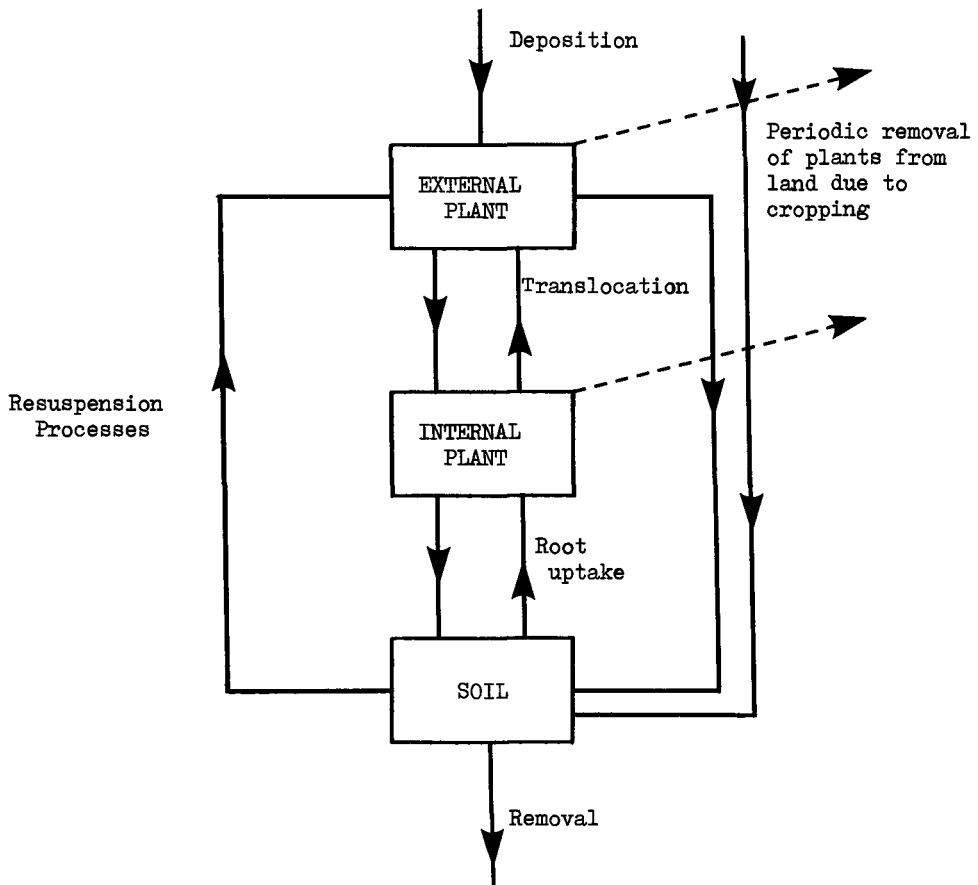
c) Application of the models

The two modules developed to describe the migration of radionuclides in soil form integral parts of the models used to evaluate the transfer to plants, the transfer to animals and the external doses from deposited activity. The time dependence of each of these quantities is determined largely by the rate of migration (together with radioactive decay) in soil and this is illustrated in subsequent sections. Some illustrative results of the rate of migration are given in Figure 3.7 where the cumulative percentage of the initial deposit is plotted as a function of depth at selected times after deposition. Results are given for the migration of two nuclides, plutonium-239 and caesium-137 with half-lives of $2.44 \cdot 10^4$ and $3.01 \cdot 10^1$ years respectively; the influence of radioactive half-life is clearly indicated.

3.3.3.3 Transfer of radionuclides to plants

The main features of the model developed to describe the transfer of radionuclides to plants are illustrated schematically below.

Diagram 3.5 Schematic representation of model for transfer of radionuclides to plants



The compartment marked "soil" represents the model for migration in soil appropriate to the plant species and agricultural conditions considered. All plants consumed directly by man are assumed in this study to be derived from land that is frequently cultivated and the migration model for well-mixed soil is most appropriate in these circumstances. Grass, however, is assumed to be produced only on undisturbed pasture in which case the migration model for undisturbed soil is applicable. Both internal and external compartments are considered for plants; transfer to the external plant surfaces may occur by interception of depositing activity or by resuspension of activity from soil; transfer to the internal plant occurs by root uptake and translocation from the external surfaces. Each process is considered in turn.

(a) Interception and retention of deposited radionuclides

The interception and retention of radionuclides on external plant surfaces varies according to the physico-chemical form of the deposit, the nature of the vegetation and the conditions prevailing both during and after the deposition process. Considerable variation has been observed in measured values of interception factors and removal rates of activity from plant surfaces; $\sqrt{3.38 - 3.40}$. Values of these parameters intermediate in their respective ranges are adopted in this study and are assumed equally applicable to all types of vegetation and radionuclides considered (with the exception of the noble gases). An interception factor of 0.2 is assumed for plant surfaces and is a compromise value taking into account both wet and dry deposition from the atmosphere; the remaining fraction of the deposit, 0.8, is transferred directly to the soil surface. The removal of the contaminant from plant surfaces due to the actions of rain, wind and plant growth is assumed to occur with a half-life of 0.038 y (14 days) for pasture grass $\sqrt{3.38}$ and 0.082 y (30 days) for all other plants $\sqrt{3.39}$.

Much of the external contamination on plants when harvested will in general be removed before consumption of the edible parts by man, for example, washing in the case of leafy green vegetables, or by removal of the outer protective layers in the production of flour from grain. The quantity of the contaminant which is transferred to man will depend on individual preparation methods and on the extent to which the contaminant adheres to the surface of the vegetation. There are few data on this subject and it is assumed that 90% of the external contaminant is removed from all plants during preparation or processing before consumption by man. Some justification for this value for transfer of plutonium from the outside surfaces of grain to flour has been provided by the measurements of Aarkrog $\sqrt{3.41}$.

(b) Resuspension of activity from soil to external plant surfaces

The general processes of resuspension (see Section 3.3.2) will result in the transfer of activity from the soil to the external surfaces of plants. Considerable variation might be expected in the importance of this route of contamination with plant type, in particular with growing habits and method of preparation before consumption. Few data are available in this area however, and the same general approach is adopted for all surface crops.

The contamination of plant surfaces by resuspension is considered in two stages. The first concerns the resuspension of the contaminant in the period soon after deposition by wind driven processes. The second

involves the resuspension by a variety of processes, of soil particles with which the contaminant becomes associated within a few months (or years) of deposition. The first process is governed by the time dependent resuspension formula described in Section 3.3.2; various approximations have been made to facilitate the incorporation of this relationship into the model and the procedures adopted are described by Simmonds et al [3.31].

The transfer of contaminant to external plant surfaces by the second process can be determined readily from the quantities of soil typically associated with the edible parts of crops when harvested. The concentration of activity in the soil on plant surfaces is assumed to be the same as that in the well mixed top 30 cm layer; the sole exception is grass, which is assumed to be derived from undisturbed soil, and the approach adopted for it is discussed in Section 3.3.3.4(a). The quantities of soil contaminating various plant surfaces are uncertain and the relevant data are summarised below.

Measurements in the United Kingdom [3.42] have shown that a value of 0.01% is typical of the quantity of soil associated with the whole grain seed when expressed in terms of the dry weight of the latter; in exceptional circumstances it could be as much as 0.1%. For vegetables (including fruit) there is even greater uncertainty in assigning an average value to the amount of soil contamination on plant surfaces. There is considerable variation in the form of vegetables and this will have a marked influence on the degree of surface contamination; for example leguminous vegetables, such as peas, are protected by a pod, whereas leafy vegetables, such as lettuce, grow close to the ground and on occasions may be subject to significant contamination by soil. A value of 0.1% of the dry plant weight has been suggested [3.42] as an average amount of soil in leafy vegetables and this value has been conservatively adopted for all vegetables and fruit.

The assumptions outlined in Section 3.3.3.3(a) concerning the amount of surface contaminant removed by preparation methods before consumption are also adopted here, namely that 90% of the surface contaminant is removed in these processes.

(c) Root uptake

The absorption of elements from soil by plants varies considerably depending on soil type and climatic conditions. There is also significant variation with the nature of the plants (eg, root crops compared with grain crops) and the chemical form of the element has a major influence. However, with the exception of a few elements such as strontium and caesium, and to a lesser extent the transuranium elements these variations have not been investigated in detail. For these and a few other elements a distinction is made between the transfer coefficients between soil and the various plant species where data permit. For most elements the transfer coefficient between soil and plant for a particular element is assumed to be independent of plant type. In some cases the paucity of data is such that the transfer coefficients are chosen by analogy with other elements for which more appropriate data exist.

Data on root uptake tend to be in the form of concentration factors between plants and soil at the end of the growing period. Such data contain no information on the time dependence of the uptake mechanisms and as such cannot be rigorously applied in that context.

Their application to a model which is time dependent in character is valid only insofar as the variation in the concentration of the nuclide in the root zone is small during the growing period. For long-lived radionuclides this assumption is in general valid. Where it is not, the assumption is made in the model that the plant rapidly comes into equilibrium with the soil as determined by the concentration factor. Where the concentration of activity in soil varies rapidly with time the activity in plants will be determined largely by the concentration in soil just prior to harvesting. The derivation of transfer coefficients, which are used in the model, from concentration factors is described by Simmonds et al [3.31]; while these coefficients represent the rate of transfer from soil to plant and vice versa the time dependence is an artefact. The coefficients are chosen solely to ensure that the concentration factor between plant and soil is attained rapidly.

(d) Translocation from external surfaces

Translocation of contamination from the surfaces of leaves and stems to the internal tissues of plants is known to occur and to be an important mechanism for some elements. For plants with their edible parts above ground the fraction translocated appears to be small compared with the residual surface contamination for most elements, even after processing and preparation for consumption. It is, therefore, ignored for the majority of elements, except for technetium, tellurium, iodine and caesium where the fraction translocated is significant [3.43]; for these elements the fraction translocated is taken as 10% of the surface deposit [3.43]. For root vegetables, translocation is the only mechanism which transfers surface contamination on the above ground portion of the plant to the edible root; it is therefore included for most elements. The fraction translocated is typically in the range 1 to 10%. Translocation of the transuranium elements, molybdenum and chromium is small and is not considered.

In addition to the mechanisms described in (a) - (d) above, account is taken in the model of removal of activity from the system by harvesting of crops; a growing period of 0.274 y (100 days) is assumed before cropping. Account is also taken of radioactive decay, and the ingrowth of daughter products, where appropriate, in each compartment in the system.

(e) Summary of the data adopted to evaluate transfer to plants

The values adopted for the non-element dependent parameters used in the model are summarised in Table 3.15. Data are given for plant yields, interception factor and half-life of activity on plant surfaces, the level of soil contamination on plants after preparation for consumption, growing period before cropping and the depth of the root zone. The values adopted for the element dependent parameters, in particular concentration factors between soil and the respective plants and the translocated fractions, are summarised in Table 3.16.

Transfer coefficients, which are used in the model, have been derived from data in Tables 3.15 and 3.16 and are summarised in Appendix 3.3.

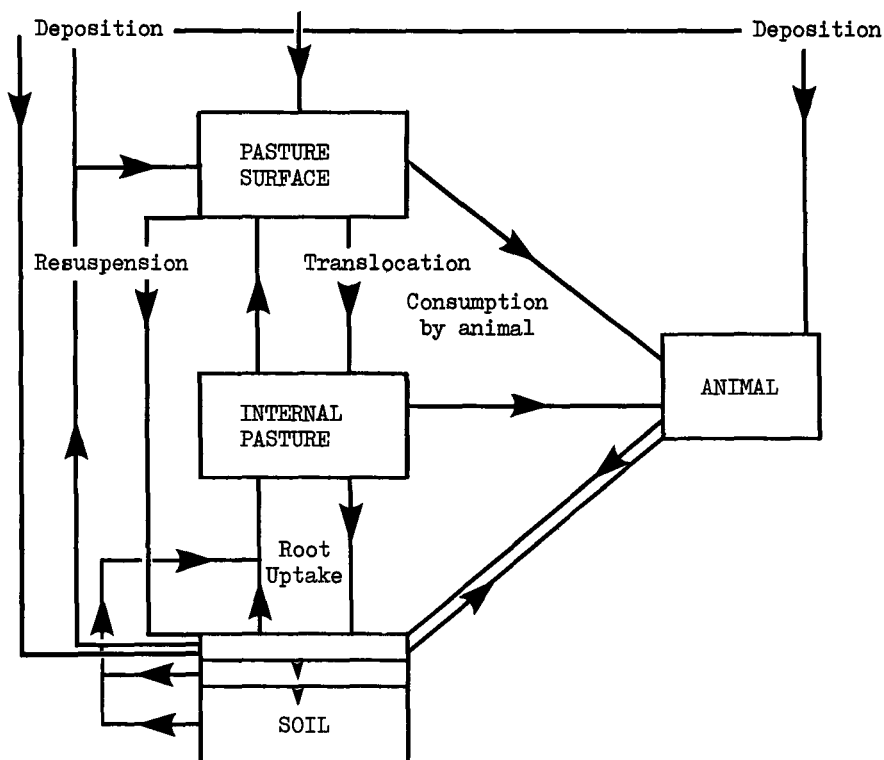
3.3.3.4 Transfer of radionuclides to animals

It is convenient to consider the transfer of radionuclides to animals in two stages; these comprise the intake of radionuclides into the animal by ingestion or inhalation and the subsequent metabolism of these radionuclides, in particular their transfer to animal tissues (and/or produce) consumed by man. The models developed to describe these transfer processes for grazing animals are described.

(a) Intake of radionuclides by grazing animals

The principal mechanisms involved in the transfer of radionuclides to grazing animals are illustrated schematically below.

Diagram 3.6 Schematic representation of the principal mechanisms for the transfer of radionuclides to grazing animals



The compartment marked "soil" corresponds to the model for undisturbed soil described in Section 3.3.3.2; grass is assumed to be derived solely from undisturbed pasture in this study. The two main routes of intake comprise ingestion and inhalation. Ingestion is by far the most important pathway for the intake of most radionuclides although inhalation may be significant for those radionuclides whose transfer across the gut of the animal is small.

The consumption of pasture grass is in general the most important mode of intake by ingestion. Three main processes contribute to the contamination of pasture grass : deposition, resuspension, root uptake.

Translocation is negligible by comparison. These processes are described in detail in the previous section where the values of the parameters required to estimate the transfer of radionuclides to grass are summarised. The inadvertent consumption of soil, together with grass, by grazing animals is a further pathway which must be considered; for nuclides which have a low transfer from soil to grass by root uptake the ingestion of soil may be the most important mode of intake. Typically the inadvertent consumption of soil is about 4% and 20% of dry matter intake for cattle and sheep respectively $\sqrt{3.51, 3.52}$; the potential significance of this pathway is evident. Resuspension of activity onto the surface of undisturbed pasture in the period shortly after deposition is governed by the time dependent resuspension formula described in Section 3.3.2; the approach is simplified by various approximations to facilitate its inclusion in the model $\sqrt{3.31}$.

In general two routes of intake must be considered for the inhalation of activity by animals; these comprise the inhalation of activity while the deposition onto pasture is taking place and the subsequent inhalation of resuspended activity. The former may not apply if the source of contamination is not deposition from the atmosphere or if, for example, the animal is introduced to the pasture after the deposition process has ceased. The intake of activity by inhalation while deposition is continuing can be readily evaluated from the breathing rate of the animal and the time dependence of the air concentration. The procedures described in Section 3.2 to evaluate air concentrations of radionuclides and their inhalation by man are equally applicable to animals and are adopted for that purpose; reference should be made to Section 3.2 for further details and this aspect is not considered further here. As before, the inhalation of resuspended activity is evaluated by the use of simplifying approximations applied to the time dependent resuspension formula (Section 3.3.2); the approximations are described by Simmonds et al $\sqrt{3.31}$. The time dependent resuspension formula applies to wind driven resuspension from undisturbed pasture. The habits of grazing animals (in particular the proximity of their head to the ground and the disturbance of the ground during grazing) may result in enhanced but localised resuspended air concentrations and thus greater intakes by inhalation. Owing to the absence of data no account is taken of this additional resuspension mechanism; it must be recognised however that the inhalation by grazing animals of resuspended activity may consequently be underestimated.

The values adopted for the various parameters concerned with the transfer of radionuclides to grass are summarised in Tables 3.15 and 3.16 together with similar data for other plants. The values adopted for the non-element dependent parameters for grazing animals (eg, ingestion and inhalation rates, animal and organ weight, milk yields etc) are summarised in Table 3.17 and their choice is discussed in more detail by Simmonds et al $\sqrt{3.31}$. Consideration is limited to cattle and sheep. The average lifetime of cattle is taken to be six years; this is based on the average lifetime of dairy cattle. The average lifetime for beef cattle is considerably shorter and the assumption is recognised as being conservative for those long-lived radionuclides which build-up in animal tissue. Sheep are taken to have a mean lifetime of 1 year.

(b) Metabolism of inhaled and ingested radionuclides

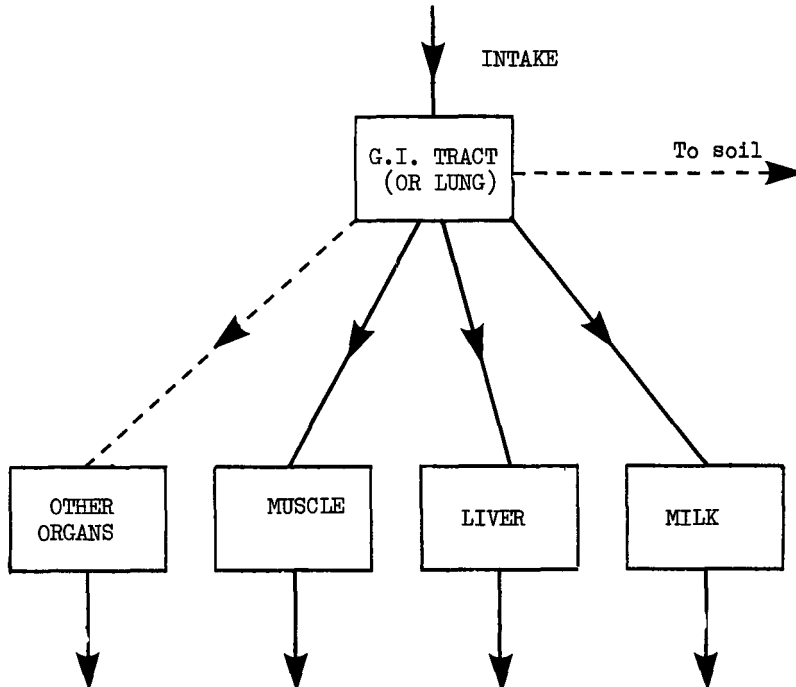
Radionuclides inhaled or ingested by grazing animals will be metabolised to varying extents depending upon the nuclide. Data on the metabolism of radionuclides in grazing animals are limited

and recourse is often made to data and models developed to represent metabolism in man. In many cases the latter are based on observations of metabolism in other, generally small, animals. The degree of complexity necessary in modelling the metabolism of a radionuclide in grazing animals depends on the nuclide and the circumstances considered. It is sufficient in general to limit consideration to the transfer of radionuclides to muscle, liver and milk which represent the main animal products consumed by man. For radionuclides whose biological half-lives in various organs are small compared with the animals' lifespan a relatively simple model can be adopted; it is sufficient to model the fractional transfer of ingested or inhaled activity to particular organs and the half-lives of the activity in those organs. For a few radionuclides, particularly those of the transuranium elements which have long biological half-lives in body organs, a more complex model is required if the metabolism is to be represented adequately. Recycling of activity between these organs and body fluids may continue to occur with particular implications for the time dependence of the transfer of activity to milk; in such cases both the transfer to and recycling of activity from these organs must be modelled. Models of both types are used in this study depending on the nature of the nuclide and availability of suitable data. The simpler model is used for all but the transuranium elements and both models are described in the following.

Simpler metabolic model

The model used to determine the metabolism of all nuclides other than those of the transuranium elements is illustrated schematically below.

Diagram 3.7 Schematic representation of the simpler metabolic model



The derivation of transfer coefficients is described by Simmonds et al [3.31] and is only briefly considered here. Most data are for cattle and are in the form of the fraction of the daily intake (assumed continuous) ingested appearing in unit mass of meat or milk. The origin and reliability of the data is variable; for example some data are based on experiments with cattle whereas others are extrapolations from experiments with other animals or even derived by analogy with the metabolism of other elements. For a comprehensive compilation of the available data reference should be made to [3.43, 3.53, 3.54]. The data adopted in this study are summarised in Table 3.18; the fraction of the daily intake (assumed continuous) of stable elements appearing in unit mass of meat and milk are given together with the biological half-life in animal muscle. These data can be used to derive the transfer coefficients for use in the model. Similar data are given in Table 3.18 for transfer to liver and are derived from data recommended for man [3.55] assuming the fractional transfer from body fluids to liver is the same in cattle as in man. For those elements where no data are available for transfer to liver the concentration and half-life of activity in liver are taken to be equal to those in muscle, although it is recognised that an alternative approach would be to make use of the physiological similarity between elements.

Few data are available on the fractional transfer of inhaled activity to the body organs of grazing animals. The values used in this study have been derived from metabolic data recommended for man [3.55]. The fraction of the daily intake by inhalation appearing in a particular organ or milk, from a grazing animal, $F(\text{inh})_c$ is obtained as

$$F(\text{inh})_c = \frac{f(\text{inh})_M}{f(\text{ing})_M} F(\text{ing})_c \dots\dots\dots(3.36)$$

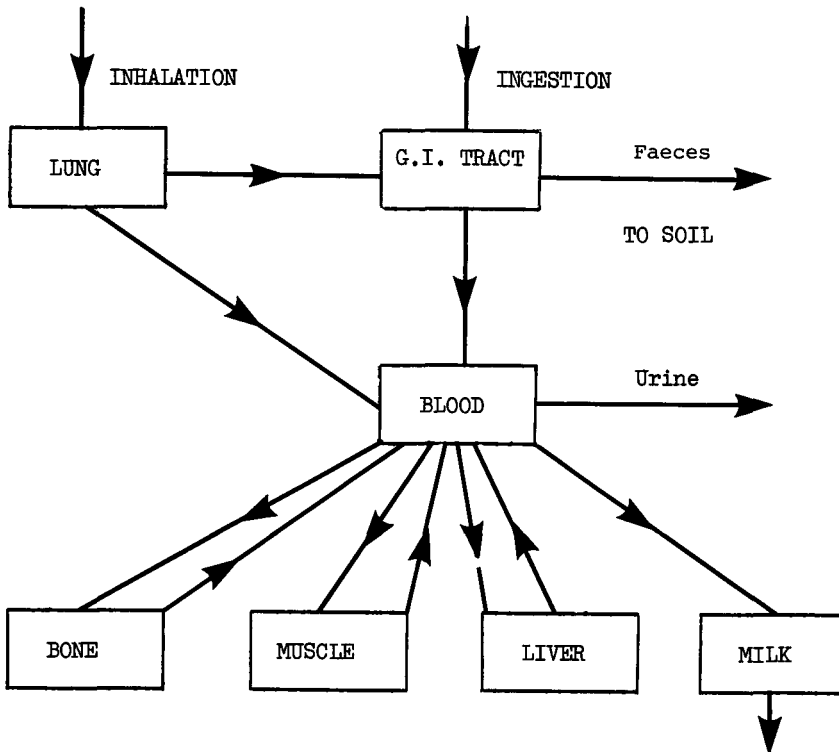
- where $f(\text{inh})_M$ is the fraction of inhaled activity reaching body fluids in man
- $f(\text{ing})_M$ is the fraction of ingested activity reaching body fluids in man
- $F(\text{ing})_c$ is the fraction of the daily intake appearing in the organ of or milk from cattle (see Table 3.18).

The fractions of ingested or inhaled activity reaching body fluids in man depends on the physico-chemical form of the element considered. Each element is assumed to be in the oxide form and when inhaled to be in the form of a 1µm AMAD aerosol. It is further assumed that the transfer of activity across the lung occurs instantaneously; in reality, depending on the compound inhaled, the time constant for transfer may be days, weeks or years. This assumption will overestimate the transfer across the lung of cattle particularly for radionuclides with radioactive half-lives short compared to the time constant for transfer across the lung. The assumption is however conservative and considered justified bearing in mind the many other uncertainties in the data used in the model. The fractions of the daily intake by inhalation appearing in unit mass of particular organs and milk of cattle derived from equation (3.36) are summarised in Table 3.18; similar data can be obtained for the fractions transferred to sheep from the procedure specified in that table.

More complex metabolic model

The model used to describe the metabolism of the transuranium elements in grazing animals is illustrated schematically below.

Diagram 3.8 Schematic representation of the more complex metabolic model



Account is taken of the transfer of material to various organs and of the recycling of activity between these organs and body fluids. Bone is included as an organ because of its importance as a source of recycled material.

The transfer of radionuclides from lung and the GI tract of the animal is based, with simplification where appropriate, on the models recommended by ICRP for man; these models are described in detail in Chapter 6 and their modification and simplification for application to grazing animals is discussed by Simmonds et al [3.31]. The time constants and the fraction of each radionuclide transferred from the animal lung and GI tract are based on data given for man in Chapter 6 assuming each radionuclide to be in the oxide form and as a 1 μ m AMAD aerosol when inhaled.

The distribution of plutonium among the various organs in cows has recently been measured by Stanley et al [3.56]. These data have been used to derive transfer coefficients appropriate to the above model; the derivation of these coefficients is described by Linsley et al [3.48]. These transfer coefficients, in the absence of further data, are assumed to be equally valid for the radionuclides of americium, curium

and neptunium. The transfer coefficients derived for cows are also assumed applicable to sheep.

The transfer coefficients used in the models to describe the intake of radionuclides into animals and to evaluate their subsequent metabolism are summarised in Appendix 3.3.

3.3.3.5 Application of the foodchain models and a summary of selected results

The foodchain models have been applied to evaluate the time dependence of the transfer of activity to foodstuffs following the continuous deposition of activity on land for a year at a rate of $1 \text{ Bq m}^{-2} \text{ s}^{-1}$. A matrix of results has been generated which contains the time integral of each nuclide per unit mass of food derived from such land. This matrix (when combined with the spatial distributions of agricultural yields and deposition rates of radionuclides) forms the basis of estimates of the time dependent transfer of activity to man via terrestrial foodstuffs following the release of activity to atmosphere. Some selected results are presented and features of interest noted. Separate consideration is given to transfer to plants and animal produce.

(a) Transfer to plants

Results are given in Table 3.19 for the transfer of six radionuclides to plants. The results are expressed in terms of the time integrals of activity per unit mass of plant (Bq y kg^{-1}) to 1, 50, 100 and 500 years after the deposition commenced and to infinity.

For surface plants, (green vegetables and grain) a large fraction of the integrated activity is accumulated in the first year primarily as a result of deposition of activity onto plant surfaces. Only in the case of strontium-90 does the time integral of activity increase significantly in subsequent years; this is due to the relatively high rate of root absorption of strontium from soils. For the short-lived iodine-131 ($t_{1/2} = 0.022\text{y}$) there is, as expected, no further contribution after the first year when the deposition has ceased.

In root crops, the time integrals of activity continue to increase while activity remains in the root zone. The only mechanism of importance for transfer of activity to root crops is absorption from the soil; absorption continues until activity is removed either by migration out of the root zone or by radioactive decay. For most nuclides considered in Table 3.19 the time integral of activity per unit mass of root crops at long times is less than that in surface plants by an order of magnitude or more; iodine-129 and strontium-90 are exceptions, and at long times their time integrals of activity in root crops approach those in grain.

The relative importance and time dependence of the important transfer mechanisms for plutonium-239 and strontium-90 to surface plants is illustrated in Figures 3.8 and 3.9 respectively.

The important mechanisms comprise surface contamination from direct deposition, initial resuspension before the surface layer of contaminant becomes uniformly mixed with soil during cultivation, the subsequent resuspension of surface soil and absorption by root uptake. Initial resuspension is due to the action of wind during the time that the surface deposit of the contaminant is present as a thin layer. The layer is assumed to be removed by annual or more frequent cultivation and

subsequently only resuspension due to contaminated soil particles is considered.

Plutonium-239, is poorly absorbed from soil into plants and the direct deposition of activity makes by far the greatest contribution to the time integrals of activity in surface plants. Root uptake and resuspension of soil continue to contribute to the time integrals of activity for extended periods until the activity has migrated from the root zone. Considerable uncertainty is associated with the half-life assumed of 100 years for the migration of activity from the root zone. The total transfer of plutonium-239 to surface plant is however determined by mechanisms independent of this parameter and the results are therefore relatively insensitive to its assumed value. If consideration were restricted to crops growing on previously contaminated soils the uncertainty in the rate of migration in soil would then be important.

The rate of absorption of strontium-90 by plant roots is some four orders of magnitude greater than for plutonium-239 and this difference is evident in Figures 3.8 and 3.9. Root uptake is particularly enhanced relative to the other transfer mechanisms in green vegetables and as a result, the time integral of activity by this route exceeds that due to direct deposition on surfaces within one or two years of deposition ceasing. The contribution of root uptake to the time integral continues for about 100 years, at which time the contribution exceeds that due to direct deposition by more than an order of magnitude in the case of green vegetables. The decline in root uptake of strontium-90 with time is predominantly due to its radioactive decay in soil. Thus, the transfer of strontium-90 to surface plant is not particularly sensitive to the uncertainty in rate of migration out of the root zone. The rate of root absorption of strontium-90 is much lower for grain than for green vegetables and contamination by direct deposition is the main contributor to the time integral of activity in grain.

Most radionuclides considered in this assessment fall between the extremes represented by plutonium-239 and strontium-90 in terms of the relative importance of root absorption. Technetium and tellurium are exceptions having root absorption rates which have been variously reported as being more than an order of magnitude greater than for strontium. The nuclides of tellurium being considered have very short half-lives (less than 1 day) and will therefore be unimportant as contaminants in food crops. Technetium-99 has an extremely long radioactive half-life (2.1×10^5 years) and the time integral of activity in food crops is quickly dominated by root uptake. For long-lived radionuclides such as technetium-99 (and iodine-129, $t_{1/2} = 1.7 \times 10^7$ years) with significant root absorption rates, the assumed rate of migration of activity from surface soil will clearly have an impact on the time integral of activity at long times. However, for most of the radionuclides considered the major contribution to the time integral of activity in surface plants is the direct deposition on plant surfaces.

(b) Transfer to animal products

The time integrals of activity in meat, liver and milk derived from cows grazing pasture on which activity is deposited continuously at a rate of $1 \text{ Bq m}^{-2} \text{ s}^{-1}$ for one year are given in Table 3.20 for selected nuclides. Similar results are given for sheep in Table 3.21; while the absolute values of the respective results differ they both exhibit the same general characteristics. No account is taken in the time integrals given in Table 3.20 and 3.21 of the inhalation of activity

by the animals while it is being deposited onto pasture; this aspect is given separate consideration later. The most notable feature in Tables 3.20 and 3.21 is that by far the majority of activity is transferred to the various food products within about 50 y of the initial deposition with little further transfer later. For short-lived nuclides the transfer is essentially complete within a short time of the deposition process terminating (eg, see iodine-131). The temporal variation of the time integral of activity differs between nuclides; this is a consequence of the varying relative importance of the different processes (each with its own characteristic time constant) which contribute to the transfer of activity to the animal.

The time dependence and relative importance of the various transfer processes are illustrated in Figures 3.10 and 3.11 for the transfer of plutonium-239 and strontium-90, respectively, to cow meat. The transfer to other products would exhibit similar characteristics. Consideration is given to transfer by consumption of pasture grass contaminated by direct deposition, resuspension and root uptake, by the inadvertent consumption of soil; and the inhalation of resuspended activity.

For plutonium-239 the greatest contributor to the time integral of activity transferred to meat is predicted to be inhalation of resuspended activity. The transfer by ingestion is much smaller with transfer by root uptake into grass being negligible compared with the other processes. This prediction of the relative importance of ingestion compared with inhalation of resuspended activity should however be treated cautiously; for example there is considerable uncertainty in the model used to evaluate the inhalation of resuspended activity by the cow (see Section 3.3.3.4) and the gut transfer fraction for plutonium varies significantly with its form when ingested.

The transfers of strontium from soil to grass and across the animal gut to blood are both several orders of magnitude greater than the corresponding transfers for plutonium. This is clearly reflected in Figure 3.11 where the ingestion pathways, and particularly root uptake into grass, make by far the greatest contribution to strontium in animal products. In contrast with plutonium-239 the inhalation of resuspended strontium-90 makes an insignificant contribution. This is likely to be so for most nuclides; the exceptions will be those which, like plutonium-239, have very low transfers from soil to grass and across the animal gut.

The time dependence of the transfer of strontium-90 to meat varies according to the transfer process. The transfer by direct deposition on grass is essentially complete once the deposition ceases owing to the relatively short biological half-life of strontium in muscle. In reality there would be a continuing transfer from remobilisation of strontium deposited with a long half-life in animal bone; this process is however not taken into account in the relatively simple metabolic model adopted for strontium-90 in the cow. The transfers by soil consumption and deposition of resuspended activity cease to contribute significantly after about 10 years. Both these mechanisms involve the transfer of activity from the top 1 cm of soil and it is the migration of activity out of this layer which determines the time dependence of these processes. Root uptake, on the other hand, is assumed to occur from the top 15 cm of soil and it therefore continues to contribute for a longer period. The time constant of transfer by root uptake is determined by a combination of the migration from the top 15 cm of soil and the radioactive half-life of strontium-90 of 28.1 years. Moreover this time constant characterises the overall

transfer of strontium owing to the dominant contribution from root uptake.

Similar considerations apply to the time dependence of the individual processes contributing to the transfer of plutonium-239. In general, however, all the processes exhibit longer time constants than for the transfer of strontium-90. This factor has two origins. The first is an artefact and is connected with the computational procedure adopted to represent the periodic slaughter of animals; for mathematical convenience this is represented by an exponential loss with the result that the time dependence of the transfer is somewhat slower than in reality; the absolute transfer however is correctly evaluated. The second is a real effect and arises from the long half-life of plutonium in liver (and bone) and the adoption of a more elaborate metabolic model (see Section 3.3.3.4) which takes account of the remobilisation of plutonium from these organs. Thus plutonium may appear in meat or liver some considerable time after its intake by the animal.

The inhalation by animals of activity as it is being deposited on pasture represents a further route which may be significant for some radionuclides particularly those which have a low transfer in the terrestrial environment and across the animal gut. The time integrals (infinite) of activity in various animals products from inhalation of selected nuclides are given in Table 3.22.

An indication of the potential significance of this route is given in Figures 3.10 and 3.11 where the contribution from inhalation of the activity while it is being deposited is contrasted with subsequent transfer from the contaminated land. The air concentration and hence the quantity of activity inhaled during the deposition process is determined by the conditions pertaining during the deposition; for the purposes of the comparison it is assumed that dry deposition, with a deposition velocity of $5 \cdot 10^{-3} \text{ m s}^{-1}$, is the sole contributor. Subject to this assumption the inhalation by the cow of plutonium-239 while it is being deposited is more important than its subsequent uptake after deposition on pasture. For strontium-90 however inhalation is not significant. The ratio of the contribution from inhalation of plutonium to that from its subsequent uptake after deposition will vary according to the deposition processes assumed; for example the ratio would increase if a lower deposition velocity were assumed but would decrease if wet deposition were considered. While considerable variation might be encountered in the relative importance of the inhalation route it is clear that it is potentially very important. For nuclides with characteristics in the terrestrial environment similar to those of plutonium it is essential that account is taken of this route.

3.3.3.6 The transfer of tritium and carbon-14 in the terrestrial environment

The transfer of tritium and carbon-14 between the atmosphere and the terrestrial environment is somewhat more complex than that described and modelled for other nuclides in previous sections. This additional complexity is primarily a consequence of the fundamental roles played by hydrogen and carbon in biological systems. The models described earlier are not appropriate for tritium and carbon-14 and a relatively simple, but conservative, specific activity approach is adopted to evaluate the transfer through the terrestrial environment to man.

It is assumed that the terrestrial environment and man come into rapid equilibrium with the carbon-14 in the atmosphere and that the specific activity of carbon taken in by man by inhalation or ingestion is equal to that in the atmosphere at the point of interest. For a release of carbon-14 to atmosphere the specific activity will be determined by the degree of atmospheric dispersion (see Section 3.2) and the carbon concentration in the atmosphere; the latter is taken as 0.15 g m^{-3} . A similar assumption is made for tritium and the specific activity of tritium taken into the body is taken as equal to that in atmospheric water vapour at the point of interest; the specific activity in the atmospheric water vapour is again determined by the degree of atmospheric dispersion and the concentration of water vapour in the atmosphere taken as 8 g m^{-3} (annual average value). The intake of carbon-14 and tritium in man by inhalation and ingestion can be determined from the respective intakes of carbon and water (see Section 5.3) by the various routes; the dose equivalent in man can then be determined from these intakes from the committed dose equivalents per unit intake given in Chapter 6.

The use of a specific activity approach for these nuclides must be qualified in two respects. The first, and perhaps most important, is that the doses evaluated will be overestimated. The second concerns the absence of information on the temporal distribution of the dose which in reality may be delivered over an extended period. It is implicit in the model however that the dose is only delivered while the specific activity, and thus discharge is maintained.

3.3.4 External irradiation due to surface deposition

The external irradiation to which man is subjected from surface deposition has been evaluated, for atmospheric releases, for an undisturbed soil into which penetration of the activity occurs by natural processes. The external irradiation due to the contamination in the top 30 cm of soil has been calculated for the photons and electrons emitted by the appropriate radionuclides. External irradiation due to the contamination in deeper soil (below 30 cm) has been neglected; it is almost zero for electrons and very small for photons compared with the external irradiation due to contamination in the upper layer (the top 30 cm).

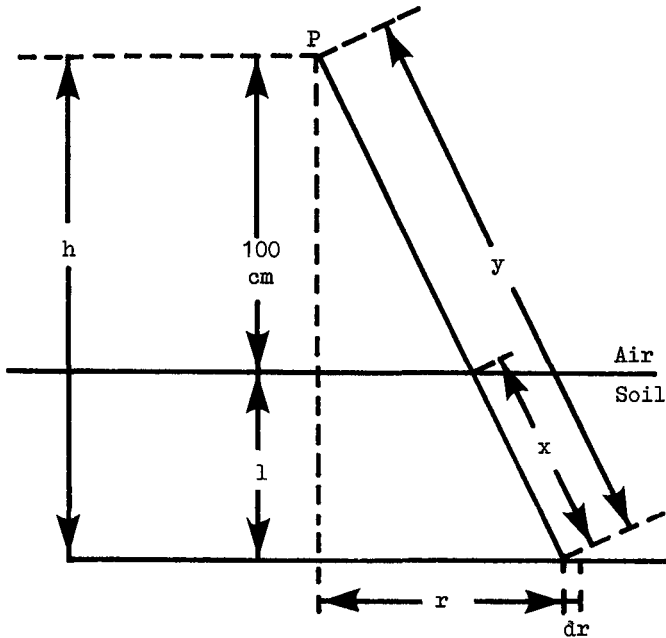
3.3.4.1 External irradiation due to photons

The relationship between land contamination and the absorbed dose in air at a metre above a layer of soil has been calculated by means of the following formula which takes account of the build-up in soil but neglects the mechanism in air.

$$\dot{dD}(r,l,E) = P C_A \frac{2\pi r dr}{4 \pi Y^2} E B_E e^{-\mu x} \left(\frac{\mu_a}{\rho} \right)_{\text{air}} \dots\dots\dots(3.37)$$

in which $\dot{dD}(r,l,E)$ is the component of dose in Gray per year corresponding to photons of energy E from an annular source between r and r + dr at a depth of l in the soil (see Diagram 3.9).

Diagram 3.9 Schematic diagram for calculation of external irradiation due to activity deposited on ground.



P is a constant

C_A is the number of photons of initial energy E, in MeV, emitted per second per m^2 of surface and per cm depth of soil in the layer considered.

x, y, and h are the lengths, in cm, indicated in the diagram.

μ , in m^{-1} is the linear attenuation coefficient for the photons of energy E in soil.

$\left(\frac{\mu_a}{\rho}\right)_{air}$ is the mass energy absorption coefficient in air, in $m^2 kg^{-1}$, for photons of energy E..

B_E is the build-up factor in soil.

It has been expressed in the form:

$$B_E = \sum_{n=1}^2 A_n e^{-\alpha_n \mu x}$$

.....(3.38)

in which $A_2 = 1 - A_1$ and A_1 , α_1 and α_2 have been obtained from the results of Beck and de Planque (3.57).

It can be shown, for contamination at depth l which is uniform over the horizontal plane that the dose at one metre above the surface is

$$\dot{D}(l, E) = P\left(\frac{\mu_a}{\rho}\right)_{\text{air}} C_A E \sum_{n=1}^2 A_n \left[-E_1(-\mu l(1 + \alpha_n)) \right] \dots\dots\dots(3.39)$$

where E_1 is the first order integral function,

$$E_1(b) = -\int_{-t}^{\infty} \frac{e^{-t}}{t} dt$$

The absorbed dose in air for a given energy E and a specified profile is calculated for each millimetre in the top 10 centimetres and for each centimetre between 10 and 30 centimetres depth.

For a particular energy E, the dose equivalents in the various organs of interest and the effective dose equivalent are then calculated by means of the conversion factors in Table 3.2. These conversion factors which have been evaluated in the case of exposure to a semi-infinite cloud, strictly do not apply to the present problem, but have been used because of the similarity of the geometries and in the absence of better data.

Finally, the dose equivalents corresponding to a given profile and radionuclide are obtained by summation over the various γ and X-ray energies for the radionuclide. In Table 3.23 the results are presented in the form of time integrals for several time periods and for the radionuclides considered in the terrestrial models.

3.3.4.2 External irradiation due to electrons

The absorbed dose in air due to electrons has been evaluated using the same general approach as for photons but because of the much greater absorption of electrons in soil, air and tissue several modifications have to be introduced:

- the absorbed dose in air, which is very variable between 0 and 2 m above the soil, has been calculated at increasing heights in steps of 10 cm;
- the attenuation of the electrons in air has been taken into account;
- the build-up factor in soil is not used.

For a given energy E, the absorbed dose in air is taken to be equal to the average of the results obtained for the heights between 0 and 170 cm.

The dose in the basal layer of skin is calculated taking account of the absorption of electrons in the 70 μm superficial layer.

After obtaining the dose in skin due to a given radionuclide, it is necessary to add the contributions of the different energy components (β particles and conversion electrons) and their intensities.

Doses in organs and tissues other than the skin have been neglected since they are negligibly small owing to the attenuation of electrons in superficial tissues.

3.3.5 Application of the results to a particular site

It has been shown in Section 3.2.5 how, for a given release the annual average deposition rate may be evaluated at any location relative to the discharge point. The annual average deposition rate, $\omega(i,d,\theta)$ at a distance d and an angle θ from the release point takes into account the frequency that the wind blows in the direction θ and the distribution of atmospheric dispersion conditions. $\omega(i,d,\theta)$ corresponds to a release of $Q_0(i)$, $Bq\ s^{-1}$, of radionuclide i and is expressed in $Bq\ m^{-2}\ s^{-1}$. The value $\omega(i,d,\theta)$ serves as the basis of the calculation of doses received by man at (d,θ) from external irradiation and inhalation of resuspended activity following its deposition in soil. It also forms the basis of the quantity of activity appearing in foodstuffs contaminated as a results of the deposit at the location (d,θ) .

The estimation of dose in man requires, in addition, detailed knowledge of dietary habits. Each mode of exposure is considered in the following sections.

3.3.5.1 External irradiation from deposited activity

External irradiation is made up of photon and electron components.

(i) External irradiation by photons

The dose equivalent in the organ or tissue, m , integrated from the beginning of the deposition up to the time, t , resulting from external irradiation by the γ and X-radiation from the activity contained in the soil due to the deposit (i,d,θ) can be expressed in the form

$$HD_{\gamma}(i,d,\theta,m,t) = \omega(i,d,\theta) \left[F_{\gamma}(i,m,t) \right] \quad (Sv) \dots\dots\dots(3.40)$$

in which $F_{\gamma}(i,m,t)$ is the dose equivalent in the organ or tissue m , integrated up to time t , which is received by a person continuously exposed to the external γ and X-ray irradiation from radionuclide i deposited continuously at a rate of $1\ Bq\ m^{-2}\ s^{-1}$ for one year on undisturbed land. The evaluation of the matrix of $F_{\gamma}(i,m,t)$ is given in Section 3.3.4 and selected values are given in Table 3.2.3.

(ii) External irradiation due to electrons

In the same manner as for photons one obtains:

$$HD_{\beta}(i,d,\theta,t) = \omega(i,d,\theta) \left[F_{\beta}(i,t) \right] \quad (Sv) \dots\dots\dots(3.41)$$

where $HD_{\beta}(i,d,\theta,t)$ is the dose equivalent (Sv) in skin integrated from the beginning of the deposition to time t resulting from external β and e^{-} irradiation from activity contained in the soil due to the deposit $\omega(i,d,\theta)$.

$F_{\beta}(i,t)$ is the dose equivalent (Sv) in skin, integrated to time t , received by people continuously exposed to the external β and e^{-} irradiation from the continuous deposit of radionuclide i for one year at a rate of $1 \text{ Bq m}^{-2} \text{ s}^{-1}$ on undisturbed land. The evaluation of the matrix $F_{\beta}(i,t)$ is given in Section 3.3.4.2.

3.3.5.2 Inhalation of resuspended activity

Equation (3.34) gives the expression for the air concentration, integrated to time t , $I_R(i,t)$, Bq s m^{-3} resulting from resuspension of radionuclide i deposited at a rate of $1 \text{ Bq m}^{-2} \text{ s}^{-1}$ continuously for one year. This leads to the quantity inhaled, $IRS(i,d,\theta,t)$ integrated to time, t , at a point d and θ .

$$IRS(i,d,\theta,t) = \frac{1}{3.15 \times 10^7} \omega(i,d,\theta) I_R(i,t) B \quad (\text{Bq})$$

.....(3.42)

where $B = 8030 \text{ m}^3 \text{ y}^{-1}$ is the volume of air breathed by an adult in a year. The evaluation of the matrix $I_R(i,t)$ is given in Section 3.3.2.2 and selected results are shown in Figures 3.5 and 3.6.

The dose equivalent integrated to time t in the organ or tissue m is given by:

$$HRS(i,d,\theta,m,t) = H_{inh}(i,m) IRS(i,d,\theta,t) \quad (\text{Sv})$$

.....(3.43)

where $H_{inh}(i,m)$ is the committed dose equivalent in tissue m from the inhalation of 1 Bq of nuclide i .

3.3.5.3 Ingestion of contaminated foodstuffs

Irradiation via ingestion of contaminated foodstuffs, unlike that from external exposure and from inhalation of airborne activity, cannot in general be readily correlated with the level of environmental contamination local to the individual. This is a consequence of much of man's diet originating from areas far removed from his place of residence. Such a correlation can only be made if it is assumed that the individual obtains his total dietary intake from an area local to his residence. Dietary habits of this type are relatively rare and are relevant only in so far as the estimation of the exposure of extreme groups or individuals; this aspect is given further consideration in Chapter 7. In the most general case the exposure of an individual at (d,θ) from ingestion must be determined from the integral over the land area of the product of the quantity and level of contamination of each foodstuff he obtains from a particular location. The spatial distribution of the dietary intakes of the many individuals comprising the exposed population is in general not well known; it is not however necessary to determine this distribution in order to evaluate the exposure of the population as a whole. The latter can be determined from the quantity of food derived from an area of known contamination and the fraction of that food ingested by the population.

The quantity of radionuclide, i , entering the diet of the population from unit mass of foodstuff, k , harvested annually at (d, θ) to time, t , can be related to the deposition rate $\omega(i, d, \theta)$ by

$$\text{CCP}(i, d, \theta, k, t) = \omega(i, d, \theta) \text{CP}(i, k, t) \text{TD}(i, k) \quad (\text{Bq y kg}^{-1})$$

.....(3.44)

where $\text{CP}(i, k, t)$ is the time integrated concentration of nuclide, i , in foodstuff, k , following the deposition of nuclide, i , at a continuous rate of $1 \text{ Bq m}^{-2} \text{ s}^{-1}$ for 1 year

$\text{TD}(i, k)$ is a factor which takes account of radioactive decay during the delay between harvesting (or animal slaughter) and consumption

and where it is assumed that the total quantity of foodstuff harvested is consumed by the population of interest.

The evaluation of $\text{CP}(i, k, t)$ for a range of nuclides and foodstuffs of interest has been described previously.

The time integral of the collective dose equivalent rate in tissue, m , of the exposed population per unit mass of foodstuff, k , harvested annually can be determined as

$$\text{HCP}(i, d, \theta, k, t, m) = \text{CCP}(i, d, \theta, k, t) \text{H}_{\text{ing}}(i, m) \quad (\text{Sv kg}^{-1})$$

.....(3.45)

where $\text{H}_{\text{ing}}(i, m)$ is the committed dose equivalent in tissue, m , from ingestion of 1 Bq of nuclide, i (see Chapter 5). The committed dose equivalent is assumed equal to the average individual dose equivalent received following intakes of 1 Bq by a population of standard age distribution (see Chapter 2).

3.3.5.4 Estimation of collective dose equivalent commitments

When combined with the spatial distributions of the population and of agricultural production the dose equivalents at (d, θ) (or quantity of activity appearing in diet from unit mass of food derived from (d, θ)) can be used to evaluate the collective dose equivalent commitments in the respective tissues. The procedure adopted is discussed in detail in Chapter 7.

3.4 Representation of the distribution of population and agricultural production within the European Community*

Representations of the distribution of the population and of the agricultural production within the European Community are required for the

* This section has been prepared in conjunction with Mme A Garnier and Mlle A M Sauve. The representation of the population distribution within the countries of the Community is the subject of a research contract between Euratom and CEA [3.587].

evaluation of collective dose in the Community. The zone considered extends between the 36°N and the 62°N parallels and the 10°W and 20°E of Greenwich meridians. The area involved is from Sicily in the south to the Shetland Islands in the north and from the south west coast of Ireland in the west to the Italian coast off the Gulf of Taranto in the east.

A grid has been established, across Member States, consisting of a series of squares of equal area defined from a given origin. The basic data have been taken from national and European statistics. These data have been transformed for the purposes of this study to provide a consistent representation.

3.4.1 The characteristics of the grid

The grid is based on a network in which each "square" is represented by an equal area of 10^4 km^2 which is subdivided into a finer grid. The zone is divided into bands on either side of the Greenwich meridian (positive values to the east and negative values to the west). The spacing of the bands, 1.5° , corresponds approximately to a distance of 100 km on the 49° parallel and is easy to locate on a map with 0.5° subdivisions. On either side of the 49° parallel the distance between parallels has been calculated in such a way as to obtain equal areas which deform progressively from a true square: the distances between parallels vary from 92.2 to 127.3 km towards the north (positive co-ordinates) and from 90.6 to 74.2 km towards the south (negative co-ordinates). The extreme latitudes are $62^\circ 27'$ and $35^\circ 49'$. Table 3.24 gives details of the numerical values and Figure 3.13 represents the grid on a map.

A "square" on the largest grid is located by means of a double reference. Each of the indices is composed of a number of two digits preceded by a sign (positive signs being omitted). The first index represents the position of the "square" on the abscissa (longitude) and varies for the zone considered between -07 to -01 and 01 to 13. The second index locates the position on the ordinate (latitude) and varies between -17 to -01 and 01 to 13. The "square" (01, 01) is found just to the north of the 49^th parallel and just to the east of Greenwich. The "square" (-01, -01) is found just to the south of the 49^th parallel and to the west of Greenwich.

A grid one hundred times finer is obtained by linear interpolation. This is made easier by an intermediate transformation of the co-ordinates into the centesimal system (grads). Each side of the grid is divided into ten equal parts.

The location of a "square" on the finest grid is done by means of two indices each of three digits, positive or negative (the first index for the abscissa and the second for the ordinate). For each of these indices the first two digits refer to the location of the large "square" and the third digit, varying between 0 and 9, represents the subdivisions of this square. Figure 3.14 illustrates the method of locating squares on the grids.

3.4.2 Population grid

3.4.2.1 Population data

The population data are obtained from the national censuses within the Member States at dates ranging from 1970 to 1975 (1970 for Belgium, Denmark, and the Federal Republic of Germany; 1971 for Italy, Luxembourg,

the Netherlands and the United Kingdom; 1975 for France). The sources of data used are given in reference [3.587]. The method of presentation of the population data varies between countries. In the majority of cases the populations are given for each administrative unit in the country and the number of these units vary between 270 in Denmark to 36,000 in France. For certain countries, the data are given in the form of the population within the squares of a grid. For Great Britain the data are used for 10 km squares on the National Grid of Great Britain since it was not considered necessary in this study to achieve greater resolution. There are 2,675 squares with non-zero population. A similar system has been adopted for Ireland (914 squares). For Italy the data are in 1 km squares adapted for the study of specific sites.

3.4.2.2 Geographical Coordinates

The location of the centres of the administrative units must be given in geographical coordinates, because each country uses a different cartographic projection (Lambert belge, Gauss-Kruger, Gauss-Boya, Mercator) in order to minimise the deformation of the area represented. The reference axes and projection coefficients used are appropriate to the position and extent of the territory and vary from country to country; hence the only way to unify these data is to use geographical coordinates*. Table 3.25 shows the system of coordinates used by each country. In the final column the method of obtaining geographical coordinates is indicated and is explained in detail for each country in reference [3.587].

3.4.2.3 Derivation of the population grid

This consists of bringing together the two kinds of information (population and co-ordinates) and dividing them up according to the scheme adopted in this study. To do this several computer programs have been written [3.597]. These allow the census data and the geographical co-ordinates to be brought together and reordered by increasing co-ordinate on the reference axes. The population may then be put into grid squares, radial bands or sectors of a given circle. In particular they can be divided amongst the 100 km² areas on the European Grid defined above. The subroutine EDIGRI [3.597] allows the addition of results on the European Grid. Table 3.26 shows, by way of an example, the results obtained for square (7, 10) situated in Denmark. Figure 3.13 illustrates the average density of population in the European Community.

3.4.3 Agricultural Grid

For the purpose of this study, the agricultural data have been presented on a grid of squares of area 10⁴ km². European and national data have been transformed and grouped into categories suitable for the subsequent calculation of collective dose.

3.4.3.1 Data collection

The basic agricultural data have been supplied by the Institute for Economic Research, State University, Groningen on the relative yields of some products for each administrative division (county (department) or its equivalent for each country in the Community). This work was carried out under

* This data was prepared with the help of the French Geographical Institute.

contract with the CEC. Other information from Member States has been used in this study. From the available information the following have been used:

- data for the years 1971, 1972 and 1973 for France, Holland, Belgium, Luxembourg, United Kingdom and Denmark.
- data for the years 1971, 1972 and 1973 for Italy with the years 1966, 1967 and 1968 for livestock.
- data for the years 1971 and 1974 for West Germany.

From this information a mean value for the following quantities has been calculated:

- surface area for vegetable production (hectares)
- numbers of cattle
- numbers of milk cows
- numbers of sheep
- numbers of pigs
- wheat production (tonnes)
- barley production (tonnes)
- potato production (tonnes)

These data had to be supplemented by other production data for milk and milk products, meat and vegetables. These have been mainly obtained on a national level from EUROSTAT reports published by the statistics office of the European Community [3.61 - 3.63]. Some regional data (by county/department) have nevertheless been used either from the same EUROSTAT reports or from official documents of the appropriate Ministries of each member country [3.60, 3.64-3.69].

These additional data have been combined with the base data in the following manner:

- (1) for milk products, the production has been determined as a function of the effective number of milk cows (several corrections have been made, notably when the calculated milk collection in a region is greater than the actual production)
- (2) for meat production, the net production of meat and liver have been related proportionally to the numbers of cattle given in the data base (the production of sheep and goats have been grouped together)
- (3) the production of
 - green vegetables (edible cabbage and other leafy vegetables)
 - leguminous vegetables (vegetables grown for their fruit and pods)

- root vegetables (root bulbs and tubers other than potatoes) has been evaluated using national statistics by assuming that the national production is distributed uniformly according to the surface areas used for vegetable production in each county or department*.

3.4.3.2 Results

Table 3.27 gives the results obtained by the process of data collection and transformation described above for a square of the agricultural grid. The data utilised in the terrestrial model are obtained by regrouping the data from the grid in the following way:

- (1) milk products are divided into two categories according to the delay between production, transformation and actual consumption:
 - delay less than or equal to a month (milk for consumption, sour cream, fresh cheese**)
 - delay greater than a month*** -(cheese, powdered milk, evaporated milk)

In this scheme the milk converted to cream and butter is not included because of the small transfer of radionuclides to fatty materials.

- (2) the meat products are grouped together as meat and liver from cattle and calves in the first group and from sheep and goats for the second
- (3) the vegetable products are grouped together as follows:
 - cereals, wheat and barley
 - green vegetables (leafy and leguminous)
 - root vegetables (potatoes are listed separately).

Figures 3.15 to 3.17 give examples of the variations in production for fresh milk, potatoes and wheat in the countries of the Community.

3.4.3.3 Discussion and commentary

The grid for agricultural production presented in this study can only be a very theoretical estimation of the existing level of production in each square of the grid. In no case could the data obtained here replace the results of a properly conceived economic study.

* for Ireland the data base does not give the surface area for vegetable production and so the national production has been divided equally between the counties.

** See later discussion of milk for consumption.

*** To a first approximation this delay can be considered to be greater than three months.

It is necessary to consider the seasonal influence on certain productions. This is particularly true for milk collection which could vary by 35% between the amount collected in November and that in May.

For milk production the milk for consumption includes milk straight from the cow, pasteurised, UHT milk and sterilised milk. For UHT milk the national consumption figures are:

Country	UHT milk consumption as a % of the total consumption
Belgium	4%
France	10%
West Germany	27%
Italy	43%

It is not possible to break this information down to local level. While consumption of UHT milk is generally greater in towns it is clear from the above data that it also varies with national and local habits.

3.4.4 Transformation of the results

In order to evaluate the collective doses received by the countries of the European Community, the results for population and agricultural production have to be combined with model predictions of airborne contamination and the resulting contamination of agricultural produce. The contamination is calculated as a function of distance from the site, ie, for atmospheric discharges in a series of sectors of a circle centred on the point of discharge, while the population and agricultural production data are contained in squares whose position is totally independent of the point of discharge. It is, therefore necessary to transform these data so that the distribution of population and agricultural production is obtained for sectors and elements of a circle centred on the different sites. A computer program has been written to do this. The method is described in Appendix 3.4 and in greater detail in reference [3.70].

The values for radii of circles are given in Table 3.28. There are 21 altogether to give an acceptable precision for the evaluation of collective doses. The width of the angular sectors are 20° and 30°, depending upon the site chosen.

Figure 3.18 and Table 3.29 show examples of results.

REFERENCES

- [3.1] Sutton, O G, The theory of Eddy diffusion in the atmosphere. Proc. R. Soc. (London) Ser. A, 135, 143 (1932).
- [3.2] Smith, F B, The application of field experiment data to the parameterisation of dispersion of plumes from ground-level and elevated sources. IN Proc. IMA Symposium on Mathematical Modelling of Turbulent Diffusion in the Environment, Liverpool, September 1978. (To be published).
- [3.3] Maul, P R, The mathematical modelling of the meso-scale transport of gaseous pollutants. Atmos. Environ., 11, 1191 (1977).
- [3.4] Scriven, R A and Fisher, B E A, The long range transport of airborne material and its removal by deposition and washout - II. The effect of turbulent diffusion. Atmos. Environ. 9, 59 (1975).
- [3.5] Islitzer, N F and Slade, D H, Diffusion and transport experiments, IN Meteorology and Atomic Energy, (Slade D H, ed). US Atomic Energy Commission, TID 24190 (1968).
- [3.6] Pasquill, F, Atmospheric dispersion. London, Van Nostrand (1962). (Revised edition, Chichester, Ellis Horwood (1974)).
- [3.7] Elliot, W P, A discussion of the Calder-Deacon equation for diffusion from a continuous point source. US Air Force Report AFCRC-TN-60-298 (1960).
- [3.8] ApSimon, H M and Goddard, A J H, Modelling the atmospheric dispersal of radioactive pollutants beyond the first few hours of travel, IN Proc. 7th International Technical Meeting on Air Pollution Modelling and Its Application, Airlie, Va., September 1976.
- [3.9] Desprès, A and Le Grand, J, Une méthode d'évaluation des transferts atmosphériques à longue distance. IN Proc. Seminar on La Dispersion en Milieu Physique Naturel, Cadarache, March 1978.
- [3.10] Bryant, P M, Methods of estimation of the dispersion of windborne material and data to assist in their application. Harwell, UKAEA, AHSB(RP)R42 (1964).
- [3.11] Jones, J A, ESCLOUD. A computer program to calculate the air concentration, deposition rate and external dose rate from a continuous discharge of radioactive material to atmosphere. Harwell, National Radiological Protection Board. (To be published).
- [3.12] Chilton, A B, Broad beam attenuation. IN Engineering Compendium on Radiation Shielding, 1, Shielding Fundamentals and Methods, section 4.5.1. (Jaeger, R G et al, eds.), New York, Springer Verlag (1968).
- [3.13] Handbook of Radiological Protection, Part I, Data. Panel of the Radioactive Substances Advisory Committee, (1971), (London, HMSO).

- 3.14] Poston, J W and Snyder, W S, A model for exposure to a semi-infinite cloud of a photon emitter, *Health Phys.*, 26, 287 (1974).
- 3.15] ICRP, Recommendations of the International Commission on Radiological Protection. Oxford, Pergamon Press, ICRP Publication 26. *Ann. ICRP*, 1, no. 3 (1977).
- 3.16] Nichols, A L, The UK Chemical Nuclear Data Committee File: A Summary of the primary data available in ENDF/B format. Harwell, UKAEA AERE-R8904 (1977).
- 3.17] Nair, S and Henning, M J, A user's guide to the reactor inventory code RICE. Berkeley, Glos., CEEGB Report RD/B/N4079 (1978).
- 3.18] Grandin, M, Lalande, R, Lorenzi, P, Bouville, A, Desprès, A, Guezengar, J M et Le Grand, J. Irradiation externe pendant et après le passage d'un nuage radioactif. Rapport CEA-R-4844 (1977).
- 3.19] Nichols, A L, Radioactive-nuclide decay data for reactor calculations: activation products and related isotopes. Harwell, UKAEA AERE-R8903 (1977).
- 3.20] Gifford, F A, Turbulent diffusion-typing schemes: a review. *Nucl. Saf.*, 17, no.1, (1976).
- 3.21] Pasquill, F, The estimation of the dispersion of windborne material, *Met. Mag.*, 90, 33 (1961).
- 3.22] Doury, A, Une méthode de calcul pratique et générale pour la prévision numérique des pollutions véhiculées par l'atmosphère, Rapport CEA-R-4280 (rev. 1) (1976).
- 3.23] Smith, F B, A scheme for estimating the vertical dispersion from a source near ground level. IN Proc. 3rd Meeting of the Expert Panel on Air Pollution Modelling, Paris, October 1972. Brussels, NATO CCMS, chap. XVII (1972).
- 3.24] Hosker, R P, Estimation of dry deposition and plume depletion over forest and grassland. IN Proc. IAEA/WHO Symposium on Physical Behaviour of Radioactive Contaminants in the Atmosphere, Vienna, 1974. Vienna, IAEA, p. 291 (1975).
- 3.25] Slinn, W G N, Parameterizations for resuspension and for wet and dry deposition of particles and gases for use in radiation dose calculations. *Nucl. Saf.*, 19, no.2 (1978).
- 3.26] Hoffman, F O, A reassessment of the deposition velocity in the prediction of the environmental transport of radioiodine from air to milk. *Health Phys.*, 32, 437 (1977).
- 3.27] ICRP, Report of the Task Group on Reference Man. Oxford, Pergamon Press, ICRP Publication 23 (1975).
- 3.28] Linsley, G S, Resuspension of the transuranium elements: A review of existing data. Harwell, National Radiological Protection Board, NRPB-R75 (1978). (London, HMSO).

- [3.29] Tamura, T, Physical and chemical characteristics of plutonium in existing contaminated soils and sediments. IN Transuranium Nuclides in the Environment. Proc. Symposium, San Francisco, 1975. Vienna, IAEA (1976).
- [3.30] Hamilton, E I, The concentration of uranium in air from contrasted natural environments. Health Phys., 19, 511 (1970).
- [3.31] Simmonds, J R, Linsley, G.S. and Jones, J A, A general model for the transfer of radioactive materials in terrestrial foodchains. Harwell, National Radiological Protection Board, NRPB-R89 (1979). (London, HMSO).
- [3.32] Bryant, P M, Derivation of working limits for continuous release rate of iodine-131 to atmosphere in a milk producing area. Health Phys., 10, 249 (1964).
- [3.33] Kelly, G N, Jones, J A, Bryant, P M and Morley F, The predicted radiation exposure of the population of the European Community resulting from discharges of krypton-85, tritium, carbon-14 and iodine-129. Luxembourg, CEC doc. V/2676/75 (1975).
- [3.34] Aarkrog, A, Comparative studies of plutonium inventories in soils and marine sediments. IN Proc. 4th International Congress of IRPA, Paris, April 1977, 3, 841, (1977).
- [3.35] Nyhan, J W, Miera, F R and Neher, R E, The distribution of plutonium in Trinity soils after 28 years. J. Environ. Qual., 5, 431, (1976).
- [3.36] Krey, P W, Hardy, E P and Toonkel, L E, The distribution of plutonium and americium with depth in soil at Rocky Flats. New York, HASL-318 (1977).
- [3.37] Bayer, A, The radiological exposure of the population in the Rhine-Meuse region by nuclear installations during normal operation. Luxembourg, CEC doc. V/1647/77 (1978).
- [3.38] Bartlett, B O, Middleton, L J, Milbourn, G M and Squire, H M, Surveys of radioactivity in human diet and experimental studies, report for 1960. Letcombe, Agricultural Research Council, ARCRL 5, p 51 (1960).
- [3.39] Garner, R J, Transfer of radioactive materials from the terrestrial environment to animals and man. Chemical Rubber Co. Ltd., Ohio, CRC Press (1972).
- [3.40] Scott-Russell, R (ed.), Radioactivity and Human Diet. Oxford, Pergamon Press, (1966).
- [3.41] Aarkrog, A, Variation of direct plutonium contamination in Danish cereal grains. Health Phys., 35, 489 (1978).
- [3.42] Reith, J W S, The Macauley Institute for Soil Research, Aberdeen. Private communication (1977).

- [3.43] Fletcher, J F and Dotson, W L, Hermes - a digital computer code for estimating regional radiological effects from the nuclear power industry. HEDL-TME-71-168 (1971).
- [3.44] Annual Abstracts of Statistics, 1976. Central Statistics Office, London, HMSO (1976).
- [3.45] Ng, Y C, Burton, A, Thompson, S E, Tandy, R K, Kretner, H K and Pratt, M W, Predictions of the maximum dosage to man from the fallout of nuclear devices, IV. IN Handbook for Estimating the Maximum Internal Dose from Radionuclides Released to the Biosphere. Univ. California, UCRL-50163, Part IV (1968).
- [3.46] Till, J E, Hoffman, F O and Dunning, D E, Assessment of Tc-99 releases to the atmosphere - a plea for applied research. Oak Ridge, Tenn., ORNL/TM-6260 (1978).
- [3.47] Delmas, J, Didier, R, Grauby, A and Bovard, P, Radiocontamination expérimentale de quelques espèces cultivées soumises à l'irrigation par aspersion. IN Proc. International Symposium on Radioecology, CEN Cadarache, September 1969.
- [3.48] Linsley, G S, Simmonds, J R and Kelly, G N, An evaluation of the foodchain pathway for transuranium elements dispersed in soils. Harwell, National Radiological Protection Board, NRPB-R81 (1979). (London, HMSO).
- [3.49] Berhardt, D E and Eadie, G G, Parameters for estimating the uptake of transuranic elements by terrestrial plants. US Environmental Protection Agency, ORP/LV-76-2 (PB-254029) (1976).
- [3.50] Madelmont, C, Centre d'Etudes Nucléaires de Fontenay-aux-Roses, France. Private communication (1978).
- [3.51] Thornton, I and Kinniburgh, D G, Intakes of lead, copper and zinc by cattle from soil and pasture. IN Proc. Symposium on Trace Element Metabolism in Animals, 3, Munich, July 1977. (To be published).
- [3.52] Thornton, I, Biogeochemical and soil ingestion studies in relation to the trace-element nutrition of livestock. IN Trace Element Metabolism in Animals 2. Proc. Symposium, Baltimore, University Park Press (1974).
- [3.53] Ng, Y C, Colsher, C S, Quinn, D J and Thompson, S E, Transfer coefficients for the prediction of the dose to man via the forage - cow - milk pathway from radionuclides released to the biosphere. Univ. California, UCRL-51939, (1977).
- [3.54] Final environmental statement, Waste Management Operations, Hanford Reservation, Volume 2. Washington DC, ERDA-1538 (1975)
- [3.55] Adams, N, Hunt, B W and Reissland, J A, Annual limits of radionuclides for workers. Harwell, National Radiological Protection Board, NRPB-R82 (1978). (London, HMSO).

- [3.56] Stanely, R E, Bretthauer, E W and Sutton, W W, Absorption distribution and excretion of plutonium by dairy cattle. IN Radioecology of Plutonium and Other Transuranics in Desert Environments. (White, M G and Dunaway, P B, eds.). Nevada Applied Ecology Group, NVO-153, (1975).
- [3.57] Beck, H and De Planque, G, The radiation field in air due to distributed gamma ray sources in the ground. New York, USAEC, HASL-195 (1968).
- [3.58] Garnier, A and Sauve, A M, Etude de la répartition géographique de la population Européenne en vue de l'évaluation des conséquences radiologiques des rejets d'effluents radioactifs. EUR/CEA Département de Protection, CEA, Fontenay-aux-Roses. (To be published).
- [3.59] Sauve, A M, Programmes informatiques (Fortran) de répartition de la population Européenne. CEA. (To be published).
- [3.60] Centre National Interprofessionnel de l'Economie Laitière, L'économie laitière en chiffre, CNIEL, Paris (1978).
- [3.61] Statistical Office of the European Communities, Milk and milk products. EUROSTAT, (1977).
- [3.62] Statistical Office of the European Communities, Vegetables and fruit products. (1966-1977) EUROSTAT, (1978).
- [3.63] Statistical Office of the European Communities, Monthly statistics of meat (July/August 1977). EUROSTAT, (1977).
- [3.64] Ministry of Agriculture, Fisheries and Food Statistical Information, Number of animals slaughtered in 1976 by Counties. Stats. 174/77, MAFF, Guildford, (1977).
- [3.65] Landund Forstwirtschaft, Fischerei, Fachserie B, Reihe 3, Viehwirtschaft, 11 Milch, 111 Schlachtungen und Fleischgewinnung, Stuttgart, FRG (1973).
- [3.66] Instituto Centrale di Statistica, 1973 Annual Report. ISTAT, Rome (1974).
- [3.67] Crapelet, C and Thibier, M, Le Mouton Vigot Frères Editeur, Paris (1947).
- [3.68] Blain, J, Les aliments d'origine animale destinés à l'homme, Vigot Freres Editeur, Paris (1947).
- [3.69] Statistiques Agricoles Ministère de l'Agriculture et du Développement Rural. Bilans alimentaires supplement 106. Ministère de l'Agriculture, (1972).
- [3.70] Bouville, A et Guezengar, J M, Transformation des données contenues dans une grille de maille rectangulaire sous forme de répartition dans des secteurs de couronne, CEA. (To be published).

Table 3.1 The radionuclides considered for release to the atmosphere⁽¹⁾

Nuclide	Half-life	Nuclide	Half-life
H-3	1.23 10 ¹ y	Zr-95	5.68 10 ⁶ s
C-14	5.70 10 ³ y	Nb-95	3.02 10 ⁶ s
Ar-41	6.59 10 ³ s	Mo-99	2.38 10 ⁵ s
Cr-51	2.39 10 ⁶ s	Tc-99	2.14 10 ⁵ y
Mn-54	2.70 10 ⁷ s	Tc-99m	2.17 10 ⁴ s
Fe-55	2.70 y	Ru-103	3.41 10 ⁶ s
Fe-59	3.90 10 ⁶ s	Ru/Rh-106	1.01 y
Co-58	6.13 10 ⁶ s	Rh-103m	3.41 10 ³ s
Co-60	5.28 y	Sb-124	5.21 10 ⁶ s
Zn-65	2.12 10 ⁷ s	Sb-125	2.74 y
Kr-83m	6.59 10 ³ s	Te-125m	5.02 10 ⁶ s
Kr-85m	1.61 10 ⁴ s	Te-127m	9.42 10 ⁶ s
Kr-85	1.07 10 ¹ y	Te-127	3.36 10 ⁴ s
Kr-87	4.57 10 ³ s	Te-129m	2.90 10 ⁶ s
Kr-88	1.01 10 ⁴ s	Te-129	4.14 10 ³ s
Kr-89	1.89 10 ² s	Te-131m	1.08 10 ⁵ s
Rb-86	1.62 10 ⁶ s	Te-132	2.81 10 ⁵ s
Rb-88	1.06 10 ³ s	I-129	1.57 10 ⁷ y
Rb-89	9.36 10 ² s	I-131	6.95 10 ⁵ s
Sr-89	4.35 10 ⁶ s	I-132	8.21 10 ³ s
Sr-90	2.82 10 ¹ y	I-133	7.52 10 ⁴ s
Y-90	2.31 10 ⁵ s	I-134	3.19 10 ³ s
Y-91	5.05 10 ⁶ s	I-135+D	2.42 10 ⁴ s

continued

Table 3.1 (continued) The radionuclides considered for release to the atmosphere

Nuclide	Half-life	Nuclide	Half-life
Xe-131m	$1.04 \cdot 10^6$ s	Ce-144	$2.45 \cdot 10^7$ s
Xe-133m	$1.93 \cdot 10^5$ s	Pr-144	$1.04 \cdot 10^3$ s
Xe-133	$4.56 \cdot 10^5$ s	Fm-147	2.62 y
Xe-135m	$9.18 \cdot 10^2$ s	Eu-154	8.50 y
Xe-135	$3.30 \cdot 10^4$ s	Eu-155	4.96 y
Xe-137	$2.30 \cdot 10^2$ s	Np-239	$1.99 \cdot 10^5$ s
Xe-138	$8.52 \cdot 10^2$ s	Pu-238	$8.60 \cdot 10^1$ y
Cs-134	2.08 y	Pu-239	$2.44 \cdot 10^4$ y
Cs-135	$3.01 \cdot 10^6$ y	Pu-240	$6.58 \cdot 10^3$ y
Cs-136	$1.12 \cdot 10^6$ s	Pu-241	$1.50 \cdot 10^1$ y
Cs-137+D	$3.01 \cdot 10^1$ y	Pu-242	$3.79 \cdot 10^5$ y
Cs-138	$1.93 \cdot 10^3$ s	Am-241	$4.58 \cdot 10^2$ y
Ba-140	$1.11 \cdot 10^6$ s	Cm-242	$1.41 \cdot 10^7$ s
La-140	$1.44 \cdot 10^5$ s	Cm-244	$1.76 \cdot 10^1$ y
Ce-141	$2.81 \cdot 10^6$ s		

Notes The transfer of the following nuclides through the terrestrial environment after their

(1) deposition from the atmosphere is modelled.

H-3, C-14, Cr-51, Mn-54, Fe-55, Fe-59, Co-58, Co-60, Zn-65, Rb-86, Sr-89, Sr-90, Y-90, Y-91, Zr-95, Nb-95, Mo-99, Tc-99, Ru-103, Ru/Rh-106, Sb-124, Sb-125, Te-127m, Te-129m, Te-131m, Te-132, I-129, I-131, I-132, I-133, I-134, I-135+D, Cs-134, Cs-136, Cs-137+D, Ba-140, La-140, Ce-141, Ce-144, Fm-147, Eu-154, Eu-155, Np-239, Pu-238, Pu-239, Pu-240, Pu-241, Pu-242, Am-241, Cm-242, Cm-244.

Table 3.2 Conversion factors to derive dose equivalent in tissue from absorbed dose in air as a function of the initial photon energy

Photon Energy MeV	Absorbed Dose in air Gy/μ/m ²	Ratio of Organ Dose Equivalent to Absorbed Dose in Air			
		Effective	Gonads	Thyroid	Skin
1.00 E-02	7.52 E-16	2.17 E-03	4.02 E-03	4.29 E-04	1.94 E-01
1.50 E-02	3.09 E-16	1.39 E-02	1.36 E-04	1.68 E-04	3.50 E-01
2.00 E-02	1.69 E-16	5.43 E-02	6.96 E-02	3.26 E-02	4.42 E-01
3.00 E-02	6.95 E-17	2.27 E-01	2.22 E-01	2.68 E-01	5.81 E-01
5.00 E-02	3.09 E-17	5.70 E-01	4.29 E-01	6.03 E-01	7.59 E-01
6.50 E-02*	2.78 E-17	6.30 E-01	4.60 E-01	7.10 E-01	8.00 E-01
1.00 E-01	3.81 E-17	7.68 E-01	5.30 E-01	9.70 E-01	9.04 E-01
2.00 E-01	8.69 E-17	7.96 E-01	7.32 E-01	7.63 E-01	9.55 E-01
5.00 E-01	2.32 E-16	7.17 E-01	5.68 E-01	6.31 E-01	9.08 E-01
1.00 E+00	4.56 E-16	7.12 E-01	5.68 E-01	5.51 E-01	9.80 E-01
1.50 E+00	6.18 E-16	7.98 E-01	7.00 E-01	8.45 E-01	9.12E-01
2.00 E+00	7.52 E-16	7.78 E-01	6.46 E-01	7.65 E-01	1.00 E+00
4.00 E+00	1.21 E-15	9.68 E-01	7.10 E-01	1.58 E+00	9.48 E-01
1.00 E+01*	2.32 E-15	9.68 E-01	7.10 E-01	1.58 E+00	9.48 E-01

* These energies were not considered by Poston and Snyder but are included to facilitate interpolation and extrapolation.

Table 3.3 The weighting factors used in calculating the effective dose equivalent from external γ irradiation

Organ	Weighting Factor
Gonads	0.25
Breast	0.15
Red Bone Marrow	0.12
Lung	0.12
Thyroid	0.03
Bone surfaces	0.03
Remainder (1)	0.30

Notes

- (1) A weighting factor of 0.06 is applied to each of the five organs or tissues of the remainder (other than skin) receiving the highest dose equivalents.

Table 3.4 β dose rates per unit air concentration

Nuclide	Absorbed dose rate in air $Gy\ y^{-1}\ per\ Bq\ m^{-3}$	Dose Equivalent rate in skin $Sv\ y^{-1}\ per\ Bq\ m^{-3}$	Nuclide	Absorbed dose rate in air $Gy\ y^{-1}\ per\ Bq\ m^{-3}$	Dose Equivalent rate in skin $Sv\ y^{-1}\ per\ Bq\ m^{-3}$
H-3	2.46 E-08	0.0	Rh-103m	1.43 E-07	0.0
C-14	2.08 E-07	2.16 E-08	Sb-124	1.40 E-06	6.46 E-07
Ar-41	1.61 E-06	7.62 E-07	Sb-125	5.06 E-07	1.48 E-07
Cr-51	2.09 E-10	9.68 E-11	Te-125m	3.92 E-07	1.00 E-07
Mn-54	8.26 E-10	4.04 E-10	Te-127m	3.08 E-07	6.00 E-08
Fe-55	0.0	0.0	Te-127	9.20 E-07	4.03 E-07
Fe-59	5.03 E-07	1.77 E-07	Te-129m	9.64 E-07	4.14 E-07
Co-58	1.10 E-09	5.37 E-10	Te-129	1.90 E-06	9.02 E-07
Co-60	4.27 E-07	1.36 E-07	Te-131m	6.03 E-07	2.46 E-07
Zn-65	0.0	0.0	Te-132	4.31 E-07	8.68 E-08
Kr-83m	9.99 E-08	0.0	I-129	2.76 E-07	1.92 E-08
Kr-85m	9.74 E-07	4.41 E-07	I-131	8.19 E-07	3.44 E-07
Kr-85	8.93 E-07	3.89 E-07	I-132	1.85 E-06	8.79 E-07
Kr-87	4.27 E-06	2.10 E-06	I-133	1.53 E-06	7.19 E-07
Kr-88	1.28 E-06	5.85 E-07	I-134	2.18 E-06	1.05 E-06
Kr-89	3.94 E-06	1.93 E-06	I-135+D	1.49 E-06	6.93 E-07
Rb-86	2.23 E-06	1.07 E-06	Xe-131m	5.40 E-07	1.98 E-07
Rb-88	6.19 E-06	3.06 E-06	Xe-133m	7.43 E-07	3.19 E-07
Rb-89	2.96 E-06	1.44 E-06	Xe-133	5.89 E-07	1.62 E-07
Sr-89	1.95 E-06	9.32 E-07	Xe-135m	3.74 E-07	1.80 E-07
Sr-90	7.28 E-07	3.02 E-07	Xe-135	1.32 E-06	5.99 E-07
Y-90	3.04 E-06	1.49 E-06	Xe-137	5.62 E-06	2.78 E-06
Y-91	2.06 E-06	9.85 E-07	Xe-138	2.31 E-06	1.10 E-06
Zr-95	5.25 E-07	1.92 E-07	Cs-134	6.90 E-07	2.87 E-07
Nb-95	2.19 E-07	2.62 E-08	Cs-135	2.79 E-07	5.43 E-08
Mo-99	1.45 E-06	6.73 E-07	Cs-136	5.26 E-07	1.77 E-07
Tc-99	3.89 E-07	1.14 E-07	Cs-137+D	9.65 E-07	4.16 E-07
Tc-99m	6.08 E-08	1.78 E-08	Cs-138	3.89 E-06	1.91 E-06
Ru-103	3.12 E-07	7.18 E-08	Ra-140	1.23 E-06	5.05 E-07
Ru/Rh-106	4.49 E-06	2.19 E-06	La-140	1.95 E-06	9.31 E-07

continued

Table 3.4 (continued) β dose rates per unit air concentration

Nuclide	Absorbed dose rate in air Gy y^{-1} per Bq m^{-3}	Dose Equivalent rate in skin Sv y^{-1} per Bq m^{-3}
Ce-141	7.30 E-07	2.83 E-07
Ce-144	4.18 E-07	1.19 E-07
Pr-144	3.96 E-06	1.95 E-06
Pm-147	2.99 E-07	6.30 E-08
Eu-154	9.87 E-07	4.31 E-07
Eu-155	2.62 E-07	2.60 E-08
Np-239	1.13 E-06	3.87 E-07
Pu-238	2.74 E-08	9.81 E-11
Pu-239	2.84 E-08	8.70 E-09
Pu-240	2.46 E-08	9.81 E-11
Pu-241	2.77 E-08	3.69 E-13
Pu-242	5.92 E-09	7.56 E-10
Am-241	8.93 E-08	3.17 E-10
Cm-242	2.38 E-08	1.01 E-14
Cm-244	2.05 E-08	0.0

Table 3.5 Coefficients given by Hosker [3.24] to derive the vertical standard deviation of the plume for the various stability categories (1,2).

Stability Category	Mean wind speed m/s	a	b	c	d
A	1	0.112	1.06	$5.38 \cdot 10^{-4}$	0.815
B	2	0.130	0.950	$6.52 \cdot 10^{-4}$	0.750
C	5	0.112	0.920	$9.05 \cdot 10^{-4}$	0.718
D	5	0.098	0.889	$1.35 \cdot 10^{-3}$	0.688
E	3	0.0609	0.895	$1.96 \cdot 10^{-3}$	0.684
F	1	0.0638	0.783	$1.36 \cdot 10^{-3}$	0.672

Notes

(1) Coefficients appropriate to a roughness length of 10cm.

(2) Vertical standard deviation, $\sigma_z = \frac{a x^b}{1 + c x^d}$

Table 3.6 Coefficients given by Doury [3.207] to derive the vertical standard deviation of the plume for various diffusion conditions (1).

Diffusion Condition	Time of travel, ⁽²⁾ t (seconds)	A	K
Normal	0 - 2.4 10 ²	0.42	0.814
	2.4 10 ² - 3.28 10 ³	1.0	0.685
	> 3.28 10 ³	20	0.5
Poor	All	0.2	0.5

Notes

- (1) The vertical standard derivation of the

$$\sigma_z = (At)^k$$

- (2) Time of travel is obtained as x/\bar{u} , that is the distance travelled divided by the mean wind speed. Wind speeds of 1, 2 and 5m s⁻¹ are considered for normal diffusion and 1, 2 and 3m s⁻¹ for poor diffusion conditions.

Table 3.7 Depth of mixing layer assumed for the various dispersion conditions

(a) Pasquill typing scheme

Stability Category	Depth of Mixing Layer (m)
A	2000
B	2000
C	1000
D	1000
E	200
F	200

(b) Doury typing scheme

Dispersion Condition	Mean Wind Speed m s^{-1}	Depth of mixing layer, m
Poor	1, 2, 3	200
Normal	1, 2	2000
Normal	5	1000

Table 3.8 Air concentration for a release at height 30m (Bq m⁻³ per Bq s⁻¹)

Pasquill category D

Nuclide	Parent	Distance (m)			
		10 ³	10 ⁴	10 ⁵	10 ⁶
H-3		4.83E-07	1.26E-08	4.38E-10	3.19E-11
C-14		4.83E-07	1.26E-08	4.38E-10	3.19E-11
MN-54		4.78E-07	1.17E-08	3.43E-10	9.65E-12
CO-60		4.78E-07	1.17E-08	3.43E-10	9.69E-12
KR-85M		4.78E-07	1.15E-08	1.86E-10	0.0
KR-85		4.83E-07	1.26E-08	4.38E-10	3.19E-11
SR-85		4.78E-07	1.17E-08	3.42E-10	9.39E-12
SR-89	RB-89	2.88E-12	3.96E-13	1.50E-14	4.12E-16
SR-90		4.78E-07	1.17E-08	3.43E-10	9.69E-12
Y-90		4.77E-07	1.16E-08	3.23E-10	5.32E-12
Y-90	SR-90	2.87E-10	7.01E-11	2.00E-11	4.38E-12
Y-91		4.78E-07	1.17E-08	3.43E-10	9.43E-12
RU/RH106		4.78E-07	1.17E-08	3.43E-10	9.65E-12
I-129		4.78E-07	1.17E-08	3.44E-10	9.70E-12
OI-129		4.83E-07	1.25E-08	4.37E-10	3.15E-11
I-131		4.77E-07	1.17E-08	3.37E-10	7.94E-12
XE-133		4.82E-07	1.25E-08	4.25E-10	2.36E-11
XE-135		4.81E-07	1.20E-08	2.88E-10	4.79E-13
CS-134		4.78E-07	1.17E-08	3.43E-10	9.68E-12
BA-140		4.77E-07	1.17E-08	3.39E-10	8.55E-12
LA-140		4.77E-07	1.16E-08	3.12E-10	3.71E-12
CE-144		4.78E-07	1.17E-08	3.43E-10	9.64E-12
NP-239		4.77E-07	1.16E-08	3.20E-10	4.83E-12
PU-239		4.78E-07	1.17E-08	3.44E-10	9.70E-12
PU-241		4.78E-07	1.17E-08	3.43E-10	9.69E-12
AM-241		4.78E-07	1.17E-08	3.44E-10	9.70E-12

Table 3.9 Deposition rate for a release at height 30m ($\text{Bq m}^{-2} \text{s}^{-1}$ per Bq s^{-1})

Pasquill category D

Nuclide	Parent	Distance (m)				
		10^3	10^4	10^5	10^6	10^7
H-3		0.0	0.0	0.0	0.0	0.0
C-14		0.0	0.0	0.0	0.0	0.0
MN-54		5.0E-3	2.39E-09	5.85E-11	1.72E-12	4.82E-14
CO-60		5.0E-3	2.39E-09	5.85E-11	1.72E-12	4.84E-14
KR-85M		0.0	0.0	0.0	0.0	0.0
KR-85		0.0	0.0	0.0	0.0	0.0
SR-85		5.0E-3	2.39E-09	5.85E-11	1.71E-12	4.70E-14
SR-85	RB-89	5.0E-3	1.44E-14	1.98E-15	7.51E-17	2.06E-18
SR-90		5.0E-3	2.39E-09	5.85E-11	1.72E-12	4.85E-14
Y-90		5.0E-3	2.39E-09	5.82E-11	1.62E-12	2.66E-14
Y-90	SR-90	5.0E-3	1.43E-12	3.50E-13	1.00E-13	2.19E-14
Y-91		5.0E-3	2.39E-09	5.85E-11	1.71E-12	4.72E-14
RU/RH106		5.0E-3	2.39E-09	5.85E-11	1.72E-12	4.83E-14
I-125		5.0E-3	2.39E-09	5.85E-11	1.72E-12	4.85E-14
OI-125		5.0E-5	2.41E-11	6.27E-13	2.19E-14	1.58E-15
I-131		5.0E-3	2.39E-09	5.84E-11	1.68E-12	3.97E-14
XE-133		0.0	0.0	0.0	0.0	0.0
XE-135		0.0	0.0	0.0	0.0	0.0
CS-134		5.0E-3	2.39E-09	5.85E-11	1.72E-12	4.84E-14
BA-140		5.0E-3	2.39E-09	5.84E-11	1.70E-12	4.28E-14
LA-140		5.0E-3	2.39E-09	5.79E-11	1.56E-12	1.86E-14
CE-144		5.0E-3	2.39E-09	5.85E-11	1.72E-12	4.82E-14
NP-235		5.0E-3	2.39E-09	5.81E-11	1.60E-12	2.41E-14
PU-239		5.0E-3	2.39E-09	5.85E-11	1.72E-12	4.85E-14
PU-241		5.0E-3	2.39E-09	5.85E-11	1.72E-12	4.85E-14
AM-241		5.0E-3	2.39E-09	5.85E-11	1.72E-12	4.85E-14

Table 3.10 Effective cloud gamma dose rates for a release at height 30m
(Sv y⁻¹ per Bq s⁻¹)

Pasquill category D

Nuclide	Parent	Distance (m)			
		10 ³	10 ⁴	10 ⁵	10 ⁶
H-3		0.0	0.0	0.0	0.0
C-14		0.0	0.0	0.0	0.0
MN-54		3.05E-13	1.23E-14	4.06E-16	1.17E-17
CO-60		9.06E-13	3.76E-14	1.28E-15	3.71E-17
KR-85M		7.28E-14	2.56E-15	4.37E-17	0.0
KR-85		8.65E-16	3.56E-17	1.36E-18	1.01E-19
SR-85		4.95E-17	2.00E-18	6.64E-20	1.86E-21
SR-89	RB-89	2.98E-22	6.78E-23	2.91E-24	8.16E-26
SR-90		0.0	0.0	0.0	0.0
Y-90		9.69E-17	4.10E-18	1.36E-19	2.31E-21
Y-90	SR-90	5.82E-20	2.47E-20	8.41E-21	1.91E-21
Y-91		9.64E-16	3.99E-17	1.35E-18	3.82E-20
RU/RH106		7.75E-14	3.04E-15	9.91E-17	2.84E-18
I-125		1.03E-15	2.70E-17	8.00E-19	2.26E-20
OI-125		1.04E-15	2.90E-17	1.02E-18	7.35E-20
I-131		1.54E-13	5.85E-15	1.84E-16	4.39E-18
XE-133		1.43E-14	4.94E-16	1.74E-17	9.69E-19
XE-135		1.17E-13	4.41E-15	1.13E-16	1.90E-19
CS-134		5.85E-13	2.32E-14	7.62E-16	2.19E-17
BA-140		6.96E-14	2.66E-15	8.44E-17	2.16E-18
LA-140		8.38E-13	3.44E-14	1.08E-15	1.32E-17
CE-144		7.62E-15	2.64E-16	8.14E-18	2.30E-19
NP-239		6.27E-14	2.23E-15	6.52E-17	9.92E-19
PU-239		3.76E-17	1.26E-18	3.89E-20	1.11E-21
PU-241		2.51E-18	8.67E-20	2.67E-21	7.58E-23
AM-241		8.56E-15	2.69E-16	8.11E-18	2.30E-19

Table 3.11 External beta dose rates in skin for a release at height 30m
(Sv y⁻¹ per Bq s⁻¹)

Pasquill category D

Nuclide	Parent	Distance (m)			
		10 ³	10 ⁴	10 ⁵	10 ⁶
H-3		0.0	0.0	0.0	0.0
C-14		0.10E-13	0.27E-15	0.95E-17	0.69E-18
MN-54		0.19E-15	0.47E-17	0.14E-18	0.39E-20
CO-60		0.65E-13	0.16E-14	0.47E-16	0.13E-17
KR-85M		0.21E-12	0.51E-14	0.82E-16	0.0
KR-85		0.19E-12	0.49E-14	0.17E-15	0.12E-16
SR-89		0.45E-12	0.11E-13	0.32E-15	0.88E-17
SR-89	RB-89	0.27E-17	0.37E-18	0.14E-19	0.38E-21
SR-90		0.14E-12	0.35E-14	0.10E-15	0.29E-17
Y-90		0.71E-12	0.17E-13	0.48E-15	0.79E-17
Y-90	SR-90	0.43E-15	0.10E-15	0.30E-16	0.65E-17
Y-91		0.47E-12	0.12E-13	0.34E-15	0.93E-17
RU/RH106		0.10E-11	0.26E-13	0.75E-15	0.21E-16
I-129		0.92E-14	0.22E-15	0.66E-17	0.19E-18
OI-129		0.93E-14	0.24E-15	0.84E-17	0.60E-18
I-131		0.16E-12	0.40E-14	0.12E-15	0.27E-17
XE-133		0.78E-13	0.20E-14	0.69E-16	0.38E-17
XE-135		0.29E-12	0.72E-14	0.17E-15	0.29E-18
CS-134		0.14E-12	0.34E-14	0.98E-16	0.28E-17
BA-140		0.24E-12	0.59E-14	0.17E-15	0.43E-17
LA-140		0.44E-12	0.11E-13	0.29E-15	0.35E-17
CE-144		0.57E-13	0.14E-14	0.41E-16	0.11E-17
NP-239		0.18E-12	0.45E-14	0.12E-15	0.19E-17
PU-239		0.42E-14	0.10E-15	0.30E-17	0.84E-19
PL-241		0.18E-18	0.43E-20	0.13E-21	0.36E-23
AM-241		0.15E-15	0.37E-17	0.11E-18	0.31E-20

Table 3.12

Fraction of a long lived nuclide remaining in the plume at various distances downwind⁽¹⁾

Stability Category	Fraction remaining in the plume					
	Deposition Velocity m s ⁻¹	Distance (m)				
		10 ³	10 ⁴	10 ⁵	10 ⁶	3 10 ⁶
A	5 10 ⁻³	0.96	0.89	0.71	0.08	6 10 ⁻⁴
D		0.99	0.93	0.79	0.30	0.042
D + rain		0.97	0.76	0.11	0	0
F		1.0	0.53	1.6 10 ⁻²	0	0
D	5 10 ⁻⁵	1.0	0.99	0.99	0.99	0.97
F		1.0	0.99	0.96	0.76	0.46

(1) for a release at a height of 30m.

Table 3.13 Values of transfer coefficients used in the models for migration in soil

Transfer Coefficient	value in y^{-1}
Well mixed soil ⁽¹⁾	
K_{11}	6.93 10^{-3}
Undisturbed land ⁽²⁾	
K_{12}	2.43 10^{-1}
K_{23}	6.29 10^{-2}
K_{34}	3.92 10^{-2}
K_{43}	1.47 10^{-3}
K_{44}	1.39 10^{-2}

(1) see diagram 3.3, section 3.3.3.2

(2) see diagram 3.4, section 3.3.3.2

Table 3.14

A comparison between the predictions of the model and the experimental results* for plutonium migration

Time (years)	Experiment	Percentage of Total Deposit							
		0-1 cm		1-5 cm		5-15 cm		15-30 cm	
		Model	Expt*	Model	Expt*	Model	Expt*	Model	Expt*
6	Aarkrog** (Thule) $\sqrt{3.34}$	23.3	25.9	61.1	51.8	14.3	21.2	1.3	1.1
7	Krey (Rocky Flats) $\sqrt{3.39}$	18.3	10.4	62.2	56.9	17.6	30.4	1.9	2.1
27	Nyhan (Trinity) $\sqrt{3.35}$	0.1	5.8	24.5	28.6	44.6	34.4	26.9	15.6

* The experimental results are specified at depths different to those given above. In evaluating experimental results at these different depths it was assumed that the plutonium in soil was log-normally distributed with depth.

** Experimental data for migration in marine sediments

Table 3.15 Non-element dependent parameters for crops and pasture

	Roots	Grain	Green Vegetables (a)	Pasture
Yield, wet weight ($\text{kg m}^{-2} \text{y}^{-1}$)	2.5 $\sqrt[3]{3.447}$	4.0 $10^{-1} \sqrt[3]{3.447}$	1.0 $\sqrt[3]{3.447}$	1.0 - cattle (b) 3.0 10^{-1} -sheep
Interception factor	-	0.2 (c)	0.2	0.2
Amount of soil on edible plant after preparation for consumption*	-	0.001	0.01	-
Half life on plant surface, y	0.082	0.082 $\sqrt[3]{3.397}$	0.082 $\sqrt[3]{3.397}$	0.038 $\sqrt[3]{3.387}$
Mean life for cropping, y	0.27	0.27	0.27	-
Depth of soil (cm)	30	30	30	15

Notes

- (a) Green vegetables includes leafy and leguminous varieties and fruit.
- (b) Different yields are proposed for pasture grazed by sheep and cattle as the former are generally on poorer pasture.
- (c) A value of 0.2 for the interception factor for general deposition is proposed as a compromise between 0.25 for dry deposition and 0.10 for wet deposition.

* percentage of dry plant weight

Table 3.16 Element dependent parameters for crops and pasture

Element	Concentration Factor $\sqrt[3]{3.43, 3.45}$ *				Pasture	Fraction deposited on plant which reaches portion eaten	
	Root Vegetables	Grain	Green Vegetables	Pasture		Root veg	Green veg, Grain
Chromium	3 10^{-4}	3 10^{-4}	3 10^{-4}	3 10^{-4}	3 10^{-4}	-	-
Manganese	3 10^{-2}	3 10^{-2}	3 10^{-2}	3 10^{-2}	3 10^{-2}	5 10^{-2}	-
Iron	3 10^{-4}	4 10^{-4}	2 10^{-4}	4 10^{-4}	4 10^{-4}	5 10^{-2}	-
Cobalt	2 10^{-3}	1 10^{-2}	1 10^{-3}	1 10^{-2}	1 10^{-2}	5 10^{-2}	-
Zinc	4 10^{-1}	4 10^{-1}	4 10^{-1}	4 10^{-1}	4 10^{-1}	5 10^{-2}	-
Rubidium	1 10^{-1}	1 10^{-1}	1 10^{-1}	1 10^{-1}	1 10^{-1}	1 10^{-2}	-
Strontium	6 10^{-2} $\sqrt[3]{3.47}$	2 10^{-2} $\sqrt[3]{3.47}$	7 10^{-1} $\sqrt[3]{3.47}$	3 10^{-1} $\sqrt[3]{3.50}$	3 10^{-1} $\sqrt[3]{3.50}$	1 10^{-2}	-
Yttrium	3 10^{-3}	3 10^{-3}	3 10^{-3}	3 10^{-3}	3 10^{-3}	1 10^{-2}	-
Zirconium	2 10^{-4}	2 10^{-4}	2 10^{-4}	2 10^{-4}	2 10^{-4}	1 10^{-2}	-
Niobium	1 10^{-2}	1 10^{-2}	1 10^{-2}	1 10^{-2}	1 10^{-2}	1 10^{-2}	-
Molybdenum	1 10^{-1}	1 10^{-1}	1 10^{-1}	1 10^{-1}	1 10^{-1}	-	-
Technetium**	50 $\sqrt[3]{3.49}$	50 $\sqrt[3]{3.46}$	50 $\sqrt[3]{3.46}$	50 $\sqrt[3]{3.46}$	50 $\sqrt[3]{3.46}$	1 10^{-1}	1 x 10^{-1}
Ruthenium	1 10^{-2}	6 10^{-2}	4 10^{-3}	4 10^{-2}	4 10^{-2}	5 10^{-2}	-
Silver	2 10^{-1}	2 10^{-1}	2 10^{-1}	2 10^{-1}	2 10^{-1}	5 10^{-2}	-

continued

Table 3.16 (continued) Element dependent parameters for crops and Pasture

Element	Concentration Factor* [3.43, 3.45]				Translocation [3.43] (c)	
	Root Vegetables	Grain	Green Vegetables	Pasture	Root veg.	Green veg, Grain
Antimony	1 10 ⁻²	1 10 ⁻²	1 10 ⁻²	1 10 ⁻²	5 10 ²	-
Tellurium	1	1	1	1	1 10 ⁻¹	1 10 ⁻¹
Iodine	2 10 ⁻²	2 10 ⁻²	2 10 ⁻²	2 10 ⁻²	1 10 ⁻¹	1 10 ⁻¹
Caesium	5 10 ⁻³ [3.47]	6 10 ⁻³ [3.47]	2 10 ⁻² [3.47]	2 10 ⁻² [3.47]	1 10 ⁻¹	1 10 ⁻¹
Barium	5 10 ⁻³	5 10 ⁻³	5 10 ⁻³	5 10 ⁻³	1 10 ⁻²	-
Lanthanum	3 10 ⁻³	3 10 ⁻³	3 10 ⁻³	3 10 ⁻³	1 10 ⁻²	-
Cerium	3 10 ⁻³	3 10 ⁻³	7 10 ⁻³	5 10 ⁻⁴	2 10 ⁻²	-
Promethium	3 10 ⁻³	3 10 ⁻³	3 10 ⁻³	3 10 ⁻³	2 10 ⁻²	-
Europium	3 10 ⁻³	3 10 ⁻³	3 10 ⁻³	3 10 ⁻³	2 10 ⁻²	-
Neptunium (a)	1 10 ⁻³	1 10 ⁻⁶	1 10 ⁻⁴	1 10 ⁻⁴	-	-
Plutonium	1 10 ⁻³ [3.48]	1 10 ⁻⁶ [3.48]	1 10 ⁻⁴ [3.48]	1 10 ⁻⁴ [3.48]	-	-
Americium	1 10 ⁻³ [3.48]	1 10 ⁻⁵ [3.48]	1 10 ⁻³ [3.48]	1 10 ⁻³ [3.48]	-	-
Curium (b)	1 10 ⁻³	1 10 ⁻⁵	1 10 ⁻³	1 10 ⁻³	-	-

*Concentration factor = activity/unit wet weight plant
 activity/unit dry weight soil

** Recent unpublished experimental data have indicated that this value may be too high

(a) Assumed to be the same as plutonium [3.49]
 (b) Assumed to behave as americium [3.49]
 (c) Translocation has been ignored for pasture as it is small compared to transfer by other routes

Table 3.17 Non-element dependent parameters for animals

Parameter	Value	
	Milk Cows	Sheep
Amount eaten per year $\sqrt[3]{3.407}$ (kg dry wt y^{-1})	5.1 10^3	5.5 10^2
Half time in $\sqrt[3]{3.407}$ G.I. Tract (s)	5.4 10^4	5.4 10^4
Mean life (y)	6	1
Soil consumption as % of dry matter intake	4 $\sqrt[3]{3.517}$	20 $\sqrt[3]{3.527}$
Weight of muscle, kg $\sqrt[3]{3.407}$	230	18*
Weight of liver, kg	6	0.8
Milk production rate ($l.y^{-1}$)	3.65 10^3	-
Number of animals/unit area	250	200
Total body weight $\sqrt[3]{3.407}$, kg	530	65
Inhalation rate $\sqrt[3]{3.407}$ ($m^3.s^{-1}$)	1.5 10^{-3}	1 10^{-4}

*This value may vary significantly with the age of slaughter of the animal.

Table 3.18 Element dependent parameters for cattle (1)

Element	Fraction of the daily intake by ingestion transferred		Fraction of daily intake by inhalation transferred		Biological half-life, $\sqrt{3.557}$	
	per litre of milk	per kg of muscle $\sqrt{3.43}, 3.54$	per litre of milk	per kg of muscle	Muscle	Liver
Chromium	$2 \cdot 10^{-3}$	$5 \cdot 10^{-3}$	$2 \cdot 10^{-3}$	$6 \cdot 10^{-3}$	$9 \cdot 10^{-2}$	$9 \cdot 10^{-2}$
Manganese	$1 \cdot 10^{-4}$	$5 \cdot 10^{-3}$	$3 \cdot 10^{-4}$	$1 \cdot 10^{-2}$	$6 \cdot 10^{-2}$	$7 \cdot 10^{-2}$
Iron	$6 \cdot 10^{-5}$	$1 \cdot 10^{-3}$	$2 \cdot 10^{-4}$	$3 \cdot 10^{-3}$	$5 \cdot 10^0$	$5 \cdot 10^0$
Cobalt	$2 \cdot 10^{-3}$	$1 \cdot 10^{-3}$	$3 \cdot 10^{-3}$	$2 \cdot 10^{-3}$	$5 \cdot 10^{-1}$	$5 \cdot 10^{-1}$
Zinc	$1 \cdot 10^{-2}$	$2 \cdot 10^{-3}$	$7 \cdot 10^{-3}$	$1 \cdot 10^{-3}$	$8 \cdot 10^{-1}$	$8 \cdot 10^{-1}$
Rubidium	$1 \cdot 10^{-2}$	$1 \cdot 10^{-2}$	$6 \cdot 10^{-3}$	$6 \cdot 10^{-3}$	$1 \cdot 10^{-1}$	$1 \cdot 10^{-1}$
Strontium(2)	$1 \cdot 10^{-3}$	$2 \cdot 10^{-3}$	$2 \cdot 10^{-3}$	$4 \cdot 10^{-3}$	$5 \cdot 10^{-2}$	$5 \cdot 10^{-2}$
Yttrium	$2 \cdot 10^{-5}$	$6 \cdot 10^{-3}$	$1 \cdot 10^{-2}$	$3 \cdot 10^0$	$4 \cdot 10^1$	$4 \cdot 10^1$
Zirconium	$8 \cdot 10^{-2}$	$5 \cdot 10^{-4}$	$8 \cdot 10^{-2}$	$6 \cdot 10^{-2}$	$2 \cdot 10^{-2}$	$2 \cdot 10^{-2}$
Niobium	$2 \cdot 10^{-2}$	$5 \cdot 10^{-4}$	$2 \cdot 10^{-2}$	$3 \cdot 10^{-3}$	$3 \cdot 10^{-1}$	$3 \cdot 10^{-1}$
Molybdenum	$1 \cdot 10^{-3}$	$1 \cdot 10^{-2}$	$2 \cdot 10^{-3}$	$2 \cdot 10^{-2}$	$1 \cdot 10^{-1}$	$1 \cdot 10^{-1}$
Technetium	$1 \cdot 10^{-2}$	$1 \cdot 10^{-2} \sqrt{3.457}$	$7 \cdot 10^{-3}$	$7 \cdot 10^{-3}$	$8 \cdot 10^{-3}$	$8 \cdot 10^{-3}$
Ruthenium	$6 \cdot 10^{-7}$	$1 \cdot 10^{-3}$	$1 \cdot 10^{-6}$	$2 \cdot 10^{-3}$	$7 \cdot 10^{-1}$	$7 \cdot 10^{-1}$

continued

Table 3.18 (Continued) Element dependent parameters for cattle (1)

Element	Fraction of the daily intake by ingestion transferred		Fraction of daily intake by inhalation transferred		Biological half-life, $\sqrt{3.55/Y}$	
	per litre of milk	per kg of muscle $\sqrt{3.43}, 3.547$	per litre of milk	per kg of muscle	Muscle	Liver
Silver	$3 \cdot 10^{-2}$	$1 \cdot 10^{-3}$	$5 \cdot 10^{-2}$	$2 \cdot 10^{-3}$	$1 \cdot 10^{-1}$	$1 \cdot 10^{-1}$
Antimony	$2 \cdot 10^{-5}$	$5 \cdot 10^{-3}$	$3 \cdot 10^{-5}$	$8 \cdot 10^{-3}$	$5 \cdot 10^{-2}$	$5 \cdot 10^{-2}$
Tellurium	$2 \cdot 10^{-4}$	$5 \cdot 10^{-3}$	$3 \cdot 10^{-4}$	$8 \cdot 10^{-3}$	$5 \cdot 10^{-2}$	$5 \cdot 10^{-2}$
Iodine	$1 \cdot 10^{-2}$	$2 \cdot 10^{-2}$	$6 \cdot 10^{-3}$	$1 \cdot 10^{-2}$	$5 \cdot 10^{-2}$	$5 \cdot 10^{-2}$
Caesium	$7 \cdot 10^{-3}$	$3 \cdot 10^{-2}$	$4 \cdot 10^{-3}$	$2 \cdot 10^{-2}$	$3 \cdot 10^{-1}$	$3 \cdot 10^{-1}$
Barium	$3 \cdot 10^{-4}$	$5 \cdot 10^{-4}$	$2 \cdot 10^{-3}$	$2 \cdot 10^{-3}$	$9 \cdot 10^{-2}$	$9 \cdot 10^{-2}$
Lanthanum	$2 \cdot 10^{-5}$	$5 \cdot 10^{-3}$	$4 \cdot 10^{-3}$	$9 \cdot 10^{-1}$	$1 \cdot 10^1$	$1 \cdot 10^1$
Cerium	$2 \cdot 10^{-5}$	$1 \cdot 10^{-3}$	$4 \cdot 10^{-3}$	$2 \cdot 10^{-1}$	$1 \cdot 10^1$	$1 \cdot 10^1$
Promethium	$2 \cdot 10^{-5}$	$5 \cdot 10^{-3}$	$1 \cdot 10^{-2}$	$3 \cdot 10^0$	$1 \cdot 10^1$	$1 \cdot 10^1$
Europium	$2 \cdot 10^{-5}$	$5 \cdot 10^{-3}$	$1 \cdot 10^{-2}$	$3 \cdot 10^0$	$1 \cdot 10^1$	$1 \cdot 10^1$

Notes

(1) The fractions transferred to unit mass of muscle and liver of sheep can be derived from the following expression

$$f_{s,i} = f_{c,i} \cdot \frac{M_{c,i}}{M_{s,i}}$$

where $f_{s,i}$ and $f_{c,i}$ are the fractions transferred to unit mass of tissue i , in sheep and cattle respectively

$M_{s,i}$ and $M_{c,i}$ are the masses of tissue i , in sheep and cattle respectively

(2) A review of data on this transfer parameter which became available after the completion of the report shows significant changes compared with the values quoted above [Ng Y.C., Colsher C.S., and Thompson, S.E., IAEA Vienna, March 1979]

Table 3.19 The time integrals of activity transferred to unit mass of various plants

Plant	Nuclide	Time integral of activity per unit mass of plant (Bq y kg ⁻¹) to time t.				
		1 y	50 y	100 y	500 y	Infinity
Green Vegetables	Sr-90	9.2E+04	1.2E+06	1.5E+06	1.5E+06	1.5E+06
	I-129	1.6E+05	2.2E+05	2.6E+05	3.5E+05	3.6E+05
	I-131	3.3E+04	3.3E+04	3.3E+04	3.3E+04	3.3E+04
	Cs-137	1.6E+05	1.9E+05	2.0E+05	2.0E+05	2.0E+05
	Pu-239	8.0E+04	8.0E+04	8.0E+04	8.1E+04	8.1E+04
	Am-241	8.0E+04	8.2E+04	8.4E+04	8.8E+04	8.8E+04
Grain	Sr-90	2.0E+05	2.3E+05	2.4E+05	2.4E+05	2.4E+05
	I-129	4.0E+05	4.6E+05	5.0E+05	5.9E+05	6.0E+05
	I-131	8.1E+04	8.1E+04	8.1E+04	8.1E+04	8.1E+04
	Cs-137	4.0E+05	4.1E+05	4.1E+05	4.1E+05	4.1E+05
	Pu-239	2.0E+05	2.0E+05	2.0E+05	2.0E+05	2.0E+05
	Am-241	2.0E+05	2.0E+05	2.0E+05	2.0E+05	2.0E+05
Root Crops	Sr-90	1.0E+05	1.0E+05	1.2E+05	1.3E+05	1.3E+05
	I-129	3.5E+02	5.5E+04	9.7E+04	1.9E+05	1.9E+05
	I-131	3.7E+01	3.9E+01	3.9E+01	3.9E+01	3.9E+01
	Cs-137	8.8E+01	8.6E+03	1.1E+04	1.1E+04	1.1E+04
	Pu-239	1.7E+01	2.8E+03	4.9E+03	9.5E+03	9.8E+03
	Am-241	1.7E+01	2.7E+03	4.6E+03	7.9E+03	8.1E+03

Notes

- (1) The time integrals per unit mass of plant have been evaluated for continuous deposition of each radionuclide for 1 year at a rate of 1 Bq m⁻² s⁻¹.
- (2) The yields of each plant in kg m⁻² y⁻¹ are given in Table 3.15

Table 3.20 The time integrals of activity in various food products derived from cows grazing contaminated pasture¹⁾

Animal Product	Nuclide	Time integral of activity in animal products (Bq y kg ⁻¹)				
		1 y	50 y	100 y	500 y	Infinity
Meat	Sr-90	6.8E+04	8.0E+05	8.5E+05	8.5E+05	8.5E+05
	I-129	3.7E+05	1.2E+06	1.3E+06	1.3E+06	1.3E+06
	I-131	4.4E+04	4.6E+04	4.6E+04	4.6E+04	4.6E+04
	Cs-137	3.5E+05	1.5E+06	1.5E+06	1.5E+06	1.5E+06
	Pu-239	7.5E+00	3.0E+02	3.0E+02	3.0E+02	3.0E+02
	Am-241	3.3E+02	5.5E+03	5.5E+03	5.5E+03	5.5E+03
Liver	Sr-90	6.8E+04	8.0E+05	8.5E+05	8.6E+05	8.6E+05
	I-129	3.7E+05	1.2E+06	1.3E+06	1.3E+06	1.3E+06
	I-131	4.4E+04	4.6E+04	4.6E+04	4.6E+04	4.6E+04
	Cs-137	3.5E+05	1.5E+06	1.6E+06	1.6E+06	1.6E+06
	Pu-239	9.0E+02	3.7E+04	3.7E+04	3.7E+04	3.7E+04
	Am-241	4.0E+04	6.8E+05	6.8E+05	6.8E+05	6.8E+05
Milk	Sr-90	3.9E+04	4.1E+05	4.3E+05	4.3E+05	4.3E+05
	I-129	2.0E+05	6.2E+05	6.5E+05	6.6E+05	6.6E+05
	I-131	7.5E+04	7.6E+04	7.6E+04	7.6E+04	7.6E+04
	Cs-137	1.4E+05	3.8E+05	3.9E+05	3.9E+05	3.9E+05
	Pu-239	1.4E+01	5.5E+00	5.5E+00	5.5E+00	5.5E+00
	Am-241	6.1E+00	1.0E+02	1.0E+02	1.0E+02	1.0E+02

Notes

- (1) The time integrals correspond to the activity in unit mass of the respective foodstuffs following the continuous deposition of activity on land at a rate of 1 Bq m⁻² s⁻¹ for one year.

Table 3.21 The time integrals of activity in various food products derived from sheep grazing contaminated pasture ¹⁾

Animal Product	Nuclide	Time integral of activity in animal products (Bq y kg ⁻¹)				
		1y	50 y	100 y	500 y	Infinity
Meat	Sr-90	2.3E+05	1.2E+06	1.2E+06	1.2E+06	1.2E+06
	I-129	1.9E+06	4.5E+06	4.6E+06	4.6E+06	4.6E+06
	I-131	2.1E+05	2.2E+05	2.2E+05	2.2E+05	2.2E+05
	Cs-137	1.6E+06	4.7E+06	4.8E+06	4.8E+06	4.8E+06
	Pu-239	3.0E+01	1.7E+02	1.7E+02	1.7E+02	1.7E+02
	Am-241	1.5E+03	7.2E+03	7.1E+03	7.1E+03	7.1E+03
Liver	Sr-90	1.3E+05	6.9E+05	7.1E+05	7.1E+05	7.1E+05
	I-129	1.1E+06	2.6E+06	2.7E+06	2.7E+06	2.7E+06
	I-131	1.2E+05	1.3E+05	1.3E+05	1.3E+05	1.3E+05
	Cs-137	9.5E+05	2.8E+06	2.8E+06	2.8E+06	2.8E+06
	Pu-239	2.1E+03	1.2E+04	1.2E+04	1.2E+04	1.2E+04
	Am-241	1.0E+05	5.1E+05	5.1E+05	5.1E+05	5.1E+05

Notes

- 1) The time integrals correspond to the activity in unit mass of the respective foodstuffs following the continuous deposition of activity on land at a rate of $1 \text{ Bq m}^{-2} \text{ s}^{-1}$ for 1 year.

Table 3.22 The time integral of activity in animal products derived from cows and sheep inhaling activity at a concentration of 1 Bq m^{-3} in the atmosphere.¹⁾

Animal Product	Nuclide	Time integral of activity in animal products (Bq y kg^{-1})	
		Cows	Sheep
Meat	Sr-90	$4.5\text{E-}01$	$3.5\text{E-}01$
	I-129	$1.6\text{E+}00$	$1.3\text{E+}00$
	I-131	$4.6\text{E-}01$	$3.8\text{E-}01$
	Cs-137	$2.4\text{E+}00$	$1.3\text{E+}00$
	Pu-239	$1.7\text{E+}00$	$1.1\text{E-}01$
	Am-241	$4.1\text{E+}00$	$4.2\text{E-}01$
Liver	Sr-90	$4.5\text{E-}01$	$2.1\text{E-}01$
	I-129	$1.6\text{E+}00$	$7.5\text{E-}01$
	I-131	$4.6\text{E-}01$	$2.2\text{E-}01$
	Cs-137	$2.4\text{E+}00$	$7.7\text{E-}01$
	Pu-239	$2.1\text{E+}02$	$7.7\text{E+}00$
	Am-241	$5.1\text{E+}02$	$3.0\text{E+}01$
Milk	Sr-90	$2.2\text{E-}01$	-
	I-129	$8.1\text{E-}01$	-
	I-131	$7.6\text{E-}01$	-
	Cs-137	$5.7\text{E-}01$	-
	Pu-239	$3.1\text{E-}02$	-
	Am-241	$7.5\text{E-}02$	-

Note

- 1) The time integral of activity corresponding to the inhalation of activity for 1 year at an air concentration of 1 Bq m^{-3}

Table 3.23

Time integral of the effective dose equivalent rate (Sv)
 from the external irradiation due to photons
 from 1 years deposition at a rate of $1 \text{ Bq m}^{-2} \text{ s}^{-1}$

Radionuclide	Time integral of the effective dose equivalent rate (Sv)			
	1 y	50 y	500 y	Infinity
Zirconium-95	0.11	0.15	0.15	0.15
Iodine-131	$9.6 \cdot 10^{-3}$	$9.9 \cdot 10^{-3}$	$9.9 \cdot 10^{-3}$	$9.9 \cdot 10^{-3}$
Caesium-137 + D	0.23	14	16	16
Plutonium-239	$7.7 \cdot 10^{-4}$	$5.5 \cdot 10^{-2}$	$7.8 \cdot 10^{-2}$	$7.8 \cdot 10^{-2}$
Plutonium-241	$6.5 \cdot 10^{-6}$	$2.4 \cdot 10^{-4}$	$2.4 \cdot 10^{-4}$	$2.4 \cdot 10^{-4}$
Americium-241*	$1.7 \cdot 10^{-6}$	$1.5 \cdot 10^{-3}$	$2.0 \cdot 10^{-3}$	$2.0 \cdot 10^{-3}$

*This component is due to the in-growth of americium-241 as the daughter of plutonium-241

Table 3.24: Definition of the large squares (10^4 km^2) on the European Grid

Degrees	Distance from Previous Parallel	Distance Between 2 Meridians	Area (km^2)
35.15		136.3	
35.81	73.6	135.2	10000.7
36.48	74.2	134.1	10002.5
37.16	74.9	132.9	10004.3
37.83	75.5	131.7	10006.1
38.52	76.3	130.4	9994.9
39.21	77.0	129.2	9997.1
39.92	77.8	127.9	9999.4
40.62	78.5	126.5	10001.8
41.34	79.4	125.2	10004.2
42.06	80.3	123.8	9904.3
42.79	81.2	122.3	9997.2
43.53	82.1	120.9	10000.2
44.28	83.2	119.4	10003.3
45.04	84.3	117.8	9994.7
45.81	85.5	116.2	9998.5
46.59	86.6	114.6	10002.3
47.38	87.9	112.9	9994.9
48.18	89.3	111.2	9999.6
49.00	90.6	109.4	10004.3
49.83	92.2	107.5	10002.9
50.68	93.9	105.6	9997.5
51.53	95.6	103.7	10002.1
52.41	97.4	101.7	9995.6
53.30	99.4	99.6	9998.8
54.22	101.5	97.5	10000.9
55.15	103.8	95.3	10001.9
56.11	106.3	93.0	10001.8
57.09	109.0	90.6	10000.3
58.10	112.0	88.1	9997.4
59.13	115.2	85.5	10001.6
60.20	118.8	82.8	10003.0
61.31	122.8	80.0	10001.7
62.45	127.3	77.1	9997.1
63.64	132.4	74.0	10003.7
64.89	138.2	70.7	9997.0
66.19	144.9	67.3	9997.7
67.57	152.9	63.6	10001.7
69.03	162.3	59.7	9998.1

Table 3.25 Acquisition of Data

COUNTRY	POPULATION DATA		GEOGRAPHICAL DATA		METHOD OF OBTAINING GEOGRAPHICAL COORDINATES
	Year	Units (number or dimension)	Centres of unit	Projection System	
Belgium	1970	Community (2355)	Centre of habitation (usually bell tower of principal church)	Lambert belge	Computer program
Germany	1970	Community (23,000)		Gauss-Kruger	Computer program
Denmark	1970	Large community (270)	Centre of habitation (0 for road distances)	-	Cartographic method
France	1975	Community (36,000)	Main point of commune	Geographical coordinates (in milligrads)	
Great Britain	1971	10km squares (2675 with non zero values)	-	National Grid of G.B.	Hand calculation
Italy		1km squares	-	Gauss-Boaga	Computer program
Ire and Northern Ireland	1971	10km squares (914)	-	Irish grid	Cartographic method
Luxembourg	1971				Cartographic method
Netherlands	1971	Community (900)	Central point (usually Town Hall)		Cartographic method

LONGITUDES

L	70	71	72	73	74	75	76	77	78	79
A	I	I	I	I	I	I	I	I	I	I
Y 109	0	I	0	I	0	I	0	I	0	I
I	I	I	I	I	I	I	I	I	I	I
Y 108	0	I	0	I	0	I	0	I	0	I
U	I	I	I	I	I	I	I	I	I	I
D 107	0	I	0	I	0	I	0	I	0	I
E	I	I	I	I	I	I	I	I	I	I
S 106	0	I	0	I	0	I	0	I	0	I
I	I	I	I	I	I	I	I	I	I	I
I 105	0	I	0	I	0	I	0	I	0	I
I	I	I	I	I	I	I	I	I	I	I
I 104	0	I	0	I	0	I	14086	0	I	0
I	I	I	I	I	I	I	I	I	I	I
I 103	0	I	0	I	0	I	31100	0	I	8695
I	I	I	I	I	I	I	I	I	I	I
I 102	0	I	0	I	0	I	9348	0	I	0
I	I	I	I	I	I	I	I	I	I	I
I 101	0	I	0	I	0	I	9217	0	I	0
I	I	I	I	I	I	I	I	I	I	I
I 100	0	I	0	I	8066	I	8819	0	I	13728
I	I	I	I	I	I	I	I	I	I	I

POPULATION IN SQUARE (7,10) = 122501

TABLE 3.26

Distribution of the population in (7,10) grid

Table 3.27

An example of the quantitative data of agricultural production obtained for one square (10,000 km²) of the grid

Data given by the program.

Number of squares: 86(1) Abscissa: 8 ordinate -5

Geographical composition of the square (2)

% surface	No code Dept	Department	No code Region	Region	No code Country	Country
20	141	Brescia	36	Lombardia	3	Italy
45	144	Mantova	36	"	3	"
81	146	Trento	37	Trentindatoadige	3	"
97	147	Verona	38	Veneto	3	"
100	148	Vicenta	38	"	3	"
6	149	Belluno	38	"	3	"
2	150	Tasuiso	38	"	3	"
52	152	Padona	38	"	3	"

Agricultural Production

- milk products (in tonnes of milk or equivalent to tonnes of milk)
- milk for consumption: 29400 Sour milk: 3600 fresh cheese: 14700
 cream: 10800 butter: 148500 other cheese: 305200 powdered milk:
 1300 evaporated milk: 1200
- meat products
- Cattle killed (100's of head): 2657 Cattle meat (tonne): 55500
- Veal " " 806 Veal " " 7600
- Pigs " " 4829 Pork " " 39600
- Sheep & Goats " 146 Sheep & Goats " 100
- Cattle liver (kg): 1434700
- Veal " " 181500
- Pigs " " 652000
- Sheep & Goats " 5100

continued

Table 3.27 (continued)

- vegetable products (tonnes fresh weight)

wheat: 447300 barley: 10500 potatoes: 175900

green vegetables (leafy): 31300 leguminous vegetables: 59000

root vegetables: 8900

Notes

- (1) The square number is a parameter which is used in the computer program. There are 267 squares of the grid listed from the south to the north and from the west to the east.
- (2) The geographic composition of the grid is only contained in the computer listing and not on the magnetic tape which only contains the grid reference and the agricultural production data.

Table 3.28 Radii used in the transformation of results

Number	Distance on the ground (km)	Length of the projection (km)
1	1	1.000
2	2	2.000
3	3	3.000
4	5	5.000
5	7	7.000
6	10	10.000
7	15	15.000
8	20	20.000
9	35	35.000
10	50	50.000
11	70	70.001
12	100	100.002
13	200	200.016
14	300	300.055
15	450	450.187
16	700	700.705
17	1100	1102.741
18	1600	1608.464
19	2000	2016.592
20	2400	2428.800
21	3000	3056.707

DISTANCE (km)								
SECTEUR	15-20	20-35	35-50	50-70	70-100	100-200	200-300	
0-20	0.1240E+02	0.6750E+02	0.1147E+03	0.4549E+03	0.1606E+04	0.2422E+05	0.7617E+05	
20-40	0.1612E+02	0.1835E+03	0.6909E+03	0.1522E+04	0.3258E+04	0.3366E+05	0.1091E+06	
40-60	0.2046E+02	0.4775E+03	0.8109E+03	0.1531E+04	0.3258E+04	0.3853E+05	0.5363E+05	
60-80	0.6122E+02	0.5285E+03	0.6181E+03	0.1528E+04	0.3276E+04	0.5120E+05	0.7711E+05	
80-100	0.7922E+02	0.5213E+03	0.8217E+03	0.1531E+04	0.3259E+04	0.5075E+05	0.7381E+05	
100-120	0.6184E+02	0.5188E+03	0.7408E+03	0.1261E+04	0.2554E+04	0.3739E+05	0.5975E+05	
120-140	0.1984E+02	0.4067E+03	0.6227E+03	0.1184E+04	0.2505E+04	0.3058E+05	0.3511E+05	
140-160	0.2467E+02	0.3092E+03	0.5887E+03	0.1179E+04	0.2496E+04	0.2998E+05	0.4437E+05	
160-180	0.3143E+02	0.1969E+03	0.3435E+03	0.7534E+03	0.1866E+04	0.3851E+05	0.8438E+05	
180-200	0.5259E+02	0.3416E+03	0.4941E+03	0.9148E+03	0.1886E+04	0.4921E+05	0.9856E+05	
200-220	0.3990E+02	0.2895E+03	0.4400E+03	0.8086E+03	0.1712E+04	0.1226E+05	0.2433E+05	
220-240	0.1922E+02	0.2209E+03	0.4323E+03	0.8029E+03	0.9651E+03	0.6905E+03	0.4096E+04	
240-260	0.1984E+02	0.9321E+02	0.2484E+03	0.6423E+03	0.1156E+03	0.5429E+02	0.0	
260-280	0.1922E+02	0.8928E+02	0.1383E+03	0.2287E+03	0.1753E+03	0.3863E+03	0.0	
280-300	0.1860E+02	0.9052E+02	0.1376E+03	0.2523E+03	0.1968E+03	0.5420E+03	0.0	
300-320	0.1984E+02	0.9052E+02	0.1376E+03	0.2592E+03	0.3845E+03	0.6083E+03	0.8060E+01	
320-340	0.2356E+02	0.9238E+02	0.1401E+03	0.2598E+03	0.5511E+03	0.1738E+04	0.3682E+03	
340-360	0.2108E+02	0.1054E+03	0.1575E+03	0.2933E+03	0.5995E+03	0.6866E+04	0.1601E+05	

TABLE 3.29

Distribution of the fresh milk production, in $t y^{-1}$, in the 20° sectors centered on a site in the Rhone valley

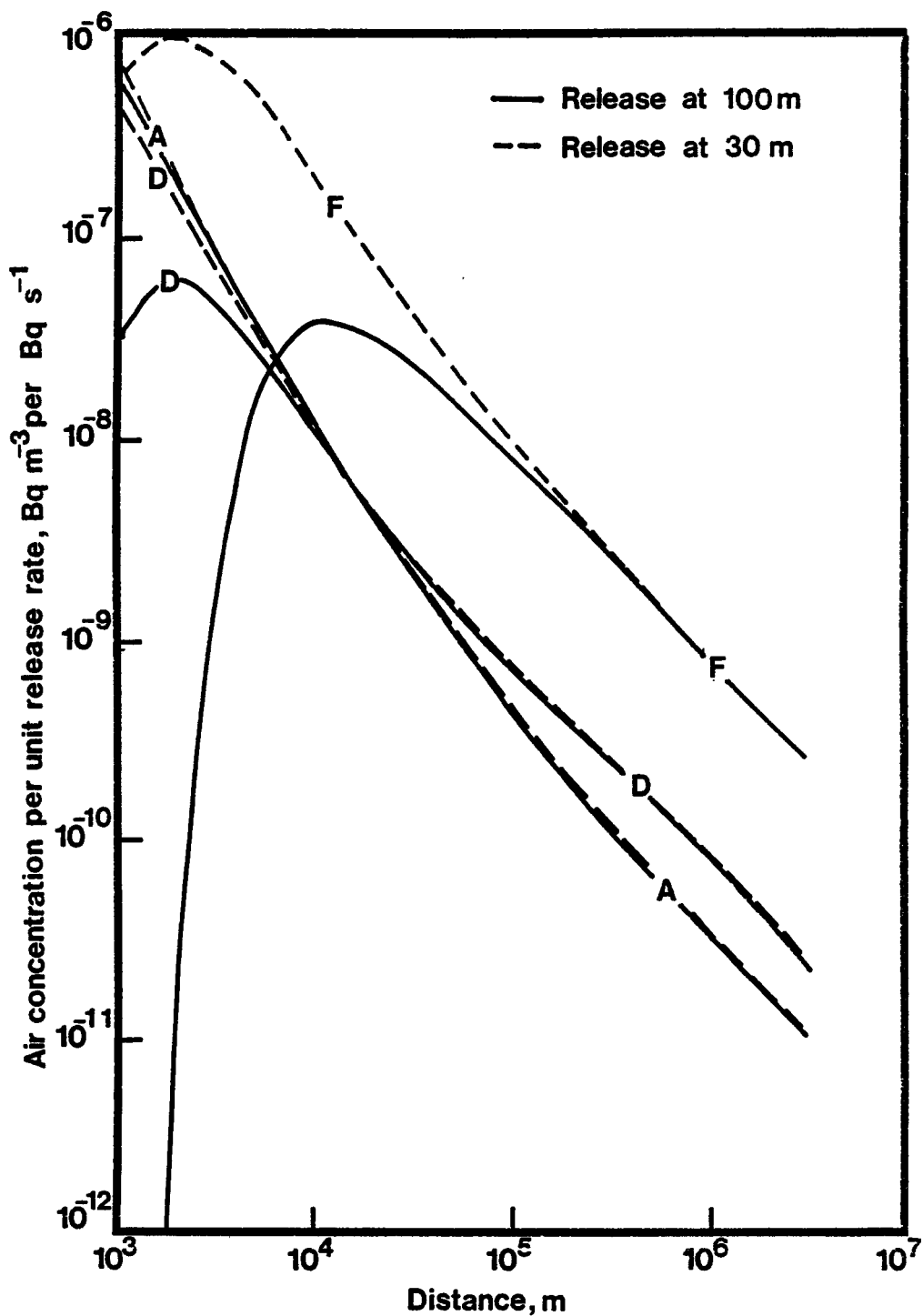


Figure 3.1 The variation of air concentration with distance for a non-depositing nuclide showing the influence of release height and dispersion conditions assuming uniform windrose

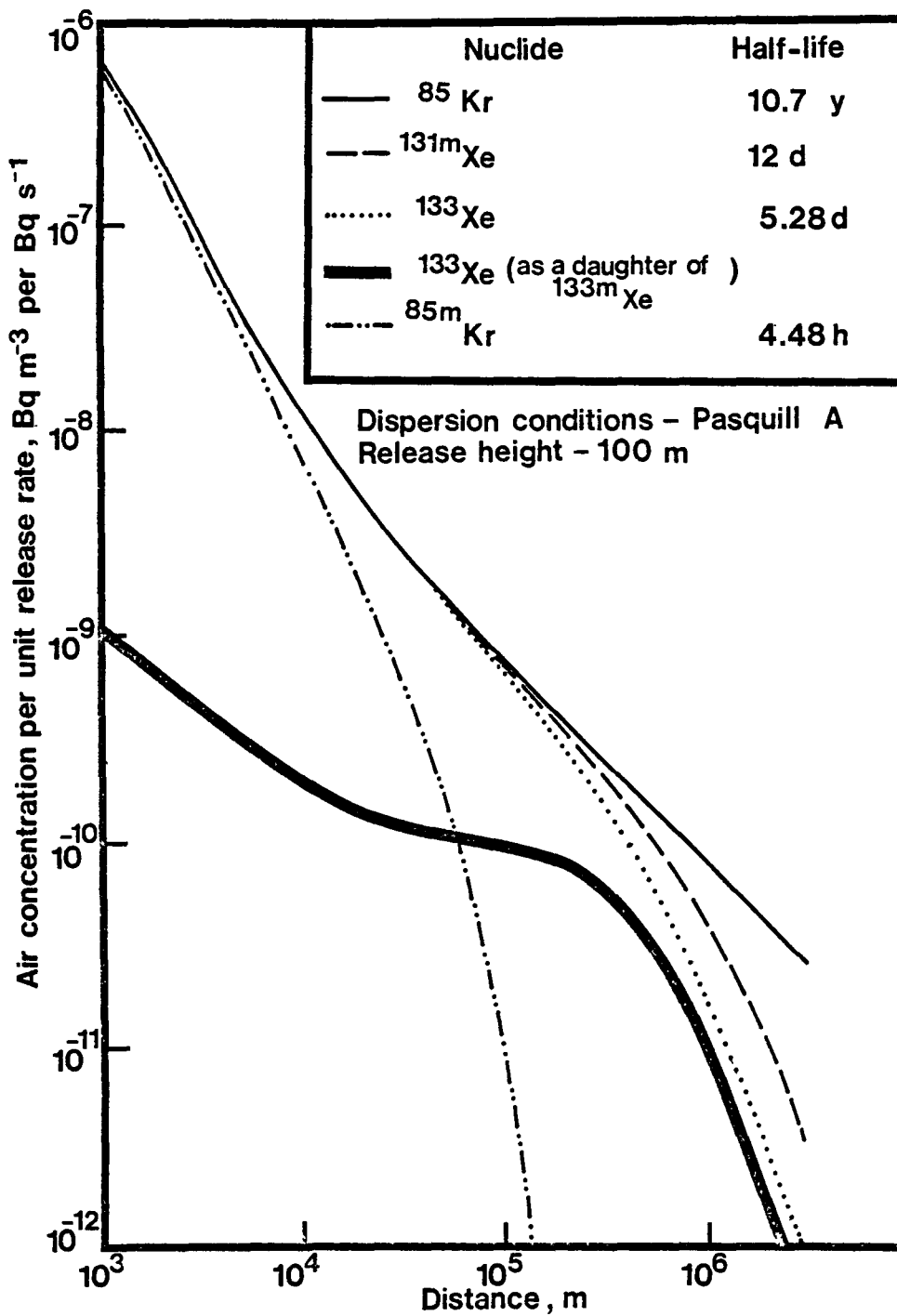


Figure 3.2 Variation in air concentration with distance for noble gases of various half-lives assuming uniform windrose

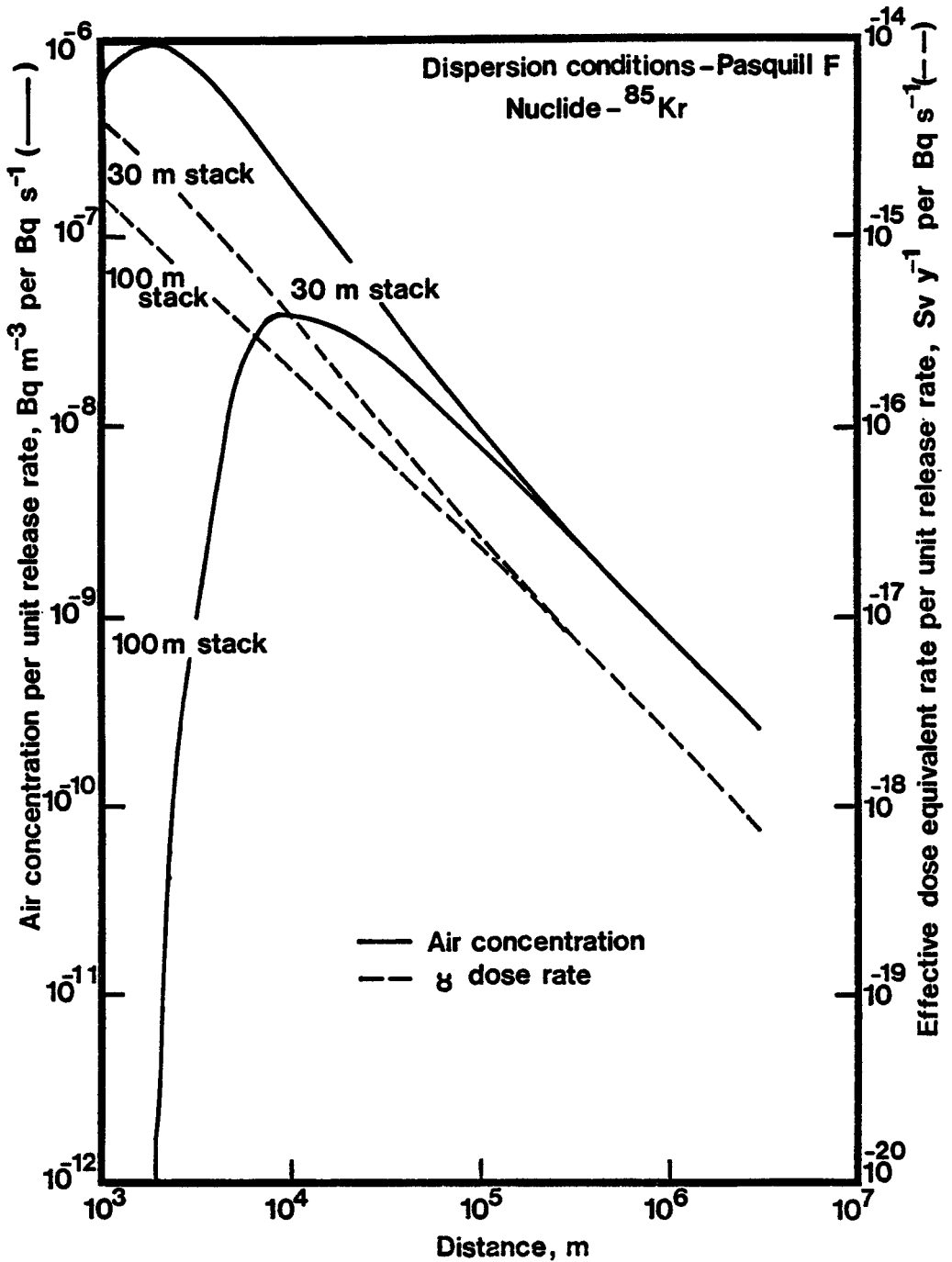


Figure 3.3 The variation of air concentration and external dose rate with release height assuming uniform windrose

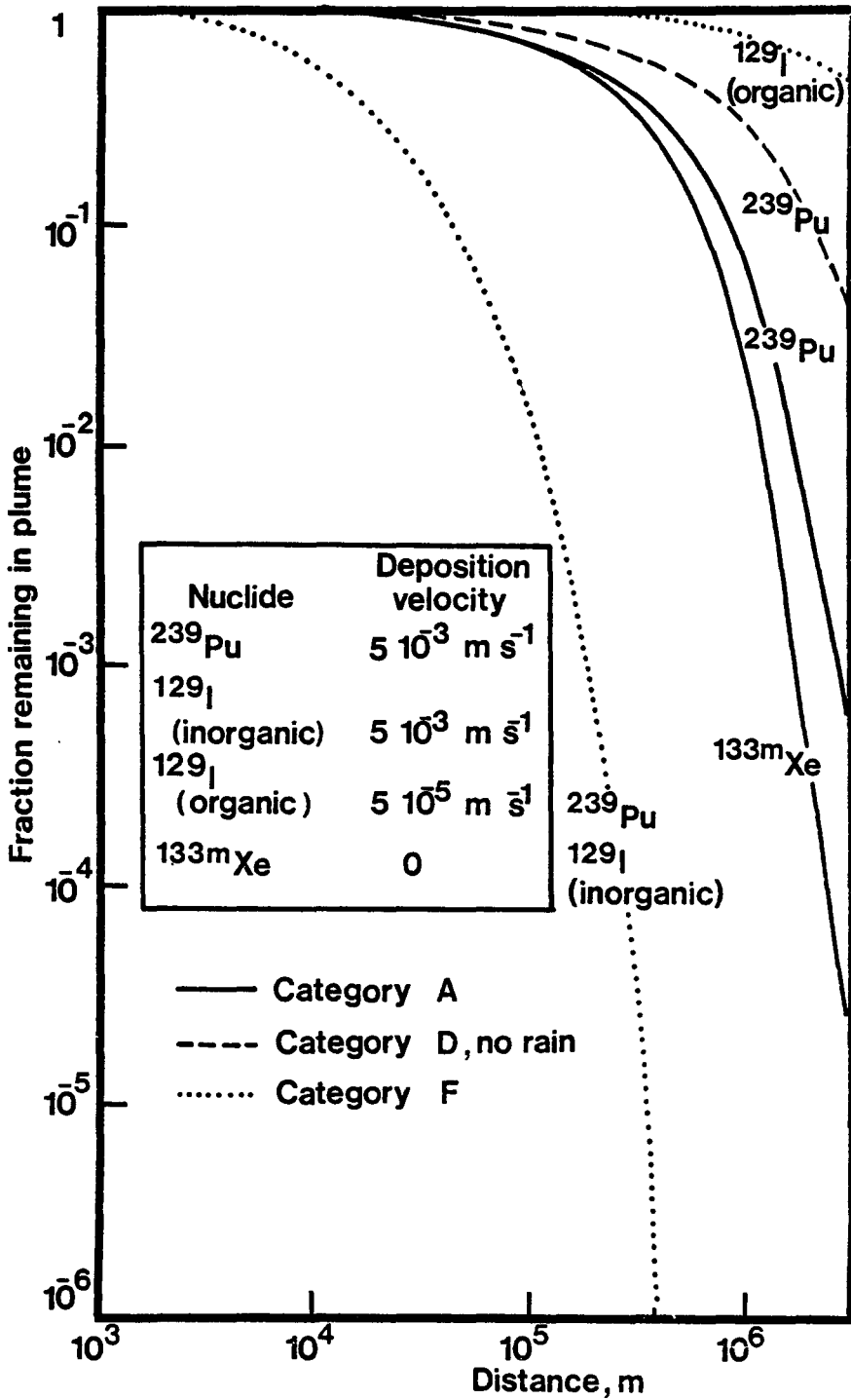


Figure 3.4 The fraction of activity remaining in the plume for the release of various nuclides at 30 m in various dispersion conditions

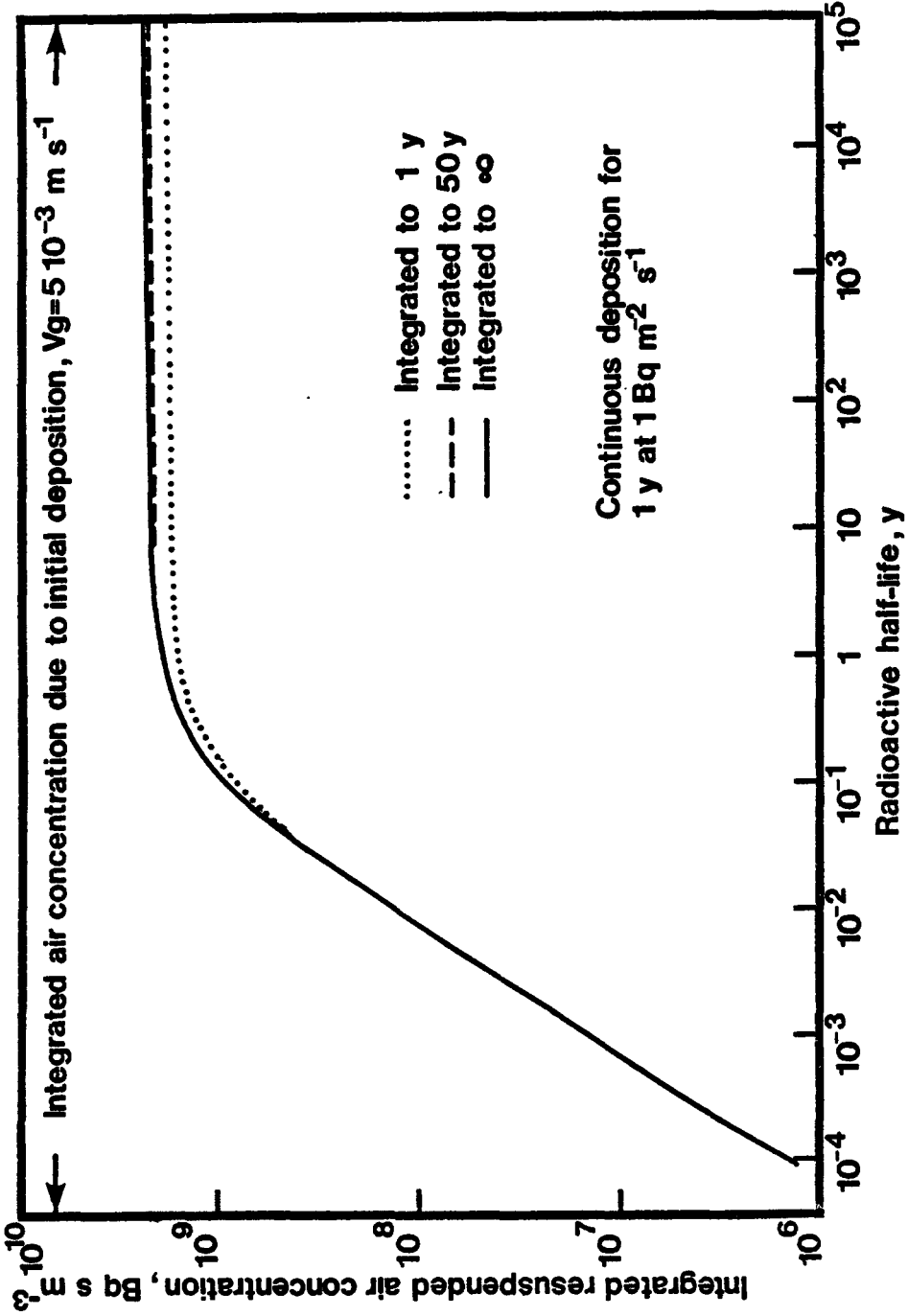


Figure 3.5 The variation of the integrated resuspended air concentration with radioactive half-life

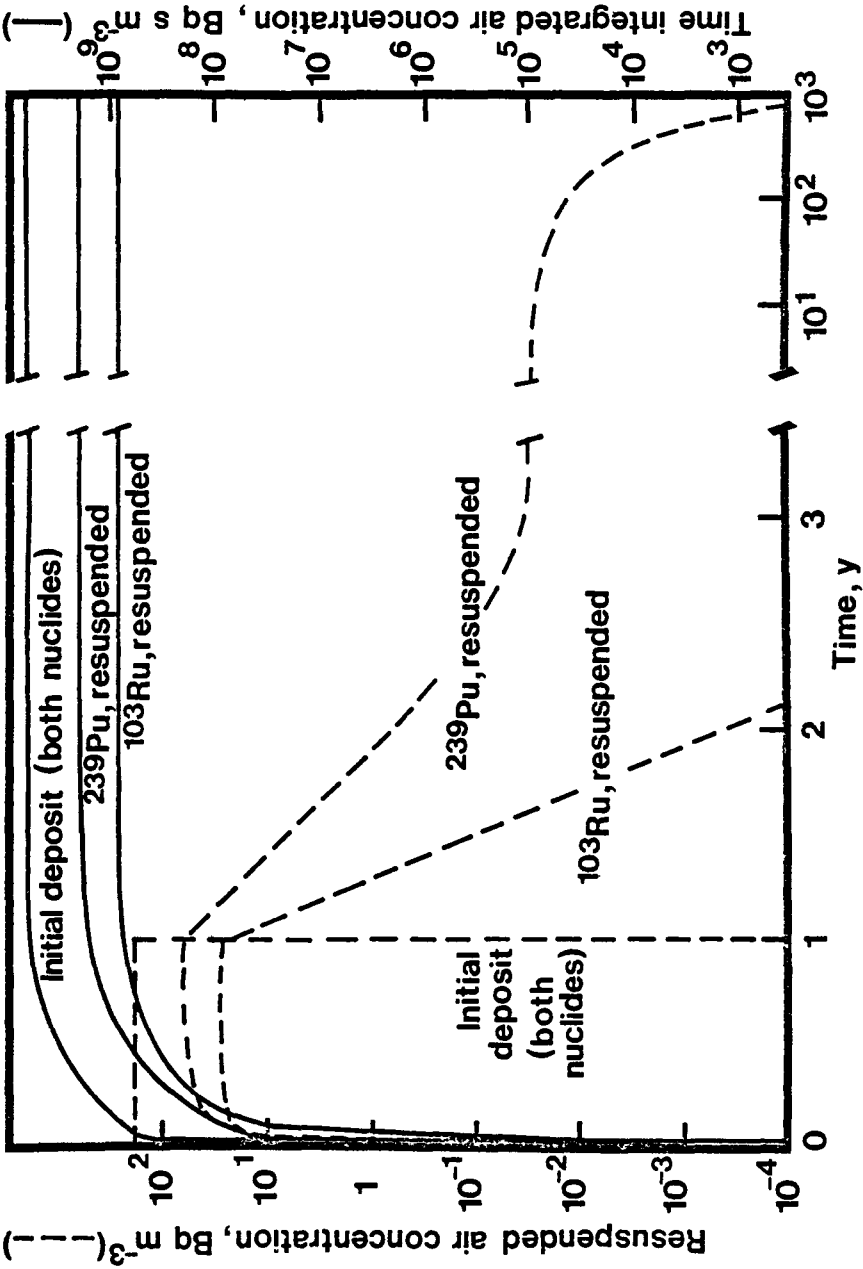


Figure 3.6 Variation of the air concentration during the initial deposition and the subsequent resuspended air concentrations with time

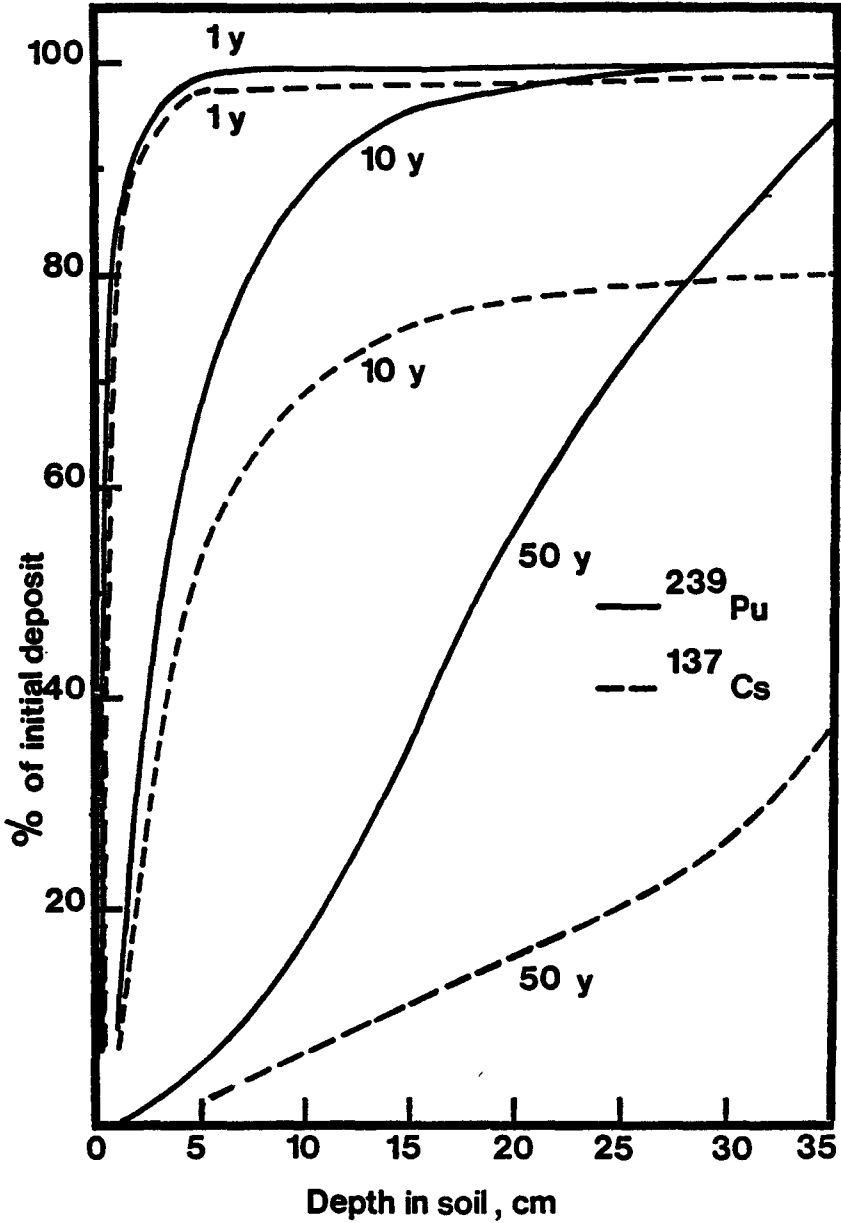


Figure 3.7 The rate of migration of plutonium-239 and caesium-137 into undisturbed soil as a function of time after the initial deposit

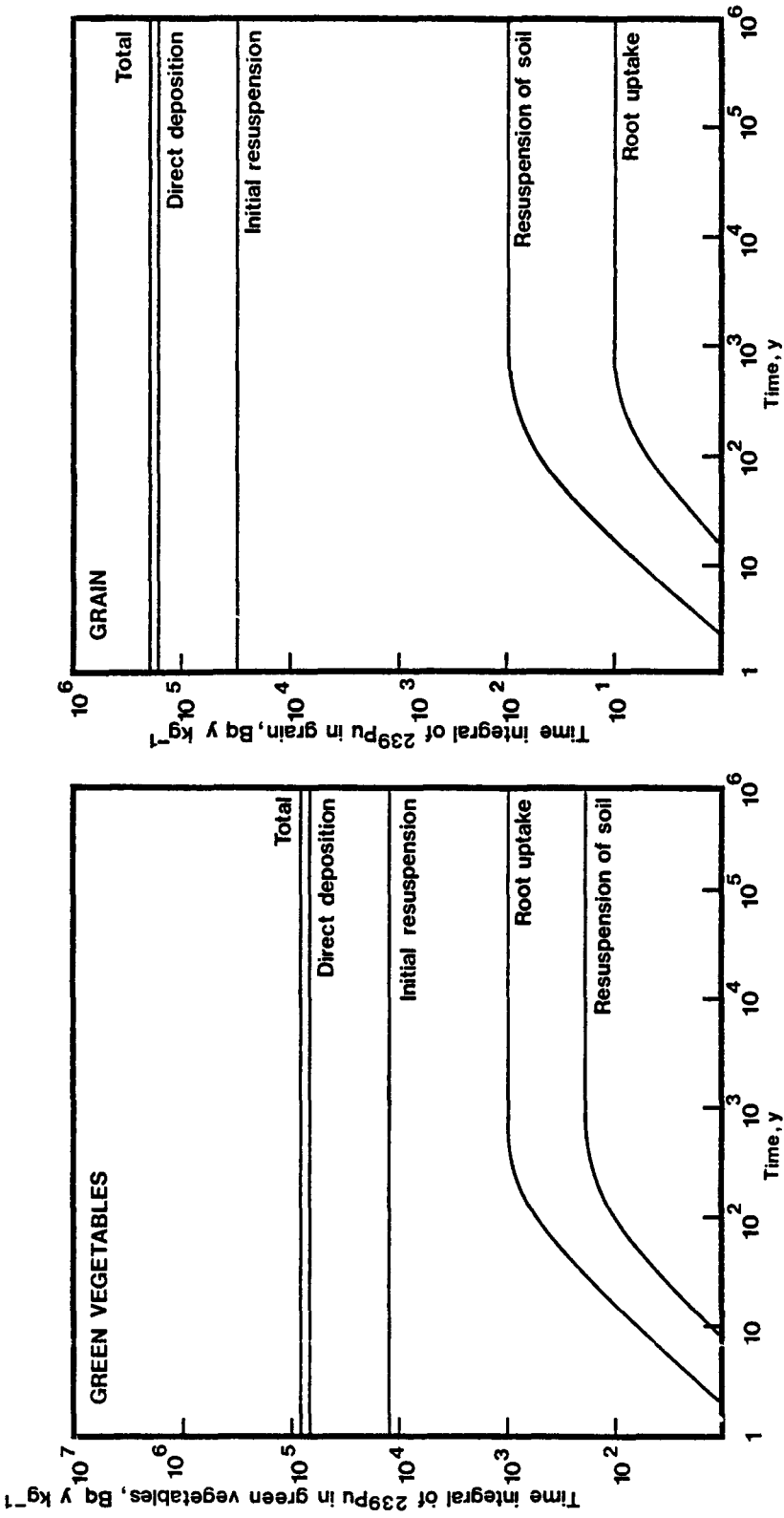


Figure 3.8 The relative importance and time dependence of the important mechanisms for the transfer of plutonium-239 to green vegetables and grain

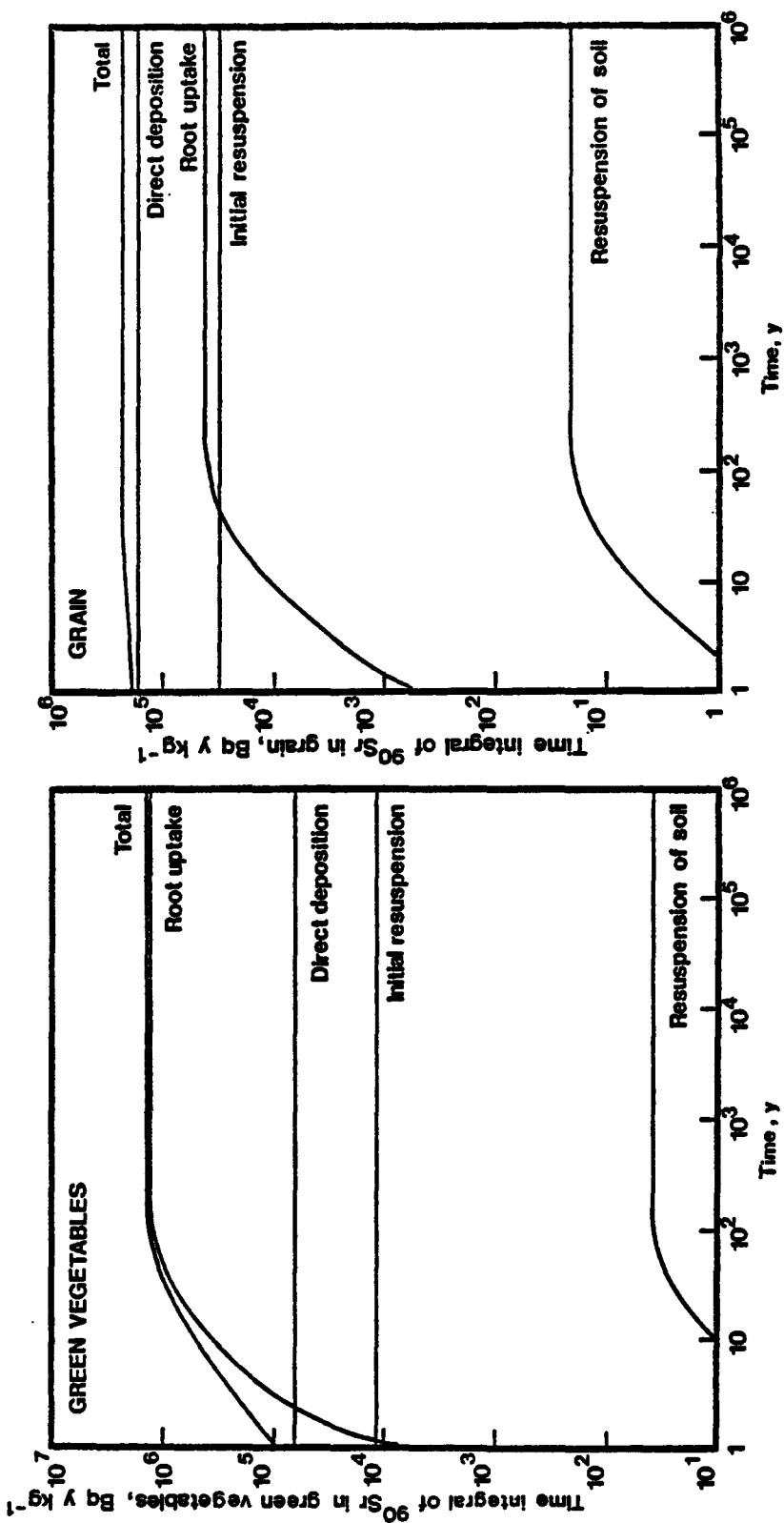
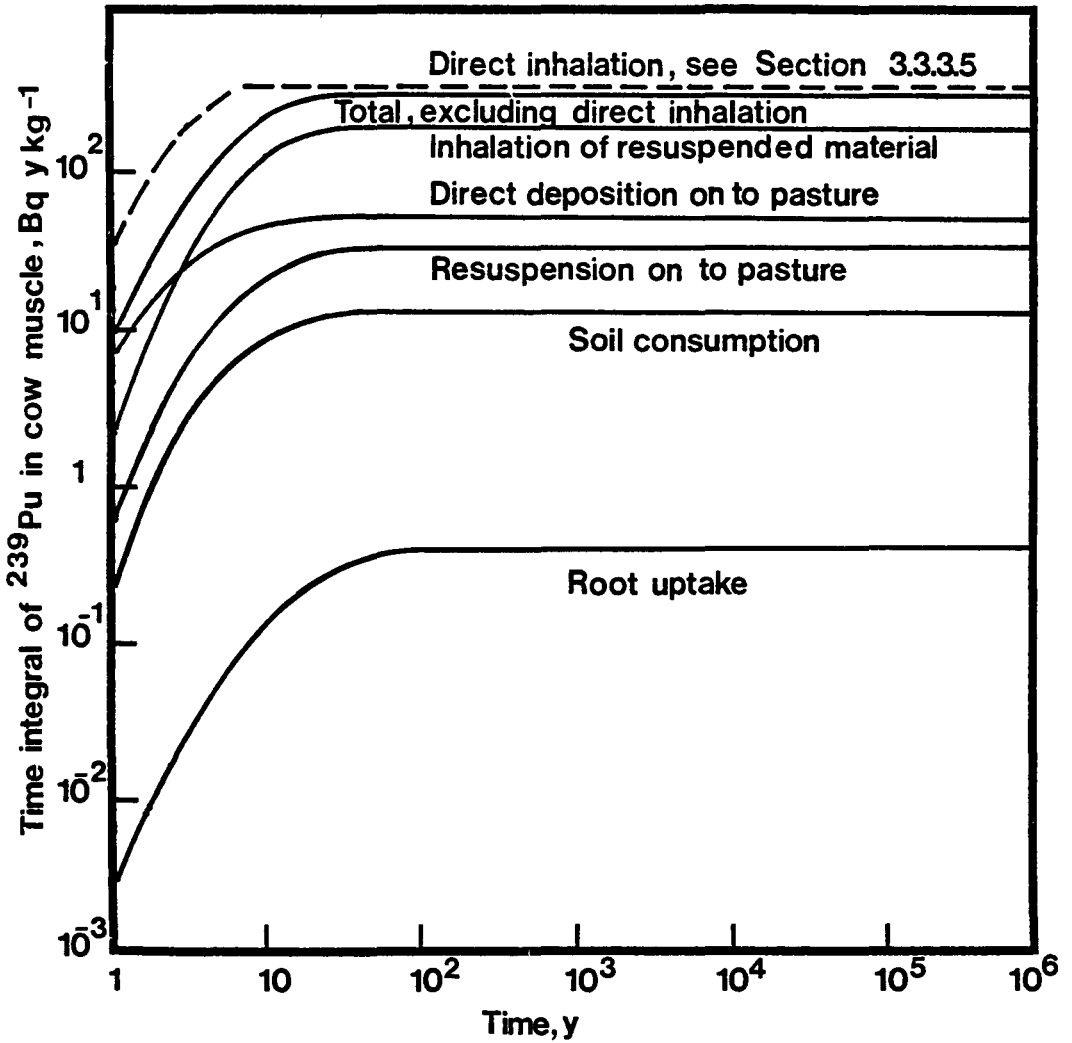


Figure 3.9 The relative importance and time dependence of the important mechanisms for the transfer of strontium-90 to green vegetables and grain



NB. While the discharge stops after 1 y the time integral continues to increase due to the long biological half-life of plutonium in the animal.

Figure 3.10 The relative importance and time dependence of the important mechanisms for the transfer of plutonium-239 to cow muscle

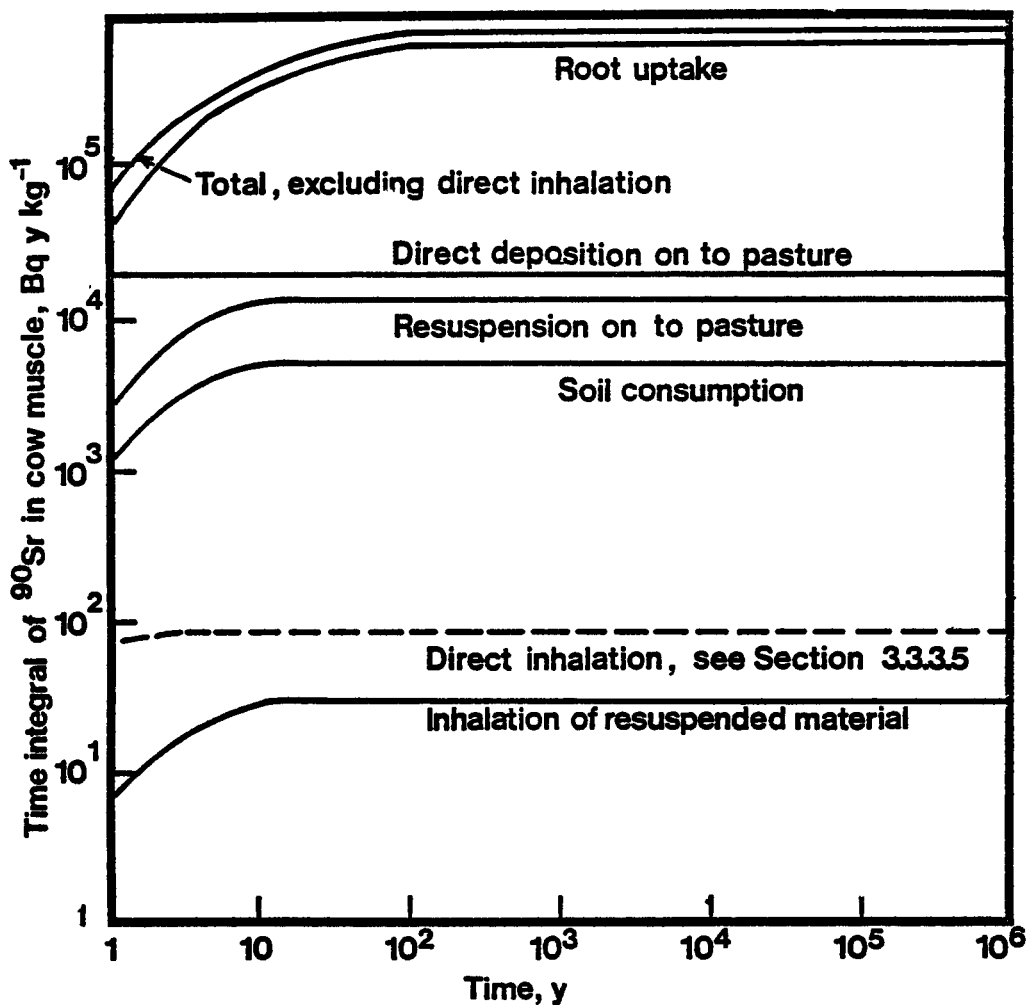


Figure 3.11 The relative importance and time dependence of the important mechanisms for the transfer of strontium-90 to cow muscle

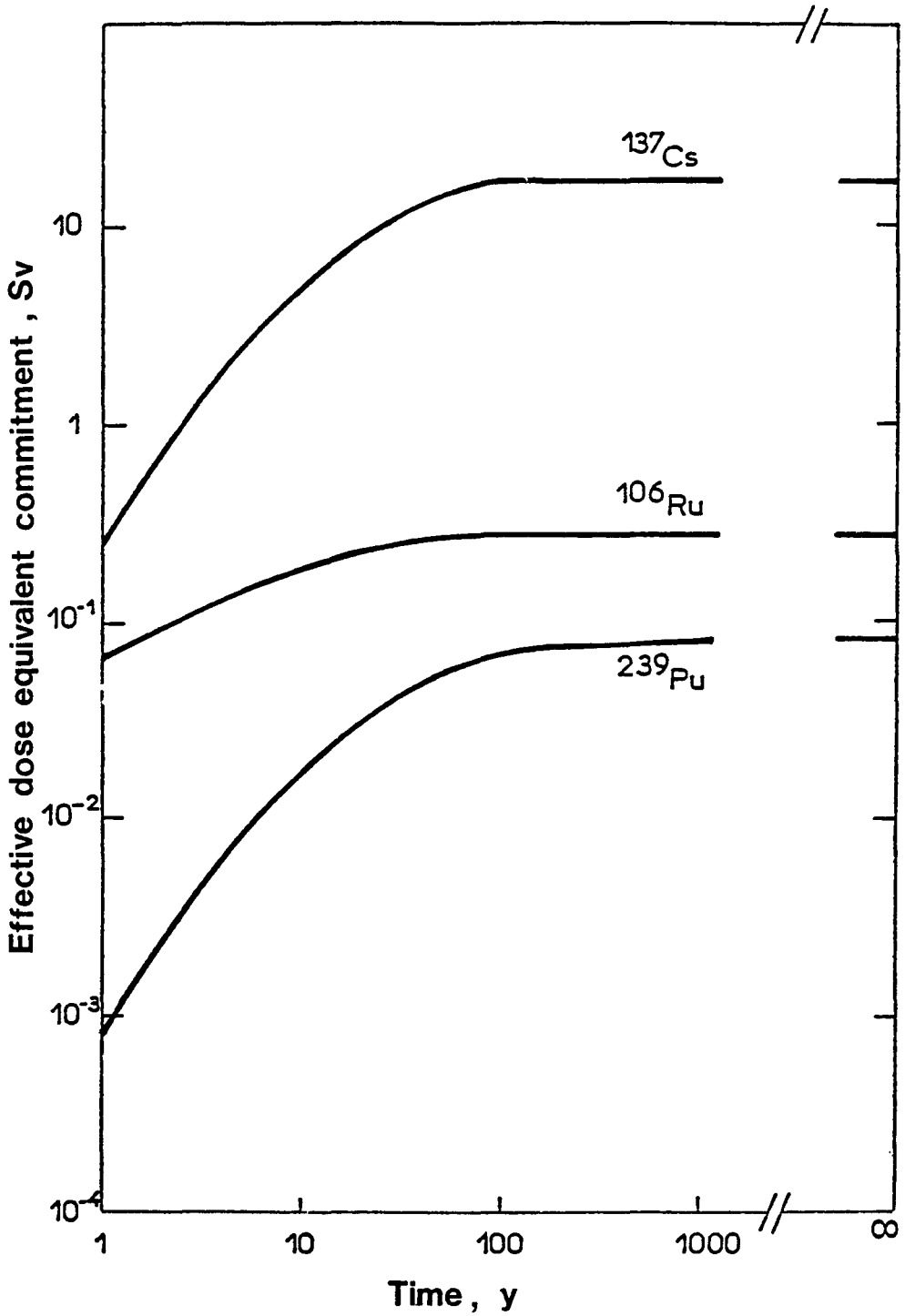


Figure 3.12 Variation of effective dose equivalent commitment with time for external X and γ irradiation from a deposition on the soil of $1 \text{ Bq m}^{-2} \text{ s}^{-1}$ during 1 y

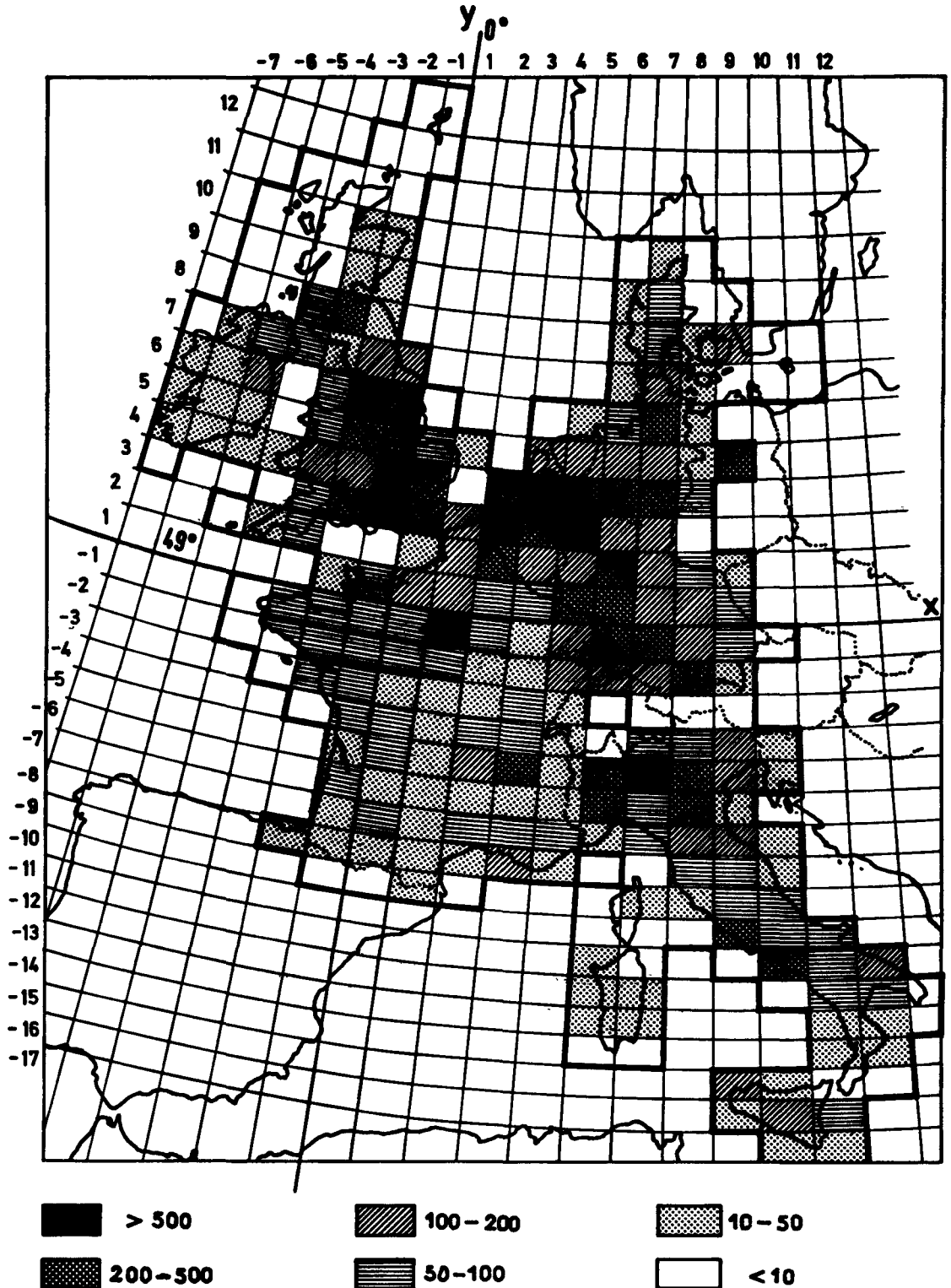


Figure 3.13 - Mean population density (man km^{-2}) in the 10^4 km^2 squares of the largest grid

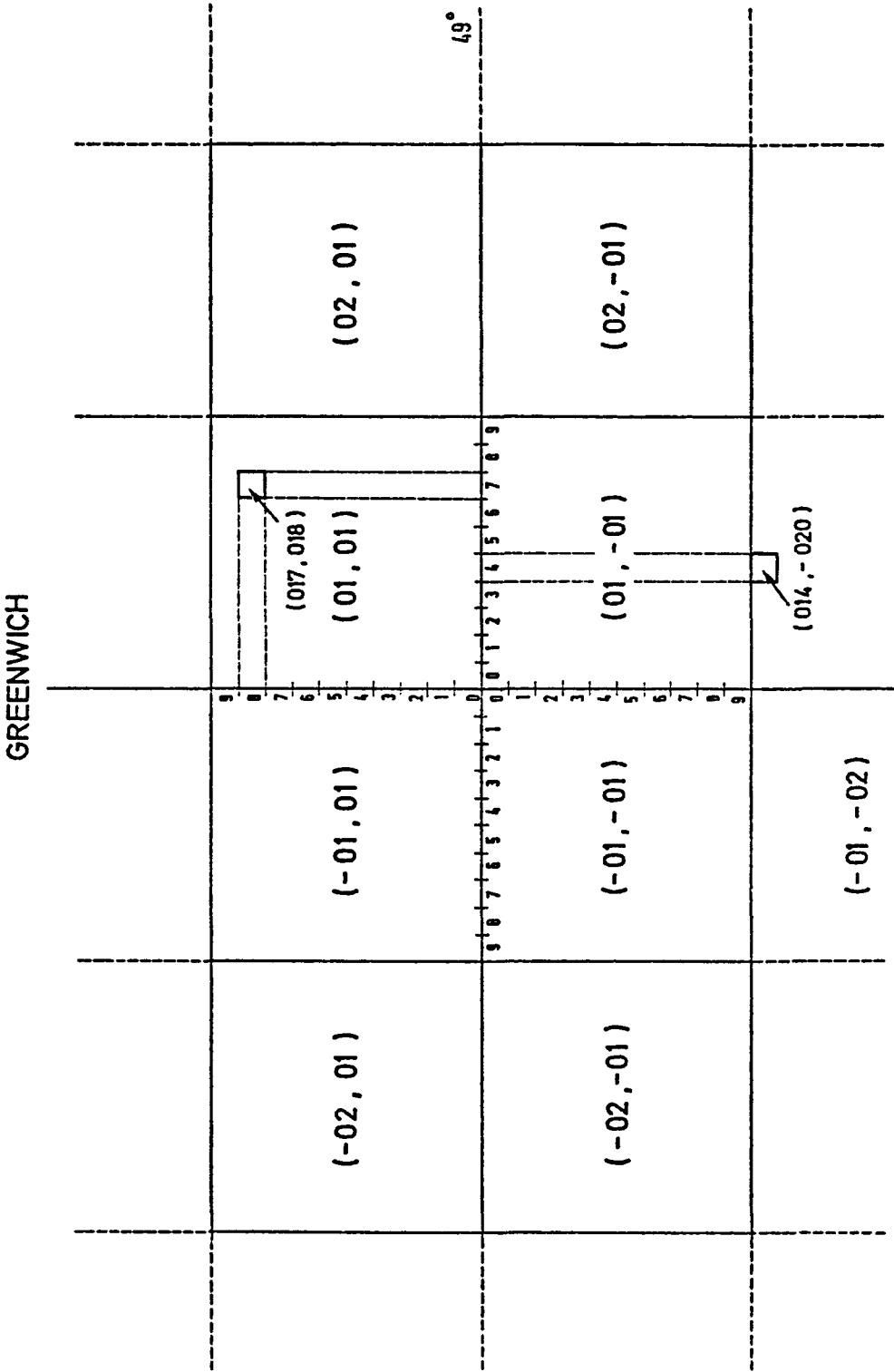


Figure 3.14 Representation of the squares forming the grid

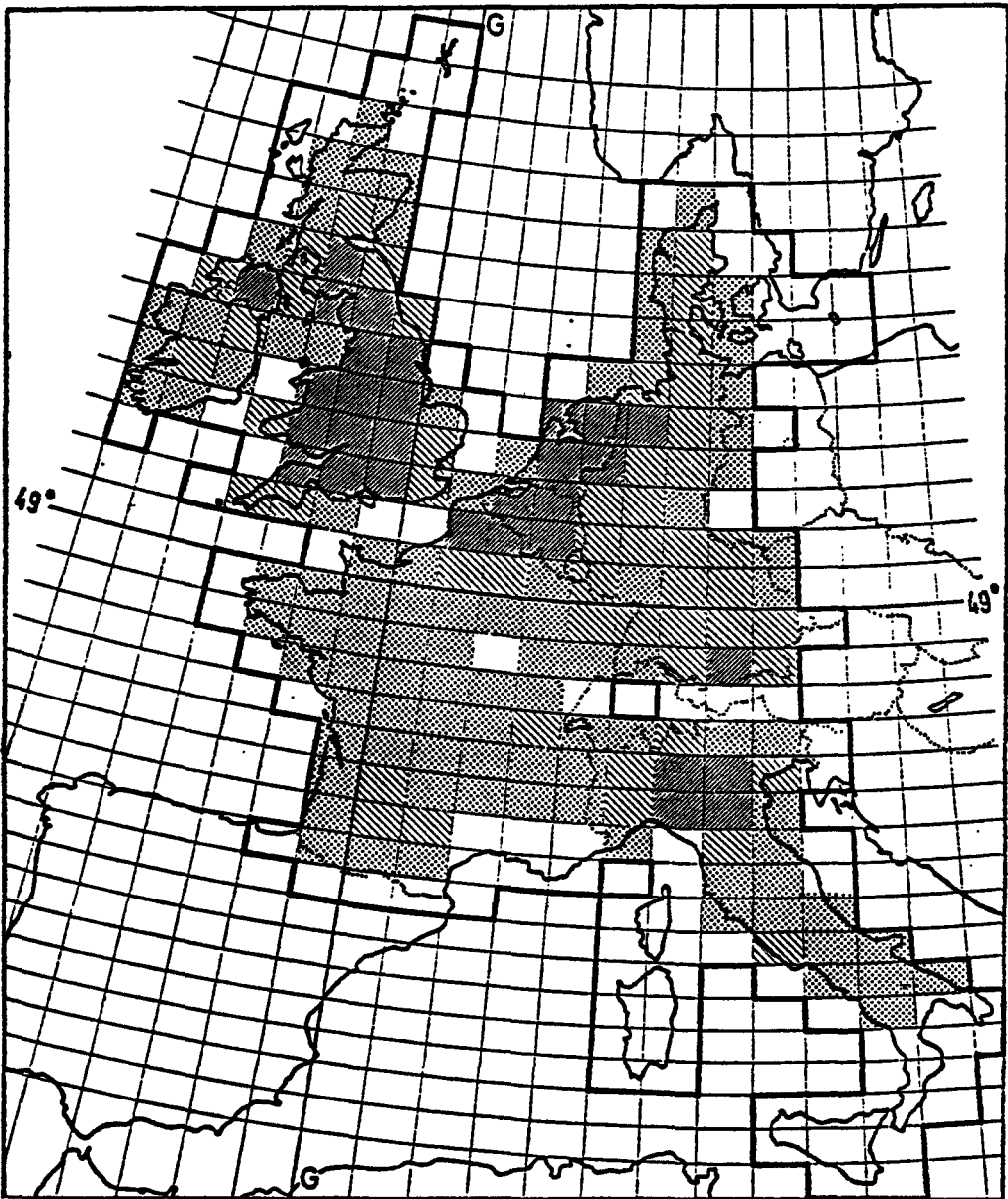


Figure 3.15 Production density of fresh milk in the European Community

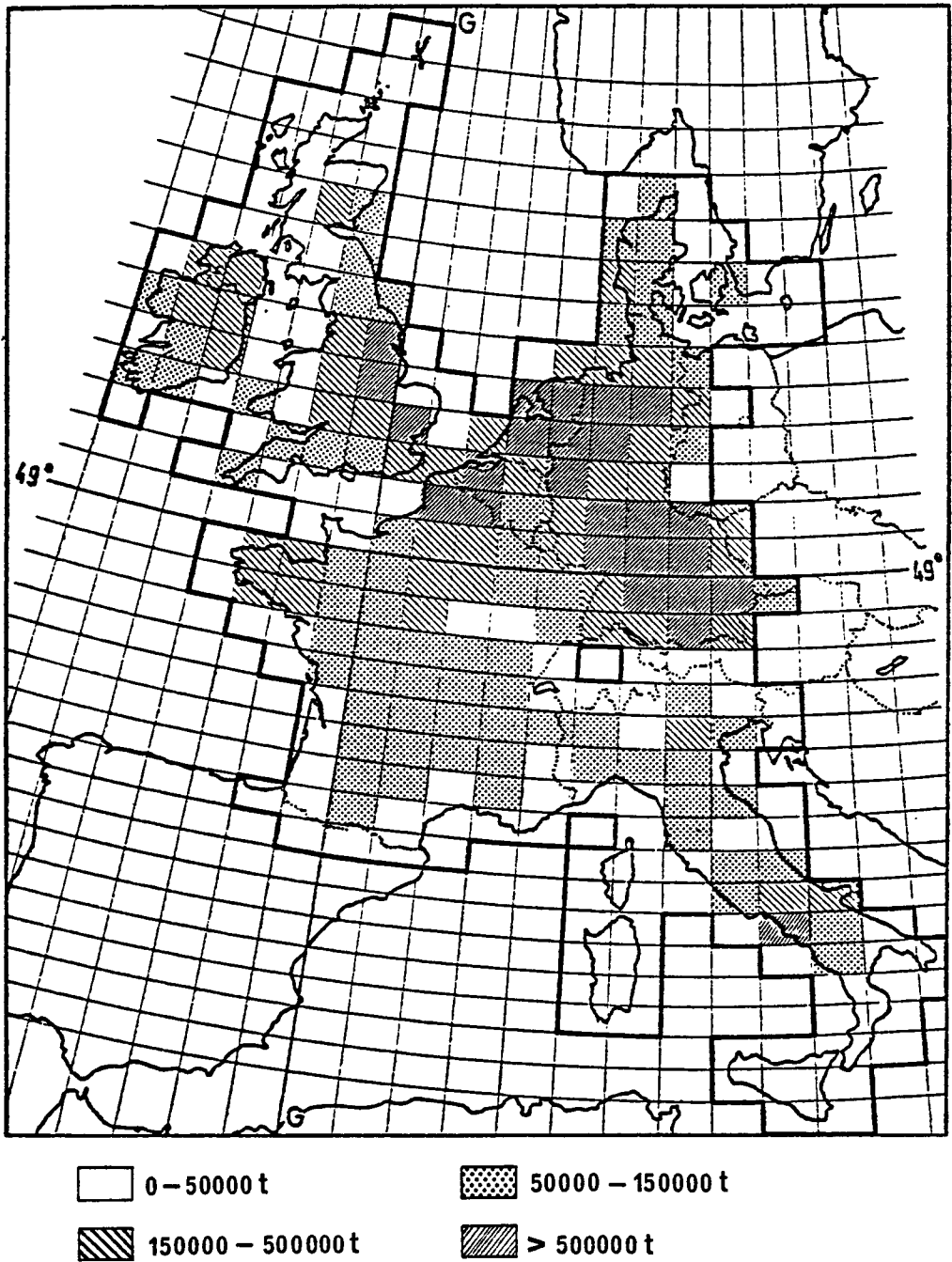


Figure 3.16 Production density of potatoes in the European Community

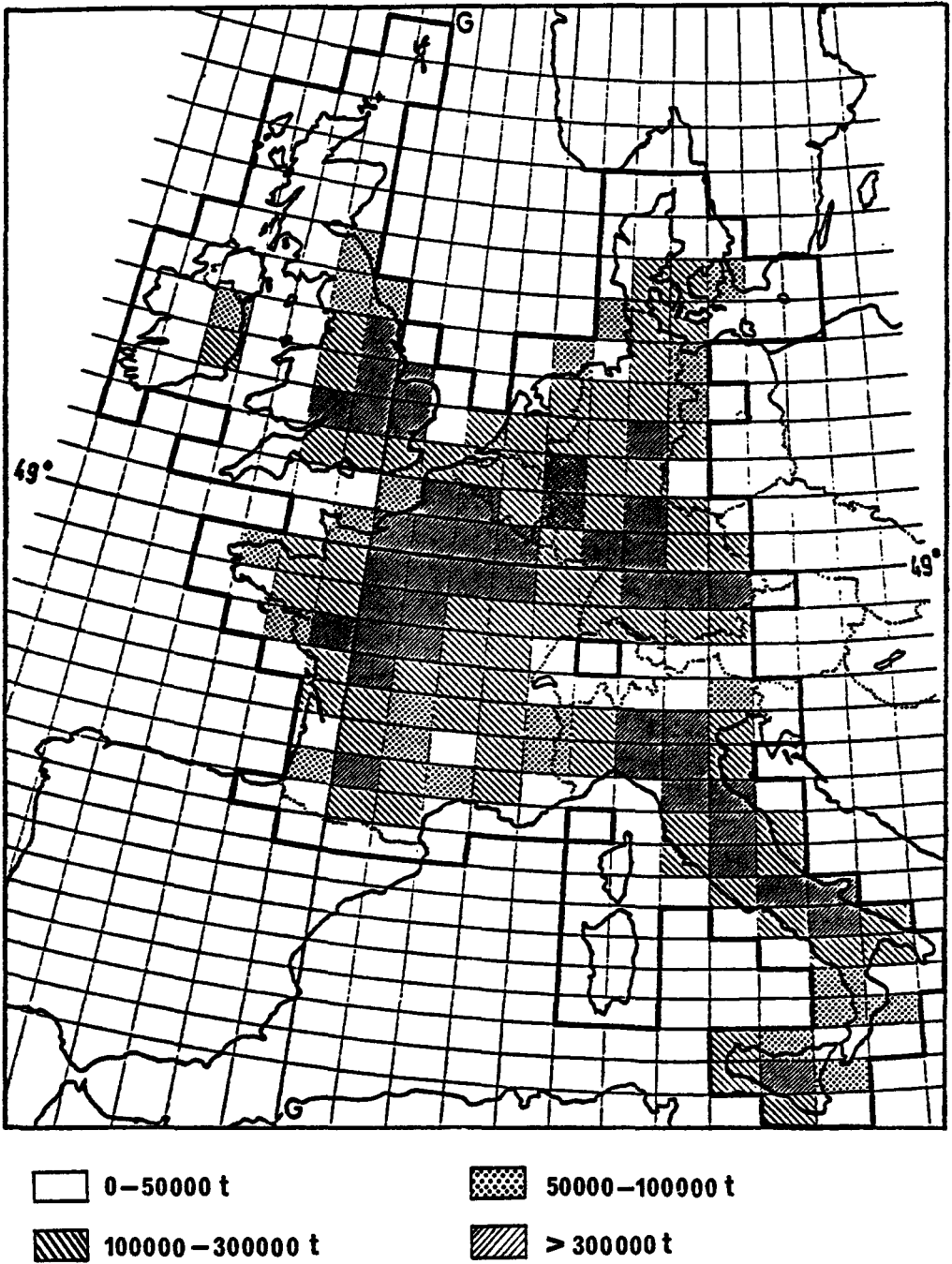


Figure 3.17 Production density of wheat in the European Community

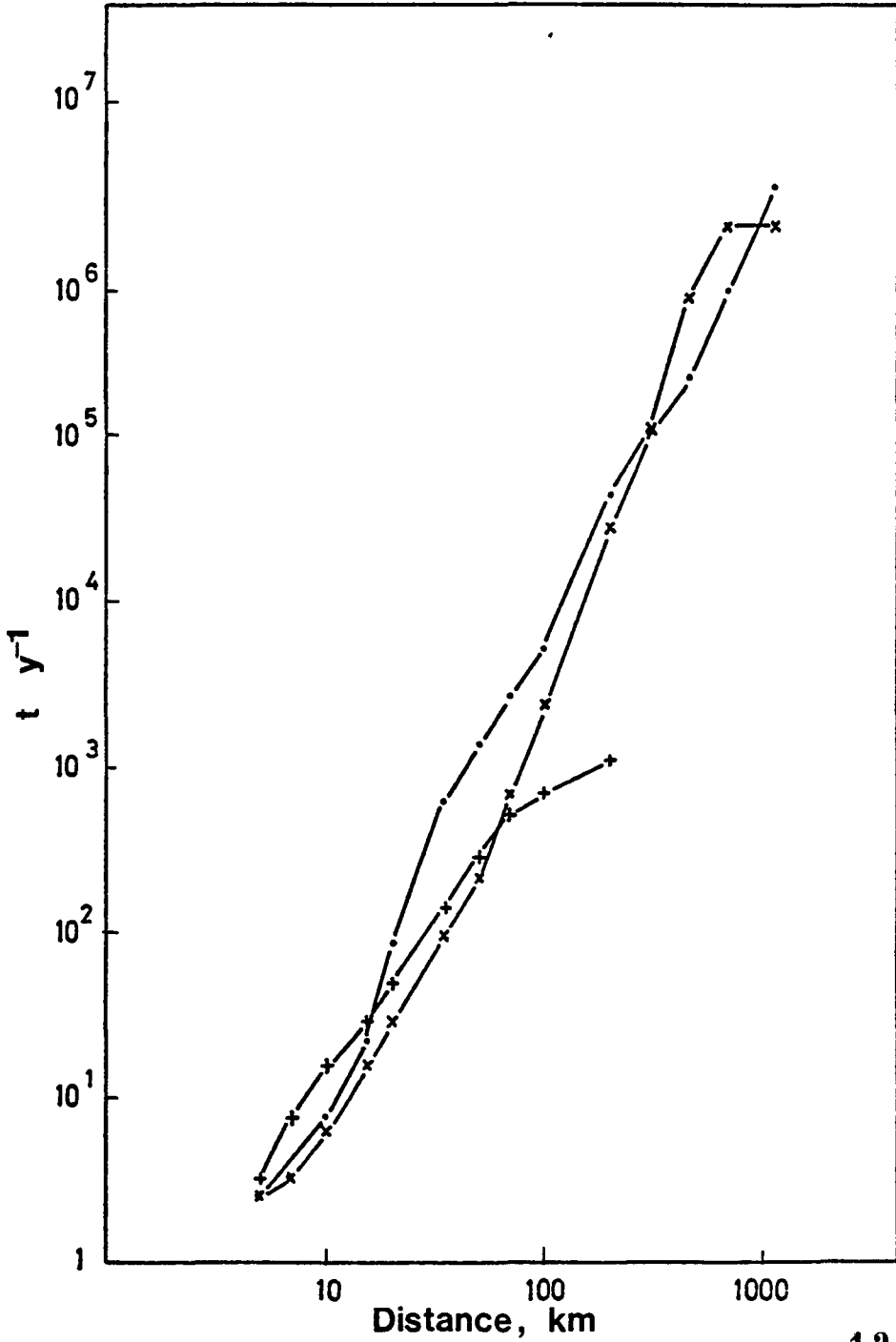


Figure 3.18 Cumulative production of fresh milk, in $t y^{-1}$, as a function of distance, in three 20° sectors centered on a site in the Rhone valley

Appendix 3.1

Wind-driven resuspension from urban surfaces

While the pollution of air in urban environments due to a variety of aerosols, eg, lead from vehicle exhausts, SO₂ from the combustion of fossil fuels, has received considerable attention, the relationship between contamination on the surfaces of city streets and pavements and the air has not been established. Some of the principal differences between wind-driven resuspension in urban and rural environments are likely to be in the mechanisms governing the removal of material from surfaces following deposition. For example, in urban environments wash-off during rainfall is likely to remove a considerable fraction of the surface deposit. Similarly, surface material will be removed by street cleaning practices.

The magnitude and time dependence of resuspension from urban surfaces is uncertain, but nevertheless, the relative importance of urban as compared to rural resuspension is investigated making some simplifying assumptions concerning the removal process from urban surfaces. It is assumed that rainfall occurs at intervals of two weeks and results in the complete removal of the resuspendible surface deposit. Using this assumption together with an initial resuspension factor of 10⁻⁵ m⁻¹ the integrated resuspended air concentration arising from deposition at unit rate for one year is compared with the result obtained using the 'rural' model.

(a) Resuspension from urban surfaces

While the deposit is on the surface, the resuspended air concentration is assumed constant with time given by

$$R_A = K D \quad \dots\dots\dots(A3.1)$$

where R_A is the resuspended air concentration (Bq m⁻³)
 K is the resuspension factor (m⁻¹)
 D is the surface deposit (Bq m⁻²)

For a continuous deposition rate of P Bq m⁻² s⁻¹, the cumulative surface deposit (D_c) after time t, assuming no losses from the surface is

$$D_c = \int_0^t P dt \quad (Bq m^{-2}) \quad \dots\dots\dots(A3.2)$$

The integrated resuspended air concentration I_u, is given after time t by

$$I_u = \int_0^t K D_c dt \quad (Bq s m^{-3}) \quad \dots\dots\dots(A3.3)$$

Substituting for D_c from equation (A3.2)

$$I_u = \int_0^t \int_0^t K P dt dt \quad \dots\dots\dots(A3.4)$$

If it is assumed that the surface contamination is completely removed by rainfall when $t = 1.21 \times 10^6$ s (14 days) and that $P = 1 \text{ Bq m}^{-2} \text{ s}^{-1}$ and $K = 10^{-5} \text{ m}^{-1}$ the integrated resuspended air concentration after 14 days is

$$\underline{I_u = 7.3 \times 10^6 \text{ Bq s m}^{-3}}$$

For continuous deposition lasting for 1 year, assuming the deposit to be removed periodically by rainfall every 14 days, the integrated resuspended air concentration is

$$\underline{I_u = 1.9 \times 10^8 \text{ Bq s m}^{-3}}$$

(b) Resuspension from rural surfaces

Following deposition on the surface, the resuspension factor, $K(t)$, is assumed to vary as (see Section 3.3.2.2)

$$K(t) = 10^{-5} \exp\left(-\frac{0.693t}{4.75 \times 10^6}\right) + 10^{-9} \text{ m}^{-1} \dots\dots\dots(A3.5)$$

where t is the time in s and the longer term decline in resuspension factor has been ignored for simplicity.

The infinite time integral of the resuspended air concentration I_R , above a surface on which a nuclide has been deposited at a rate P , continuously for a year is

$$I_R = \int_0^{\infty} K(t) P \times 3.15 \times 10^7 \text{ dt} \dots\dots\dots(A3.6)$$

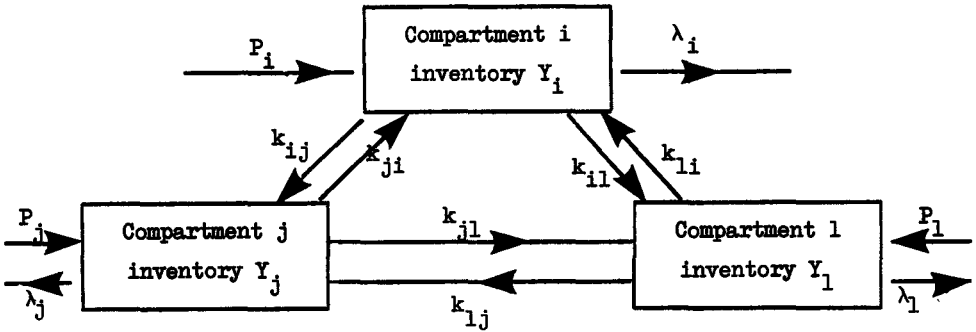
Substituting for $K(t)$ in equation (A3.6) from (A3.5) and assuming $P = 1 \text{ Bq m}^{-2} \text{ s}^{-1}$

$$\underline{I_R = 2.2 \times 10^9 \text{ Bq s m}^{-3}}$$

Subject to the assumptions adopted the resuspension above rural surfaces is significantly in excess of that above urban surfaces. Bearing in mind the uncertainties associated with the respective estimates a conservative approach is adopted in this study and the model developed for rural surfaces is used to estimate resuspension from all deposits.

Appendix 3.2

General form of compartmental model



A dynamic compartmental model has been used in which the transfer rate of material between compartments is proportional to the inventory of material in the source compartment. The relationship can be generally represented by:

$$\frac{dY_i}{dt} = \sum_{j=1}^n k_{ji} Y_j - \left[\sum_{j=1}^n k_{ij} \right] Y_i - \lambda_i Y_i + P_i \dots\dots\dots(A3.7)$$

where $2 \leq i, j \leq n$ and $k_{ii} = 0$

and k_{ij} and k_{ji} are transfer coefficients between two compartments having inventories Y_i and Y_j .

λ_i is an effective transfer coefficient from compartment i which takes account of loss of material from the compartment without transfer to another, for example, radioactive decay.

P_i is a source of continuous input into compartment i . The time integral of the inventory in any compartment is obtained as

$$Y_i^t = \int_0^t Y_i dt \dots\dots\dots(A3.8)$$

The time variation and time integrals of the respective inventories are obtained by solution of the sets of simultaneous equations (A3.7) and (A3.8).

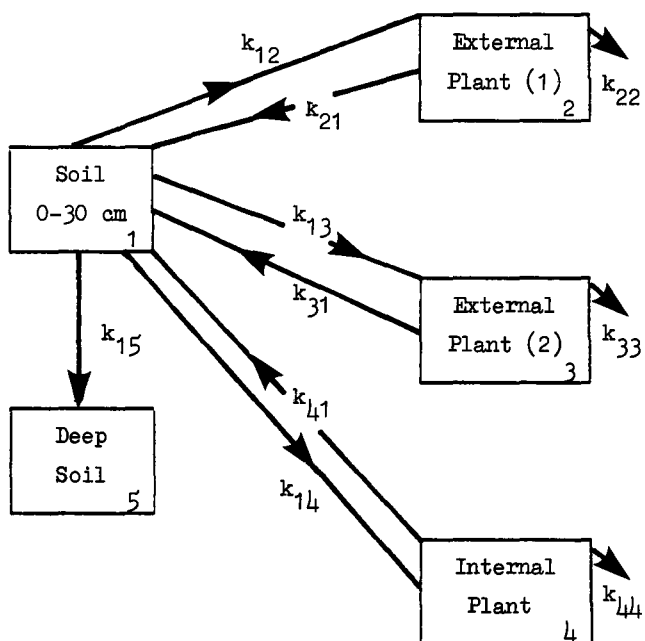
Appendix 3.3

Transfer coefficients used in the terrestrial food chain models

The transfer coefficients used in each of the terrestrial foodchain models are summarised in the following sections. Each model is illustrated schematically. In some cases the models differ from the simplified versions presented in the main text; the modifications are made to facilitate computation.

Transfer coefficients are given separately for element dependent and element independent groups.

I Green Vegetables and Grain



Note

External plant (1) is for direct deposition and initial resuspension

External plant (2) is for soil contamination

Internal plant is for root uptake

k_{22} , k_{33} and k_{44} represent periodic cropping of the plant.

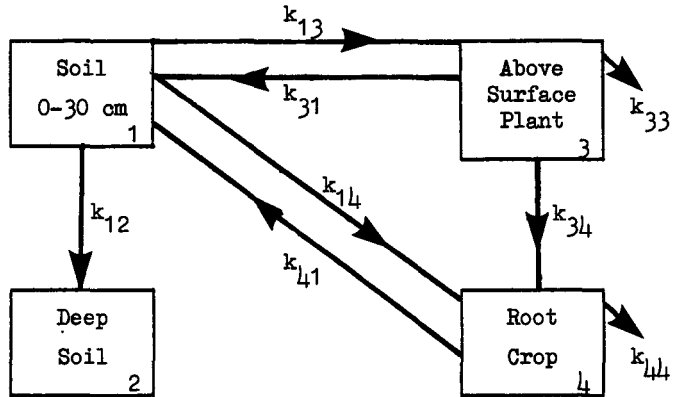
Element Independent Transfer Coefficients

Transfer Coefficient	Value s ⁻¹	
	Green vegetables	Grain
k ₁₂	7.0 10 ⁻⁹	7.0 10 ⁻⁹
k ₂₁	2.7 10 ⁻⁷	2.7 10 ⁻⁷
k ₁₃	4.4 10 ⁻⁸	8.9 10 ⁻⁹
k ₃₁	1.0	1.0
k ₄₁	1.0	1.0
k ₁₅	2.2 10 ⁻¹⁰	2.2 10 ⁻¹⁰
k ₂₂ , k ₃₃ , k ₄₄	3.2 10 ⁻⁸	3.2 10 ⁻⁸

Element Dependent Transfer Coefficients

Element	Value of k ₁₄ s ⁻¹	
	Green vegetables	Grain
Chromium	6.7 10 ⁻⁷	2.7 10 ⁻⁷
Manganese	6.7 10 ⁻⁵	2.7 10 ⁻⁵
Iron	4.4 10 ⁻⁷	3.6 10 ⁻⁷
Cobalt	2.2 10 ⁻⁶	8.9 10 ⁻⁶
Zinc	8.9 10 ⁻⁴	3.6 10 ⁻⁴
Rubidium	2.2 10 ⁻⁴	8.9 10 ⁻⁵
Strontium	1.6 10 ⁻³	1.8 10 ⁻³
Yttrium	6.7 10 ⁻⁶	2.7 10 ⁻⁶
Zirconium	4.4 10 ⁻⁷	1.8 10 ⁻⁷
Niobium	2.2 10 ⁻⁵	8.9 10 ⁻⁶
Molybdenum	2.2 10 ⁻⁴	8.9 10 ⁻⁵
Technetium	1.1 10 ⁻¹	4.4 10 ⁻²
Ruthenium	8.9 10 ⁻⁶	5.3 10 ⁻⁵
Silver	4.4 10 ⁻⁴	1.8 10 ⁻⁴
Antimony	2.2 10 ⁻⁵	8.9 10 ⁻⁶
Tellurium	2.2 10 ⁻³	8.9 10 ⁻⁴
Iodine	4.4 10 ⁻⁵	1.8 10 ⁻⁵
Caesium	4.4 10 ⁻⁵	5.3 10 ⁻⁶
Barium	1.1 10 ⁻⁵	4.4 10 ⁻⁶
Lanthanum	6.7 10 ⁻⁶	2.7 10 ⁻⁶
Cerium	1.6 10 ⁻⁵	2.7 10 ⁻⁶
Neptunium	2.2 10 ⁻⁷	8.9 10 ⁻¹⁰
Plutonium	2.2 10 ⁻⁷	8.9 10 ⁻¹⁰
Americium	2.2 10 ⁻⁶	8.9 10 ⁻⁹
Curium	2.2 10 ⁻⁶	8.9 10 ⁻⁹

II Root Crops



Notes

k_{13} represents initial resuspension

k_{31} removal due to weathering processes

k_{14} and k_{41} represent root uptake

k_{34} represents translocation

k_{33} and k_{44} represent periodic cropping of the plant

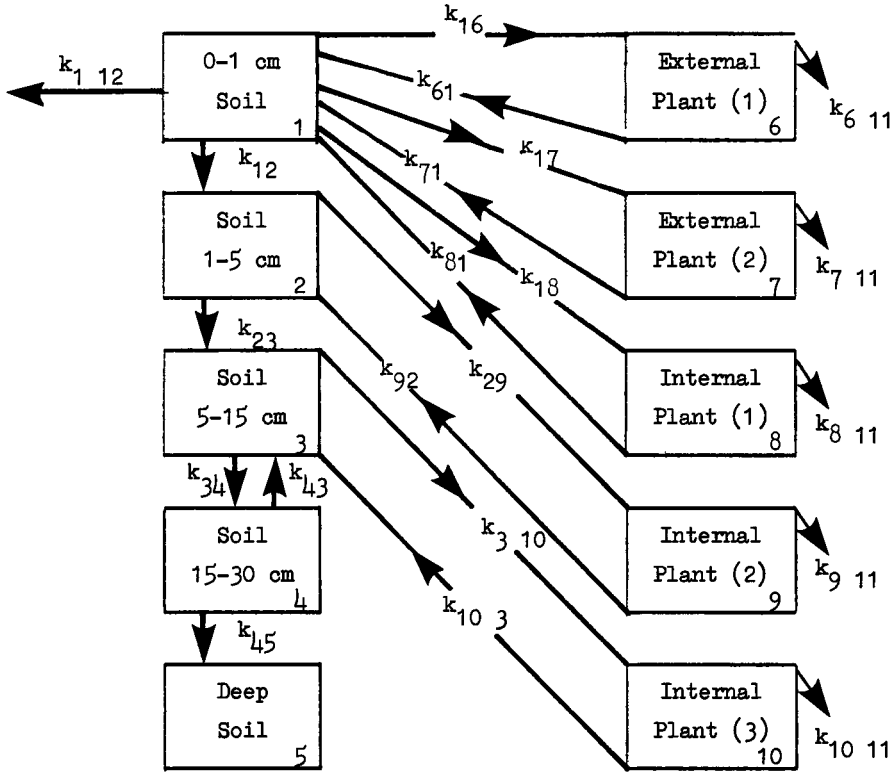
Element Independent Transfer Coefficients

Transfer coefficient	Value, s ⁻¹
k ₁₂	2.2 10 ⁻¹⁰
k ₁₃	7.0 10 ⁻⁹
k ₃₁	2.7 10 ⁻⁷
k ₄₁	1.0
k ₃₃ , k ₄₄	3.2 10 ⁻⁸

Element Dependent Transfer Coefficients

Element	Value, s ⁻¹	
	k ₁₄	k ₃₄
Chromium	1.7 10 ⁻⁶	0.0
Manganese	1.7 10 ⁻⁴	1.4 10 ⁻⁸
Iron	1.7 10 ⁻⁶	1.4 10 ⁻⁸
Cobalt	1.1 10 ⁻⁵	1.4 10 ⁻⁸
Zinc	2.2 10 ⁻³	1.4 10 ⁻⁸
Rubidium	5.6 10 ⁻⁴	2.7 10 ⁻⁹
Strontium	3.3 10 ⁻⁴	2.7 10 ⁻⁹
Yttrium	1.7 10 ⁻⁵	2.7 10 ⁻⁹
Zirconium	1.1 10 ⁻⁶	2.7 10 ⁻⁹
Niobium	5.6 10 ⁻⁵	2.7 10 ⁻⁹
Molybdenum	5.6 10 ⁻⁴	0.0
Technetium	2.8 10 ⁻⁴	3.0 10 ⁻⁸
Ruthenium	5.6 10 ⁻⁵	1.4 10 ⁻⁸
Silver	1.1 10 ⁻³	1.4 10 ⁻⁸
Antimony	5.6 10 ⁻⁵	1.4 10 ⁻⁶
Tellurium	5.6 10 ⁻³	3.0 10 ⁻⁸
Iodine	1.1 10 ⁻⁴	3.0 10 ⁻⁸
Caesium	2.8 10 ⁻⁵	3.0 10 ⁻⁸
Barium	2.8 10 ⁻⁵	2.7 10 ⁻⁹
Lanthanum	1.7 10 ⁻⁵	2.7 10 ⁻⁹
Cerium	1.7 10 ⁻⁵	5.5 10 ⁻⁹
Neptunium	5.6 10 ⁻⁶	0.0
Plutonium	5.6 10 ⁻⁶	0.0
Americium	5.6 10 ⁻⁶	0.0
Curium	5.6 10 ⁻⁶	0.0

III Undisturbed Pasture Model



Notes

1. Compartments 1-5 are the undisturbed soil model described in Section 3.3.3.2.
2. k_{16} represents resuspension onto the plant surface, k_{61} represents losses due to weathering processes.
External plant (1) is also used for direct deposition.
3. External plant (2) represents surface contamination by soil and represents all soil consumed by the animal.
4. The internal plant compartments represent root uptake from the different layers of soil.
5. k_{12} represents inhalation by the animal of resuspended material.
6. k_{611} , k_{711} , k_{811} , k_{911} , k_{1011} represent losses due to consumption of the pasture by animals.

Element Independent Parameters

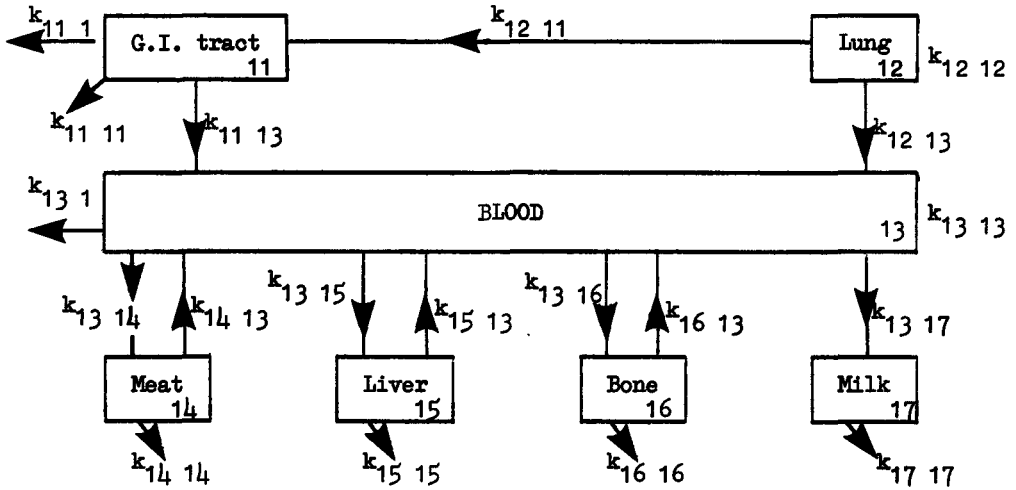
Transfer coefficient	Value, s ⁻¹	
	Cows	Sheep
k ₁₂	7.7 10 ⁻⁹	7.7 10 ⁻⁹
k ₂₃	2.0 10 ⁻⁹	2.0 10 ⁻⁹
k ₃₄	1.2 10 ⁻⁹	1.2 10 ⁻⁹
k ₄₃	4.7 10 ⁻¹¹	4.7 10 ⁻¹¹
k ₄₅	4.4 10 ⁻¹⁰	4.4 10 ⁻¹⁰
k ₁₆	1.0 10 ⁻⁹	1.0 10 ⁻⁹
k ₆₁	5.7 10 ⁻⁷	5.7 10 ⁻⁷
k ₁₇	5.3 10 ⁻⁴	8.0 10 ⁻⁴
k ₇₁	1.0	1.0
k ₈₁	1.0	1.0
k ₉₂	1.0	1.0
k ₁₀₃	1.0	1.0
k _{6 11} , k _{7 11} , k _{8 11} , k _{9 11} , k _{10 11}	2.0 10 ⁻⁷	5.8 10 ⁻⁸
k _{1 12}	3.75 10 ⁻¹³ (*)	2.0 10 ⁻¹⁴ (*)

* For the actinides, k_{1 12} is multiplied by 0.63 as that is the fraction of a 1.0 μm AMAD aerosol which is deposited in the lung, this fraction is already included in the animal transfer coefficients for other elements.

Element Dependent Parameters

Element	Value, s ⁻¹					
	k ₁₈		k ₂₉		k _{3 10}	
	Cow	Sheep	Cow	Sheep	Cow	Sheep
Chromium	2.0 10 ⁻⁵	6.0 10 ⁻⁶	5.0 10 ⁻⁶	1.5 10 ⁻⁶	2.0 10 ⁻⁶	6.0 10 ⁻⁷
Manganese	2.0 10 ⁻³	6.0 10 ⁻⁴	5.0 10 ⁻⁴	1.5 10 ⁻⁴	2.0 10 ⁻⁴	6.0 10 ⁻⁵
Iron	2.7 10 ⁻⁵	8.0 10 ⁻⁶	6.7 10 ⁻⁶	2.0 10 ⁻⁶	2.7 10 ⁻⁶	8.0 10 ⁻⁷
Cobalt	6.7 10 ⁻⁴	2.0 10 ⁻⁴	1.7 10 ⁻⁴	5.0 10 ⁻⁵	6.7 10 ⁻⁵	2.0 10 ⁻⁵
Zinc	2.7 10 ⁻²	8.0 10 ⁻³	6.7 10 ⁻³	2.0 10 ⁻³	2.7 10 ⁻³	8.0 10 ⁻⁴
Rubidium	6.7 10 ⁻³	2.0 10 ⁻³	1.7 10 ⁻³	5.0 10 ⁻⁴	6.7 10 ⁻⁴	2.0 10 ⁻⁴
Strontium	2.0 10 ⁻²	6.0 10 ⁻³	5.0 10 ⁻³	1.5 10 ⁻³	2.0 10 ⁻³	6.0 10 ⁻⁴
Yttrium	2.0 10 ⁻⁴	6.0 10 ⁻⁵	5.0 10 ⁻⁵	1.5 10 ⁻⁵	2.0 10 ⁻⁵	6.0 10 ⁻⁶
Zirconium	1.3 10 ⁻⁵	4.0 10 ⁻⁶	3.3 10 ⁻⁶	1.0 10 ⁻⁶	1.3 10 ⁻⁶	4.0 10 ⁻⁷
Niobium	6.7 10 ⁻⁴	2.0 10 ⁻⁴	1.7 10 ⁻⁴	5.0 10 ⁻⁵	6.7 10 ⁻⁵	2.0 10 ⁻⁵
Molybdenum	6.7 10 ⁻³	2.0 10 ⁻³	1.7 10 ⁻³	5.0 10 ⁻⁴	6.7 10 ⁻⁴	2.0 10 ⁻⁴
Technetium	3.3	1.0	8.3 10 ⁻¹	2.5 10 ⁻¹	3.3 10 ⁻¹	1.0 10 ⁻¹
Ruthenium	2.7 10 ⁻³	8.0 10 ⁻⁴	6.7 10 ⁻⁴	2.0 10 ⁻⁴	2.7 10 ⁻⁴	8.0 10 ⁻⁵
Silver	1.3 10 ⁻²	4.0 10 ⁻³	3.3 10 ⁻³	1.0 10 ⁻³	1.3 10 ⁻³	4.0 10 ⁻⁴
Antimony	6.7 10 ⁻⁴	2.0 10 ⁻⁴	1.7 10 ⁻⁴	5.0 10 ⁻⁵	6.7 10 ⁻⁵	2.0 10 ⁻⁵
Tellurium	6.7 10 ⁻²	2.0 10 ⁻²	1.7 10 ⁻²	5.0 10 ⁻³	6.7 10 ⁻³	2.0 10 ⁻³
Iodine	1.3 10 ⁻³	4.0 10 ⁻⁴	3.3 10 ⁻⁴	1.0 10 ⁻⁴	1.3 10 ⁻⁴	4.0 10 ⁻⁵
Caesium	1.3 10 ⁻³	4.0 10 ⁻⁴	3.3 10 ⁻⁴	1.0 10 ⁻⁴	1.3 10 ⁻⁴	4.0 10 ⁻⁵
Barium	3.3 10 ⁻⁴	1.0 10 ⁻⁴	8.3 10 ⁻⁵	2.5 10 ⁻⁵	3.3 10 ⁻⁵	1.0 10 ⁻⁶
Lanthanum	2.0 10 ⁻⁴	6.0 10 ⁻⁵	5.0 10 ⁻⁵	1.5 10 ⁻⁵	2.0 10 ⁻⁵	6.0 10 ⁻⁶
Cerium	3.3 10 ⁻⁵	1.0 10 ⁻⁵	8.3 10 ⁻⁶	2.5 10 ⁻⁶	3.3 10 ⁻⁶	1.0 10 ⁻⁶
Neptunium	6.7 10 ⁻⁶	2.0 10 ⁻⁶	1.7 10 ⁻⁶	5.0 10 ⁻⁷	6.7 10 ⁻⁷	2.0 10 ⁻⁷
Plutonium	6.7 10 ⁻⁶	2.0 10 ⁻⁶	1.7 10 ⁻⁶	5.0 10 ⁻⁶	6.7 10 ⁻⁶	2.0 10 ⁻⁶
Americium	6.7 10 ⁻⁵	2.0 10 ⁻⁵	1.7 10 ⁻⁵	5.0 10 ⁻⁶	6.7 10 ⁻⁶	2.0 10 ⁻⁶
Curium	6.7 10 ⁻⁵	2.0 10 ⁻⁵	1.7 10 ⁻⁵	5.0 10 ⁻⁶	6.7 10 ⁻⁶	2.0 10 ⁻⁶

IV Animal model for the transuranium elements



Notes

$k_{11 \ 11}$ and $k_{13 \ 1}$ represent return to soil via excreta

$k_{11 \ 11}$, $k_{12 \ 12}$, $k_{13 \ 13}$, $k_{14 \ 14}$, $k_{15 \ 15}$ and $k_{16 \ 16}$ represent losses due to the periodic slaughter of animals and are equal to $5.3 \cdot 10^{-9} \text{ s}^{-1}$ for cows and $3.2 \cdot 10^{-8} \text{ s}^{-1}$ for sheep.

$k_{17 \ 17}$ represents losses due to regular milking

This model is used with inputs from the undisturbed pasture model (III) and also for inhalation in the initial cloud, with an input to the lung compartment only.

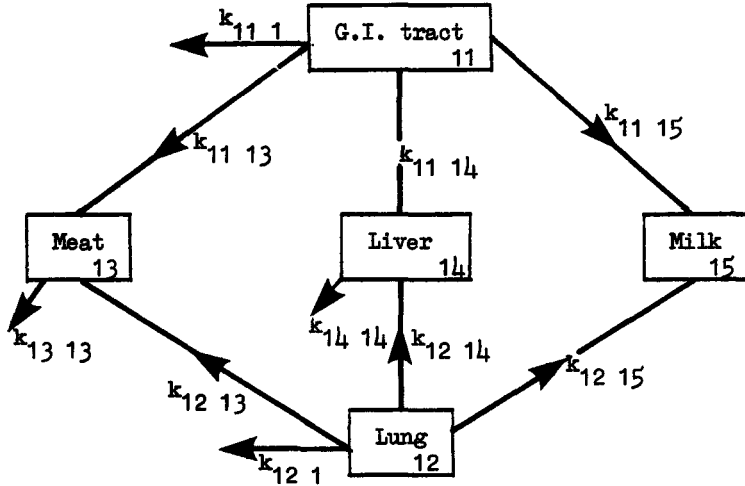
Element Independent Parameters for Cows and Sheep

Parameter	Value, s ⁻¹
k ₁₁ 1	1.3 10 ⁻⁵
k ₁₃ 1	1.2 10 ⁻⁷
k ₁₃ 14	2.3 10 ⁻⁵
k ₁₄ 13	5.5 10 ⁻⁶
k ₁₃ 15	2.3 10 ⁻⁵
k ₁₅ 13	1.7 10 ⁻⁶
k ₁₃ 16	2.3 10 ⁻⁵
k ₁₆ 13	2.8 10 ⁻⁷
k ₁₃ 17	1.2 10 ⁻⁷
k ₁₇ 13	3.5 10 ⁻⁵

Element Dependent Parameters

Element	Value, s ⁻¹		
	k ₁₁ 13	k ₁₂ 11	k ₁₂ 13
Neptunium	1.3 10 ⁻⁷	1.2 10 ⁻⁶	2.4 10 ⁻⁷
Plutonium	1.3 10 ⁻¹⁰	9.3 10 ⁻⁸	7.2 10 ⁻⁹
Americium	6.4 10 ⁻⁹	1.2 10 ⁻⁶	2.4 10 ⁻⁷
Curium	6.4 10 ⁻⁹	1.2 10 ⁻⁶	2.4 10 ⁻⁷

V Cow model for elements other than the transuranium elements



Notes

$k_{11\ 1}$ and $k_{12\ 1}$ are returns to soil to represent excretion processes via blood.

$k_{13\ 13}$ and $k_{14\ 14}$ represent losses from the organs due to biological processes.

In addition there is a loss from each compartment to represent the periodic slaughter of cows, the value of this transfer coefficient is $5.3 \cdot 10^{-9} \text{ s}^{-1}$.

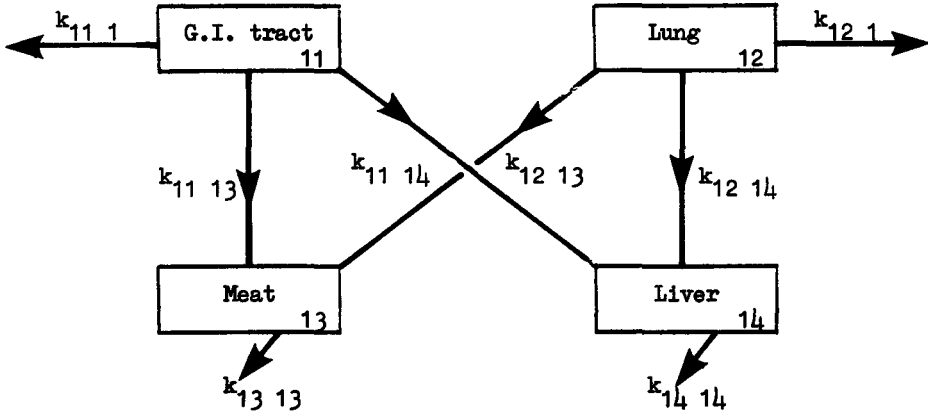
Element Independent Transfer Coefficients

Transfer coefficient	Value, s^{-1}
$k_{11\ 1}$	$1.3 \cdot 10^{-5}$
$k_{12\ 1}$	$1.2 \cdot 10^{-5}$

Element Dependent Transfer Coefficients

Element	$k_{11} 13$	$k_{11} 14$	$k_{11} 15$	$k_{12} 13$	$k_{12} 14$	$k_{12} 15$	$k_{13} 13$	$k_{14} 14$
Chromium	$3.1 \cdot 10^{-7}$	$8.1 \cdot 10^{-9}$	$2.7 \cdot 10^{-8}$	$3.1 \cdot 10^{-6}$	$8.1 \cdot 10^{-9}$	$2.7 \cdot 10^{-7}$	$2.3 \cdot 10^{-7}$	$2.3 \cdot 10^{-7}$
Manganese	$4.9 \cdot 10^{-9}$	$3.4 \cdot 10^{-7}$	$1.4 \cdot 10^{-9}$	$1.3 \cdot 10^{-9}$	$9.0 \cdot 10^{-7}$	$3.6 \cdot 10^{-8}$	$3.6 \cdot 10^{-7}$	$3.1 \cdot 10^{-9}$
Iron	$1.0 \cdot 10^{-8}$	$1.0 \cdot 10^{-7}$	$7.7 \cdot 10^{-7}$	$2.5 \cdot 10^{-8}$	$2.5 \cdot 10^{-8}$	$1.9 \cdot 10^{-7}$	$4.0 \cdot 10^{-9}$	$4.0 \cdot 10^{-8}$
Cobalt	$1.2 \cdot 10^{-8}$	$3.3 \cdot 10^{-10}$	$2.6 \cdot 10^{-6}$	$1.8 \cdot 10^{-9}$	$4.8 \cdot 10^{-10}$	$3.9 \cdot 10^{-7}$	$4.6 \cdot 10^{-8}$	$4.6 \cdot 10^{-8}$
Zinc	$1.6 \cdot 10^{-7}$	$4.1 \cdot 10^{-8}$	$1.4 \cdot 10^{-6}$	$9.4 \cdot 10^{-9}$	$2.4 \cdot 10^{-9}$	$8.4 \cdot 10^{-7}$	$2.8 \cdot 10^{-7}$	$2.8 \cdot 10^{-7}$
Rubidium	$5.9 \cdot 10^{-7}$	$1.5 \cdot 10^{-9}$	$1.5 \cdot 10^{-7}$	$3.2 \cdot 10^{-7}$	$8.3 \cdot 10^{-9}$	$8.0 \cdot 10^{-7}$	$2.0 \cdot 10^{-7}$	$2.0 \cdot 10^{-7}$
Strontium	$2.2 \cdot 10^{-10}$	$5.7 \cdot 10^{-10}$	$1.3 \cdot 10^{-9}$	$3.6 \cdot 10^{-7}$	$9.3 \cdot 10^{-7}$	$2.1 \cdot 10^{-6}$	$4.2 \cdot 10^{-10}$	$4.2 \cdot 10^{-10}$
Yttrium	$8.7 \cdot 10^{-7}$	$1.9 \cdot 10^{-8}$	$2.5 \cdot 10^{-5}$	$4.8 \cdot 10^{-5}$	$1.1 \cdot 10^{-7}$	$1.4 \cdot 10^{-4}$	$5.7 \cdot 10^{-6}$	$5.7 \cdot 10^{-6}$
Zirconium	$7.7 \cdot 10^{-8}$	$2.0 \cdot 10^{-8}$	$5.4 \cdot 10^{-6}$	$2.0 \cdot 10^{-8}$	$5.3 \cdot 10^{-9}$	$1.3 \cdot 10^{-4}$	$1.1 \cdot 10^{-8}$	$1.1 \cdot 10^{-8}$
Niobium	$1.2 \cdot 10^{-7}$	$3.2 \cdot 10^{-7}$	$3.2 \cdot 10^{-7}$	$6.5 \cdot 10^{-7}$	$1.7 \cdot 10^{-7}$	$2.9 \cdot 10^{-7}$	$7.8 \cdot 10^{-7}$	$7.8 \cdot 10^{-7}$
Molybdenum	$4.8 \cdot 10^{-5}$	$2.0 \cdot 10^{-6}$	$1.4 \cdot 10^{-6}$	$7.3 \cdot 10^{-6}$	$3.1 \cdot 10^{-6}$	$2.1 \cdot 10^{-6}$	$1.8 \cdot 10^{-6}$	$1.8 \cdot 10^{-6}$
Technetium	$2.6 \cdot 10^{-5}$	$3.0 \cdot 10^{-6}$	$4.6 \cdot 10^{-11}$	$8.8 \cdot 10^{-8}$	$1.0 \cdot 10^{-6}$	$1.6 \cdot 10^{-6}$	$2.8 \cdot 10^{-6}$	$2.8 \cdot 10^{-6}$
Ruthenium	$7.9 \cdot 10^{-9}$	$2.1 \cdot 10^{-7}$	$7.6 \cdot 10^{-6}$	$1.2 \cdot 10^{-7}$	$3.0 \cdot 10^{-6}$	$1.1 \cdot 10^{-5}$	$3.1 \cdot 10^{-7}$	$3.1 \cdot 10^{-7}$
Silver	$6.8 \cdot 10^{-8}$	$7.8 \cdot 10^{-7}$	$5.8 \cdot 10^{-6}$	$1.5 \cdot 10^{-7}$	$1.7 \cdot 10^{-7}$	$1.3 \cdot 10^{-5}$	$1.8 \cdot 10^{-7}$	$1.8 \cdot 10^{-7}$
Antimony	$5.4 \cdot 10^{-7}$	$3.8 \cdot 10^{-8}$	$2.7 \cdot 10^{-8}$	$7.8 \cdot 10^{-7}$	$5.5 \cdot 10^{-8}$	$3.9 \cdot 10^{-8}$	$4.0 \cdot 10^{-7}$	$4.0 \cdot 10^{-7}$
Tellurium	$5.3 \cdot 10^{-6}$	$1.4 \cdot 10^{-8}$	$2.7 \cdot 10^{-6}$	$7.5 \cdot 10^{-6}$	$1.9 \cdot 10^{-8}$	$3.7 \cdot 10^{-7}$	$4.0 \cdot 10^{-7}$	$4.0 \cdot 10^{-7}$
Iodine	$3.0 \cdot 10^{-7}$	$7.8 \cdot 10^{-8}$	$1.8 \cdot 10^{-6}$	$1.5 \cdot 10^{-6}$	$3.9 \cdot 10^{-9}$	$8.8 \cdot 10^{-7}$	$4.3 \cdot 10^{-8}$	$4.3 \cdot 10^{-8}$
Caesium	$6.9 \cdot 10^{-8}$	$1.8 \cdot 10^{-8}$	$1.0 \cdot 10^{-8}$	$3.8 \cdot 10^{-7}$	$9.8 \cdot 10^{-9}$	$5.5 \cdot 10^{-7}$	$8.0 \cdot 10^{-7}$	$8.0 \cdot 10^{-7}$
Barium	$3.1 \cdot 10^{-9}$	$8.1 \cdot 10^{-9}$	$3.8 \cdot 10^{-8}$	$1.4 \cdot 10^{-7}$	$3.7 \cdot 10^{-9}$	$1.7 \cdot 10^{-7}$	$2.4 \cdot 10^{-7}$	$2.4 \cdot 10^{-9}$
Lanthanum	$2.9 \cdot 10^{-9}$	$2.3 \cdot 10^{-9}$	$2.5 \cdot 10^{-9}$	$5.1 \cdot 10^{-8}$	$4.1 \cdot 10^{-7}$	$4.5 \cdot 10^{-7}$	$2.3 \cdot 10^{-9}$	$2.3 \cdot 10^{-9}$
Cerium	$5.8 \cdot 10^{-10}$	$2.3 \cdot 10^{-9}$	$2.5 \cdot 10^{-9}$	$9.9 \cdot 10^{-8}$	$3.9 \cdot 10^{-7}$	$4.3 \cdot 10^{-7}$	$2.3 \cdot 10^{-9}$	$2.3 \cdot 10^{-9}$

VI Sheep model for elements other than the transuranium elements



Notes

$k_{11 \ 1}$ and $k_{12 \ 1}$ represent return of soil from excretion process via blood.

$k_{13 \ 13}$ and $k_{14 \ 14}$ represent loss from the organs due to biological processes.

In addition there is a loss from each compartment to represent the periodic slaughter of sheep, the value of this transfer coefficient is $3.2 \cdot 10^{-8} \text{ s}^{-1}$.

Element Independent Transfer Coefficients

Transfer coefficient	Value, s^{-1}
$k_{11 \ 1}$	$1.3 \cdot 10^{-5}$
$k_{12 \ 1}$	$1.2 \cdot 10^{-5}$

Element Dependent Transfer Coefficients

Element	k_{11}^{13}	k_{11}^{14}	k_{12}^{13}	k_{12}^{14}	k_{13}^{13}	k_{14}^{14}
Chromium	$3.0 \cdot 10^{-7}$	$7.9 \cdot 10^{-9}$	$3.0 \cdot 10^{-6}$	$7.9 \cdot 10^{-9}$	$2.3 \cdot 10^{-7}$	$2.3 \cdot 10^{-7}$
Manganese	$4.9 \cdot 10^{-9}$	$3.4 \cdot 10^{-7}$	$1.3 \cdot 10^{-9}$	$9.0 \cdot 10^{-7}$	$3.6 \cdot 10^{-9}$	$3.1 \cdot 10^{-9}$
Iron	$1.0 \cdot 10^{-8}$	$1.0 \cdot 10^{-7}$	$2.5 \cdot 10^{-8}$	$2.5 \cdot 10^{-8}$	$4.0 \cdot 10^{-8}$	$4.0 \cdot 10^{-8}$
Cobalt	$1.2 \cdot 10^{-8}$	$3.2 \cdot 10^{-10}$	$1.7 \cdot 10^{-8}$	$4.7 \cdot 10^{-10}$	$4.6 \cdot 10^{-8}$	$4.6 \cdot 10^{-8}$
Zinc	$1.4 \cdot 10^{-7}$	$3.7 \cdot 10^{-8}$	$8.7 \cdot 10^{-7}$	$2.3 \cdot 10^{-9}$	$2.8 \cdot 10^{-7}$	$2.8 \cdot 10^{-7}$
Rubidium	$5.3 \cdot 10^{-7}$	$1.4 \cdot 10^{-9}$	$3.0 \cdot 10^{-7}$	$7.8 \cdot 10^{-9}$	$2.0 \cdot 10^{-7}$	$2.0 \cdot 10^{-7}$
Strontium	$2.2 \cdot 10^{-10}$	$5.7 \cdot 10^{-10}$	$3.5 \cdot 10^{-7}$	$9.1 \cdot 10^{-9}$	$4.2 \cdot 10^{-7}$	$4.2 \cdot 10^{-7}$
Yttrium	$8.7 \cdot 10^{-7}$	$1.9 \cdot 10^{-9}$	$4.3 \cdot 10^{-6}$	$9.4 \cdot 10^{-8}$	$5.7 \cdot 10^{-10}$	$5.7 \cdot 10^{-10}$
Zirconium	$1.5 \cdot 10^{-9}$	$3.8 \cdot 10^{-10}$	$1.7 \cdot 10^{-8}$	$4.4 \cdot 10^{-8}$	$1.1 \cdot 10^{-8}$	$1.1 \cdot 10^{-8}$
Niobium	$9.9 \cdot 10^{-7}$	$2.6 \cdot 10^{-7}$	$5.2 \cdot 10^{-7}$	$1.4 \cdot 10^{-9}$	$7.8 \cdot 10^{-7}$	$7.8 \cdot 10^{-7}$
Molybdenum	$4.7 \cdot 10^{-5}$	$2.0 \cdot 10^{-6}$	$7.2 \cdot 10^{-6}$	$3.1 \cdot 10^{-7}$	$1.8 \cdot 10^{-6}$	$1.8 \cdot 10^{-6}$
Technetium	$1.9 \cdot 10^{-5}$	$2.2 \cdot 10^{-10}$	$7.8 \cdot 10^{-8}$	$8.9 \cdot 10^{-7}$	$2.8 \cdot 10^{-8}$	$2.8 \cdot 10^{-8}$
Ruthenium	$7.9 \cdot 10^{-8}$	$2.1 \cdot 10^{-7}$	$1.2 \cdot 10^{-8}$	$3.0 \cdot 10^{-10}$	$3.1 \cdot 10^{-7}$	$3.1 \cdot 10^{-7}$
Silver	$4.7 \cdot 10^{-7}$	$5.3 \cdot 10^{-7}$	$7.1 \cdot 10^{-8}$	$8.1 \cdot 10^{-7}$	$1.8 \cdot 10^{-7}$	$1.8 \cdot 10^{-7}$
Antimony	$5.4 \cdot 10^{-7}$	$3.8 \cdot 10^{-8}$	$7.8 \cdot 10^{-7}$	$5.5 \cdot 10^{-8}$	$4.0 \cdot 10^{-7}$	$4.0 \cdot 10^{-7}$
Tellurium	$5.3 \cdot 10^{-6}$	$1.4 \cdot 10^{-8}$	$7.4 \cdot 10^{-6}$	$1.9 \cdot 10^{-8}$	$4.0 \cdot 10^{-7}$	$4.0 \cdot 10^{-7}$
Iodine	$2.6 \cdot 10^{-7}$	$6.9 \cdot 10^{-8}$	$1.4 \cdot 10^{-7}$	$3.6 \cdot 10^{-9}$	$4.3 \cdot 10^{-8}$	$4.3 \cdot 10^{-8}$
Caesium	$6.4 \cdot 10^{-8}$	$1.7 \cdot 10^{-10}$	$3.6 \cdot 10^{-7}$	$9.4 \cdot 10^{-9}$	$8.0 \cdot 10^{-7}$	$8.0 \cdot 10^{-7}$
Barium	$3.1 \cdot 10^{-9}$	$8.1 \cdot 10^{-9}$	$1.4 \cdot 10^{-7}$	$3.6 \cdot 10^{-7}$	$2.4 \cdot 10^{-9}$	$2.4 \cdot 10^{-9}$
Lanthanum	$2.9 \cdot 10^{-10}$	$2.3 \cdot 10^{-9}$	$4.9 \cdot 10^{-8}$	$3.9 \cdot 10^{-7}$	$2.3 \cdot 10^{-9}$	$2.3 \cdot 10^{-9}$
Cerium	$5.8 \cdot 10^{-10}$	$2.3 \cdot 10^{-9}$	$9.5 \cdot 10^{-8}$	$3.8 \cdot 10^{-7}$	$2.3 \cdot 10^{-9}$	$2.3 \cdot 10^{-9}$

Appendix 3.4

Transformation into sectors of the data contained in the population and agricultural grids

It is necessary to divide into sectors, around the site being studied the data on the population and agricultural production contained in the grid of equal areas (100 to 10⁴ km²).

The earth is considered to be a sphere with all the points on the surface a distance R equal to 6370 km from its centre; they are represented by their latitude θ and their longitude λ in a coordinate system whose origin is the centre of the earth. The axes Ox and Oy are in the plane of the equator and the axis Oz intercepts the surface of the earth at the north pole (Figure A3.4.1). For a given site S₀ (θ_0, λ_0) a double rotation (Figure A3.4.1) of axes allows it to be placed in a geometry which is more favourable for calculation. The first rotation, of λ_0 about Oz transforms Oxyz to Ox'y'z'; this rotation does not change the latitude of S₀ but gives it a longitude of zero. The second rotation of $\frac{\pi}{2} - \theta$ about Oy' transforms Ox'y'z' into Ox''y''z'', the latitude of S₀ becomes equal to $\frac{\pi}{2}$ and its longitude is undetermined.

A point M on the surface of the earth with coordinates (θ, λ) in the representation Oxyz goes to, in the representation Ox''y''z'', coordinates θ'' and λ'' such that:

$$\sin \theta'' = \sin \theta \sin \theta_0 + \cos \theta \cos (\lambda - \lambda_0) \cos \theta_0 \dots\dots\dots (A3.9)$$

$$\sin \lambda'' = \frac{\cos \theta \sin (\lambda - \lambda_0)}{\cos \theta''} \dots\dots\dots (A3.10)$$

In the representation Ox''y''z'', circles centred on S₀ will be the locus of points such that θ'' is constant whilst the radii of these circles will be such that λ'' is a constant.

To simplify the problem further, the position of points are represented on a map by their cartesian coordinates X'' and Y''. For this a Polar Stereographic projection is used (Figure A3.4.2) which transforms the point M(R, θ'' , λ'') on the surface of the earth to a point M'(X'', Y'') on a plane which is tangential to the surface of the earth at S₀. The axes S₀X'' and S₀Y'' as parallel to Ox'' respectively. This projection is congruent that is to say it conserves directions.

$$X'' = 2R \tan \left(\frac{\pi}{4} - \frac{\theta''}{2} \right) \cos \lambda'' \dots\dots\dots (A3.11)$$

$$Y'' = 2R \tan \left(\frac{\pi}{4} - \frac{\theta''}{2} \right) \sin \lambda'' \dots\dots\dots (A3.12)$$

It only remains to determine how the squares of equal area of 100 km² for population and 10⁴ km² for agricultural production should be divided among the sectors and distance bands given. It is assumed that within a square the distribution of population and agricultural production is uniform. Figure A3.4.2 shows an example where the entire "square" of 10⁴ km² is not contained in one of the distance bands and sectors given. In this case the "square" is divided into 100 parts each of approximately 100 km² and it is determined which of the given distance bands and sectors contains each of

the parts. For the smaller squares which are still distributed through several distance bands and sectors a supplementary division into 100 elements of area 1 km^2 is made. The allocation of these elements into the various distance bands and sectors is made according to the position of their centre, which sometimes introduces a small error but avoids ambiguity.

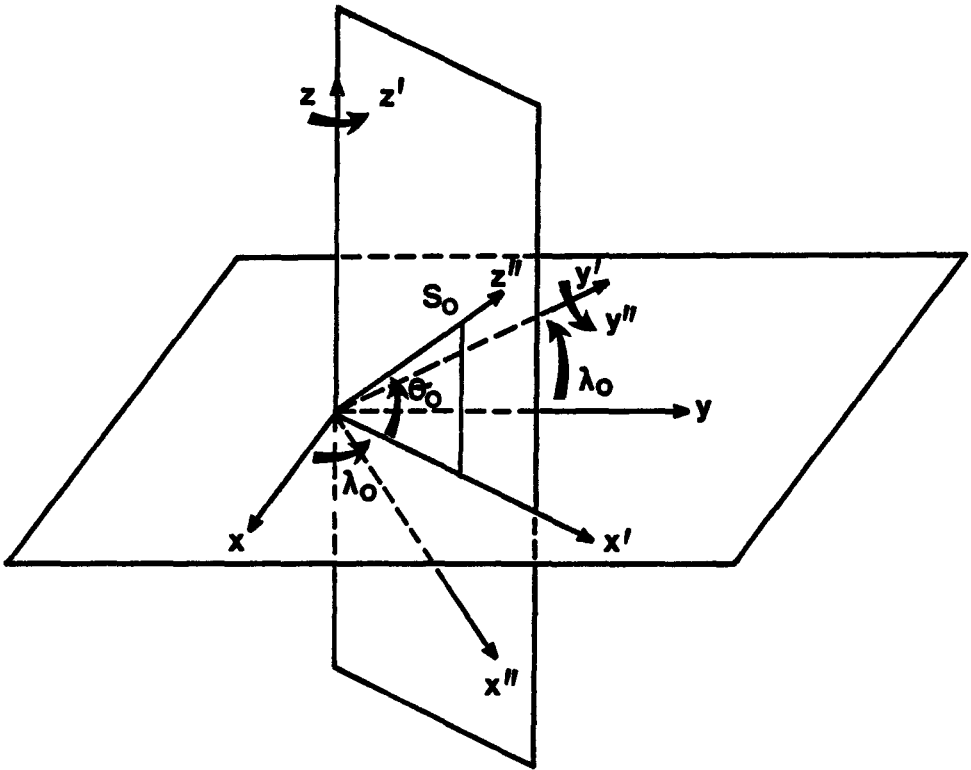


Figure A3.4.1 Schematic diagram of the representation used in the calculation

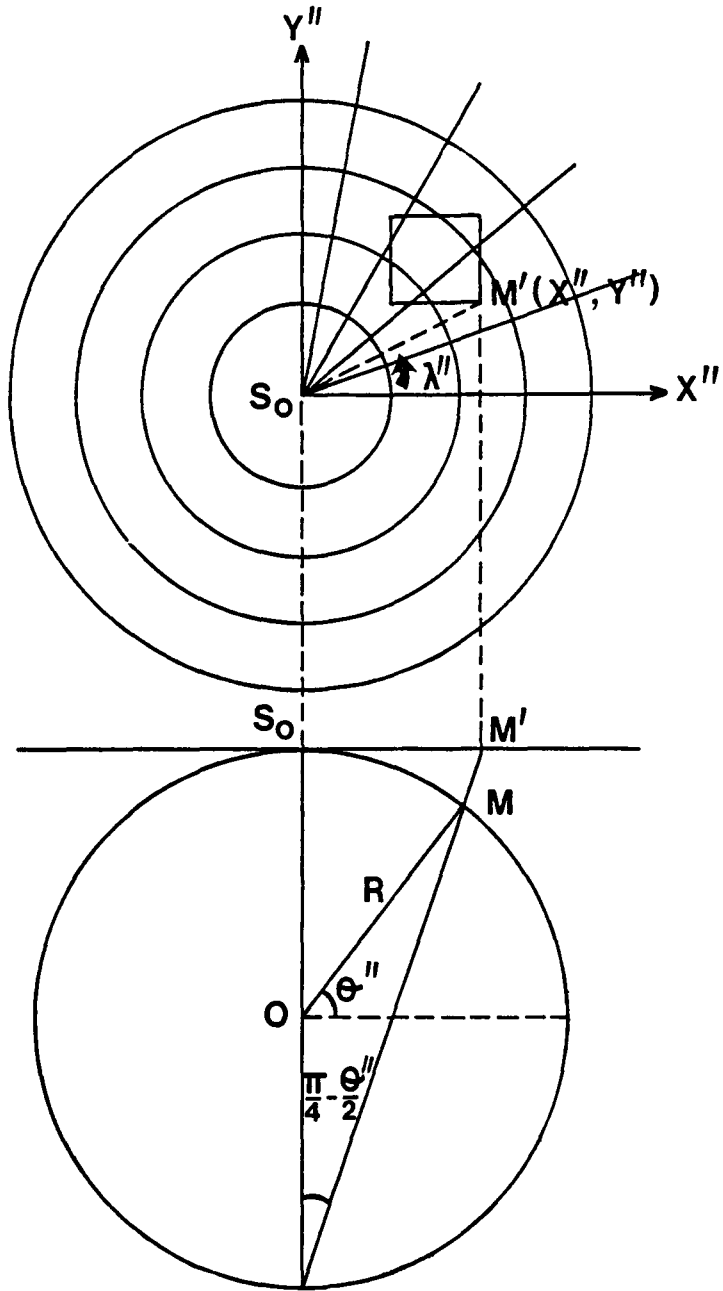


Figure A3.4.2 Locating a square on the grid in the representation $S_0 X'', Y''$

CHAPTER 4

ASSESSMENT OF RADIONUCLIDES RELEASED TO THE AQUATIC ENVIRONMENT

4.1 Introduction

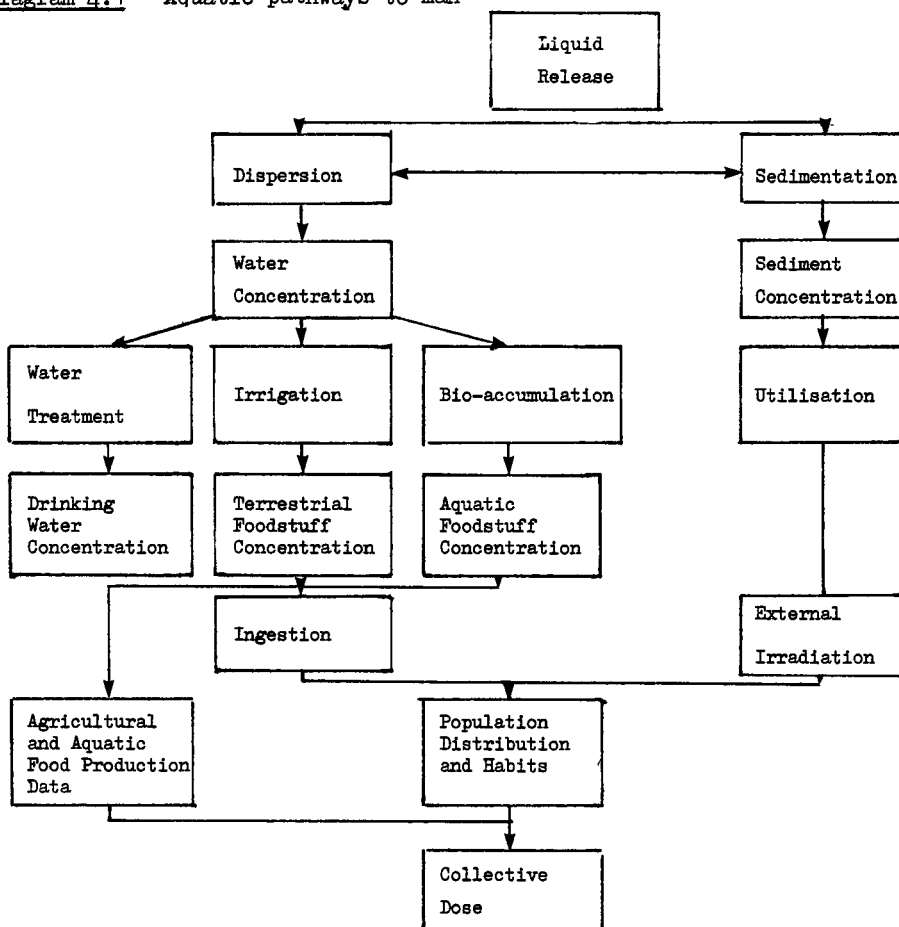
In order to evaluate the consequences of discharges of radioactive effluents into surface waters, mathematical models have been used which represent four sectors of the hydrosphere:

- rivers
- estuaries
- local marine zones
- regional marine zones

A discharge into a river may involve the movement of radionuclides through all four sectors whereas for a discharge into the sea it is only necessary, in general, to consider the local and regional marine zones.

The pathways to man considered in this study are shown schematically in Diagram 4.1.

Diagram 4.1 Aquatic pathways to man



The pathways considered for an effluent discharge into a river, are drinking water, ingestion of fish, irrigation leading to contamination of foodstuffs and external radiation from sediments. For discharges to the marine environment the situation is simplified in that only the ingestion of marine foodstuffs has been considered.

The radionuclides considered in this study are summarised in Table 4.1. They were selected on the basis of either their potential absolute significance or because they were known to be of public concern; other nuclides could however, be readily treated by the models developed.

For releases to both river and marine zones, the models developed have been used to evaluate the activity concentrations in both the water and the sediments per unit discharge rate. These models take into account the physical movement and dispersion of water masses, the interaction of radionuclides with suspended matter and bed sediments, and radioactive decay. The resulting concentrations of radionuclides in water are the source terms for the calculation of ingestion of the various radionuclides via specific pathways by the population of the European Community.

In the case of river discharges it is also necessary to consider the dispersion of radionuclides by irrigation practices; the concentration of radionuclides in river water is calculated and this, together with quantities of water used, serves as an input into the terrestrial models described in Section 3.3.3. For the estuarine situation only the interface between river and seawater is considered: the mechanisms of adsorption and desorption of radionuclides on suspended sediments produced in this zone have been evaluated by using partition factors between river and sea water.

The dispersion models for marine discharges have been defined separately for Northern European waters and the Mediterranean. Each consists of a local model and a regional marine model; the local model acts as an interface between the point of discharge and the regional marine model, both taking account of the effects of water flows, radioactive decay and sedimentation.

Given the objectives of the present study and the potentially vast scope of a study of hydrospheric dispersion, the models described in this section necessarily contain considerable simplifications of complex phenomena. The models developed represent time dependent behaviour but rely heavily on equilibrium concentration factor data (Table 4.2) to estimate the transfer of activity both to sediments and marine foodstuffs. The flows of water in the marine systems considered have been approximated by exchange rates between regional compartments and, while this can never give a strictly accurate representation of seawater movements, such a model reflects the availability and precision of seafood catch data and the mobility of fish. *

* Examples of complex hydrodynamic models in marine systems may be found in Porte and Bohet [4.10] and Nihoul and Runday [4.55]

In addition the number of pathways to man which have been taken into account has been limited to those which are considered important in terms of the collective dose in the exposed population, the quantity of major interest in this study. Pathways, such as the resuspension of marine and river sediments, the use of land reclaimed from the sea, etc, which may be significant in the context of individual doses in the locality of the discharge, have been discounted because of this; moreover the evaluation of such pathways is not amenable to the generic methodology developed in this report since much depends on local environmental conditions.

4.2 River models

4.2.1 Introduction

In general there are three different theoretical approaches to river modelling:

1. hydraulic models based on diffusion/advection equations
2. simple dilution models
3. semi-empirical models

The first category of model has been developed from water flow studies and the US NRC 4.1 have recommended their use in calculating doses from nuclear installations on river sites. The major problem with this approach is that sediment interactions are usually ignored, although these interactions are important both in the transport and removal of radionuclides from river water. The models are often very complicated 4.2 but are, nevertheless, applicable to radionuclides which do not interact strongly with sediments.

The second category of model is, by contrast, very simple: it is assumed that the effluent is immediately diluted in the total river volume and again the effects of sedimentation are ignored. Murray and Avogadro 4.3 have used this type of approach but have taken sedimentation effects into account.

The method adopted in this study comes under the third category, semi-empirical models. The model is that proposed by Schaeffer 4.4 which includes the fixation and transport of radionuclides on sedimentary material, but assumes instantaneous dilution of the effluent in the total flow of the river. The model is based on the results of measurements in the Rhone and thus gives realistic values for this river. For the other European rivers considered in this study (Loire, Po, Rhine) the same model has been used with modifications to basic parameters which are functions of the physical characteristics of the river being studied. For the purposes of the model the rivers are divided into sections and Figures 4.1 and 4.2 show the assumed discharge point and sections used for the Rhone and Loire.

The assumption of instantaneous dilution in a river is an approximation of the real physical situation where a finite length of time is required for an effluent to become well mixed. This will not lead to great inaccuracies when calculating collective

doses from drinking water, fish consumption or irrigation, but may give rise to underestimates if applied to calculation of the maximum individual doses.

4.2.2 Description of the model

The model of Schaeffer [4.4] assumes that radioactive effluents are diluted in the river flow and that activity is adsorbed on suspended and bed sediments to an extent depending on the nuclide. Activity is transported downstream by the river flow and by the slower movement of contaminated bed sediments. After the termination of the discharge the activity in water is zero because it has been assumed that there is no desorption of activity adsorbed on sediments.

4.2.2.1. Activity in water

Observation of activity levels in water downstream of nuclear installations shows an exponential decline in activity with distance from the plant [4.4]. Since instantaneous dilution of activity has been assumed in the flow rate of the river, the concentration C_w in the river at a distance x from the point of release is given by equation (4.1) per unit discharge rate,

$$C_w = \frac{1}{q} e^{-kx} \quad (\text{Bq m}^{-3} \text{ per Bq s}^{-1})$$

.....(4.1)

where x = distance (m)
 k = factor dependent on river and radionuclide, (m^{-1})
 q = river flow rate ($\text{m}^3 \text{s}^{-1}$)

For a given nuclide the value of k depends on its half life, the river water velocity and the extent of sedimentation effects

$$k = \frac{\lambda}{w} + k' \quad (\text{m}^{-1})$$

....(4.2)

where λ = radioactive decay constant, (s^{-1})
 w = river velocity (m s^{-1})
 k' = depletion factor for sedimentation, (m^{-1})

The concentration C_w includes the activity dissolved in water, C_f and the activity adsorbed on suspended sediments C_m per unit release rate.

$$C_w = C_f + C_m M \quad (\text{Bq m}^{-3} \text{ per Bq s}^{-1})$$

.....(4.3)

where C_f = activity in water, (Bq m^{-3} per Bq s^{-1})
 C_m = activity on suspended sediments, (Bq t^{-1} per Bq s^{-1})
 M = mass of suspended sediments, (t m^{-3})

The activity on suspended sediments is assumed to be related to the activity in the river water,

$$C_m = K_d C_f$$

where K_d = distribution (or concentration) factor of nuclide on sediments (Bq t^{-1} per Bq m^{-3})

Substituting in equation (4.3) enables the activity in water and that on suspended elements to be evaluated:-

$$C_f = \frac{C_w}{1 + K_d M} = \frac{1}{q} \frac{e^{-kx}}{1 + K_d M} \quad (\text{Bq m}^{-3} \text{ per } \text{Bq s}^{-1}) \quad \dots(4.4)$$

$$C_m = \frac{K_d}{q} \frac{e^{-kx}}{1 + K_d M} \quad (\text{Bq t}^{-1} \text{ per } \text{Bq s}^{-1}) \quad \dots(4.5)$$

4.2.2.2. Sediment activity

Unconsolidated river bed sediments act as a fluid under the influence of the shear force exerted by the river flow and to a lesser extent gravity. The following equation is defined for v , the average velocity of river bed sediments [4.56]

$$v = \alpha \sqrt{hJ} \quad (\text{m s}^{-1}) \quad \dots(4.6)$$

where α = constant ($\text{m}^{\frac{1}{2}} \text{s}^{-1}$)

h = water depth, (m)

J = slope of the river bed

and the full mathematical expressions for the model are given in Appendix A4.1. The basic equations were originally derived by Schaeffer [4.4] and some simple cases are considered below.

The activity Q_s in the sediments is a function of the distance x from the point of discharge and of the time t when the observation is made. During a period of release the profile is given by

$$Q_s(x,t) = \frac{k' Q_w}{kv - \lambda} \left[e^{(kv - \lambda)t} - 1 \right] \dots(4.7)$$

where $Q_w(x)$ is the activity in water, (Bq)

$Q_s(x)$ is the activity in sediments, (Bq m⁻¹ per Bq s⁻¹)

and other symbols having been defined in Section 4.2.2.1.

The variation of activity on sediments can be derived using equation(4.7) and a maximum activity is predicted at distance x_m from the discharge point

$$x_m = \frac{\log(kv/\lambda)}{k - \frac{\lambda}{v}} \dots(4.8)$$

The values of Q_s and x_m change with the duration, t , of the discharge, until the loss of activity due to radioactive decay gives an equilibrium: from this moment the position of the maximum stays unchanged although the front of the contaminated sediments continues to progress.

The model can be adapted to consider the more complex situation where the river is divided into several sections, the velocity of water and sediment being assumed constant in each section. In addition, certain radionuclides, eg, plutonium-241, give rise to radioactive daughter products and the expressions needed to include this phenomenon are given in Appendix 4.1 and in reference [4.57].

4.2.3 Application of the model

The model has been applied to the Rhone, Rhine, Loire and Po and this section describes its application to the Rhone. The other rivers have been treated in a comparable manner. Equally the model could be readily applied to other rivers subject to acquisition of the appropriate data.

4.2.3.1. Selection of parameters

Each river has been divided into several sections (Figures 4.1 and 4.2); the criteria used to define these sections depend on the physical characteristics of the river and also the utilisation of river water and sediments. For each of the sections it is assumed that the slope of the river bed, its width, the amount of suspended sediments, the river flow and the bed sediment velocity are constant. The values for these parameters are given in Table 4.3.

The parameter k' represents the potential interaction of radionuclides with sediments and Schaeffer has proposed values based on measurements in the Rhone river for the following radionuclides:

Caesium-137	:	10^{-5} m^{-1}
Cobalt-60 and ruthenium-106	:	5.10^{-6} m^{-1}
Strontium-90	:	2.10^{-6} m^{-1}

The above values are defined for a river velocity of 2 m s^{-1} . In this study k' values for all radionuclides were obtained in the following way: the radionuclides were separated into three categories based on knowledge of the freshwater concentration factors (Table 4.2) and then k' values, typical of those measured in the Rhone, were assigned to the categories.

Category A : strong interaction with sediments. These elements have concentration factors (K_d) values greater than 10^4 (Bq t^{-1} per Bq m^{-3}) : chromium, manganese, cobalt, zirconium, ruthenium, caesium, europium, neptunium, cerium, plutonium, americium and curium. For $w = 2 \text{ m s}^{-1}$, k' is equal to 10^{-5} m^{-1} .

Category B : moderate interaction with sediments. For elements with concentration factor (K_d) values between 10^3 and 10^4 (Bq t^{-1} per Bq m^{-3}) : carbon, zinc, strontium and yttrium. For $w = 2 \text{ m s}^{-1}$, k' is equal to 2.10^{-6} m^{-1} .

Category C : weak interaction with sediments. For elements with concentration factor (K_d) values less than $10^3 \text{ Bq t}^{-1} \text{ Bq m}^{-3}$: hydrogen, niobium, technetium, silver, antimony, tellurium and iodine. For this category k' has been assumed to be zero.

It has been assumed in this study that the values of k' are not river dependent even though there are great differences between the physical and chemical characteristics of each river.

4.2.3.2. Representative results

For each radionuclide discharged the variation in water concentration has been evaluated as a function of distance from the discharge point. Figure 4.3 shows a concentration profile for caesium-137 in filtered and non filtered water downstream of the release point on the Rhone which was shown in Figure 4.1. The profile is for a release of 1 Bq s^{-1} continuing for one year and the examples given in this section will be for radionuclides, manganese-54, cobalt-60, strontium-90 and caesium-137.

The estimation of doses received from the ingestion of drinking water, of fish, and of agricultural products contaminated by irrigation practices, follows from the calculation of the radionuclide concentration in the river water. The contamination of river sediments can lead to external irradiation of people either on the river banks or by other pathways such as the utilisation of river sediments for building

materials. Only the external irradiation of people on river banks has been considered in this study.

(a) Ingestion of drinking water

River water, or water from the water-table close to a river may be extracted and utilised, after treatment, as drinking water. The concentration of activity in drinking water is normally less than the concentration in river water by a factor which varies with the methods of extraction and treatment. For simplicity it has been assumed here that the river water is extracted directly from the river and undergoes a single filtration treatment which removes suspended sediments. Consequently the activity in drinking water is assumed to be equal to that of filtered river water.

The quantities of water extracted for drinking purposes have been taken from published documents 4.6 or have been estimated on the assumption that the populations of the small administrative areas bordering the river take their drinking water from it at an individual rate of $1.5 \cdot 10^{-8} \text{ m}^3 \text{ s}^{-1}$ (1.2 l d^{-1}) 4.7. Table 4.4 gives the quantities of water assumed to be extracted for each section of the Rhone and Loire.

For a given radionuclide, the collective intake of activity is obtained by multiplying the average concentration of activity in filtered water for each river section with the quantity of water extracted for drinking purposes from that section. Table 4.5 shows as an example the collective intakes by ingestion of caesium-137 and strontium-90 corresponding to a release of 1 Bq s^{-1} of each nuclide continuously for one year from an installation on the Rhone (see Figure 4.1).

(b) Ingestion of fish

Various species of river flora and fauna can enter the human diet but for the rivers in this study only the consumption of fish has been considered. The concentration of a given radionuclide in the edible parts of fish is calculated by multiplying the concentration of activity in filtered river water with the appropriate concentration factor given in Table 4.2.

The quantities of fish caught in each section of the Rhone and the Loire are shown in Table 4.6; they have been obtained from the production of fish per km of river (depending on the river and the section of the river) and from fishing habits on the river 4.7 and 4.47. It has been assumed that all the fish caught are consumed within the EC. The edible fraction of fish is assumed to be 50% on average.

The collective intake of a given radionuclide from ingestion of fish per section of the river is calculated by multiplying the average concentration of activity in the edible fraction of fish with the quantity of fish caught in each section of the river. Table 4.5 gives, as an example, the collective intakes of caesium-137 and strontium-90 corresponding to a release of each nuclide of 1 Bq s^{-1} continuously for one year from an installation on the Rhone (see Figure 4.1).

(c) Ingestion of agricultural products contaminated by irrigation practices

In this study consideration is limited to the spray irrigation of cultivated crops; this is considered to be the most important route by which radioactivity can reach man from irrigated crops bearing in mind irrigation practices and the transfer mechanisms for radionuclides.

Account is taken of the transfer of activity to the external surfaces of the plants and also root uptake and translocation in a manner comparable to that described for the deposition of activity from the atmosphere (see Section 3.3.3). The transfer coefficients used to describe the movement of activity are identical with those adopted in Section 3.3.3 with the exception of the fraction intercepted on plant surfaces during the deposition process. Experimental evidence [4.8, 4.9] indicates that the fraction deposited on vegetation during spray irrigation is about 0.05 in contrast to the fraction of 0.2 adopted for the deposition of activity from the atmosphere.

The models in Section 3.3.3 have been used to estimate the time integrated concentrations in Bq y kg^{-1} of agricultural produce derived from land irrigated at a rate of $1 \text{ Bq m}^{-2} \text{ s}^{-1}$ for the harvest period. The rate of deposition of each nuclide is obtained by multiplying the concentration in non-filtered water, in Bq m^{-3} , by the irrigation rate in $\text{m}^3 \text{ s}^{-1}$ per m^2 .

The quantity of agricultural products derived from irrigated land varies considerably from one river to another, and within the various sections of a river. The flow of an Alpine river like the Rhone varies little during the year but the river is utilised heavily for irrigation in certain sections: conversely the Loire has a water flow that varies considerably during the year but there is little use of river water for such purposes by comparison.

Table 4.7 shows as an example the quantities of irrigated crops produced along the length of the Rhone river [4.50 and 4.53]; the classification of the various foodstuffs into the product categories modelled in Section 3.3.3 (green vegetables, root crops, grain) is indicated. In all cases the production of crops by irrigation is assumed to be consumed totally within the EC.

For a given radionuclide and agricultural product, the collective intake of activity in each section of a river is obtained by multiplying the time integrated concentration in the product by the quantity produced in that river section. It is noted that it may be possible for activity to reach man by other routes from irrigation practices such as suspension of contaminated soil and subsequent inhalation by man or external irradiation by contaminated soil. It is assumed that these pathways are negligible in terms of collective dose compared with the ingestion of agricultural products.

4.2.3.3. Sediment activity

The model calculates the activity on bed sediments and river banks as a function of time and distance. The relevant equations are given in Appendix A4.1. Figure 4.4 shows the variation, as a function of distance, of caesium-137 and strontium-90 concentrations in sediments

at the end of a year's continuous discharge rate into the Rhone, while Figure 4.5 shows the variation of these concentrations at a point on the mouth of the Rhone river during and after the period of discharge (assumed to continue at 1 Bq s^{-1} for 1 year and then cease).

In order to calculate doses from external irradiation by contaminated sediments, it is assumed that the sediment activity on the river banks is constantly in equilibrium with the activity on river sediments and that this activity is uniformly distributed to a depth of 30 cm. Individual and collective doses have been obtained using the models described in Section 3.3.4 and assuming a population density for all rivers of 20 km^{-1} , this population spending on average 200 h hours per year on the river bank at the sections being considered 4.7.

Table 4.8 shows, for each section of the Rhone, the average concentrations of manganese-54, cobalt-60 and caesium-137 in river bank sediments and the resulting truncated collective effective dose equivalent commitments from external irradiation (truncation at 50 years). The particular radionuclides chosen for this example give rise to relatively high external γ radiation.

4.3 Estuarine models

The mathematical modelling of river estuaries is complex and must reflect the individuality of each river estuary. The physical mixing of fresh water which can have a variable composition (the pH of river water is typically in the range 6.5 to 8.5, dissolved salts 0.1 kg m^{-3}) and sea water which has a relatively constant composition (pH 7.5 to 8.0, dissolved salts 30 kg m^{-3}) can lead to significant chemical changes to dissolved radionuclides.

The estuarine region is generally an area where sedimentation effects are important; the behaviour of suspended sediments is particularly complex in estuaries with significant tidal movements and with complex patterns of sedimentation and resuspension. The presence of marine currents also makes it difficult to measure basic parameters for environmental models.

Given the obvious complexity of each estuarine region and that the possible contributions from such areas to the total collective dose are in general small, a simplified approach is adopted. The estuary is assumed to be a simple interface between the end of the river and the sea. At this interface adsorption and desorption of activity between the sediments and water occur as a result of the mixing of fresh and marine waters. A schematic representation of the model is shown in Figure 4.6.

The fraction of each nuclide retained on sediments has been estimated from the distribution (concentration) factors between water and sediments in the fresh-water and marine environments (cf Table 4.2). For this purpose the radionuclides have been divided into six classes. Each of the 3 classes used for the river model is further divided into two sub-classes which reflect the adsorption of radionuclides in marine sediments. The resulting classification is given in Table 4.9. The values adopted for the fraction of activity desorbed from river sediments in the estuarine region are as follows:

Class A1	0%
Class A2	30%
Class B1	0%
Class B2	30%
Class C1	0%
Class C2	0%

Consequently the only radionuclides (of those considered in this study) assumed to desorb in estuarine regions are carbon-14, strontium-90, caesium-134, caesium-136 and caesium-137. For these radionuclides, the period during which the activity discharged from the estuary to the sea is not limited to the period of discharge; contaminated bed sediments which move at a much lower speed than the river water, gradually reach the estuarine region and may then release a fraction of absorbed activity. This transfer pathway may lead to a release of activity spread over an extended period of time; Figures 4.7 and 4.8 show some results obtained for strontium-90 and caesium-137 where the activity transferred directly from the water phase and that desorbed from sediments are shown separately.

These two components have been derived in the following manner. The rate R_s , at which sediments reach the estuary is given by

$$R_s = v E_s L P_s \quad \dots(4.9)$$

where v = sediment velocity ($m s^{-1}$)

E_s = sediment thickness (m)

L = width of river (m)

P_s = density of sediments ($t m^{-3}$)

The rate of activity release into seawater can be evaluated by multiplying R_s by the activity on sediments at the river mouth and by the percentage desorbed.

4.4 Marine modelling

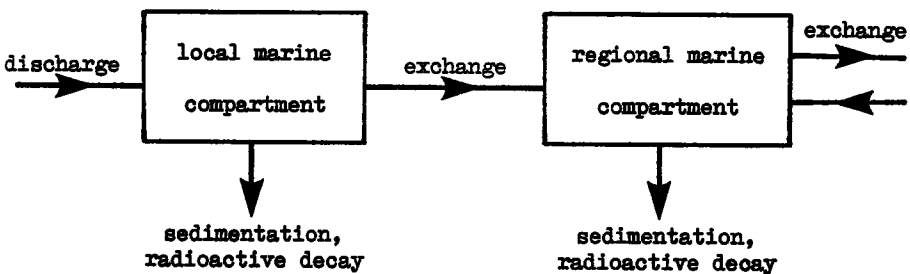
In order to calculate collective intakes of activity resulting from discharges of activity to the sea it is necessary to model the dispersion of radionuclides in marine waters, their possible reconcentration in environmental materials and the pathways to man. Of the various pathways by which man might be exposed the ingestion of marine foodstuffs is the most important in terms of collective intake, the most significant foods being fish, crustacea and molluscs.

Other pathways could be important in the context of maximum individual doses, notably external doses from contaminated sediments, the resuspension of contaminated sediments and the use of reclaimed coastal land for agricultural purposes [4.12]. These have been ignored because their contributions to collective dose are liable to be small, and moreover will be very dependent on local environmental conditions and habits and thus not amenable to modelling in the generic manner.

The models described below calculate time dependent water concentrations in various sea areas for discharges of a range of nuclides at particular locations. The models take into consideration the dispersion of the water masses, the intercation of nuclides with sediments and radioactive decay. The calculated water concentrations are then used in association with concentration factors in marine species and fisheries statistical data to evaluate collective intakes of activity by the population of the EC.

Activity may be discharged into the marine environment either directly or indirectly via a fresh-water body. In the latter case the environmental characteristics of the fresh-water system will influence the fraction of activity which eventually reaches the sea; this fraction can be evaluated using the models described in the previous Sections 4.2 and 4.3. For direct discharges the local environmental conditions determine the fraction of activity which becomes more widely dispersed and which, in general, contributes most significantly to the collective dose in the exposed population. For this reason the model chosen to characterise dispersion in the marine environment is subdivided into "local" and "regional" components which are subsequently suitably interfaced. The local model is concerned with two aspects: first, the estimation of water and sediment concentrations in the vicinity of the discharge which can be used to estimate the exposure of the critical group, and second, the prediction of the fraction of the discharged activity which leaves the local area and becomes more widely dispersed in coastal waters bordering the EC. This more widespread dispersion is estimated using the regional model. The models are applied independently but subsequently interfaced in the manner indicated in Diagram 4.2 to evaluate the collective dose for a discharge at a particular location.

Diagram 4.2 Schematic diagram showing interface between local and regional marine models



In this way the results of the regional model (which are independent of the location of discharge over relatively large areas) can be readily combined with a number of local models each representing different local environmental conditions. In a similar manner the discharge from the river/estuary model is interfaced with the regional model.

4.4.1 Local model

Dispersion on the local scale occurs by different mechanisms depending on whether the discharge is made from the coast of tidal seas

(eg, English Channel, North Sea) or from the coast of non-tidal seas (eg, Mediterranean Sea). In the case of tidal seas, the effluent trajectories are determined by the marine currents which can be predicted accurately. Eddy diffusion also contributes to marine dispersion but in the local zone marine currents are assumed to dominate. For non-tidal seas the effluent trajectories are essentially dependent on the wind. The currents are less strong than those in tidal seas and therefore the influence of eddy diffusion can determine the extent of dispersion. Experience of discharges of tracers [4.11 and 4.14], and the results of measurements of the currents in the local zone of the Gulf of Taranto [4.12 and 4.13] shows it is possible to represent the dispersion with a one compartment model. For simplification, such a model is also adopted in the case of tidal seas, and such an approach can predict concentrations close to observed values [4.37].

The variation in time of the activity in the local compartment is expressed by the differential equation:

$$\frac{dA}{dt} = Q - \lambda A - \lambda_s A - \lambda_r A$$

....(4.10)

in which A is the activity in the local compartment at time t (Bq)

Q is the rate at which activity is discharged (Bq s⁻¹)

λ is the radioactive decay constant (s⁻¹)

λ_s is the rate of loss by sedimentation (s⁻¹)

and λ_r is the rate of renewal of water in the compartment (s⁻¹)

This model assumes a one way exchange between the local compartment and the adjacent regional compartment governed by the loss term λ_rA. There will however be some activity returning to the local compartment from the regional compartment, but to a good approximation this return can be ignored in most practical cases.

As will be shown later (equation (4.19)), the rate of loss by sedimentation λ_s, is given by:

$$\lambda_s = \frac{K_d s}{h (1 + K_d ss)}$$

....(4.11)

in which K_d is the sediment-water concentration factor (Bq t⁻¹ per Bq m⁻³) (See Table 4.2).

h is the water depth in the compartment (m),

s is the rate of sedimentation (t m⁻² s⁻¹), and

ss is the suspended sediment load (t m⁻³)

The solution of equation (4.10) is:

$$A(t) = \frac{Q}{\Lambda_e} (1 - \exp(-\Lambda_e t))$$

....(4.12)

where $\Lambda_e = \lambda + \lambda_r + \lambda_s$

For a volume V of the compartment (m^3) the concentration of activity C(t) in Bq m^{-3} is given by

$$C(t) = \frac{A(t)}{V}$$

....(4.13)

This concentration can be used to assess the exposure of the critical group residing in the vicinity of the discharge, subject to the specification of dietary and other habits together with concentration factors between sea water and other environmental media. In general, this exposure contributes insignificantly to the collective dose and has been ignored in this context. The main role of the local model in this study is to act as an interface between a discharge and the regional marine compartments.

The rate of activity leaving the local compartment is a function of time given by

$$Q_{1r}(t) = \lambda_r A(t) = \lambda_r \frac{Q}{\Lambda_e} (1 - \exp(-\Lambda_e t))$$

....(4.14)

where $Q_{1r}(t)$ is the amount of activity going from the local compartment ($Bq s^{-1}$)

The equilibrium rate of activity leaving the local compartment for a continuous discharge is therefore

$$Q_{1r}(\infty) = \lambda_r \frac{Q}{\Lambda_e}$$

....(4.15)

To a good approximation, this equilibrium rate can be equated to the total activity over all time leaving the compartment for a discharge which continued for 1 year. This quantity is dependent on the ratio λ_r/Λ_e which is both site and nuclide dependent. The values of site dependent parameters are given in Table 4.10 and some results for

different nuclides at two different sites, on the Gulf di Taranto and on the eastern Irish Sea, respectively, are given in Tables 4.11 and 4.12. These tables show that for most nuclides the equilibrium rate of removal from the local compartment for a continuous discharge is attained within the first year. There are slight variations for the Gulf di Taranto because the local compartment has a relatively low rate of exchange with the regional compartment. However these differences between $Q_{1R}(1\text{ y})$ and $Q_{1R}(\infty)$ are not considered significant and only amount to 1 or 2 per cent for this site. The Eastern Irish Sea local box has both high water exchange rates and sedimentation rates and therefore $Q_{1R}(1\text{ y})$ and $Q_{1R}(\infty)$ can be considered equal.

4.4.2 Regional model

Figures 4.9 and 4.10 show the various regions used in the regional models as well as the discharge locations considered. It has been decided to separate the Mediterranean Sea from the seas of Northern Europe because of the limited exchange between the Mediterranean and the Atlantic via the Straits of Gibraltar. This separation simplifies the mathematical treatment considerably.

4.4.2.1 Description of the model used

The model can conveniently be described under five headings: water movements, sediments, marine foodstuffs, radionuclide decay chains and the calculation of collective intakes.

(a) Water movements

The technique of compartmental analysis is used to model the movements of water, and the associated activity, between the various sea areas. This technique assumes instantaneous uniform mixing within each compartment, with the rates of transfer between compartments being defined by transfer coefficients. Figures 4.11 and 4.12 show the compartments used in the two models (North European waters and the Mediterranean Sea) and the relations between them.

In order to allow for the return of long-lived nuclides to the regional waters of Northern Europe or the Mediterranean Sea following their dispersion in the rest of the world's oceans, two large compartments have been included, namely those representing the Atlantic Ocean (or the remainder of it) and the remainder of the world's oceans.

The differential equation which describes the variation of the activity in compartment i of the model is of the form:

$$\frac{dA_i}{dt} = \sum_{j=1}^{j=N} K_{ji} A_j - K_{ij} A_i - K_i A_i + Q_i$$

for all $i = 1, N$

....(4.16)

where A_i is the activity present at time t in compartment i (Bq),

K_{ij} is the rate of transfer from compartment i to compartment j (s^{-1}), with $K_{ii} = 0$

K_i is the rate of loss from compartment i by radioactive decay, sedimentation etc (s^{-1}),

Q_i is the rate of discharge into compartment i ($Bq\ s^{-1}$),

and N is the number of compartments in the system.

A quantity often used is the volume exchange, $R_{ij}\ km^3\ s^{-1}$, from compartment i to compartment j ,

$$R_{ij} = K_{ij} V_i \dots\dots(4.17)$$

V_i being the volume of compartment i (km^3)

(b) Sediments

The adsorption of activity by sediments can result in significant depletion of activity from the water phase. Such depletion is due to both the partitioning of the activity between the liquid phase and the solid phase (suspended sediments) and the removal of activity from the water column to bottom sediments. The amount of activity which is in solution is the quantity which needs to be calculated because the concentration factors for sediments and marine organisms are defined with respect to this soluble fraction.

The sediment concentration factor, or distribution coefficient, K_d , is defined as the ratio of amount of radionuclide per unit weight of dry sediment to the amount per unit volume of water ($Bq\ g^{-1}$ per $Bq\ cm^{-3}$ or $Bq\ t^{-1}$ per $Bq\ m^{-3}$). Table 4.2 gives values of the sediment concentration factor, K_d , which have been adopted for the nuclides being studied 4.39 and 4.40. For a given element, it is common to obtain variations in K_d by two orders of magnitude according to the physical and chemical properties of the radionuclides and the sediments. The values given in Table 4.2 are considered most appropriate to the sediments of the continental shelf and in particular to the sediments in the zone where sedimentation is most marked.

Depletion by sediments is greater for those nuclides with the higher values of the sediment concentration factor; it will also be greatest in those sea areas with high suspended sediment loads and/or high rates of sediment deposition, particularly if such sediments are of small grain size, such as mud and silts, which have a high surface area to volume ratio. At any given time the activity in the water column is partitioned between the water phase and the suspended sediment material. The fraction of the activity in the water column which is in solution (the filtrate fraction), F_w , is given by:

$$F_w = \frac{1}{1 + K_d ss} \dots(4.18)$$

where ss is the suspended sediment load ($t m^{-3}$).

Figure 4.13 shows the possible variation in F_w as a function of suspended sediment load ss for ruthenium-106, caesium-137 and plutonium-239. Enhanced values for the K_d factors (ie, not those given in Table 4.2) are assumed for the purposes of an example. For radionuclides with small values of K_d , such as caesium-137, the fraction of activity adsorbed on the suspended sediments is only a few percent, even in areas with high suspended sediment loads ($10^{-5}/10^{-4} t m^{-3}$). However, for radionuclides such as plutonium-239 which have high values of K_d , the value F_w is reduced by a factor of 1.4 for a sediment load of $2 \cdot 10^{-6} t m^{-3}$, as has been observed [4.33] and a factor of 5 for a sediment load of $3 \cdot 10^{-5} t m^{-3}$.

In order to take account of higher adsorption of the finer grain suspended sediments it may be necessary to assume enhanced values for the K_d 's given in Table 4.2 for all radionuclides [4.19] so that agreement with measured values can be attained [4.33]. However in this study no such enhancement has been assumed, mainly because to assume no enhancement is a conservative assumption, but also the data on this phenomenon exist only for certain nuclides. Hence the values for K_d shown in Table 4.2 have been used.

The removal of activity to bottom sediments is evaluated using a particle scavenging model. This assumes that removal of a radionuclide from solution in sea water and its transport to the ocean floor is determined by two main factors: the sediment concentration factor and the rate of settling of particulate matter from the water column to bottom sediments. The particle scavenging model assumes that the radioactivity is uniformly distributed as a function of water column depth, a reasonable assumption in most continental shelf waters except in the vicinity of the discharge point itself. The fractional removal of activity from the water to sediments, λ_s (s^{-1}) is given by:

$$\frac{F_w K_d s}{h} = \frac{K_d s}{h (1 + K_d ss)} \dots(4.19)$$

where s is the sedimentation rate ($t m^{-2} s^{-1}$) and

h is the mean water depth (m).

Values for s , ss and h for each regional compartment of the marine models are given in Tables 4.3 and 4.7 for the Northern European waters and Mediterranean respectively. These data are averaged over quite large sea areas and therefore there may be some variations from the mean at particular positions within these areas [4.19].

It is assumed that the adsorption of activity by bottom sediments is irreversible and therefore no return of activity to the water phase occurs. This is a mechanism into which further research is being carried out [4.19], especially the effect of remobilisation of bottom sediments and the desorption of activity due to chemical changes occurring on the sea bed.

(c) Marine foodstuffs

Having calculated the concentrations of the filtrate fraction of the water in each of the sea areas of the regional model for a given discharge, these are combined with concentration factors for the edible part of marine foodstuffs (given in Table 4.2) and with catch data for each of the sea areas in order to calculate the collective intakes of activity.

The concentration factors are taken from two references [4.39] and [4.40] and the adopted values in some cases reflect a compromise between different data. There are many acknowledged difficulties in both the measurement of K_d 's and their use in time dependent models and therefore Table 4.2 should not be used uncritically. There could be local and regional variations and certain species of fish may have different K_d values from those given in Table 4.2. Nevertheless it is felt that this tabulation represents the best available current data.

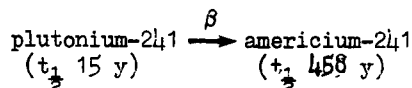
In using the catch data it is assumed that catches by EC countries can be equated to total consumption within those countries, ie, in terms of total intakes of activity the effects of imports by and exports from the EC are negligible. Included in the total catches of fish are those species, for example Norwegian pout and sand eels, which are not caught for human consumption but are used in the manufacture of cattle food and other materials. This will lead to conservative estimates of collective intakes of activity by man, particularly from the Northern, Central and Southern North Seas areas in which the catches of such species represent a significant fraction of the total catch. The catch data need to be corrected to allow for the edible fraction, and this is taken to be 50% of all marine foodstuffs. This is a conservative assumption for crustacea and particularly molluscs whose realistic edible fractions are closer to 35% and 15% respectively [4.19].

(d) Radionuclide daughter products

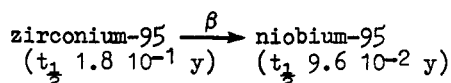
A radiological assessment requires the consideration of the daughter products of radionuclides where these are significant. For many of the fission products which have radioactive daughter nuclides and which are of concern in discharges to the aquatic environment, the daughter nuclides are very short-lived relative to their parents, for example caesium-137 ($t_{1/2} = 30.1y$) and its daughter product barium-137m, ($t_{1/2} = 2.55 min$). If the radioactive half-life of the daughter nuclide is of the order of a day or less, as is often the case, the behaviour of the daughter product in the environment will essentially be determined by that of its parent. In these cases the two nuclides can be considered to be in secular equilibrium throughout the environment.

However for long-lived daughter products it is necessary to consider the behaviour of the daughter separately from its parent.

Two examples for which this may be particularly important are:



and



In the former case equilibrium between parent and daughter are never achieved, and a peak americium-241 activity will occur about 75 years after discharge of plutonium-241. The ratio of peak americium-241 to initial plutonium-241 activity is approximately 0.03. The possible importance of this nuclide pair arises because of the greater dose equivalent per unit intake and greater concentration factors for americium-241 relative to plutonium-241, and the generally greater arisings of americium-241 due to decay of plutonium-241 than from the direct discharge of americium-241. In the case of zirconium/niobium-95, a state of transient equilibrium is approximately reached after a period of about six months after release of zirconium-95 and from then onwards the niobium-95 ratio is approximately 2.

A daughter product chain is modelled by adding for each daughter product in a decay chain a further set of compartments identical to those shown in Figures 4.11 and 4.12. For each set of compartments the physical oceanographic parameters are the same but the nuclide dependent terms such as radioactive decay and sedimentation rates are varied between the sets of compartments according to the properties of the various nuclides in the decay chain. Transfer between the sets then occurs between compartments representing the same sea areas, the value of transfer coefficient being the appropriate radioactive decay constant. Thus daughter products are modelled in a "mirror" system of the parent nuclide, with interaction between each system being the radioactive decay terms.

(e) Collective intake by the population of the EC

The solution of the system of differential equations (4.16) allows the calculation of activity present in each compartment, as a function of time, for a discharge into any one of the compartments. The concentration of activity in the water (Bq m^{-3}) is then obtained for each compartment by dividing its activity by the compartment volume.

The time integral of the collective intake from ingestion of a marine foodstuff, f , contaminated by the discharge of a radionuclide is given by:

$$\text{IC}(t) = \sum_{i=1}^N C_i(t) K_d^f P_i^f F_e^f \dots (4.20)$$

where $IC(t)$ is the time integral of the collective intake to time t (Bq)

$C_i(t)$ is the time integral of nuclide concentration in filtered sea water in region i ($Bq\ y\ m^{-3}$) to time t

K_d^f is the nuclide dependent concentration factor for seafood f ($Bq\ t^{-1}\ Bq\ m^{-3}$)

P_c^f is the annual catch of seafood f in region ($t\ y^{-1}$)

F_e^f is the edible fraction of the seafood f

This time integral of the collective intake can be used to calculate the collective effective dose equivalent commitments (or truncated values of this quantity) in the manner outlined in Chapter 2 and using the dose per unit intake by ingestion evaluated in Chapter 6. In this chapter however only the time integrated collective intakes are considered.

(f) Some limitations of the regional models

Both the Northern European Waters model and the Mediterranean model take account of exchange with the Worlds Oceans but not of exchange with the atmosphere.

For the great majority of the nuclides considered, the exchange with the atmosphere is at a low rate and it is reasonable to limit the model to the marine environment. In these cases the predominant means of transfer to man is the ingestion of marine organisms; this is the only route of transfer which has been considered in this study for the majority of the radionuclides.

The exceptions are tritium, carbon-14 and iodine-129 which, because of their chemical properties, environmental behaviour and their long radioactive half-lives, may undergo significant exchange between the aquatic environment and the atmosphere. The transfer of activity to the atmosphere and subsequently to the terrestrial environment may lead to additional significant pathways of exposure, not so far considered in the regional model.

In order to study this more widespread dispersion of these three nuclides, models have been used which consider all the sectors of the environment. For these nuclides, the regional marine model is used first, for a period of 50 years following the discharges, to evaluate the regional marine component of the collective intakes. After 50 years, the dispersion is relatively homogeneous in all the seas around the European coasts and global models, involving the other sectors of the environment are adopted; these are the subject of Chapter 5.

4.4.2.2. Results obtained with the regional marine models

The results of the calculations are values of collective intakes of activity from consumption of fish, crustacea and molluscs by the population of the EC from unit discharge per second continuously for one

year from a local to a regional marine compartment. These collective intakes from the three types of marine foodstuff have been summed to give a total collective intake. The values of the collective intakes by the three foodstuffs and the total collective intake have also been integrated over various time periods following the discharge to give integrated collective intakes.

The presentation and discussion of these results, as well as the values of the parameters adopted are given separately for the discharges from local compartments to the North European waters and the Mediterranean Sea respectively.

(i) Northern European waters

(a) Water movements

A computer code NOCEAN has been written to solve the series of differential equations (4.16) which represent the rates of movement of water between the various compartments 4.15, the source input and loss terms due to radioactive decay and sedimentation effects. This code utilises some general numerical methods developed at AERE, Harwell 4.16.

The choice of sea area for each compartment has been determined by consideration of the dispersion characteristics of the region, the availability of various oceanographic data, the sites of discharges of radioactivity and the availability of fisheries statistics. Figure 4.9 shows the area covered by each compartment within the continental shelf region of Northern Europe; not included in Figure 4.9 are those additional compartments which model the subsequent global ocean dispersion and which are included in the model to allow for the possible return of long-lived nuclides to continental shelf waters.

All the compartments used in the model and their inter-relationships are shown schematically in Figure 4.11, which gives values for the water volumes 4.17 to 4.23 of each of the compartments ($V \text{ km}^3$) and for the volume flow rates between compartments ($R \text{ km}^3 \text{ y}^{-1}$). As far as possible these flow rates have been obtained from a review of the literature 4.17 to 4.20, 4.24 to 4.30, but where data were not available estimates have been made based on water currents, likely residence times in an area and by considering conservation of water volumes for each compartment. In some cases the adequacy of the data is good, for example that for the Irish Sea which has been the subject of considerable study 4.19, 4.31, 4.32. However, for some sea areas the rates of exchange could only be estimated and are therefore to be regarded as speculative. The reliability of these transfer coefficients is discussed further in reference 4.15.

(b) Sediments

The values adopted for the suspended sediment load of each marine compartment are given in Table 4.13 4.25, 4.34, 4.35; many of these are values relative to coastal zones which have been extended to the whole of the compartment. The values adopted range from $1 \cdot 10^{-7}$ to $6 \cdot 10^{-6} \text{ t m}^{-3}$.

The values of sedimentation rates s 4.15, 4.18, 4.25, 4.33, 4.36 to 4.38 and depths h 4.18, 4.19, 4.21, 4.22, 4.39 for each

marine compartment are given in Table 4.13.

(c) Marine foodstuffs

Table 4.14 gives the assumed annual catches by EC countries of the principal marine foodstuffs - fish, crustacea and molluscs - from each area of the regional model. The data are based on the 1975 figures given by the International Council for the Exploration of the Sea [4.43] and the 1976 data by the Food and Agriculture Organisation [4.44]. It is assumed that such a level of fish catches will be maintained for the indefinite future.

For the Irish Sea the ICES only tabulates data for the whole of that sea. Since no more specific data for EC fish catches are available, the value for the total Irish Sea has been split to provide estimates for three sub-divisions of the Irish Sea in the regional model, using values of the percentage of UK fish catches in each of these areas [4.19]. This will not introduce a large error as approximately 50% of the total EC fish catch from this area is by the UK.

(d) Collective intakes

Table 4.15 shows values of the total collective intakes for a range of nuclides integrated over 1, 10, 50, 100, 500 years and infinity for a unit discharge per second continuously for one year from a local compartment into the southern North Sea.

The integrated collective intakes for discharges from local boxes into four regional compartments are given in Table 4.16. The results for inputs into any other sea area could be represented in a similar way. They have been tabulated as intakes resulting from a discharge from a local box so that they may be used for a number of different sites having unique local characteristics but discharging into the same regional sea areas.

When comparison of collective intakes from different discharges is required, the results contained in Tables 4.15 and 4.16 need to be combined with the results of the appropriate local box model for the different sites. Hence Tables 4.15 and 4.16 do not provide a comparison of actual discharges into the different regional sea areas. As the Mediterranean Sea is not a compartment of the model used for discharges into North European Waters, the water concentrations in the Mediterranean are taken to be equal to those in the Atlantic Ocean when calculating collective intakes from catches in the Mediterranean Sea.

The total collective intakes shown in Table 4.15 vary considerably with the radioactive half-life, the concentration factor in marine foodstuffs and the behaviour with respect to sediments of each nuclide. For example, the collective intakes (integrated to 50 y) per unit discharge of iodine-131 ($t_{1/2}$ 2.2 10^{-2} y) are a factor of at least 10 lower than those for iodine-129 ($t_{1/2}$ 1.57 10^7 y) due to the very short half-life of the former nuclide. However the difference is only a factor of about 2 for cobalt-58 ($t_{1/2}$ 1.94 10^{-1} y) compared with cobalt-60 ($t_{1/2}$ 5.28 y), and is less than a factor of 2 for caesium-134 ($t_{1/2}$ 2.08 y) compared with caesium-137 ($t_{1/2}$ 30.1 y).

The effect of differing concentration factors can be seen most markedly by comparing the collective intakes (integrated to 50 y) for

tritium and carbon-14, for which the concentration factors are 1.0 and 5×10^3 Bq t⁻¹ per Bq m⁻³ respectively (values for fish, crustacea and molluscs being the same). These two nuclides behave in a qualitatively similar manner with respect to sediments and, when account is taken of their differing half-lives, it is the difference in concentration factors which determine the relative magnitude of the collective intakes.

The effect of adsorption of activity on sediments and the subsequent depletion of the water column can be significant for certain nuclides such as plutonium-239. In this case the effect of depletion of activity by adsorption onto sediments is as much as 25%. Since plutonium-239 has a very high sediment concentration factor, the effect will be smaller for most other nuclides. This depletion is due to both adsorption onto suspended sediments and also removal to bottom sediments. For the southern North Sea it is the former which is estimated to be by far the more important due to the relatively high value of the suspended sediment load and the relatively low rate of sedimentation in the North Sea. However, for the eastern Irish Sea, the effect of removal of activity to bottom sediments is more significant due to the very much greater rate of sedimentation in this area. The effect of depletion to sediments is about a factor of 10, with suspended sediments only causing a depletion by a factor of 1.2. For cobalt-60 in the Irish Sea the factor is about 2.

It is of interest to compare the different values of total collective intakes for discharges into the various regional sea areas. It should be noted, however, that the comparison makes no allowance for local environmental conditions prior to the discharge into the required sea area. For an explicit comparison of discharges from particular sites it would be necessary to take such factors into account. Table 4.14 shows that of the four regions considered the integrated total collective intakes are highest for discharges into the southern North Sea and English Channel East, which tend to be very similar due to their proximity; those for the eastern Irish Sea are generally lower by factors of about 2 for many nuclides but with certain exceptions; collective intakes are lowest for the Bay of Biscay, these being about two orders of magnitude below those for the southern North Sea.

The relative importance of the different sea regions is determined by two factors; firstly, the oceanographic parameters of the sea area and those of adjacent sea areas. For example exchange of waters in the Bay of Biscay with the large water masses of the Atlantic is relatively rapid and so results in relatively lower collective intakes. Also, the effect of the high rate of sedimentation in the Irish Sea is to considerably reduce the collective intakes of plutonium-239 from the Eastern Irish Sea (as discussed above).

The relative significance of inputs into different sea regions is determined by the relative importance of the catches of the various marine foodstuffs combined with the nuclide concentration factors in the marine organisms. For example Figures 4.14 and 4.15 show the relative importance of fish, crustacea and molluscs for the collective intakes of three nuclides - cobalt-60, caesium-137 and plutonium-239 - from two sea areas - the 50 year integrated intakes have been used in these illustrations. From these it can be seen that the percentage contributions from the three marine foodstuffs varies depending on both the nuclide and the sea area. It is interesting to note that for

those nuclides that behave in a non-conservative manner in sea water and therefore have relatively high concentration factors in shellfish, the mollusc catch is often the marine foodstuff giving rise to the largest collective intake.

The relative contributions from different sea areas to the 50 year integrated total collective intakes are shown in Figure 4.16 for unit discharge rate from a local box to the southern North Sea of caesium-137 and plutonium-239. From Figures 4.14 and 4.16 and Table 4.14 it can be seen that for caesium-137 it is the large fish catches from in order of importance, the central, southern and northern North Sea and Baltic Sea which largely determine the total collective intake, whereas for plutonium-239 the dominant foodstuff is molluscs and the order of importance of the sea areas is southern, central and northern North Sea and the English Channel East.

Lastly, it can be seen from Table 4.15 that for many nuclides the values of the integrated total collective intakes do not increase significantly after about 50 years, or even after 10 years for the nuclides with half-lives of a few years or less. However, for very long-lived nuclides such as technetium-99 and plutonium-239 the integrated collective intakes can be seen to increase to some degree at very long periods of time after the initial release. This is due to the integration over very long time periods of very small annual collective intakes. This is shown for technetium-99 in Figure 4.17.

(ii) Mediterranean Sea

(a) Water movements

Mediterranean type seas [4.45] lie either between continental land masses or between a continent and a group of islands; in particular they are only in exchange with the world's oceans by very narrow straits whose depths are less than those of the seas themselves. The Mediterranean seas have, therefore, very little circulation. They often have salinity anomalies in relation to the oceans and in particular have an anomalous temperature profile. The characteristics of the Mediterranean are to be found in the "Mediterranean of the Ancient World" (Figure 4.10) [4.17 and 4.45]. The sea exchanges with the western Atlantic Ocean by the Straits of Gibraltar and to the east with an inland sea, the Black Sea, by the Dardanelles and the Bosphorous. The mean depth is 1400 m. The Straits of Gibraltar have a depth of about 300 m, the Bosphorous 40 m and the Dardanelles 80 m [4.17].

The Mediterranean Sea itself can be divided into two basins clearly separated by the narrowing across a line Italy-Sicily-Tunisia where the depth is a maximum of 400 m. The thermocline in the west basin is only temporary whereas it can be considered to be permanent in the eastern basin. Its mean depth has been estimated as 100 m [4.17].

These characteristics have led to the choice of compartments shown in Figure 4.12 which also gives the volumes of the compartments (km^3) and the volume exchange between them ($\text{km}^3 \text{y}^{-1}$). In general, these exchanges are less well known than those for Northern European waters. The exchanges between the Mediterranean and the Atlantic and the Black Sea have been taken from the literature [4.17] but the exchanges between the west and east basins have been derived by calculations. This has been done partly from the measurements of strontium-90 resulting from nuclear

explosions in the northern hemisphere [4.47] and partly from balancing the water inputs (from the Atlantic, the Black Sea, rivers and rain-fall) with evaporation. The method used is described in the Appendix A4.2.

(b) Sediments

The values adopted for the rate of sedimentation, the suspended sediment load and the water depth in each compartment are shown in Table 4.17. Due to the lack of data these are mostly estimates and are not necessarily based on measurements; they reflect therefore a considerable measure of scientific judgement.

(c) Marine foodstuffs

The fish catches in the Mediterranean by the European Community (essentially by France and Italy) are 12000 t y⁻¹ of crustacea, 91000 t y⁻¹ of molluscs and 281000 t y⁻¹ of fish [4.48]. For the east-Mediterranean basin, it has been estimated that 2/3 of the catches are from the upper layer and 1/3 from the bottom layer of the sea. The fish catches are given in Table 4.16. The quantities of fish from the Atlantic Ocean are taken to be equal to the total quantity from the Northern European waters:

3.68	10 ⁶ t y ⁻¹	of fish
9.9	10 ⁴ t y ⁻¹	of crustacea
4.0	10 ⁵ t y ⁻¹	of molluscs

(d) Collective intakes

Table 4.19 shows total collective intakes integrated to various times for unit discharge rate of 1 Bq s⁻¹ for 1 year from a local box into the eastern Mediterranean. For all radionuclides the intakes are less than those from releases into Northern European waters, with the exception of releases into the Bay of Biscay. This is because EC countries consume more seafoods from Northern European waters than they do from the Mediterranean (the collective intakes resulting from releases into the Bay of Biscay are low because this area exchanges directly with the North Atlantic and is not extensively fished). Depletion of activity in water by sedimentation effects is however less pronounced in Mediterranean waters due to the lower suspended sediments loads and the greater average depth of the Mediterranean (Tables 4.13 and 4.17). This latter effect will lead to enhanced collective intakes for nuclides experiencing significant sedimentation but it is a small effect in comparison to the difference in seafood consumption. It can be seen however in comparisons between regional values of the ratio of total collective intakes integrated to 50 y for plutonium-239 and caesium-137. In the case of releases to the southern North Sea this ratio is 2.9, while for releases to the western and eastern Mediterranean it is 8 and 7.7 respectively. This indicates the lower rate at which plutonium-239 is depleted by sedimentation effects in Mediterranean waters.

Table 4.20 shows the total collective intakes integrated to various times for a discharge of 1 Bq s⁻¹ for 1 year from a local box into the western Mediterranean. There are marked differences between the collective intakes for discharges into the eastern and western Mediterranean for short periods of integration; in general these differences, at least for the longer-lived radionuclides,

decrease with increasing integration time. The differences between intakes at short times in these regions are essentially a reflection of the different volumes and seafood catches; because the compartment volumes are large the fractional exchanges and thus the contributions from adjacent compartments to collective intakes, are small at the end of 1 year. For example the total collective intakes of tritium at the end of 1 year given in Tables 4.17 and 4.18 are in proportion to the ratio of the volumes of the eastern and western Mediterranean. This proportionality is not present when the radionuclides have a short half-life or interact strongly with sediments.

Figures 4.18 and 4.19 show the relative contributions of different marine foodstuffs to the 50 year integrated total collective intake for discharges via a local box to the upper layer of the eastern Mediterranean and to the western Mediterranean for cobalt-60, caesium-137 and plutonium-239. These two figures are very similar, with molluscs forming the largest contribution for cobalt-60 and plutonium-239, whilst fish dominate in the case of caesium-137.

Figures 4.20 and 4.21 show the relative contributions of different sea areas to the 50 year integrated total collective intake for discharges of cobalt-60, caesium-137 and plutonium-239 via a local box to the upper layer of the eastern Mediterranean and to the western Mediterranean. The relative importance of the upper eastern Mediterranean compartment can be seen; evaporation is an important mechanism in this region and hence there is a compensatory movement of water from west to east.

Finally Figure 4.22 shows the variation of total collective intake as a function of time and the contribution of different sea areas in the case of technetium-99. The long half-life of this nuclide means that intakes from seas outside the Mediterranean become significant at long times. The contribution from other seas is less important for integration to 500 years (11% of the total collective intake) but becomes dominant when integrating to infinity (76% of the total collective intake). This is due principally to the fact that the quantity of marine foodstuffs consumed in the EC from Northern European waters is about 10 times more than the quantity consumed from the Mediterranean.

REFERENCES

- 4.1] US Nuclear Regulatory Commission, Calculation of annual doses to man from routine release of reactor effluents for the purpose of evaluating compliance with 10 CFR, Part 50, Appendix I. USNRC, Regulatory Guide 1.109 (1976).
- 4.2] Prakash, A, Convective dispersion in perennial streams. Proc. ASCE, J. Environ. Eng. Div., 103 (EE2) 321 (1977).
- 4.3] Murray, C N and Avogadro, A, Preliminary report on modelling the transfer of activity through a marine ecosystem. ISPRA Establishment Office, Report of the Chemistry Division, N3801 (1978).
- 4.4] Schaeffer, R, Conséquences du déplacement des sédiments sur la dispersion des radionucléides. IN Proc. Conference on Impacts of Nuclear Releases into the Aquatic Environment, Otaniemi 1975. Vienna, IAEA, p. 263 (1976) IAEA-SM 198/4 (see also ORNL-tr-4348).
- 4.5] Bouville, A and Fabre, H, Etude de la dispersion des radioéléments dans une rivière. CEA (To be published).
- 4.6] Le bassin Loire-Bretagne - Publication Agence de Bassin Loire-Bretagne, Avenue de Buffont 45018 Orléans.
- 4.7] Bayer, A, The radiological exposure of the population in the Rhine-Meuse region by nuclear installations during normal operation. Luxembourg, CEC doc. V/1647/77 (1978).
- 4.8] Delmas, J, Grauby, A and Disdier R, Etudes expérimentales sur le transfert dans les cultures de quelques radionucléides présents dans les effluents des centrales électronucléaires. IAEA SM-172/61 321-332 (1973).
- 4.9] Delmas, J, Disdier, R, Grauby, A and Bovard, P, Radiocontamination expérimentale de quelques espèces cultivées soumises à l'irrigation par aspersion. IN Proc. International Symposium on Radioecology, CEN Cadarache, September 1969.
- 4.10] Porte, R and Bohet, C, Etude de la dispersion d'un polluant en milieu marin et dans les eaux continentales de surface; Séminaire sur la dispersion en milieu physique naturel - Cadarache, Paris, Société Française de Radioprotection (1978).
- 4.11] Bernhard, M, Cagnetti, P and Zattera, A, La diffusione in acque basse di mare: prime esperienze con Rodamina B. G. Fis. Sanit. Prot. Radiaz., 16, no. 2 (1972).
- 4.12] Bernhard, M, Cagnetti, P, Zattera, A and Schreiber, B, Processi e modelli di diluizione, riconcentrazione della ricettività ambientale del sito marini della Trisaia (Golfo di Taranto) Estratto da: "La scelta dei siti per gli impianti nucleari" Atti Convegno Trisaia P. 169-209, RT/PROT (74) 17. (1972).

- 4.13] Branca, G and Cagnetti, P, Disposal into the sea of radioactive wastes in Italy. Marine Pollution and Marine Waste Disposal by Pearson and Frangiapane - Pergamon Press - Oxford and New York (1975).
- 4.14] Cagnetti, P, Expériences de diffusion dans l'atmosphère et dans l'eau des rejets des installations nucléaires - Siting of nuclear facilities - IAEA-SM-188/28 - Vienna (1975).
- 4.15] Grimwood, P D and Clark, M J, A model of the dispersion of radioactivity discharged into the seas of northern Europe. Harwell, National Radiological Protection Board. (To be published).
- 4.16] Chance, E M, et al. FACSIMILE: A computer program for flow and chemistry simulation, and general initial value problems. Harwell, UKAEA, AERE-R8775. (1977).
- 4.17] Sverdrup, H U, Johnson, M W, and Fleming, R H, The Oceans. London, Prentice-Hall (1942).
- 4.18] Bialek, E K, Handbook of Oceanographic Tables. US Naval Oceanographic Office (1966).
- 4.19] Jefferies, D F, FRL, MAFF, Lowestoft, Personal communications (1977, 78, 79).
- 4.20] Kautsky, H, The caesium-137 content in the water of the North Sea during the years 1969 to 1975. Dent. Hydro. Zeit., 29, 217 (1976).
- 4.21] Heaps, N S, Development of a three-dimensional numerical model of the Irish Sea. Rapp. P - V Ruen. Cons. Int. Explor. Mar., 167, 147 (1974).
- 4.22] Lee, A J and Ramster, J W, Atlas of the seas around the British Isles. Lowestoft, MAFF Fisheries Research Technical Report 20, (1977).
- 4.23] Weichart, G, Pollution of the North Sea, *Ambio*, 11, (4) 99 (1973).
- 4.24] McCave, I N, Mud in the North Sea. IN Proc. NATO Conference on North Sea Science, Aviemore, 1971. (Goldberg, E D, ed) MIT Press (1973).
- 4.25] Postma, H, Transport and budget of organic matter in the North Sea. Proc. NATO Conference on North Sea Science, Aviemore, 1971. (Goldberg, E D, ed), MIT Press (1973).
- 4.26] Cartwright, D E, A study of currents in the Straits of Dover. J. Inst. Navig., XIV, (2), 130 (1961).
- 4.27] Prandle, D, Residual flows and elevations in the southern North Sea. Proc. R. Soc. (London) Ser. A, 359, 189 (1978).

- 4.28] Prandle, D, Monthly-mean residual flows through the Dover Strait; 1949-1972. J. Mar. Biol. Assoc. (To be published).
- 4.29] Bergman, R et al, Ecological transport and radiation doses from radioactive substances carried by groundwater. KBS-40 (1977).
- 4.30] Jefferies, D F, et al, Distribution of caesium-137 in British coastal waters. Mar. Pollut. Bull., 4, 118 (1973).
- 4.31] Mitchell, N T, Radioactivity in surface and coastal waters of the British Isles, 1976. Part 1: The Irish Sea and its environs. Lowestoft, MAFF, FRL 13 (1977). (See also earlier reports in this series).
- 4.32] Hetherington, J A, The behaviour of plutonium nuclides in the Irish Sea. IN Proc. International Conference on Environmental Toxicity, Univ. of Rochester, June 1975.
- 4.33] Hetherington, J A, et al, Some investigations into behaviour of plutonium in the marine environment. IN Proc. Symposium on Impacts of Nuclear Releases into the Aquatic Environment, Otaniemi, 1975. Vienna, IAEA (1976) IAEA-SM-198/29.
- 4.34] Turnekian, K K, Some aspects of the geochemistry of marine sediments. IN Chemical Oceanography, Vol. 2, (Riley, J P and Skirrow, G, eds.) Academic Press (1965).
- 4.35] Simola, K et al. Plutonium in Baltic sediments. IN Proc. 4th International Congress of IRPA, Paris, April 1977.
- 4.36] Belderson, R H, Holocene sedimentation in the western half of the Irish Sea. Mar. Geol., 2, 147 (1964).
- 4.37] Shepherd J, FRL MAFF, Lowestoft. Personal communications (1977).
- 4.38] National Academy of Sciences. Radioactivity in the Marine Environment, NAS Washington (1971).
- 4.39] Ancellin, J., Guegueniat, P and Germain, P, Radioécologie Marine. Edition Eyrolles, Paris (1979).
- 4.40] The radiological basis of the IAEA revised definition and recommendations concerning high-level radioactive waste unsuitable for dumping at sea. IAEA-211. (1978).
- 4.41] Horne, R A, Marine Chemistry. Wiley Interscience (1969).
- 4.42] Chester, R, and Aston, S R, The geochemistry of deep-sea sediments. IN Chemical Oceanography, Vol. 6 (Riley, J P and Skirrow, G, eds.) Academic Press (1976).
- 4.43] Conseil international pour l'exploitation de la mer. Bull. Stat. Pêches Maritimes, 60, 1975, Copenhagen (1978).

- 4.44] Food and Agriculture Organisation. Conseil général des pêches pour la Méditerranée. FAO Bull. Stat., no. 2, Captures nominales 1966-1976 (1978).
- 4.45] Peres, J M, Océanographie biologique et biologie marine. Presses Universitaires de France (96) (1961).
- 4.46] Thompson, S E, Burton, C A, Quinn, D J and Ng, Y C, Concentration factors of chemical elements in edible aquatic organisms, Univ. California, Lawrence Livermore Laboratory, UCRL-5-564 Rev. 1 (1972).
- 4.47] Batrakov, G F, Ereemeev, V N, Zemlyanoi, A D, Ivanova, T M and Pavlidi, I M, ⁹⁰Sr content in the Mediterranean Sea. At. Energ., 43, 197 (1977).
- 4.48] Booth, R S, A systems analysis model for calculating radionuclide transport between receiving waters and bottom sediments. IN Environmental Toxicity of Aquatic Radionuclides: Models and Mechanisms, Chap. 7. Ann Arbor Science Publishers Inc (1976).
- 4.49] Pouthier, J, Personal communication (1978).
- 4.50] Salenc, P, Le rôle de la Compagnie Nationale du Rhône dans la mise en valeur agricole de la vallée. Cah.Ing.Agron., 302, January (1976).
- 4.51] Neil, P, Irrigation des cultures legumieres de plein air Water Management, 10, July-September (1976); 12, January-March (1977).
- 4.52] Recensement général de l'Agriculture (1970-1). Ministère de l'Agriculture et du développement rural (1972).
- 4.53] CNABRL Etude des investissements hydro-agricoles dans la Vallée du Rhône au cours du VII^{ème} Plan. (Compagnie nationale d'aménagement du Bas-Rhône-Languedoc) (Janvier 1973).
- 4.54] ICRP. Recommendations of the International Commission on Radiological Protection, Report of Committee 2 on Permissible Dose for Internal Radiation (1959). Oxford, Pergamon Press, ICRP Publication 2 (1960).
- 4.55] Nihoul, J C J, and Runday, F G, Hydrodynamic models of the North Sea. Mémoires Société Royale des Sciences de Liège 6^e série tome X pp 61 - 96 (1976).
- 4.56] Leliavsky S, Précis d' hydraulique fluviale. Paris, Dunod (1961).

Table 4.1

Radionuclides considered in the evaluation
of the radiological consequences of aquatic releases

Nuclide	Half-life (y)	Nuclide	Half-life (y)
H-3	$1.23 \cdot 10^1$	Te-127m	$2.98 \cdot 10^{-1}$
C-14	$5.70 \cdot 10^3$	Te-129m	$9.21 \cdot 10^{-2}$
Cr-51	$7.58 \cdot 10^{-2}$	Te-132	$8.90 \cdot 10^{-3}$
Mn-54	$8.54 \cdot 10^{-1}$	I-129	$1.57 \cdot 10^7$
Fe-55	2.70	I-131	$2.20 \cdot 10^{-3}$
Fe-59	$1.23 \cdot 10^{-1}$	Cs-134	2.08
Co-58	$1.94 \cdot 10^{-1}$	Cs-136	$3.56 \cdot 10^{-2}$
Co-60	5.28	Cs-137	$3.01 \cdot 10^1$
Zn-65	$6.70 \cdot 10^{-1}$	Ce-144	$7.77 \cdot 10^{-1}$
Sr-89	$1.38 \cdot 10^{-1}$	Eu-154	8.50
Sr-90	$2.82 \cdot 10^1$	Eu-155	4.96
Y-90	$7.31 \cdot 10^{-3}$	Np-239	$6.30 \cdot 10^{-3}$
Y-91	$1.60 \cdot 10^{-1}$	Pu-238	$8.60 \cdot 10^1$
Zr-95	$1.80 \cdot 10^{-1}$	Pu-239	$2.44 \cdot 10^4$
Nb-95	$9.58 \cdot 10^{-2}$	Pu-240	$6.58 \cdot 10^3$
Tc-99	$2.14 \cdot 10^5$	Pu-241	$1.50 \cdot 10^1$
Ru-106	1.01	Pu-242	$3.79 \cdot 10^5$
Ag-110m	$6.87 \cdot 10^{-1}$	Am-241	$4.58 \cdot 10^2$
Sb-125	2.74	Cm-242	$4.46 \cdot 10^{-1}$
		Cm-244	$1.76 \cdot 10^1$

Table 4.2
Concentration factors for specified radionuclides (1)

Radio-nuclides	Marine concentration factors (2)					Freshwater concentration factors (3)	
	Fish	Crustacea	Molluscs	Sediments	Seaweed	Sediments	Fish
H-3	1	1	1	0	1	0	1
C-14	5000	5000	5000	100	4000	2000	5000
Cr-51	100	1000	1000	10000	30000	20000	100
Mn-54	500	10000	10000	10000	10000	10000	300
Fe-55	1000	1000	1000	10000	10000	10000	100
Fe-59	1000	1000	1000	10000	10000	10000	100
Co-58	100	1000	1000	10000	1000	30000	300
Co-60	100	1000	1000	10000	1000	30000	300
Zn-65	2000	5000	100000	10000	1000	1000	1000
Sr-89	1	10	10	500	10	2000	30
Sr-90	1	10	10	500	10	2000	30
Y-90	10	100	500	10000	1000	4000	30
Y-91	10	100	500	10000	1000	4000	30
Zr-95	1	100	1000	10000	500	60000	30
Nb-95	1	100	1000	10000	500	100	30000
Tc-99	10	1000	1000	10000	10000	200	30
Ru-106	1	500	2000	10000	2000	40000	10
Ag-110m	1000	5000	50000	10000	1000	200	3
Sb-125	500	300	100	10000	100	300	1000
Te-127m	1000	1000	1000	10000	10000	30	1000
Te-129m	1000	1000	1000	10000	10000	30	1000
Te-132	1000	1000	1000	10000	10000	30	1000
I-129	10	100	100	100	1000	200	30
I-131	10	100	100	100	1000	200	30
Cs-134	50	30	30	500	30	30000	1000
Cs-136	50	30	30	500	30	30000	1000
Cs-137	50	30	30	500	30	30000	1000
Ce-144	10	1000	1000	10000	1000	30000	30
Eu-154	100	1000	1000	10000	1000	30000	30
Eu-155	100	1000	1000	10000	1000	30000	30
Np-239	10	100	1000	50000	1000	30000	10
Pu-238	10	100	1000	50000	1000	30000	10
Pu-239	10	100	1000	50000	1000	30000	10
Pu-240	10	100	1000	50000	1000	30000	10
Pu-241	10	100	1000	50000	1000	30000	10
Pu-242	10	100	1000	50000	1000	30000	10
Am-241	10	200	2000	50000	2000	30000	30
Cm-242	10	200	2000	50000	2000	30000	30
Cm-244	10	200	2000	50000	2000	30000	30

See over for notes.

Table 4.2 - Notes

- (1) The concentration factors given here are the ratio of the quantity per unit weight of the material considered (fish, crustacea, etc...) and the quantity of activity per unit volume of filtered water, Bq tonne⁻¹ per Bq m⁻³. These are based on the dry weight of sediments and wet weight of the edible part of the other materials. They are assumed to be independent of the discharge site.
- (2) The assumed values of marine concentration factors are based on information in references 4.39 and 4.40.
- (3) The freshwater concentration factors for fish are from reference 4.46. Those for sediments are from reference 4.48, except for that for technetium, which is assumed to have the same value as iodine, and the actinides which have been assumed to have the same value as cerium.

Table 4-3

Physical characteristics of the Rhone and Loire

	Section number	Slope %	Water velocity (m s ⁻¹)	Sediment velocity (m s ⁻¹)	Width (m)	Suspended sediment load (t m ⁻³)
R H O N E	1	0.94	1.1	9.3 10 ⁻⁵	200	2.5 10 ⁻⁵
	2	0.70	1.0	1.2 10 ⁻⁴	180	2.4 10 ⁻⁵
	3	0.32	0.98	8.2 10 ⁻⁵	220	2.7 10 ⁻⁵
	4	0.54	0.92	1.1 10 ⁻⁴	220	3.1 10 ⁻⁵
	5	0.64	0.88	1.5 10 ⁻⁴	200	3.5 10 ⁻⁵
	6	0.72	0.83	1.7 10 ⁻⁴	200	3.7 10 ⁻⁵
	7	0.65	0.79	1.6 10 ⁻⁴	210	4.0 10 ⁻⁵
	8	0.38	0.75	1.3 10 ⁻⁴	220	4.5 10 ⁻⁵
	9	0.18	0.70	9.2 10 ⁻⁵	230	5.0 10 ⁻⁵
L O I R E	1	0.50	1.3	1.1 10 ⁻⁴	200	2.0 10 ⁻⁵
	2	0.40	1.1	9.5 10 ⁻⁵	250	3.0 10 ⁻⁵
	3	0.30	0.8	6.3 10 ⁻⁵	280	4.0 10 ⁻⁵
	4	0.10	0.7	3.2 10 ⁻⁵	310	5.0 10 ⁻⁵

Table 4-4

Quantities of water extracted from each section
of the Rhone and Loire for drinking purposes ($m^3 y^{-1}$)

Section number	Rhone	Loire
1	$8.3 \cdot 10^4$	$4.7 \cdot 10^4$
2	$4.8 \cdot 10^5$	$8.2 \cdot 10^4$
3	$4.8 \cdot 10^4$	$9.1 \cdot 10^4$
4	$2.7 \cdot 10^4$	$1.9 \cdot 10^5$
5	$7.4 \cdot 10^4$	
6	$3.6 \cdot 10^4$	
7	$1.1 \cdot 10^5$ ($5.7 \cdot 10^4$)*	
8	$1.4 \cdot 10^5$	
9	$3.1 \cdot 10^4$	

*Point of discharge in the middle of the section.

Table 4-5

Collective ingestion of strontium-90 and caesium-137
activity in drinking water and fish for each section of the Rhone
(Bq, for a discharge of 1 Bq s^{-1} for 1y)

Section	Collective ingestion (Bq)			
	Drinking water		Fish	
	Sr-90	Cs-137	Sr-90	Cs-137
1	-	-	-	-
2	-	-	-	-
3	-	-	-	-
4	-	-	-	-
5	-	-	-	-
6	-	-	-	-
7	31	11	0.4	5.0
8	57	9.5	0.4	2.3
9	9.8	0.7	2.8	6.3

Table 4-6

Quantities of fish caught in each section
of the Rhone and Loire (t y⁻¹)

Section	Rhone	Loire
1	340	68
2	57	70
3	94	92
4	75	140
5	94	-
6	75	-
7	100 (50)*	-
8	66	-
9	590	-

*discharge point in the middle of the section.

Table 4-7

Quantities of food produced by surface irrigation from the Rhone

Section number	Leaf vegetables and fruit (kg y ⁻¹)	Root vegetables (kg y ⁻¹)	Cereals(kg y ⁻¹)
1	2.0 10 ⁶	1.8 10 ⁶	0
2	2.6 10 ⁷	5.9 10 ⁶	0
3	5.6 10 ⁷	5.8 10 ⁶	0
4	1.4 10 ⁸	1.4 10 ⁷	0
5	2.7 10 ⁸	1.4 10 ⁷	0
6	3.4 10 ⁷	1.1 10 ⁷	0
7	2.2 10 ⁸	1.4 10 ⁸	0
8	1.3 10 ⁹	6.7 10 ⁸	8.0 10 ⁶
9	5.0 10 ⁷	3.8 10 ⁷	3.2 10 ⁷

Table 4-8

Time integral of activity concentration in
sediments and truncated collective effective
dose equivalent commitments (truncation at 50 y)

Section of Rhône	Time integral of activity concentration in sediment ⁽¹⁾ (Bq y kg ⁻¹)			Collective effective dose equivalent commitment ⁽¹⁾ (man-Sv)		
	Mn-54	Co-60	Cs-137	Mn-54	Co-60	Cs-137
1	-	-	-	-	-	-
2	-	-	-	-	-	-
3	-	-	-	-	-	-
4	-	-	-	-	-	-
5	-	-	-	-	-	-
6	-	-	-	-	-	-
7	4.1 10 ⁻²	1.1 10 ⁻¹	1.4 10 ⁻¹	1.4 10 ⁻⁶	1.2 10 ⁻⁵	3.2 10 ⁻⁶
8	3.2 10 ⁻³	2.1 10 ⁻²	4.1 10 ⁻²	6.9 10 ⁻⁸	1.5 10 ⁻⁶	6.0 10 ⁻⁷
9	1.0 10 ⁻³	1.1 10 ⁻²	4.1 10 ⁻²	3.1 10 ⁻⁸	1.1 10 ⁻⁶	8.8 10 ⁻⁷

(1) Truncated at 50 y

Table 4-9
Classification of radionuclides according to their partition
between dissolved and particulate forms in seawater

Radionuclide	Adsorption class in rivers	Degree of adsorption on marine sediments	Class in estuarine and marine areas
Cr-51 Mn-54 Fe-55, Fe-59 Co-58, Co-60 Zr-95 Ru-106 Ce-144 Eu-154, Eu-155 Np-239 Pu-238, Pu-239, Pu-242 Am-241 Cm-242, Cm-244	A (strong adsorption)	High	A 1
Cs-134, Cs-136, Cs-137		Weak	A 2
Zn-65 Y-90 Y-91	B (medium adsorption)	High	B 1
C-14 Sr-89, Sr-90		Weak	B 2
Nb-95 Tc-99 Ag-110m Sb-125 Te-127	C (adsorption weak or zero)	High	C 1
H-3 I-129		Weak or zero	C 2

Table 4-10

Site dependent parameters used in the
local marine model

	h (m)	V (km ³)	r (y ⁻¹)	$(t \ m^{-2} \ y^{-1})$	ss (t m ⁻³)
Site 1 Gulf of Tarante	15	1.5	4	10^{-4}	$5 \cdot 10^{-7}$
Site 2 English Channel	15	2.25	50	10^{-4}	$5 \cdot 10^{-6}$
Site 3 Eastern Irish Sea	20	10	10	10^{-2}	$1.25 \cdot 10^{-5}$

Table 4.11

Results* obtained for a discharge of
1 Bq s⁻¹ for 1 year into a local marine
compartment in the Gulf of Taranto

Nuclides	C(1y) (Bq m ⁻³)	Q _{1r} (1y) (Bq)	Q _{1r} (∞) (Bq)
H-3	5.10 10 ⁻³	3.05 10 ⁷	3.11 10 ⁷
C-14	5.17 10 ⁻³	3.09 10 ⁷	3.15 10 ⁷
Co-58	2.75 10 ⁻³	1.65 10 ⁷	1.65 10 ⁷
Co-60	4.95 10 ⁻³	2.96 10 ⁷	3.00 10 ⁷
Sr-90	5.13 10 ⁻³	3.07 10 ⁷	3.13 10 ⁷
Tc-99	5.10 10 ⁻³	3.05 10 ⁷	3.11 10 ⁷
Ru-106	4.38 10 ⁻³	2.63 10 ⁷	2.65 10 ⁷
I-129	5.17 10 ⁻³	3.09 10 ⁷	3.15 10 ⁷
I-131	5.92 10 ⁻⁴	3.56 10 ⁶	3.56 10 ⁶
Cs-134	4.79 10 ⁻³	2.87 10 ⁷	2.91 10 ⁷
Cs-137	5.13 10 ⁻³	3.07 10 ⁷	3.13 10 ⁷
Pu-239	4.79 10 ⁻³	2.88 10 ⁷	2.91 10 ⁷

*For explanation of symbols see Section 4.4.1

Table 4.12

Results* obtained for a discharge of 1 Bq s⁻¹ for
1 year into a local marine compartment in
the eastern Irish Sea

Nuclides	C(1y) (Bq m ⁻³)	Q _{1r} (1y) (Bq)	Q _{1r} (∞) (Bq)
H-3	3.1 10 ⁻⁴	3.1 10 ⁷	3.1 10 ⁷
C-14	3.1 10 ⁻⁴	3.1 10 ⁷	3.1 10 ⁷
Co-58	1.8 10 ⁻⁴	1.8 10 ⁷	1.8 10 ⁷
Co-60	2.2 10 ⁻⁴	2.2 10 ⁷	2.2 10 ⁷
Sr-90	3.1 10 ⁻⁴	3.1 10 ⁷	3.1 10 ⁷
Tc-99	2.2 10 ⁻⁴	2.2 10 ⁷	2.2 10 ⁷
Ru-106	2.1 10 ⁻⁴	2.1 10 ⁷	2.1 10 ⁷
I-129	3.1 10 ⁻⁴	3.1 10 ⁷	3.1 10 ⁷
I-131	7.6 10 ⁻⁵	7.6 10 ⁶	7.6 10 ⁶
Cs-134	3.0 10 ⁻⁴	3.0 10 ⁷	3.0 10 ⁷
Cs-137	3.1 10 ⁻⁴	3.1 10 ⁷	3.1 10 ⁷
Pu-239	1.2 10 ⁻⁴	1.2 10 ⁷	1.2 10 ⁷

*For explanation of symbols see Section 4.4.1

Table 4-13
Assumed values of parameters used to model loss by
sedimentation in North European Waters

Compartment	Rate of sedimentation s (t m ⁻² y ⁻¹)	Mean depth, h (m)	Suspended sediment load ss (t m ⁻³)
Northern Sea North	1 10 ⁻⁴	240	6 10 ⁻⁶
Central North Sea	1 10 ⁻⁴	50	6 10 ⁻⁶
Southern North Sea	1 10 ⁻⁴	20	6 10 ⁻⁶
English Channel East	1 10 ⁻⁴	40	1 10 ⁻⁶
English Channel West	1 10 ⁻⁴	60	1 10 ⁻⁶
Bristol Channel	1 10 ⁻⁴	50	1 10 ⁻⁶
Irish Waters	1 10 ⁻⁴	150	1 10 ⁻⁶
Bay of Biscay	1 10 ⁻⁴	1700	1 10 ⁻⁶
Irish Sea South	1 10 ⁻⁴	60	1 10 ⁻⁶
Irish Sea West	2 10 ⁻³	75	3 10 ⁻⁶
Irish Sea East	5 10 ⁻³	35	3 10 ⁻⁶
Scottish Waters	1 10 ⁻⁴	110	1 10 ⁻⁶
Baltic Sea	5 10 ⁻³	55	1 10 ⁻⁶
Arctic Ocean	1 10 ⁻⁵	1200	1 10 ⁻⁷
North East Atlantic	1 10 ⁻⁵	3500	1 10 ⁻⁷
Atlantic Ocean	1 10 ⁻⁵	3500	1 10 ⁻⁷
Other Oceans	5 10 ⁻⁶	4000	1 10 ⁻⁷

Table 4-14
Quantities of fish caught in various regions (t y⁻¹)

Compartment	Fish	Crustacea	Molluscs
Northern North Sea	773000	3800	25000
Central North Sea	1062000	30000	24000
Southern North Sea	133000	9000	137000
English Channel East	56000	3200	35000
English Channel West	77000	13000	37000
Bristol Channel	19000	320	380
Irish Waters	93000	5100	2600
Bay of Biscay	58000	17000	119000
Irish Sea South	7200	670	1200
Irish Sea West	22000	2000	3500
Irish Sea East	43000	4000	7000
Scottish Waters	288000	6700	6700
Baltic Sea	457000	3600	4700
Arctic Ocean	290000	0	0
North East Atlantic	302000	640	1700
Atlantic Ocean	281000	12000	91000
Other Oceans	0	0	0

Table 4-15

Total integrated collective intakes for a release of
1 Bq s⁻¹ for 1 year from a local box into the southern North Sea[†]

Nuclide	Total integrated collected intake (Bq)					
	1 y	10 y	50 y	100 y	500 y	Infinity
H-3*	8.5 10 ⁻¹	2.5	2.6	(2.6)	(2.6)	(2.6)
C-14*	4.4 10 ³	1.4 10 ⁴	1.5 10 ⁴	(1.5 10 ⁴)	(1.5 10 ⁴)	(1.7 10 ⁴)
Co-58	2.0 10 ²	2.3 10 ²	2.3 10 ²	2.3 10 ²	2.3 10 ²	2.3 10 ²
Co-60	3.3 10 ²	6.0 10 ²	6.0 10 ²	6.0 10 ²	6.0 10 ²	6.0 10 ²
Sr-90	3.6	6.9	7.3	7.3	7.3	7.3
Tc-99	3.0 10 ²	5.0 10 ²	5.0 10 ²	5.0 10 ²	5.0 10 ²	7.3 10 ²
Ru-106	4.8 10 ²	6.6 10 ²	6.6 10 ²	6.6 10 ²	6.6 10 ²	6.6 10 ²
I-129*	3.7 10 ¹	7.3 10 ¹	7.6 10 ¹	(7.6 10 ¹)	(7.9 10 ¹)	(3.2 10 ³)
I-131	4.9	5.0	5.0	5.0	5.0	5.0
Cs-134	3.4 10 ¹	8.2 10 ¹	8.2 10 ¹	8.2 10 ¹	8.2 10 ¹	8.2 10 ¹
Cs-137	3.7 10 ¹	1.2 10 ²	1.2 10 ²	1.2 10 ²	1.2 10 ²	1.2 10 ²
Pu-239	2.9 10 ²	3.5 10 ²	3.5 10 ²	3.5 10 ²	3.5 10 ²	3.5 10 ²

*For these nuclides the regional model is used only to calculate the total collective intake integrated to 50 y. Beyond this time, the global model is used.

†These data should not be interpreted as resulting from a direct discharge from a coastal site. That is, they must be used in conjunction with a local box model of the type described in Section 4.4.1.

Table 4-16
Total integrated collective intakes for a release of
1 Bq s⁻¹ for 1 year from local box into four different sea regions†

Location	Nuclide	Total integrated collective intake (Bq)					
		1 y	10 y	50 y	100 y	500 y	Infinity
Southern North Sea	Co-60	3.3 10 ²	6.0 10 ²	6.0 10 ²	6.0 10 ²	6.0 10 ²	6.0 10 ²
	Sr-90	3.6 10 ²	6.9 10 ²	7.3 10 ²	7.3 10 ²	7.3 10 ²	7.3 10 ²
	Ru-106	4.8 10 ²	6.6 10 ²	6.6 10 ²	6.6 10 ²	6.6 10 ²	6.6 10 ²
	I-131	4.9 10 ¹	5.0 10 ²	5.0 10 ²	5.0 10 ²	5.0 10 ²	5.0 10 ²
	Cs-137	3.7 10 ²	1.2 10 ²	1.2 10 ²	1.2 10 ²	1.2 10 ²	1.2 10 ²
Bay of Biscay	Pu-239	2.2 10 ²	3.5 10 ²	3.5 10 ²	3.5 10 ²	3.5 10 ²	3.5 10 ²
	Co-60	2.5 10 ²	1.2 10 ¹	1.2 10 ¹	1.2 10 ¹	1.2 10 ¹	1.2 10 ¹
	Sr-90	2.6 10 ²	1.7 10 ⁻¹	2.0 10 ⁻¹	2.1 10 ⁻¹	2.1 10 ⁻¹	2.1 10 ⁻¹
	Ru-106	3.8 10 ⁻²	8.8 10 ⁻²	8.8 10 ⁻²	8.8 10 ⁻²	8.8 10 ⁻²	8.8 10 ⁻²
	I-131	2.0 10 ⁻²	2.1 10 ⁻²	2.1 10 ⁻²	2.1 10 ⁻²	2.1 10 ⁻²	2.1 10 ⁻²
Irish Sea East	Cs-137	1.4 10 ⁻¹	2.0 10 ¹	2.7 10 ¹	2.9 10 ¹	3.0 10 ¹	3.0 10 ¹
	Pu-239	2.1 10 ²	1.0 10 ¹	1.3 10 ¹	1.5 10 ¹	2.0 10 ¹	5.0 10 ¹
	Co-60	1.5 10 ²	3.1 10 ²	3.1 10 ²	3.1 10 ²	3.1 10 ²	3.1 10 ²
	Sr-90	2.0 10 ²	7.3 10 ²	7.3 10 ²	7.3 10 ²	7.3 10 ²	7.3 10 ²
	Ru-106	1.3 10 ²	2.1 10 ²	2.1 10 ²	2.1 10 ²	2.1 10 ²	2.1 10 ²
English Channel East	I-131	1.8 10 ¹	1.8 10 ²	1.8 10 ²	1.8 10 ²	1.8 10 ²	1.8 10 ²
	Cs-137	3.4 10 ¹	1.5 10 ²	1.5 10 ²	1.5 10 ²	1.5 10 ²	1.5 10 ²
	Pu-239	3.3 10 ¹	5.0 10 ¹	5.0 10 ¹	5.0 10 ¹	5.0 10 ¹	5.4 10 ¹
	Co-60	3.0 10 ²	6.9 10 ²	6.9 10 ²	6.9 10 ²	6.9 10 ²	6.9 10 ²
	Sr-90	3.2 10 ²	8.2 10 ²	8.5 10 ²	8.5 10 ²	8.5 10 ²	8.5 10 ²
	Ru-106	4.1 10 ²	6.9 10 ²	6.9 10 ²	6.9 10 ²	6.9 10 ²	6.9 10 ²
	I-131	2.0 10 ¹	2.0 10 ²	2.0 10 ²	2.0 10 ²	2.0 10 ²	2.0 10 ²
	Cs-137	3.1 10 ²	1.3 10 ²	1.3 10 ²	1.3 10 ²	1.3 10 ²	1.3 10 ²
	Pu-239	2.1 10 ²	4.4 10 ²	4.4 10 ²	4.4 10 ²	4.4 10 ²	4.4 10 ²

†These data should not be interpreted as resulting from a direct discharge from a coastal site. That is, they must be used in conjunction with a local box model of the type described in Section 4.4.1.

Table 4-17
Assumed values of parameters used to model loss by
sedimentation in the Mediterranean

Compartment	Rate of sedimentation ($t\ m^{-2}\ y^{-1}$)	Mean depth (m)	Suspended sediment load ($t\ m^{-3}$)
West Mediterranean	$1\ 10^{-4}$	1400	$1\ 10^{-7}$
East Mediterranean	$5\ 10^{-5}$	1400	$1\ 10^{-7}$
Black Sea	$1\ 10^{-4}$	1200	$1\ 10^{-7}$
Atlantic Ocean	$1\ 10^{-5}$	3500	$1\ 10^{-7}$
Other Oceans	$5\ 10^{-6}$	4000	$1\ 10^{-7}$

Table 4-18
Quantities of fish caught in regions of the Mediterranean
and other waters

Compartment	Fish ($t\ y^{-1}$)	Crustacea ($t\ y^{-1}$)	Molluscs ($t\ y^{-1}$)
West Mediterranean	$1.13\ 10^5$	$2.4\ 10^3$	$2.7\ 10^4$
East Mediterranean (surface waters)	$1.12\ 10^5$	$6.3\ 10^3$	$4.3\ 10^4$
East Mediterranean (deep waters)	$5.6\ 10^4$	$3.2\ 10^3$	$2.1\ 10^4$
Black Sea	0	0	0
Atlantic Ocean	$3.7\ 10^6$	$9.9\ 10^4$	$4.0\ 10^5$
Other Oceans	0	0	0

Table 4-19

Total integrated collective intake for a release of
1 Bq s⁻¹ for 1 year from a local box into the eastern Mediterranean†

Radio-nuclides	Total integrated collective intake (Bq for a discharge of 1 Bq s ⁻¹ for 1 year)					
	1 y	10 y	50 y	100 y	500 y	Infinite
H-3	6.9 10 ⁻³	5.7 10 ⁻²	7.6 10 ⁻²	7.7 10 ⁻²	7.7 10 ⁻²	7.7 10 ⁻²
C-14	3.5 10 ¹	3.5 10 ²	6.7 10 ²	7.8 10 ²	1.1 10 ³	3.3 10 ³
Co-58	1.1	1.5	1.5	1.5	1.5	1.5
Co-60	2.5	1.7 10 ¹	1.8 10 ¹	1.8 10 ¹	1.8 10 ¹	1.8 10 ¹
Sr-90	2.6 10 ⁻²	2.3 10 ⁻¹	3.5 10 ⁻¹	3.7 10 ⁻¹	3.7 10 ⁻¹	3.7 10 ⁻¹
Tc-99	2.2	2.1 10 ¹	3.7 10 ¹	4.3 10 ¹	5.5 10 ¹	4.2 10 ²
Ru-106	3.1	9.1	9.1	9.1	9.1	9.1
I-129	2.6 10 ⁻¹	2.5	4.7	5.4	7.3	5.6 10 ³
I-131	1.7 10 ⁻²	1.7 10 ⁻²	1.7 10 ⁻²	1.7 10 ⁻²	1.7 10 ⁻²	1.7 10 ⁻²
Cs-134	2.8 10 ⁻¹	1.3	1.3	1.3	1.3	1.3
Cs-137	3.1 10 ⁻¹	2.8	4.5	4.7	4.8	4.8
Pu-239	1.9	1.8 10 ¹	3.2 10 ¹	3.6 10 ¹	4.4 10 ¹	8.9 10 ¹

† See footnotes to Table 4-15

Table 4-20

Total integrated collective intake for a release of
1 Bq s⁻¹ for 1 year from a local box into the western Mediterranean†

Radio- nuclides	Total integrated collective intake (Bq for a discharge of 1 Bq s ⁻¹ for 1 y)					
	1 y	10 y	50 y	100 y	500 y	Infinity
H-3	9.8 10 ⁻⁴	1.8 10 ⁻²	3.3 10 ⁻²	3.3 10 ⁻²	3.3 10 ⁻²	3.3 10 ⁻²
C-14	5.0	1.2 10 ²	3.8 10 ²	4.8 10 ²	8.2 10 ²	3.0 10 ³
Co-58	1.2 10 ⁻¹	1.6 10 ⁻¹	1.6 10 ⁻¹	1.6 10 ⁻¹	1.6 10 ⁻¹	1.6 10 ⁻¹
Co-60	2.8 10 ⁻¹	4.1	5.5	5.5	5.5	5.5
Sr-90	2.9 10 ⁻³	6.6 10 ⁻²	1.6 10 ⁻¹	1.7 10 ⁻¹	1.8 10 ⁻¹	1.8 10 ⁻¹
Tc-99	2.2 10 ⁻¹	5.9	1.9 10 ¹	2.4 10 ¹	3.7 10 ¹	4.0 10 ²
Ru-106	3.2 10 ⁻¹	1.4	1.4	1.4	1.4	1.4
I-129	3.0 10 ⁻²	7.5 10 ⁻¹	2.5	3.1	5.0	5.6 10 ³
I-131	1.7 10 ⁻³	1.7 10 ⁻³	1.7 10 ⁻³	1.7 10 ⁻³	1.7 10 ⁻³	1.7 10 ⁻³
Cs-134	4.1 10 ⁻²	3.0 10 ⁻¹	3.1 10 ⁻¹	3.1 10 ⁻¹	3.1 10 ⁻¹	3.1 10 ⁻¹
Cs-137	4.5 10 ⁻²	9.4 10 ⁻¹	2.3	2.5	2.5	2.5
Pu-239	2.0 10 ⁻¹	5.1	1.6 10 ¹	2.0 10 ¹	2.8 10 ¹	7.4 10 ¹

† See footnotes to Table 4-15

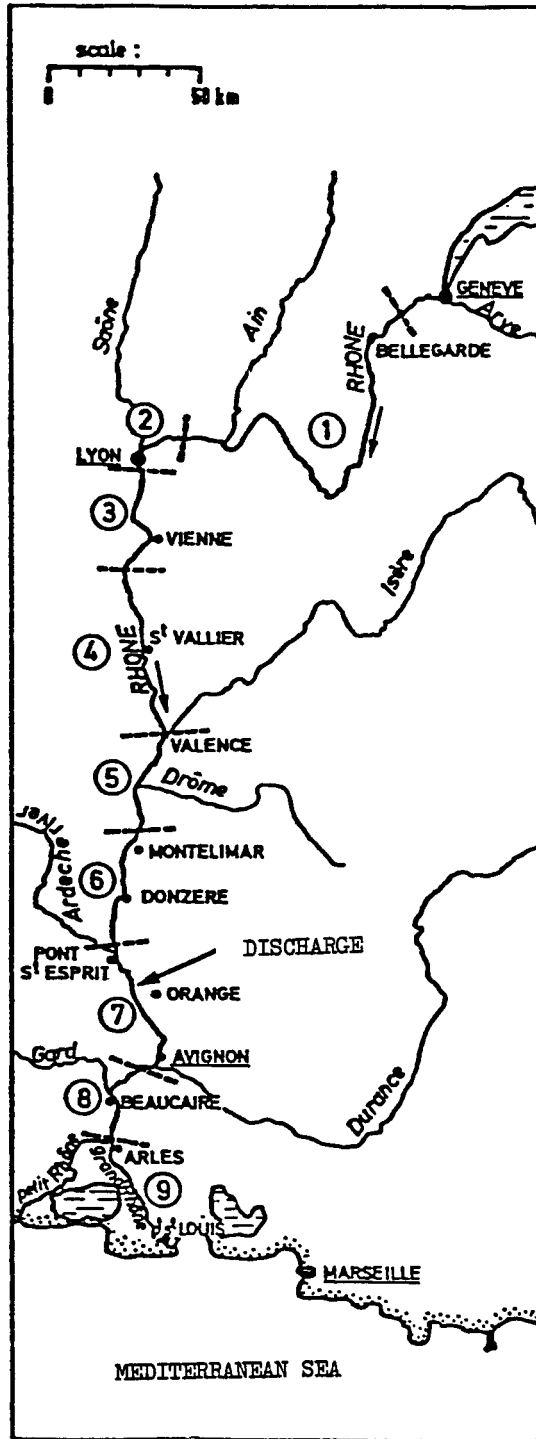


Figure 4-1 Sections of Rhone and point of discharge

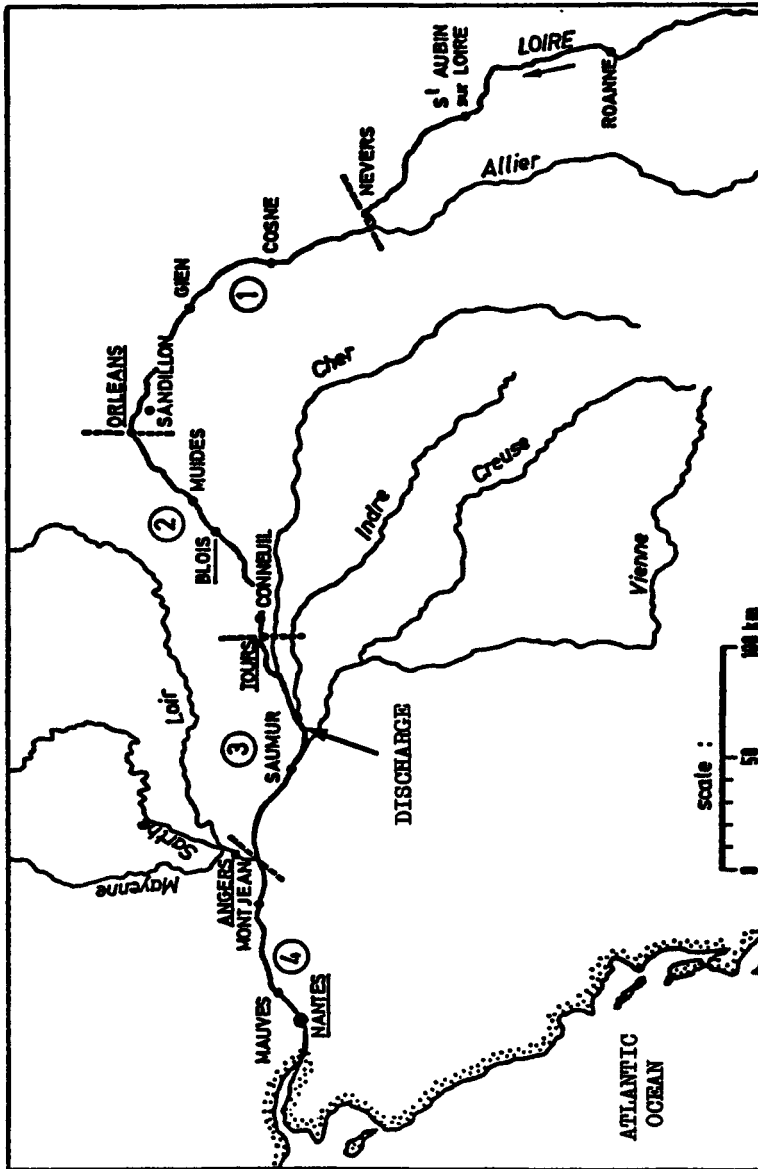


Figure 4-2 Sections of the Loire and point of discharge

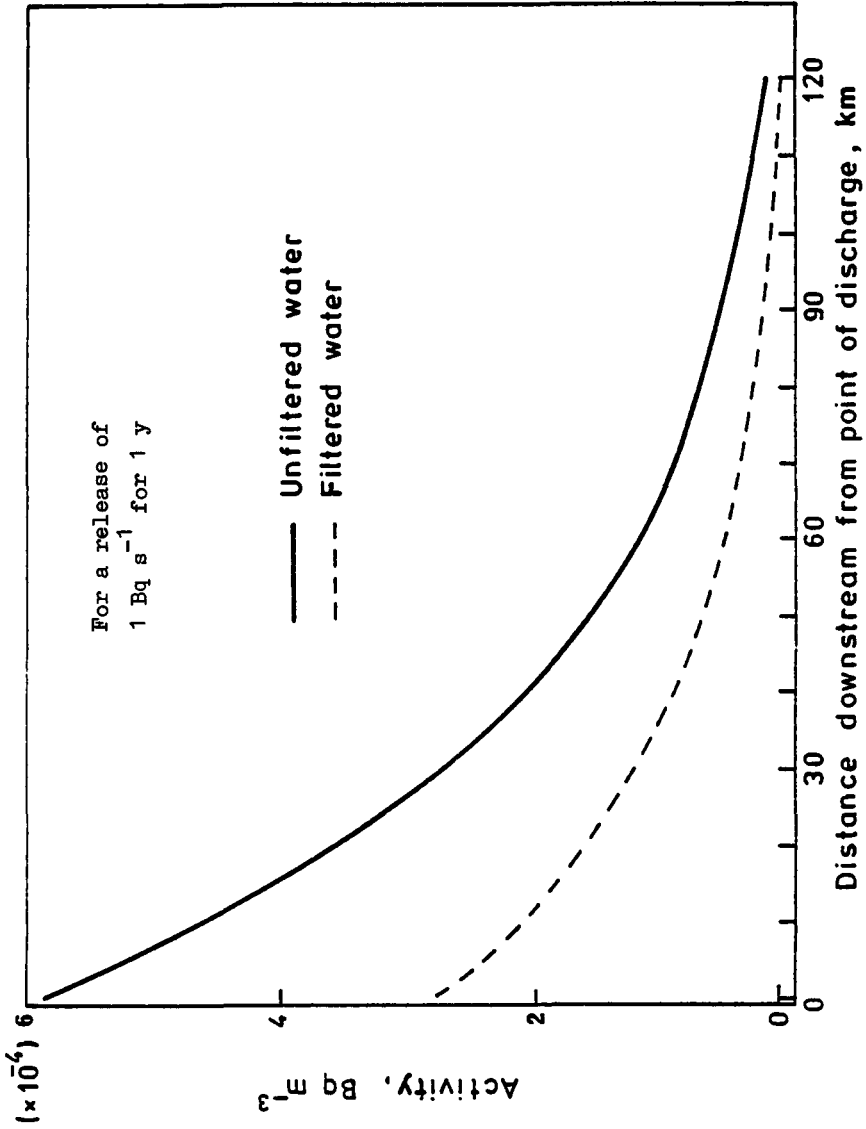


Figure 4 - 3. Variation of caesium-137 activity in filtered and non-filtered water downstream of a point of discharge on the Rhone

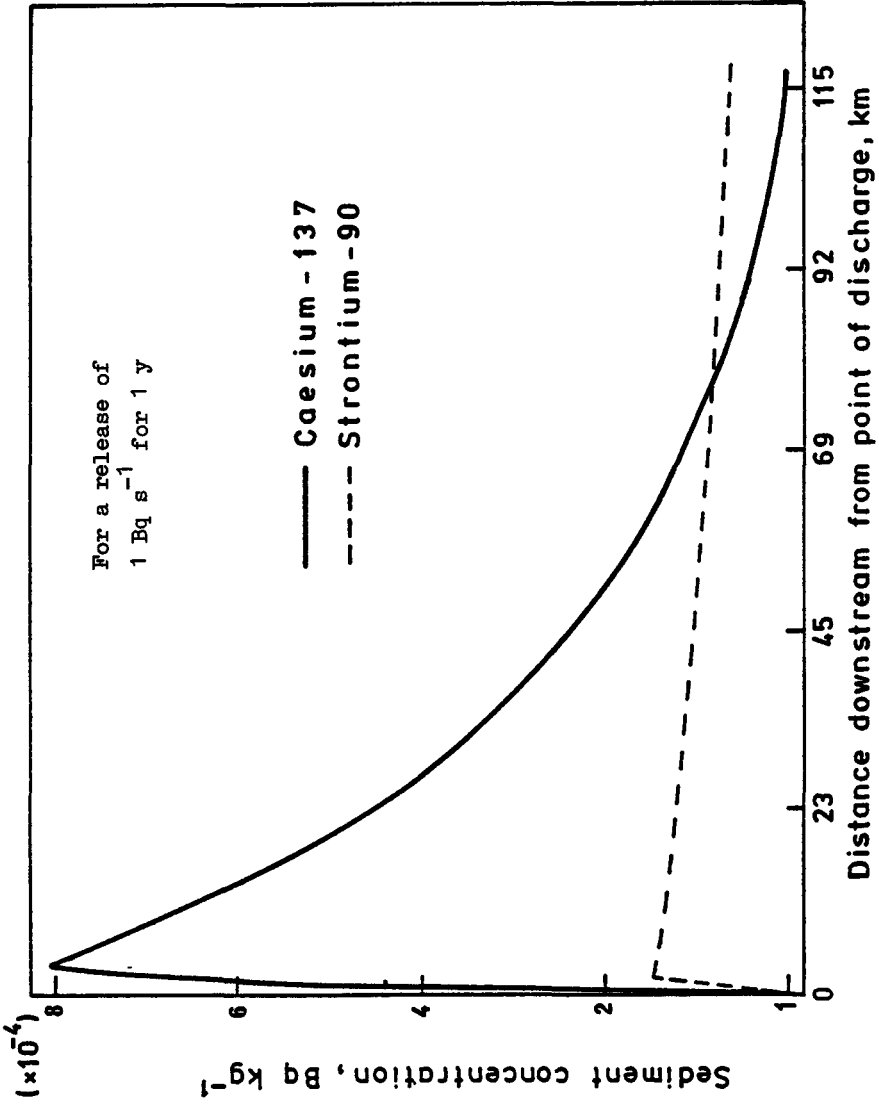


Figure 4-4 . Strontium -90 and caesium -137 sediment activity in the Rhone after 1 year of operation

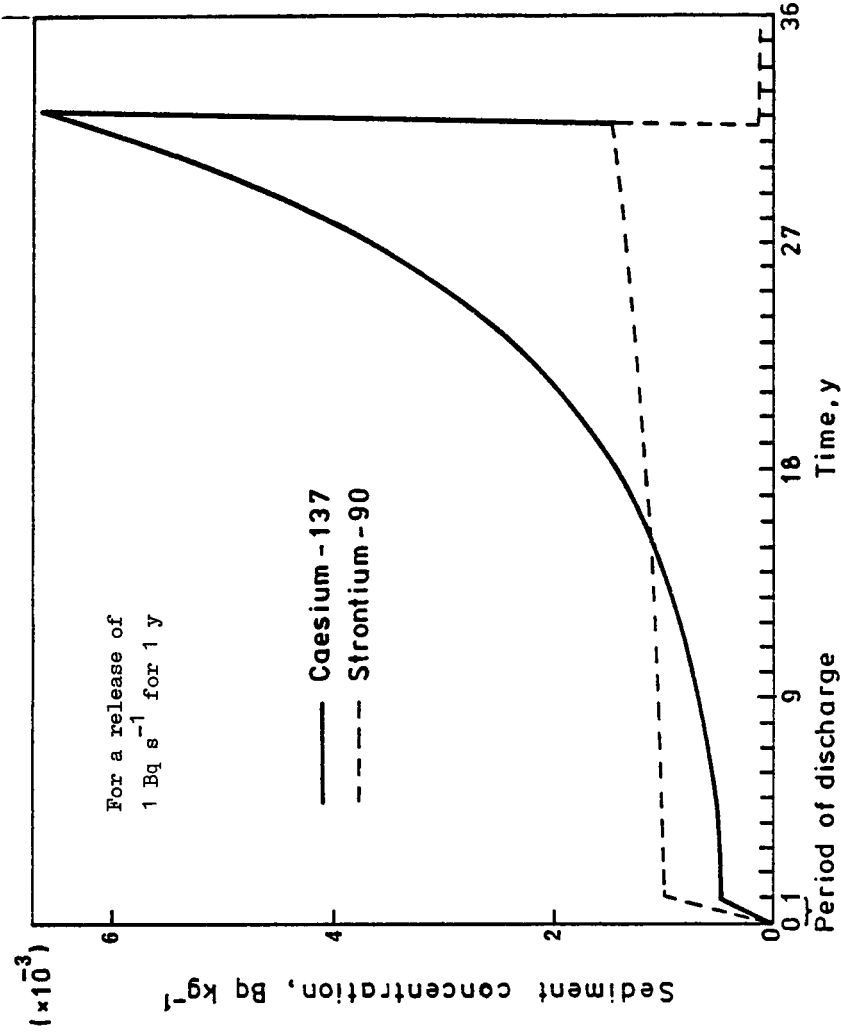


Figure 4-5 . Variation of strontium-90 and caesium - 137 in sediments as a function of time at a point situated at the mouth of the Rhone

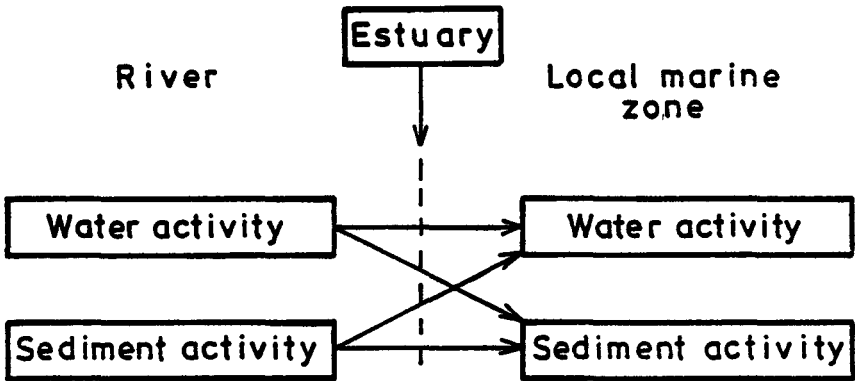


Figure 4 - 6 . Diagram of transfers between river and estuary

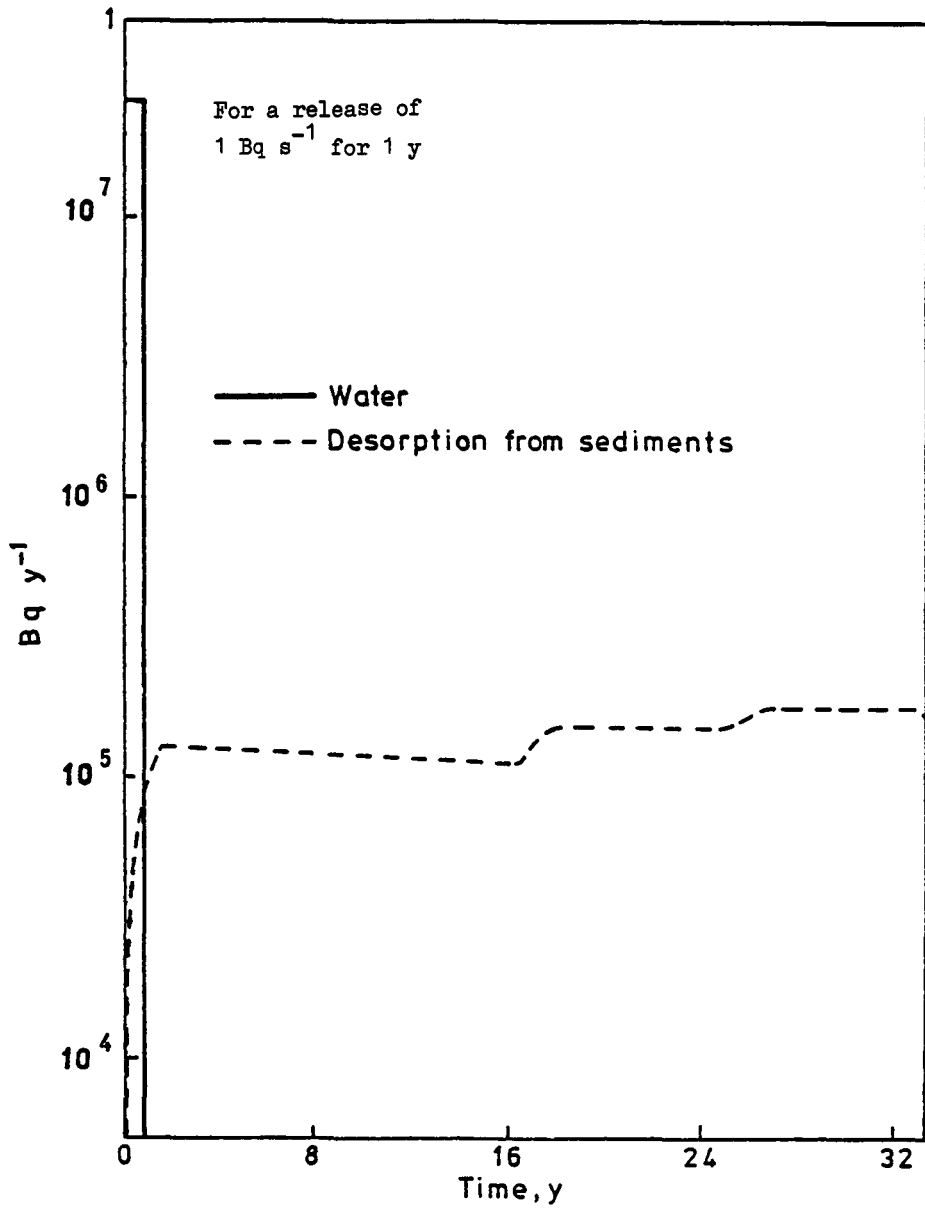


Figure 4 - 7 . Release to sea of strontium-90 originating from a discharge in to the Rhone

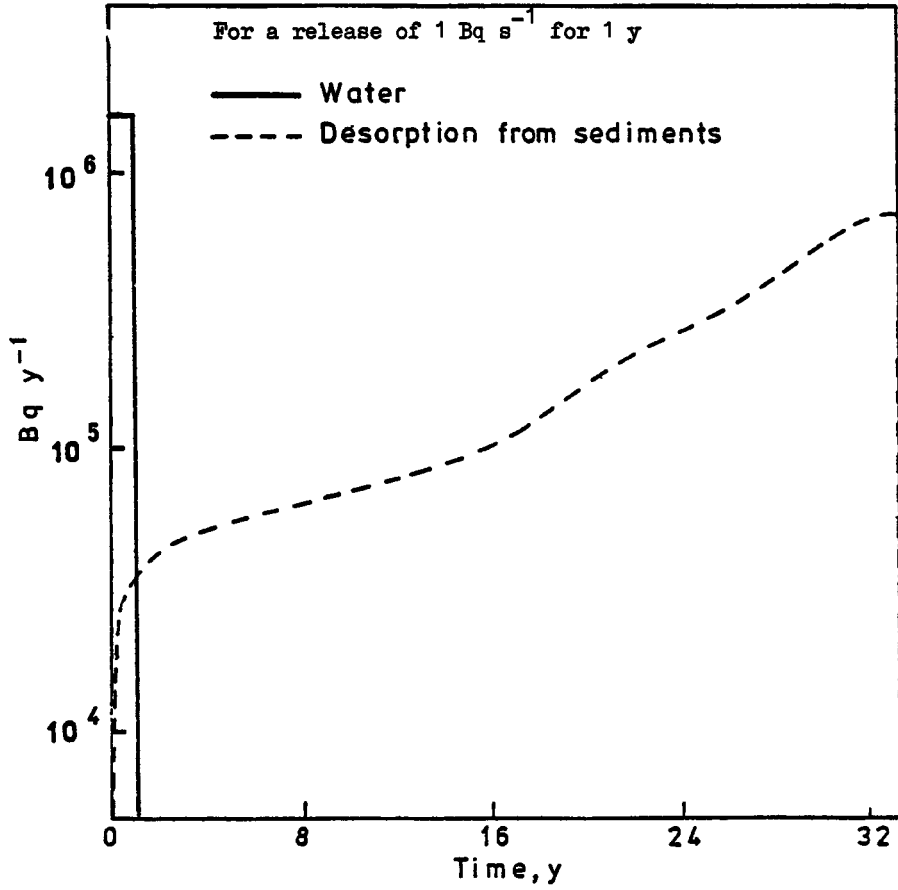


Figure 4-8. Release to sea of caesium-137 originating from a discharge in to the Rhone

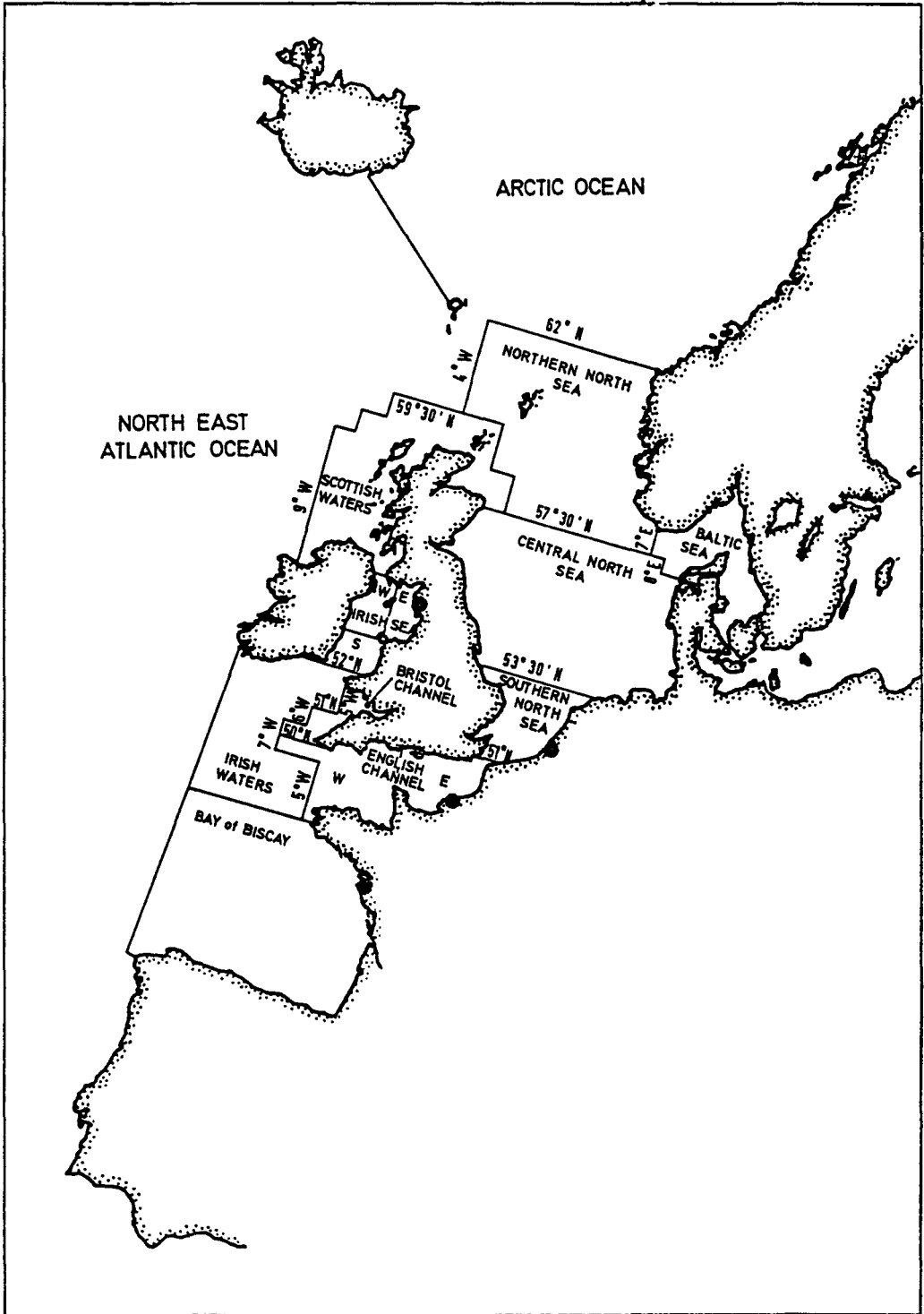


Figure 4-9 Compartment model of the Northern European waters

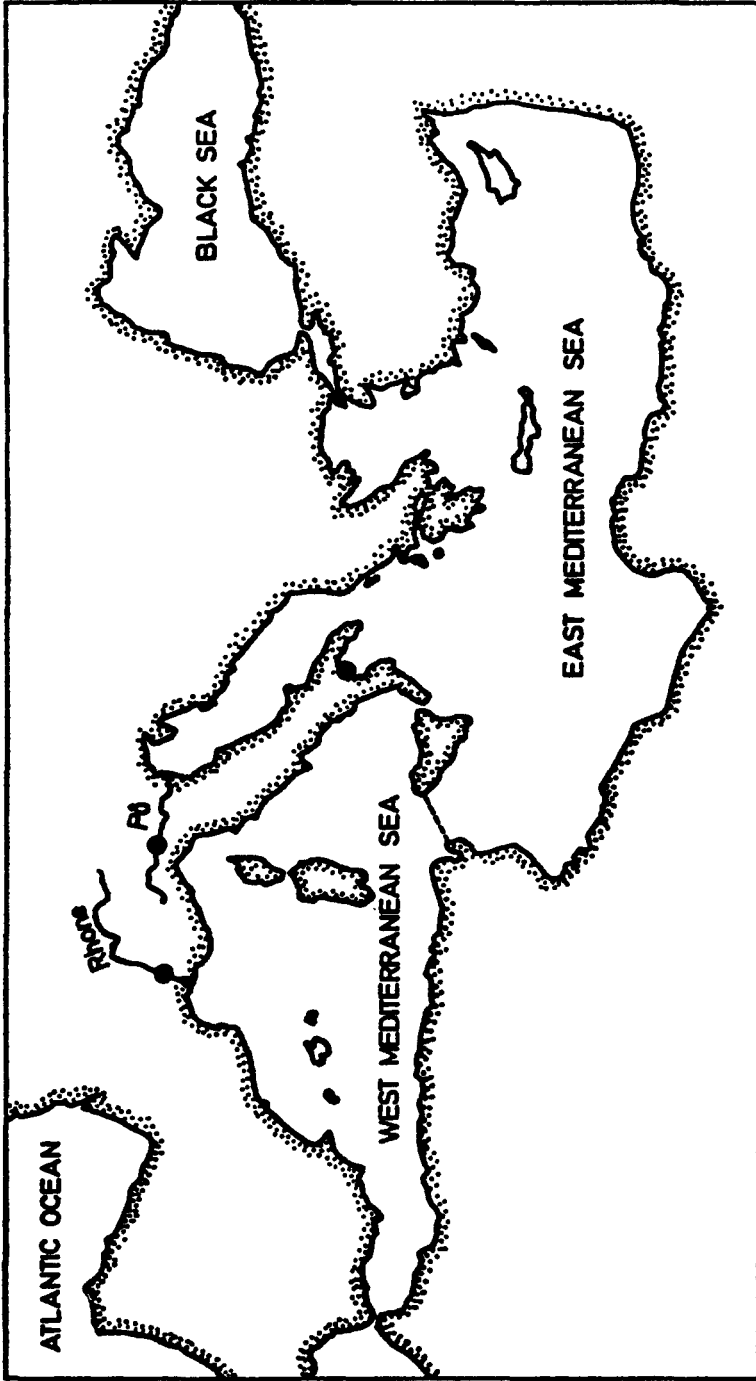
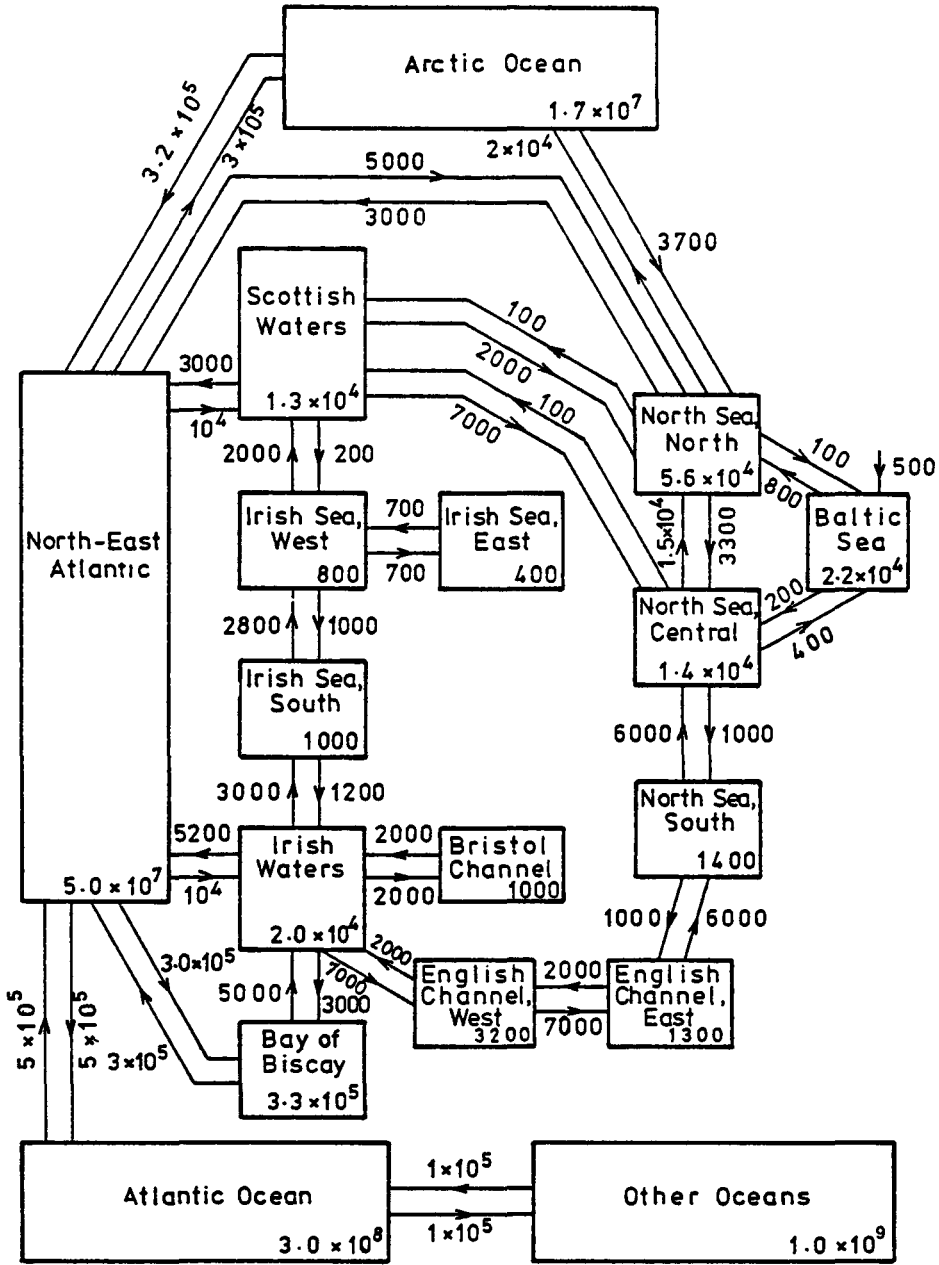


Figure 4-10 Compartment model of the Mediterranean sea



KEY:-

Volume km^3

Volume exchange rate, $\text{km}^3 \text{y}^{-1}$

Figure 4 - 11 . Compartments of North European regional model

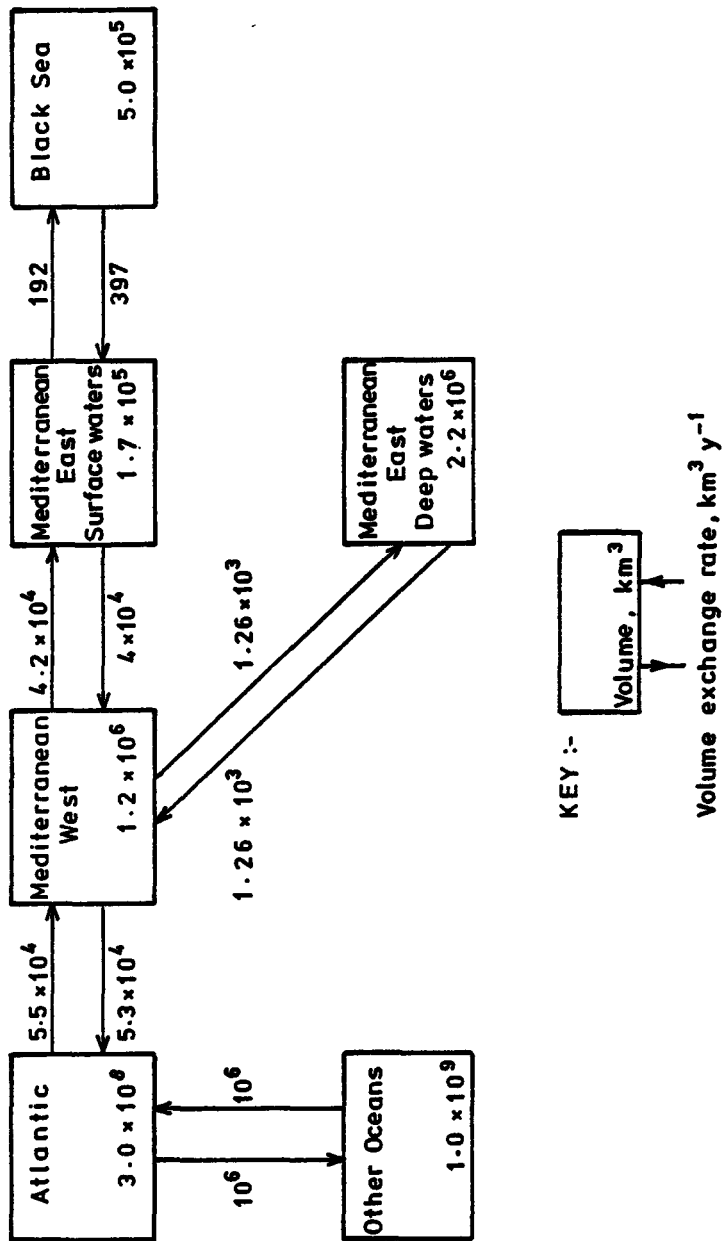


Figure 4-12. Compartments of Mediterranean regional model

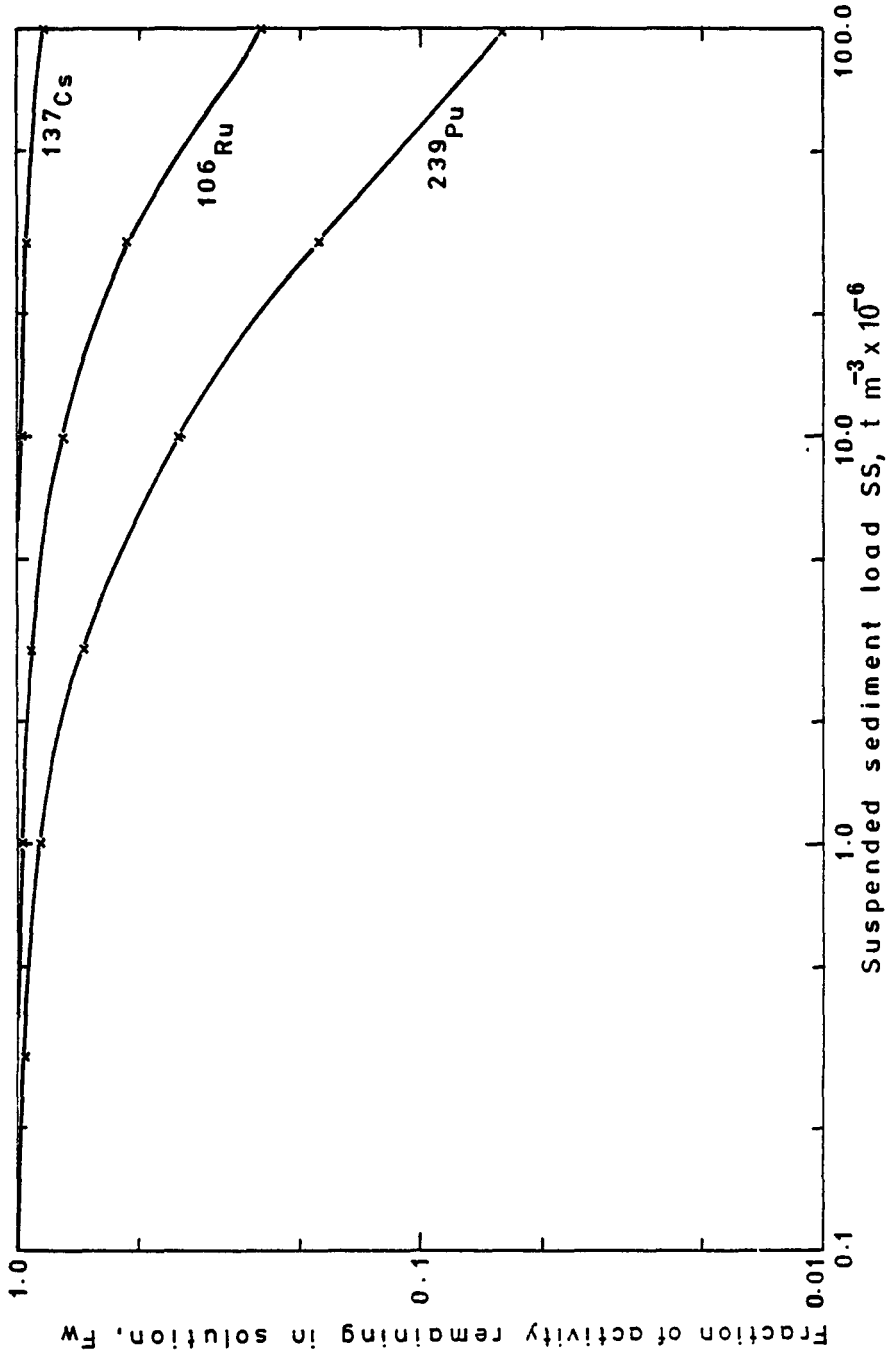


Figure 4-13 Effect of suspended sediment load on the depletion of activity from the water phase

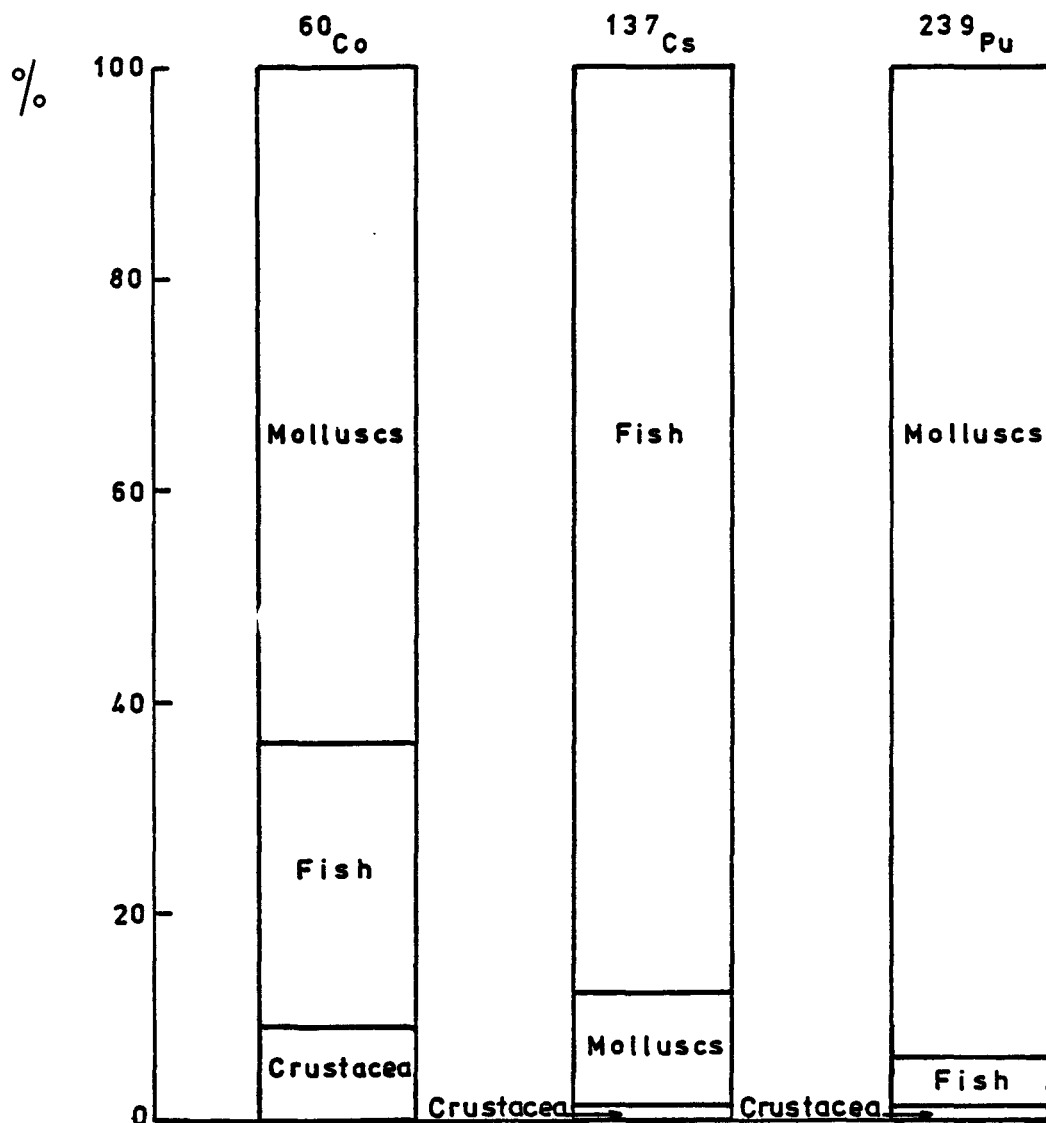


Figure 4-14 Percentage contributions of different marine foodstuffs to the 50 year integrated total collective intake for a discharge to Southern North Sea

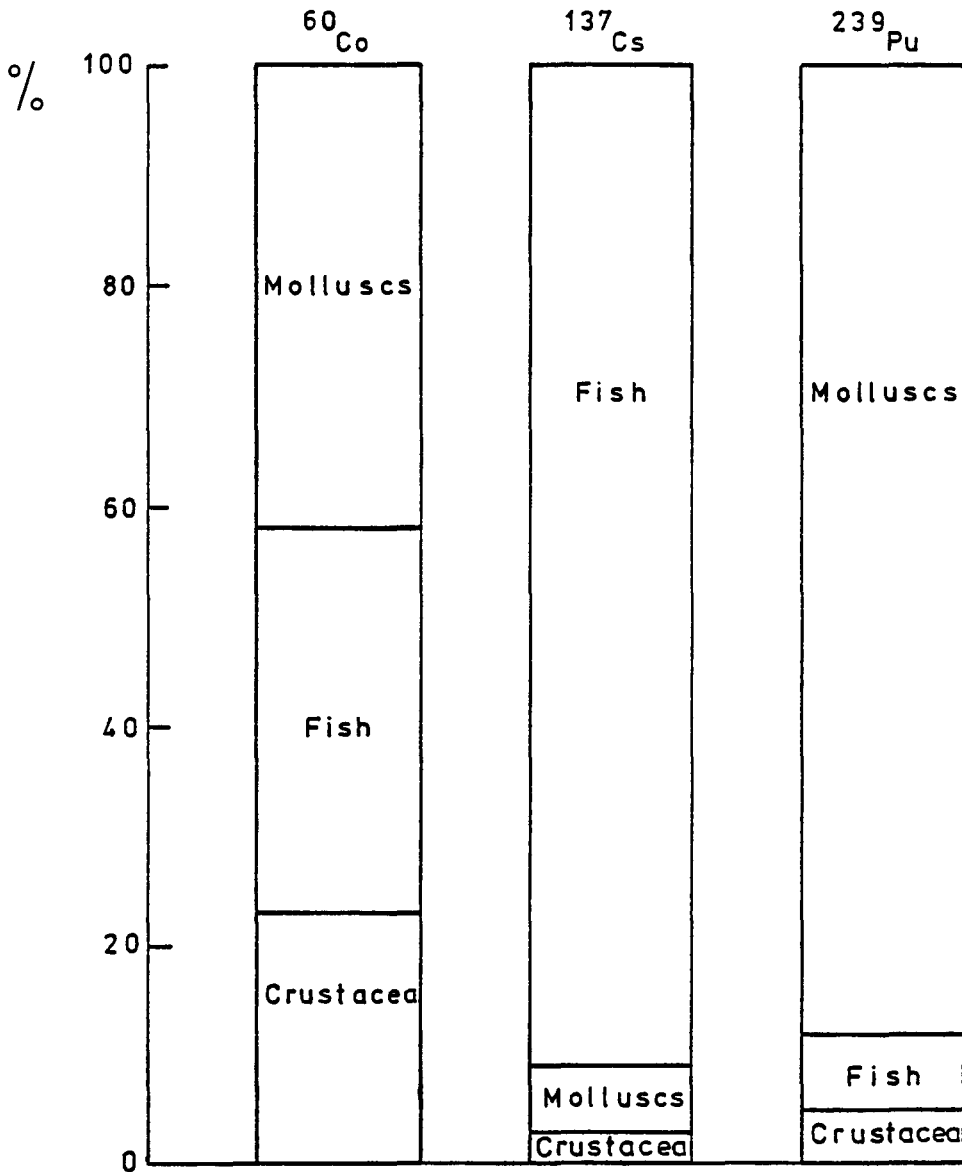


Figure 4-15 Percentage contributions of different marine foodstuffs to the 50 year integrated total collective intake for a discharge to the Eastern Irish Sea

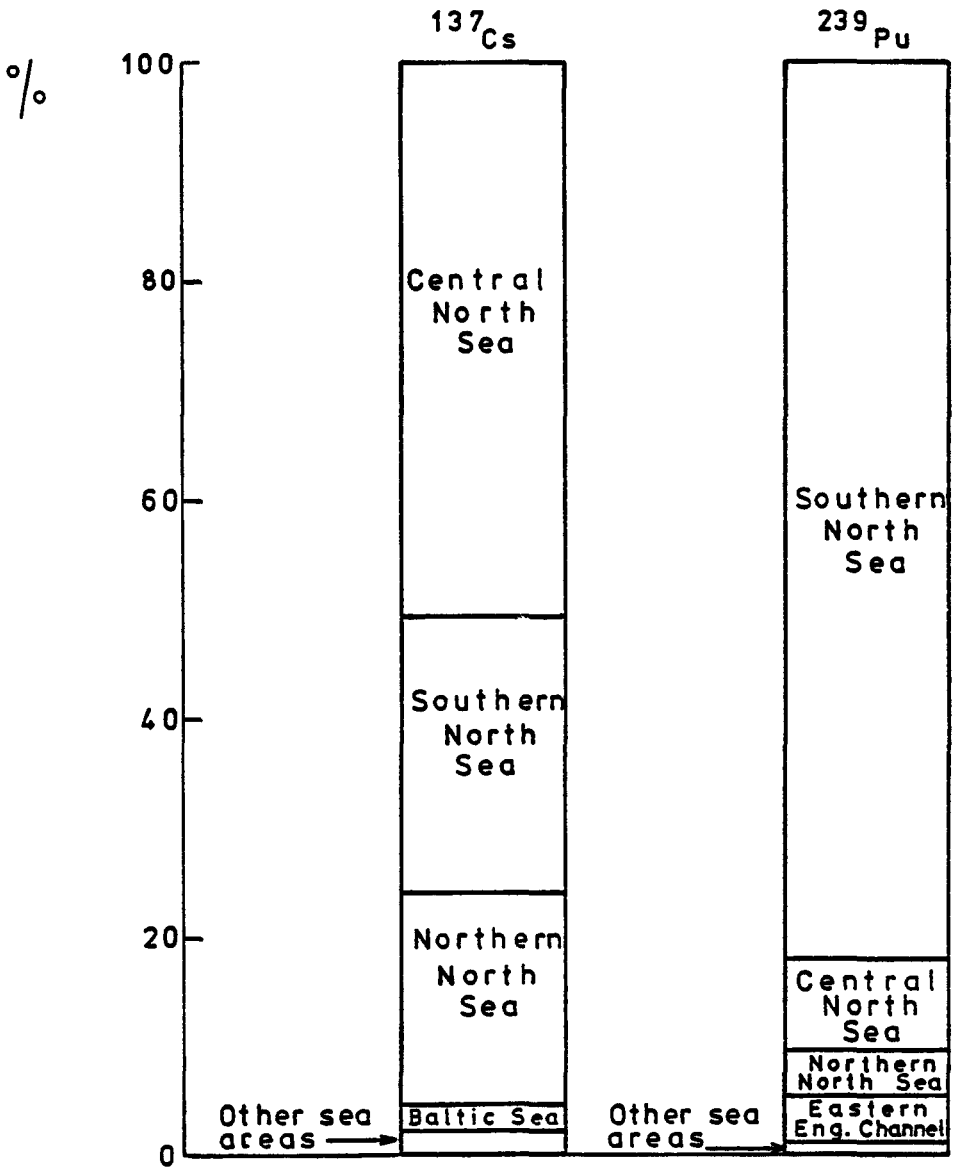


Figure 4-16 Percentage contributions of different sea areas to the 50 year integrated total collective intake for a discharge to the Southern North Sea

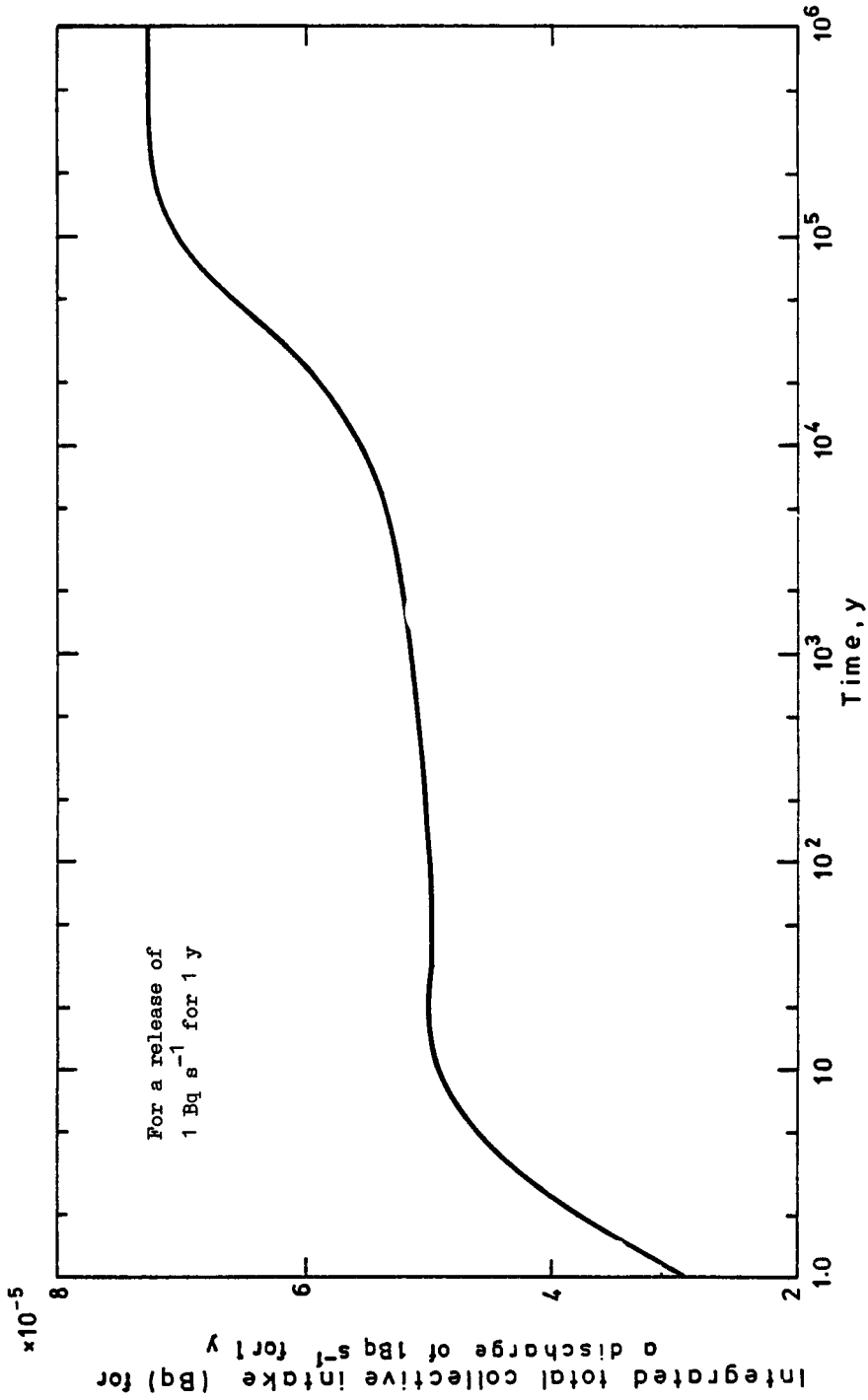


Figure 4-17 Integrated total collective intake for a discharge of ^{99}Tc from a local box in to Southern North Sea

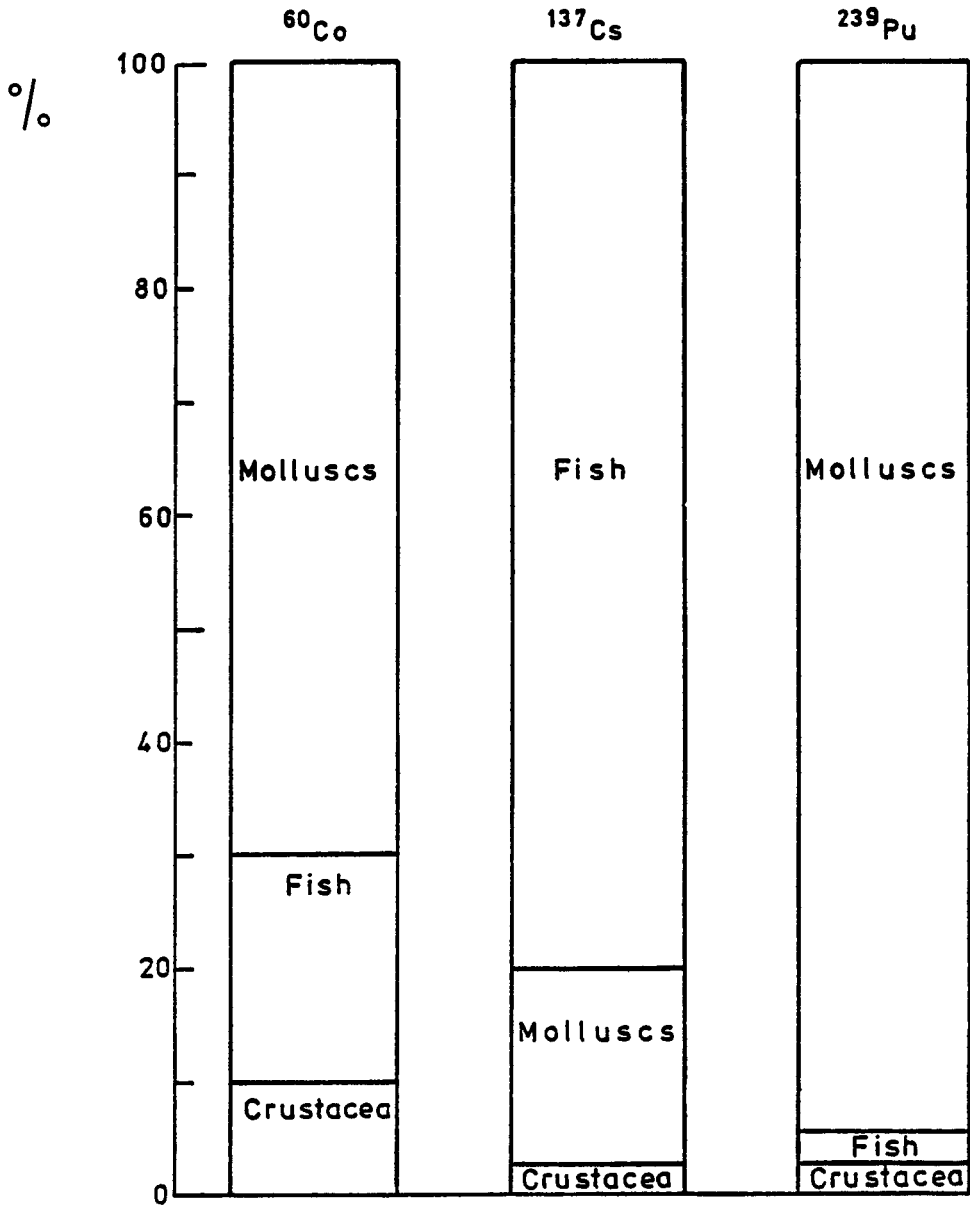


Figure 4 - 18 . Percentage contributions of different marine foodstuffs to the 50 year integrated total collective intake for a discharge to the upper layer of the Eastern Mediterranean

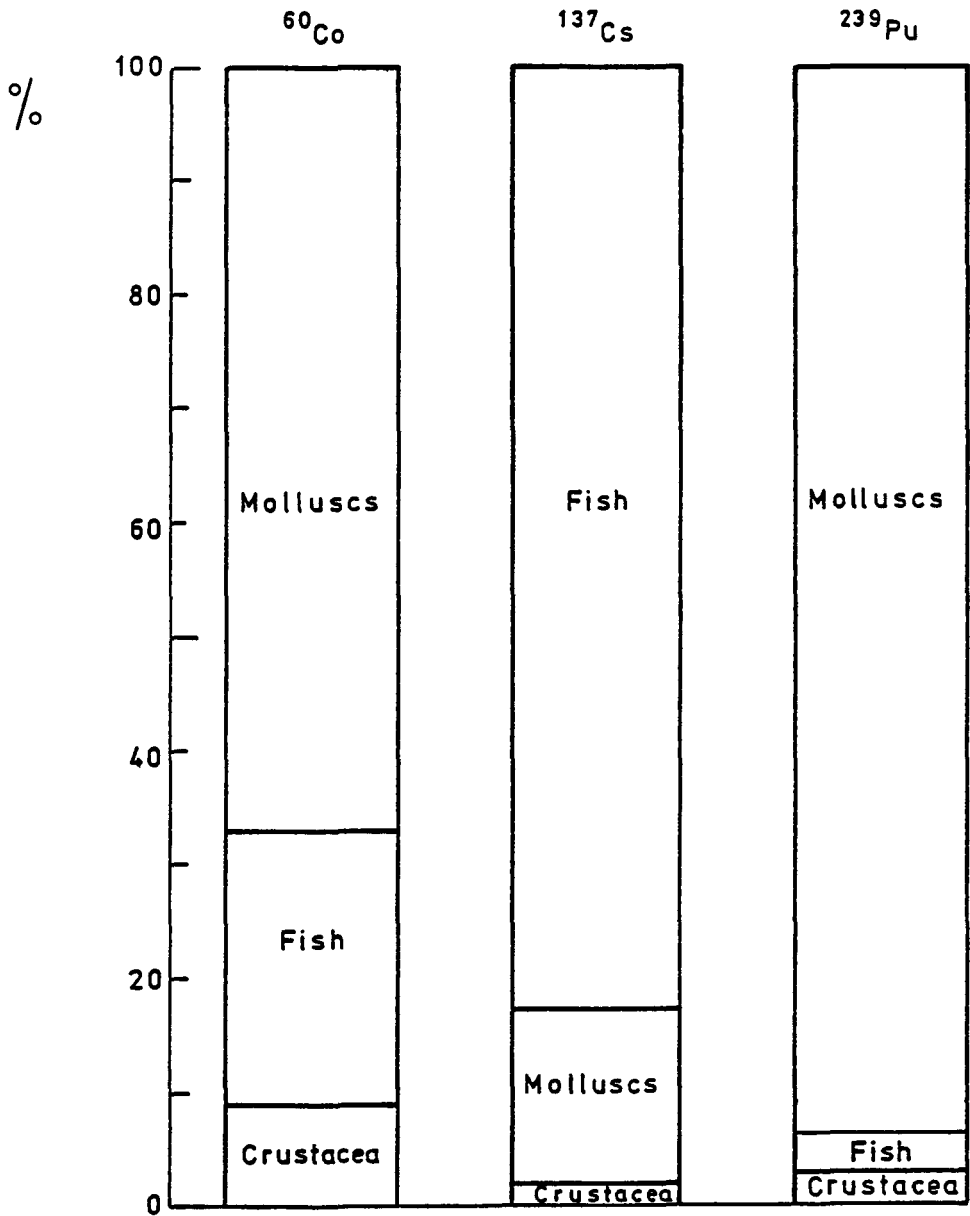


Figure 4-19 . Percentage contributions of different marine foodstuffs to the 50 year integrated total collective intake for a discharge to the Western Mediterranean

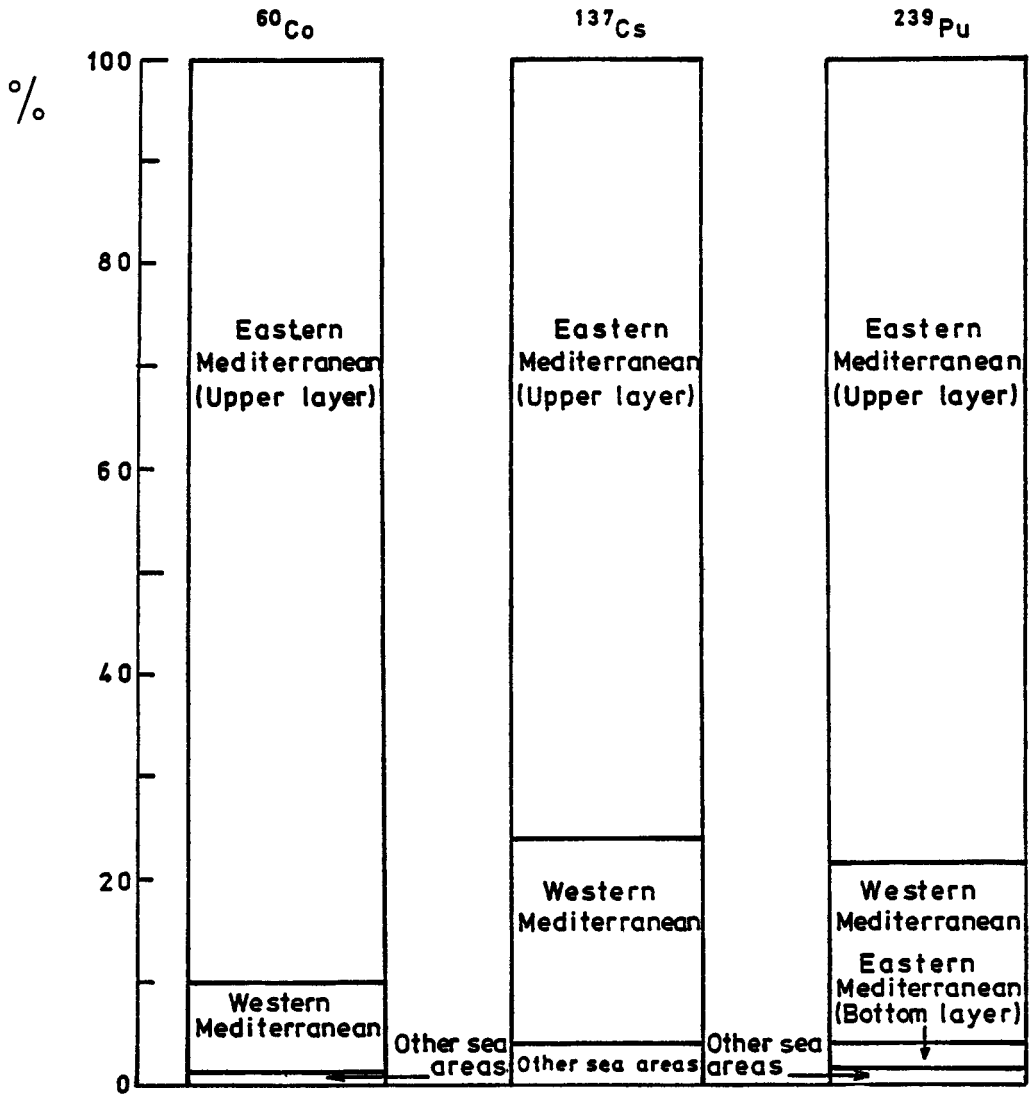


Figure 4 -20. Percentage contributions of different sea areas to the 50 year integrated total collective intake for a discharge to the upper layer of the Eastern Mediterranean

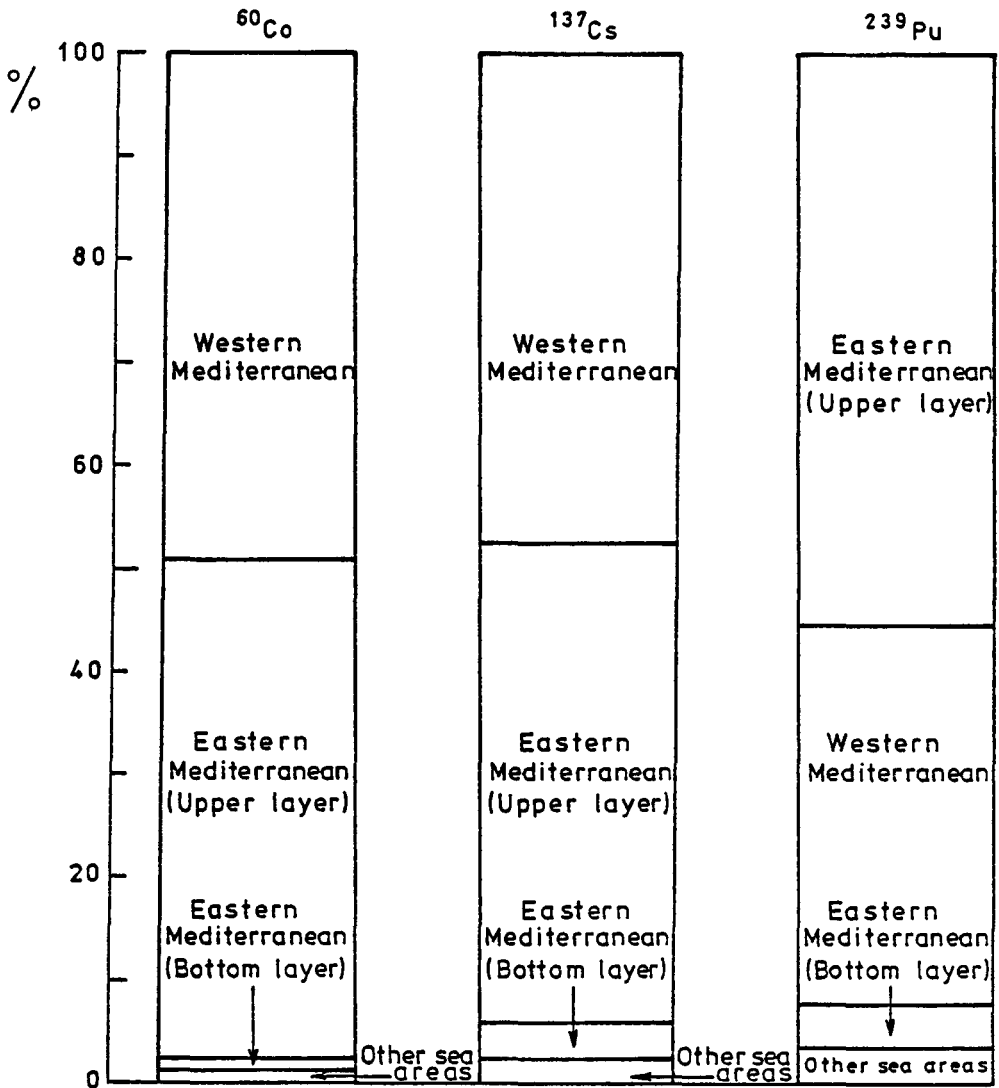


Figure 4 -21. Percentage contributions of different sea areas to the 50 year integrated total collective intake for a discharge to the Western Mediterranean

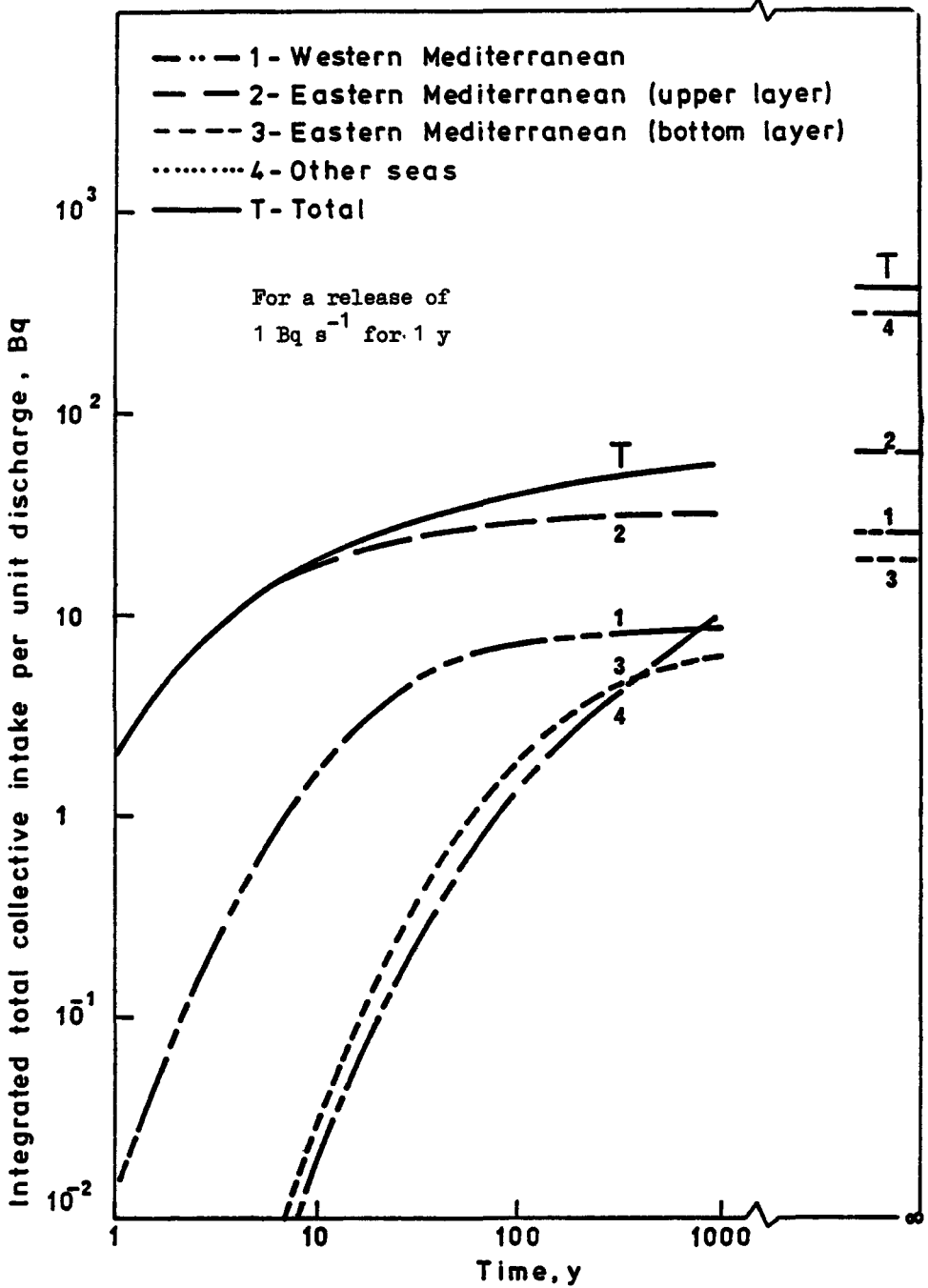


Figure 4 -22 . Integrated total collective intake for a discharge of technetium -99 to the upper layer of the Eastern Mediterranean

Appendix 4.1

Mathematical expression for sediment concentrations in rivers

This appendix describes the model used to calculate the transport of sediment contamination.

In order to simplify the mathematical expressions it has been assumed that the river flow has a constant average value downstream from the release point, that the river has a regular cross-section, that resuspended sediments travel with the same constant velocity and that there is no desorption phenomena occurring. Figure A4.1.1 shows a situation schematically.

The following terms may be defined

- aΔt = activity corresponding to a single release of short duration (Bq)
- t = time elapsed since the release (s)
- T = time of observation (s)
- T₁ = the time taken for the sediments to travel the distance X between the point of release O and the point of observation C (s)

The water velocity is considerably higher than the bed sediment velocity, it can be assumed however that the activity in water produces contamination on sediments instantaneous from t = 0. The profile of contamination travels the length of the river bed with velocity v. At time T the contamination s of sediments at point C is equal, allowing for radioactive decay, to the contamination at t = 0 at a point B situated at a distance vT upstream of C, which is a distance X = x - vT from the point of emission. Thus

$$\Delta s (C) = \Delta s (B) e^{-\lambda T} \quad \dots (A4.1)$$

$$s (x, T) = s (X, 0) e^{-\lambda T} \quad \dots (A4.2)$$

The calculation of sediment activity at B and t = 0 is carried out in the following way.

For a given radionuclide the activity of water, Q, in the river water at point B is

$$Q (X, 0) = a\Delta t e^{-kX} \quad \dots (A4.3)$$

whereas the activity lost from the water between X and X + ΔX is

$$\Delta Q (X, 0) = -k a\Delta t e^{-kX} \Delta X = k Q(X, 0) \Delta X \quad \dots (A4.4)$$

this decrease in activity is due to decay and sediment deposition. The decrease due to sediment deposition is

$$\Delta Q' (X, 0) = -k' Q (X, 0) \Delta X \quad \dots (A4.5)$$

this quantity being equal to the quantity deposited on ΔX, thus

$$\Delta s' (X, 0) = k' Q (X, 0) \Delta X \quad \dots (A4.6)$$

Thus for unit length,

$$\Delta s (X, 0) = \frac{\Delta s'}{\Delta X} = k' Q (X, 0) = k' a\Delta t e^{-kX} \quad \dots (A4.7)$$

where

$$\Delta s(x, T) = k' a \Delta t e^{-kX} e^{-\lambda T} \dots (A4.8)$$

A series is now considered of n emissions of short duration at times $t_1 \dots t_n$ spread out between times $t = 0$ and $t = T$. Each emission will contribute to the sediment activity at point C at time T, giving,

$$s(x, T) = \sum_{i=1}^n \Delta s(x, t_i) e^{-\lambda(T-t_i)} \dots (A4.9)$$

with

$$X(t_i) = x - v(T - t_i) \dots (A4.10)$$

For a continuous emission of duration t greater than T

$$S(x, T) = \int_0^T ds(x, t) e^{-\lambda(T-t)} \dots (A4.11)$$

therefore after equation A1.7.

$$s(x, T) = \int_0^T k' a e^{-kX(t)} e^{-\lambda(T-t)} dt \dots (A4.12)$$

with $X(t) = x - v(T - t)$

This means that:

$$s(x, T) = k' a e^{-k(x-vT)} e^{-\lambda T} \int_0^T e^{(\lambda - kv)t} dt \dots (A4.13)$$

and therefore

$$s(x, T) = \frac{k' a}{kv - \lambda} e^{-k(x-vT)} e^{-\lambda T} [1 - e^{(\lambda - kv)T}] \dots (A4.14)$$

giving finally

$$s(x, T) = \frac{k' Q(x)}{kv - \lambda} [e^{(kv - \lambda)T} - 1] \dots (A4.15)$$

So far situations have been considered where time T is less than T_1 , that is the time of observation is less than the time taken for the sediments to travel the distance x. In the case where T is greater than T_1 the sediment concentration at point C cannot be calculated in the above manner at $T_1 = x/v$ because the sediments situated upstream of the outfall cannot be contaminated. In this case the lower band of the integral is not 0 but $T - T_1$ and

$$s(x, T) = \int_{T-T_1}^T k' a e^{-kX(t)} e^{-\lambda(T-t)} dt \dots (A4.16)$$

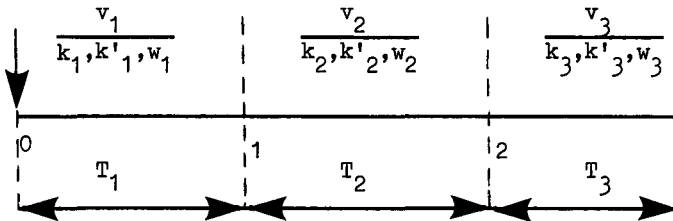
which gives

$$s(x, T) = \frac{k' Q(x)}{kv - \lambda} [e^{(kv - \lambda)T_1} - 1] \dots (A4.17)$$

It is important to note that in this case the sediment concentration at a given point is independent of time. A study of the variation as a function of distance shows a maximum x_m given by the expression.

$$x_m = \frac{\ln(kv/\lambda)}{k - \lambda/v} \quad \dots (A4.18)$$

The model can be adapted to consider the more complex case where the river is divided into several sections and the velocity of water and sediment is constant.



In the case where there are 3 sections the formulation is as follows:

$$\text{Water: } C_{\text{water}} = \frac{1}{V} \left[a e^{-k_1 X_1} e^{-k_2 (X_2 - X_1)} e^{-k_3 (x - X_2)} \right] \quad \dots (A4.19)$$

where V is the water flow at point x .

In the case of daughter product ingrowth we have

$$C_{\text{water}} = \frac{a}{V} \frac{\lambda_D}{\lambda_D - \lambda} \left(e^{-k_1 X_1} e^{-k_2 (X_2 - X_1)} e^{-k_3 (x - X_2)} \right) \quad \dots (A4.20)$$

$$- e^{-k_{D1} X_1} e^{-k_{D2} (X_2 - X_1)} e^{-k_{D3} (x - X_2)} \quad \dots (A4.20)$$

where λ = decay constant of parent nuclide
 λ_D = decay constant of daughter nuclide
 k_D = Schaeffer parameter for the daughter product

The sediment concentration at $T < T_3$ is given by

$$s(x, T) = \frac{k'_3 Q(x)}{k_3 v_3 - \lambda} \left[e^{(k_3 v_3 - \lambda) T} - 1 \right] \quad \dots (A4.21)$$

for $T_3 < T < T_2 + T_3$

$$s(x, T) = \frac{k'_2 Q(X_2)}{k_2 v_2 - \lambda} e^{-\lambda T_3} [e^{(k_2 v_2 - \lambda)(T - T_3)} - 1] + \frac{k'_3 Q(x)}{k_3 v_3 - \lambda} [e^{(k_3 v_3 - \lambda) T_3} - 1] \dots (A4.22)$$

for $T_2 + T_3 < T < T_1 + T_2 + T_3$

$$s(x, T) = \frac{k'_1 Q(X_1)}{k_1 v_1 - \lambda} e^{-\lambda(T_2 + T_3)} [e^{(k_1 v_1 - \lambda)(T - T_2 - T_3)} - 1] + \frac{k'_2 Q(X_2)}{k_2 v_2 - \lambda} e^{-\lambda T_3} [e^{(k_2 v_2 - \lambda) T_2} - 1] + \frac{k'_3 Q(x)}{k_3 v_3 - \lambda} [e^{(k_3 v_3 - \lambda) T_3} - 1] \dots (A4.23)$$

for $T > T_1 + T_2 + T_3$

$$s(x, T) = \frac{k'_1 Q(X_1)}{k_1 v_1 - \lambda} e^{-\lambda(T_2 + T_3)} [e^{(k_1 v_1 - \lambda) T_1} - 1] + \frac{k'_2 Q(X_2)}{k_2 v_2 - \lambda} e^{-\lambda T_3} [e^{(k_2 v_2 - \lambda) T_2} - 1] + \frac{k'_3 Q(x)}{k_3 v_3 - \lambda} [e^{(k_3 v_3 - \lambda) T_3} - 1] \dots (A4.24)$$

In the parallel case for daughter products for $T > T_1 + T_2 + T_3$

$$\begin{aligned}
 s(x, T) = & \frac{a \cdot \lambda_D}{\lambda_D - \lambda} [k'_1 e^{-k_1 x_1} e^{-\lambda (T_2 + T_3)} \left(\frac{e^{(k_1 v_1 - \lambda) T_1} - 1}{k_1 v_1 - \lambda} \right) \\
 & - k'_1 e^{-k_{D1} x_1} e^{-\lambda_D (T_2 + T_3)} \left(\frac{e^{(k_{D1} v_1 - \lambda_D) T_1} - 1}{k_{D1} v_1 - \lambda_D} \right) \\
 & + k'_2 e^{-k_1 x_1} e^{-k_2 (x_2 - x_1)} e^{-\lambda T_3} \left(\frac{e^{(k_2 v_2 - \lambda) T_2} - 1}{k_2 v_2 - \lambda} \right) \\
 & - k'_2 e^{-k_{D1} x_1} e^{-k_{D2} (x_2 - x_1)} e^{-\lambda_D T_3} \left(\frac{e^{(k_{D2} v_2 - \lambda_D) T_2} - 1}{k_{D2} v_2 - \lambda_D} \right) \\
 & + k'_3 e^{-k_1 x_1} e^{-k_2 (x_2 - x_1)} e^{-k_3 (x - x_2)} \left(\frac{e^{(k_3 v_3 - \lambda) T_3} - 1}{k_3 v_3 - \lambda} \right) \\
 & - k'_3 e^{-k_{D1} x_1} e^{-k_{D2} (x_2 - x_1)} e^{-k_{D3} (x - x_2)} \left(\frac{e^{(k_{D3} v_3 - \lambda_D) T_3} - 1}{k_{D3} v_3 - \lambda_D} \right)] \\
 & \dots (A4.25)
 \end{aligned}$$

These expressions can be easily adapted for the general case where the river is divided into n sections and V_i , w_i and k_i are constants.

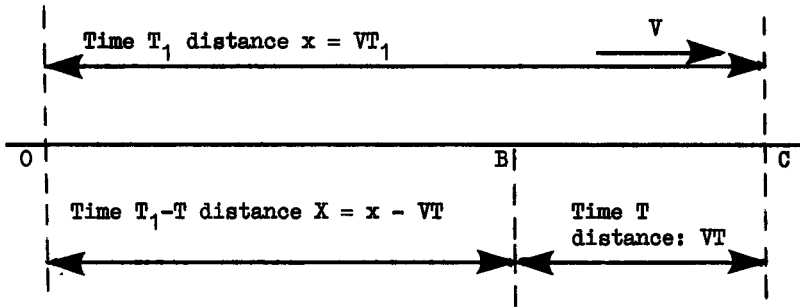


Figure A4.1.1 Diagram of the river bed

Appendix 4.2

Determination of the rates of transfer between the western and eastern Mediterranean

The rates of transfer between the western Mediterranean and the Atlantic Ocean, and between the eastern Mediterranean and the Black Sea, are known [A-4.2.17]

The water volumes must be conserved: the inputs of water (rainfall, rivers, Atlantic and Black Sea inflows) balance the loss of water (evaporation, loss to the Black Sea and Atlantic).

This is expressed by the following equations corresponding to the three defined compartments of the Mediterranean (Figure A4.2.1)

$$k_{21}V_2 + k_{31}V_3 + k_{51}V_5 + p_1 + f_1 - (k_{12} + k_{13} + k_{15})V_1 - e_1 = 0 \quad \text{..... (A4.26)}$$

$$k_{12}V_1 + k_{42}V_4 + p_2 + f_2 - (k_{21} + k_{24})V_2 - e_2 = 0 \quad \text{..... (A4.27)}$$

$$k_{13}V_1 - k_{31}V_3 = 0 \quad \text{..... (A4.28)}$$

where k_{ij} is the fraction of the volume of compartment i passing to compartment j per unit time.

V_i is the volume of compartment i

e_1, e_2 are the annual losses by evaporation in compartments 1 and 2

p_1, p_2 are the annual precipitation into compartments 1 and 2

f_1, f_2 are the annual input from rivers into compartments 1 and 2

These 3 equations are not independent, because the total volume of the Mediterranean is also constant. Only 2 of them can be used to determine the transfer coefficients k_{12}, k_{21}, k_{13} and k_{31} .

The two supplementary equations can be found in using the results of measurements of Strontium-90 in the Mediterranean basin [A-4.2.17]. Although atmospheric fallout from nuclear explosions has only existed for about 30 years it is assumed that equilibrium has been established in the Mediterranean: ie, that the concentration is constant in time in each compartment.

It is necessary to formulate this hypothesis because there is only one value for the concentration in each compartment, that measured in 1973.

The following 3 equations describe the balance of exchanges between the compartments, the inputs and losses of activity:

$$k_{21}C_2V_2 + k_{31}C_3V_3 + k_{51}C_5V_5 + P_1 + F_1 - (K_1 + \lambda + k_{13} + k_{15})C_1V_1 = 0 \quad \text{..... (A4.29)}$$

$$k_{12}C_1V_1 + k_{42}C_4V_4 + S_2 + P_2 + F_2 - (K_2 + \lambda + k_{21} + k_{24})C_2V_2 = 0 \quad \text{..... (A4.30)}$$

$$k_{13}C_1V_1 - (K_3 + \lambda + k_{31})C_3V_3 = 0 \quad \text{..... (A4.31)}$$

where C_i is the concentration in compartment i Bq m^{-3}
 λ is the radioactive decay constant at Strontium-90 (y^{-1})
 K_i is the rate of loss by sedimentation in compartment i (y^{-1})
 S_1, S_2 are the annual inputs of Strontium-90 by dry deposition into compartments 1 and 2 respectively (Bq y^{-1})
 P_1, P_2 are the annual inputs of Strontium-90 by rainfall into compartments 1 and 2 respectively (Bq y^{-1})
 F_1, F_2 are the annual inputs of Strontium-90 by rivers into compartments 1 and 2 respectively (Bq y^{-1})

These three equations are not independent because if the concentrations are constant in each compartment, the volumes being constant, the total activity present in the Mediterranean is also constant.

As a consequence, only two of the equations can be used.

It is necessary to determine the transfer coefficients k_{12}, k_{21}, k_{13} and k_{31} , since four equations are used, it is therefore possible to determine their values if one knows the rates of sedimentation, the inputs and losses of Mediterranean water and the inputs of Strontium-90 into the Mediterranean. These data are shown in Table A4.2.1 and Figure A4.2.1.

The dry deposition of Strontium-90 is evaluated from the measurements of air concentration at ISPRA in 1973 and 1974 $\overline{A-4.2.2}$: a mean of $10^{-3} \text{ pCi m}^{-3}$ being a dry deposition of 0.15 m Ci h^{-1} . The value used for Strontium-90 concentrations in rainfall is the mean of measurements taken at ISPRA and at CASACCIA during 1973-74, being 408 pCi m^{-3} . The value used for the concentration in river water is that measured in 1972 in drinking water from the Paris region from a treatment works which takes water from the Seine $\overline{A-4.2.3}$: 220 pCi m^{-3} .

The data on inputs from rivers and by precipitation and losses of water by evaporation are only known for the whole of the Mediterranean basin. It is therefore assumed that the rainfall and evaporation are uniform over the whole of the Mediterranean: ie, that the inputs and losses are proportional to the surface areas.

Finally it is assumed that the input of rivers is the same in the two basins.

The values of the transfer coefficients obtained are shown in Table A4.2.2 and Figure A4.2.1. These values, as a function of the simplifying hypothesis which are necessary to derive them, should be verified and specified; they allow however a representation of the water circulation in the Mediterranean which conforms to the generally accepted ideas.

References

- [A-4.2.1] Sverdrup, H V, Johnson, M N and Fleming, R H, The Oceans. New York, Prentice-Hall (1942).
- [A-4.2.2] CEC, Radiological protection no.11 - Results of environmental radioactivity measurements in the Member States of the European Community for air, deposition and water. Luxembourg, CEC, EUR5630 (1977).
- [A-4.2.3] Jeanmaire, I, Patti, F and Gros, R, Activite en strontium-90 d'une eau potable de la region parisienne, de 1963 à 1972. Radioprotection, 11, 57 (1976).
- [A-4.2.4] Batrakov, G F, Erenev, V N, Zemlyanoi, A D, Iranova, T M and Pavlidi, I M, ⁹⁰Sr content in the Mediterranean Sea. At. Energ., 43, 197 (1977).

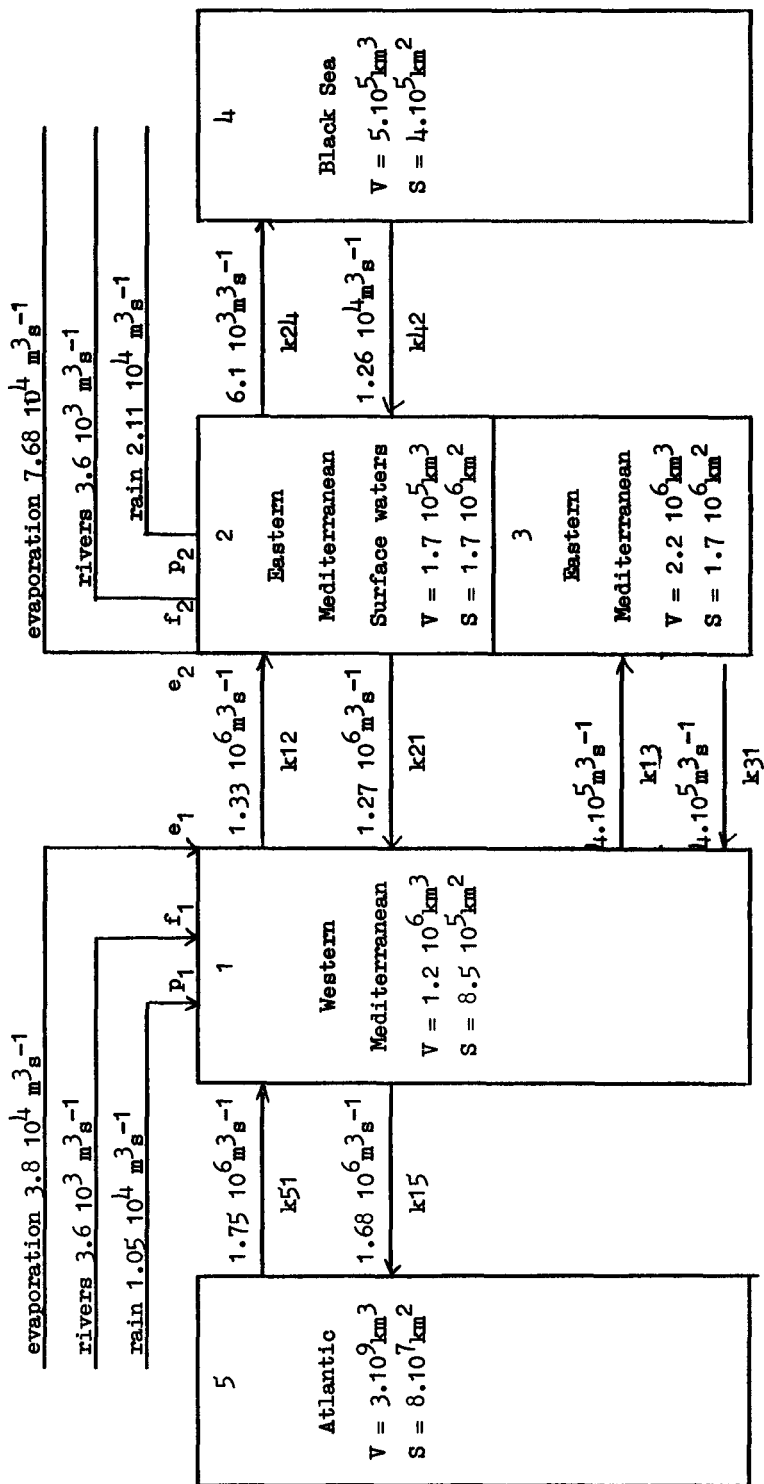
Table A4.2.1

	<u>Data Used</u>	
Input by precipitation	3.16	$10^4 \text{ m}^3 \text{ s}^{-1}$
Input by rivers	7.30	$10^3 \text{ m}^3 \text{ s}^{-1}$
Loss by evaporation	1.15	$10^5 \text{ m}^3 \text{ s}^{-1}$
Concentration in:		
- rainfall	408 pCi m^{-3}	(mean ISFRA.CASACCIA 1972-1973 [A-4.2.27])
- river water	220 pCi m^{-3}	(Seine 1972 [A-4.2.37])
- air	10^{-3} pCi m^{-3}	(ISFRA - 1973, 1974 [A-4.2.17]).
Rate of sedimentation of Strontium-90:		
- western Mediterranean	4	10^{-5} y^{-1}
- eastern Mediterranean	2	10^{-5} y^{-1}
Surface:		
of western Mediterranean	8.5	10^5 km^2
of eastern Mediterranean	1.7	10^6 km^2
Concentration of Strontium-90:		
Black Sea	530	pCi m^{-3}
Upper layer of eastern Mediterranean	140	pCi m^{-3}
Lower layer of eastern Mediterranean	14	pCi m^{-3}
Western Mediterranean	81	pCi m^{-3}
Atlantic	68	pCi m^{-3}

Table A4.2.2 Values used in the regional model for the Mediterranean

v_1	$1.2 \cdot 10^{15} \text{m}^3$
v_2	$1.7 \cdot 10^{14} \text{m}^3$
v_3	$2.2 \cdot 10^{15} \text{m}^3$
v_4	$5.0 \cdot 10^{14} \text{m}^3$
v_5	$3.2 \cdot 10^{17} \text{m}^3$
v_6	$1.0 \cdot 10^{18} \text{m}^3$
k_{12}	$3.5 \cdot 10^{-2} \text{y}^{-1}$
k_{13}	$1.0 \cdot 10^{-2} \text{y}^{-1}$
k_{15}	$4.4 \cdot 10^{-2} \text{y}^{-1}$
k_{21}	$2.4 \cdot 10^{-1} \text{y}^{-1}$
k_{24}	$1.1 \cdot 10^{-3} \text{y}^{-1}$
k_{31}	$5.7 \cdot 10^{-3} \text{y}^{-1}$
k_{42}	$7.9 \cdot 10^{-4} \text{y}^{-1}$
k_{51}	$1.8 \cdot 10^{-4} \text{y}^{-1}$
k_{56}	$3.1 \cdot 10^{-3} \text{y}^{-1}$
k_{65}	$1.0 \cdot 10^{-3} \text{y}^{-1}$

Figure A4.2.1 - Circulation of water in the Mediterranean basin



V = volume

S = surface area

CHAPTER 5

GLOBAL CIRCULATION OF RADIONUCLIDES

5.1 Introduction

Some radionuclides, owing to the magnitude of their radioactive half-lives and their behaviour in the environment, may become globally dispersed and act as a long term source of irradiation of both regional and world populations; this is an addition to the irradiation of the population exposed during the initial dispersion of these nuclides from their points of discharge. The radionuclides which are important in this context have already been identified in sections 3.2.6 and 4.4.2.1 for discharges to the atmospheric and the aquatic environments: they are krypton-85, tritium, iodine-129 and carbon-14.

Once these nuclides become globally distributed essentially the whole of the population of the European Community will be irradiated at the same level. Krypton-85 is not readily incorporated into body tissues and it is significant only in respect of external irradiation of the population. The nature of the radiation emitted by the other three nuclides is such that external irradiation is not important compared with that from the incorporation of these nuclides in the body.

5.2 Global circulation models

The models used to estimate the global circulation of krypton-85, tritium, iodine-129 and carbon-14 are essentially those given by Kelly et al [5.17]. Some minor modifications, in the interests of simplification, have been made to these models without any undue loss of precision; these modifications are identified where appropriate. Only the principal features of each model are described and reference may be made to Kelly et al [5.17] for further detail. In each case a compartment model is adopted to evaluate the global circulation and the general technique of compartmental analysis is outlined in the Appendix 3.2.

5.2.1 Krypton-85

The compartment model for krypton-85 is shown in Figure 5.1 and is a simplified version of that used by Kelly et al [5.17]. The discharged krypton-85 is assumed to be dispersed uniformly, and instantaneously, throughout the troposphere of the northern hemisphere which is assumed to have a height of 10 km and a mass of 1.9×10^{21} g. Exchange takes place between the tropospheres of the two hemispheres with a half time of about 2 years. The model adopted by Kelly et al [5.17] included a more detailed representation of the dispersion in the troposphere of the northern hemisphere. Within a few years the krypton-85 becomes uniformly mixed through the whole troposphere and the sole loss from the system is by radioactive decay.

Krypton-85 in the atmosphere results in the exposure of man by external irradiation from both photons and electrons. The dose in man is estimated from the time integral of the concentration of krypton-85 in the troposphere of the northern hemisphere (expressed in terms of Bq per kg in air) and the dose equivalent commitment per unit time integral of the air concentration.

5.2.2 Tritium

The model used for tritium is shown in Figure 5.2 and is identical with that given by Kelly et al [5.17]. Discharged tritium (whether to the atmospheric or the aquatic environment) is assumed to be immediately dispersed and exchanged with the hydrogen content of the circulating waters of the hemisphere into which the discharge is made. The subsequent circulation of tritium is then determined by the exchange of the circulating waters between the two hemispheres and the deep oceans. The circulating waters of the northern hemisphere comprise essentially the surface waters of the sea to a depth 75m and have a mass of 10^{22} g. The intake of tritium by man is determined assuming that all water taken into the body has a specific activity of tritium equal to that in the circulating waters of the Northern Hemisphere.

5.2.3 Iodine-129

The model used for iodine-129 is identical with that for tritium and is shown in Figure 5.2. Little is known of the long term global circulation of iodine-129 but clearly the model is a considerable oversimplification. For example no account is taken of possible sedimentation of iodine-129 on to the ocean bed; bearing in mind the extremely long half life of the nuclide this mechanism could be important. However the approach adopted here is conservative. The discharged iodine-129 (whether to the atmospheric or to the aquatic environment) is assumed to be mixed instantaneously through the circulating waters of the northern hemisphere and subsequently to follow the general patterns of water movement. The intake of iodine-129 by man is determined assuming the specific activity of iodine taken into the body is identical to that in the circulating waters of the northern hemisphere. The stable iodine content of these waters is taken as 60 μ g per g water [5.17].

5.2.4 Carbon-14

The model used for carbon-14 is shown in Figure 5.3 and is slightly modified compared to that adopted by Kelly et al [5.17]. The modification, as for krypton-85, comprises a less detailed representation of the dispersion in the troposphere of the northern hemisphere. The model is considerably more elaborate than that adopted for tritium and iodine-129 and is possible because of the extensive measurements made of carbon in the carbon cycle. The compartment "circulating carbon" comprises carbon in the troposphere and in those parts of the terrestrial biosphere which are subject to rapid cycles of growth and decay. The compartment "humus" comprises the carbon content of the terrestrial biosphere that is recycled more slowly. Carbon-14 discharged to the atmospheric or aquatic environment is assumed to be uniformly and instantaneously mixed with the carbon content of the compartment into which the discharge is made. The subsequent circulation between the respective compartments is governed by the transfer coefficients given in Figure 5.3. The intake of carbon-14 by man is determined assuming the specific activity of all carbon ingested or inhaled by man is equal to that in the circulating carbon of the northern hemisphere. The mass of circulating carbon in the northern hemisphere has been calculated as $3.6 \cdot 10^{17}$ g from the work of Ekdahl and Keeling [5.2].

5.3 Application of the models and selected results

The models have been applied to evaluate the time variation of the concentrations of each nuclide in the respective compartments following the discharge of each nuclide continuously at a rate of 1 Bq s^{-1} for 1 year.

Consideration is given to the discharge of each nuclide to the atmospheric and to the aquatic environment, apart from krypton-85 which is discharged only to the atmosphere. In each model, for the compartment most appropriate to the estimation of dose in man, the time variation of the concentration and time-integral of concentration of each nuclide are shown in Figures 5.4 and 5.5. The concentrations of each nuclide are expressed in terms of the activity concentrations of each nuclide in an appropriate medium (eg, Bq per kg air for krypton-85) as specified in sections 5.2.1 - 5.2.4. A matrix of results has been generated which contains the time-integrals of the activity concentrations of each nuclide in the respective media to times of 50, 100, 500 years and infinity (see table 5.1). The matrix corresponds to the continuous discharge into the appropriate parts of the environment of each nuclide at a rate of 1 Bq s⁻¹ for one year. This matrix of time integrals of concentration forms the basis of the assessment of the collective exposure of the Community population. In the case of carbon-14, tritium and iodine-129, the matrix is used first to evaluate the intake by the population, by ingestion and inhalation, of these nuclides. The collective intakes to time, t, of carbon-14 by the population by ingestion is obtained as

$$\text{TIC}(t) M_{\text{ing}} \text{ PEC} \quad (\text{Bq})$$

.....(5.1)

where TIC(t) is the time integral to t, of the concentration of carbon-14 per unit mass of carbon (Bq y kg⁻¹)

M_{ing} is the average annual individual intake of carbon by ingestion, (kg y⁻¹)

PEC is the population of the Community taken as 2.55 10⁸

and similarly the collective intake of carbon-14 by the EC population by inhalation is

$$\text{TIC}(t) M_{\text{inh}} \text{ PEC} \quad (\text{Bq})$$

.....(5.2)

where M_{inh} is the average annual individual intake of carbon by inhalation

Comparable equations can be written for the intake, by ingestion and inhalation, of tritium and iodine-129 with appropriate substitution for the time integrals of concentration in, and intakes of, the relevant media (water and iodine respectively). The annual intakes of carbon, water and iodine by inhalation and ingestion are summarised in Table 5.2 and are taken from Reference Man [5.3]. The collective dose in the exposed population is obtained as the product of these collective intakes and the appropriate committed dose equivalents per unit intake by the respective routes (see Chapter 6).

In the case of krypton-85 the only significant mode of exposure is by external irradiation and a slightly different procedure is adopted in which the collective dose in the exposed population is evaluated directly from the time integral of the air concentration. The collective effective dose equivalent commitment (truncated at time t) in the population is given

by

$$\text{TIC}(t) \text{ DK PEC} \quad (\text{man Sv})$$
$$\dots\dots\dots(5.3)$$

where TIC(t) is the time integral to t, of the concentration of krypton-85 per unit mass of air (Bq y kg^{-1})

DK is the effective dose equivalent commitment per unit time integral of the concentration of krypton-85 per unit mass of air ($\text{Sv per Bq y kg}^{-1}$)

The effective dose equivalent commitment per unit time integral of the concentration of krypton-85 per unit mass of air, DK, is summarised in Table 5.3, together with dose equivalent commitments in other appropriate organs.

At short times the time dependence of the concentrations of iodine-129 and tritium, and of carbon-14 when discharged to the aquatic environment, should be regarded with caution. In reality there will be a significant time delay before these nuclides become uniformly distributed through the circulating waters of the northern hemisphere; dispersion is assumed to be instantaneous in the models adopted. In practice the uncertainties introduced by such an approximation are rarely of importance; the infinite time integral of concentration (and thus dose commitment) is in general determined by the concentrations over much greater time periods.

5.4 Interface between the regional marine and global models

In addition to the global models described above, the regional marine models take some account of the global circulation of activity in seawater, so it is necessary to consider the interface between the two.

The global models for iodine-129, carbon-14 and tritium take account of the circulation of activity not only in the seas but also in the atmosphere and terrestrial biosphere. In contrast, the regional marine models consider only the circulation of activity in the seas themselves, and the estimated transfer of activity to man is essentially that due to the consumption of marine foodstuffs. The results of the two types of models are compared for iodine-129 in Figure 5.6, which shows the variations with time of the time-integrals of the transfer of iodine-129 to the population of the European Communities, as calculated by each model. It was assumed that the iodine-129 was discharged into the Southern North Sea, though that does not affect the general conclusions to be drawn. Figure 5.6 shows that the regional marine model significantly underestimates the time-integral of activity ingested by the population after about 10^4 years, and would thus underestimate the collective dose commitment. Similar considerations can be shown to apply to carbon-14, but less so for tritium because of its shorter half-life. As mentioned in section 5.3 the assumption in the global models that activity is dispersed instantaneously into the compartment receiving the discharge means that the short-term results of these models should be regarded with caution.

The approach adopted in this study to interface the regional marine and global models for iodine-129, carbon-14 and tritium is therefore as follows. The contributions to the time-integrals of ingested activity from the regional marine models are added to those from the global models, but only

for the first 50 years following the discharge. After 50 years the contributions to the time integrals are determined by the global models only. Inspection of figure 5.6 shows that this is a satisfactory approximation for iodine-129, and the same can be demonstrated for carbon-14 and tritium.

REFERENCES

- [5.1] Kelly, G N, Jones, J A, Bryant, P M and Morley, F. The predicted radiation exposure of the population of the European Community resulting from discharges of krypton-85, tritium, carbon-14 and iodine-129. Luxembourg, CEC doc. V/2676/75 (1975).
- [5.2] Ekdahl, C A, Bacastow, R and Keeling, C D, Atmospheric carbon dioxide and radiocarbon in the natural carbon cycle IN Proc. Symposium on Carbon in the Biosphere. CONF-720510 (1972).
- [5.3] ICRP. Report of the Task Group on Reference Man. Oxford, Pergamon Press, ICRP Publication 23 (1975).

Table 5.1 The time integrals of the activity concentration of each nuclide in various media from their global circulation (1)

Nuclide	Discharged to	(2) Time-integral of activity concentration (Bq. y kg ⁻¹)			
		to 50 y	to 100 y	to 500 y	to infinity
Krypton-85	Atmosphere	1.31 10 ⁻¹⁰	1.36 10 ⁻¹⁰	1.36 10 ⁻¹⁰	1.36 10 ⁻¹⁰
Tritium	Atmosphere and Aquatic	1.37 10 ⁻¹¹	1.38 10 ⁻¹¹	1.38 10 ⁻¹¹	1.38 10 ⁻¹¹
Iodine-129	Atmosphere and Aquatic	3.25 10 ⁻⁴	3.41 10 ⁻⁴	4.58 10 ⁻⁴	6.62 10 ⁰
Carbon-14	Atmosphere	3.60 10 ⁻⁷	4.07 10 ⁻⁷	7.04 10 ⁻⁷	4.35 10 ⁻⁶
	Aquatic	1.69 10 ⁻⁷	1.99 10 ⁻⁷	4.07 10 ⁻⁷	4.01 10 ⁻⁶

Notes

- (1) Evaluated for the continuous discharge of each nuclide at a rate of 1 Bq s⁻¹ for one year.
- (2) The time integrals of activity concentration in the appropriate compartments refer to unit mass of air for krypton-85, of water for tritium, of stable iodine for iodine-129, and of stable carbon for carbon-14.

Table 5.2 Annual intakes of stable materials by Reference Man

Material	Annual intake, kg per y	
	Ingested	Inhaled
Water	$8.0 \cdot 10^2$ ^(b)	$1.3 \cdot 10^2$ ^(b)
Carbon	$9.3 \cdot 10^1$	1.2 ^(a)
Iodine	$7 \cdot 10^{-5}$	$0.3-13 \cdot 10^{-6}$

Notes

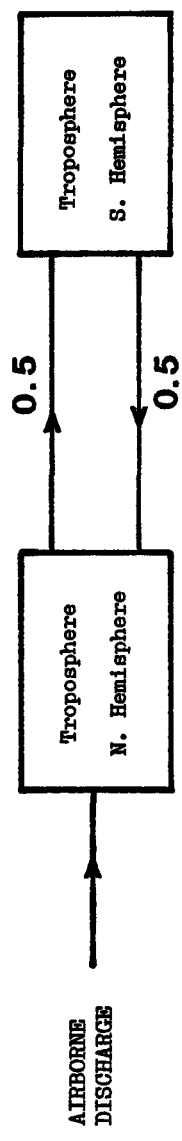
- (a) Calculated from average levels of carbon in air and an average adult inhalation rate of 22m^3 per day [5.3]
- (b) A total water intake rate by all routes of 3000 g per day for man and 2100 g per day for women is given in Reference Man [5.3]. The respective intakes by inhalation and ingestion have been evaluated assuming an annual average of $8.1\text{g H}_2\text{O}$ per m^3 air and a mean adult inhalation rate of 22m^3 per day. The intake by inhalation given in the Table also contains the intake by skin absorption which is assumed equal to the intake by inhalation.

Table 5.3 Dose equivalent commitments from external radiation (β, γ) per unit time integral of air concentration of krypton-85

Organ	Dose equivalent commitment per unit time integral of air concentration of krypton-85 (Sv per Bq y kg ⁻¹)
Effective	4.03 10 ⁻⁹
Gonads	3.19 10 ⁻⁹
Thyroid	3.53 10 ⁻⁹
Skin ⁽¹⁾	5.42 10 ⁻⁷

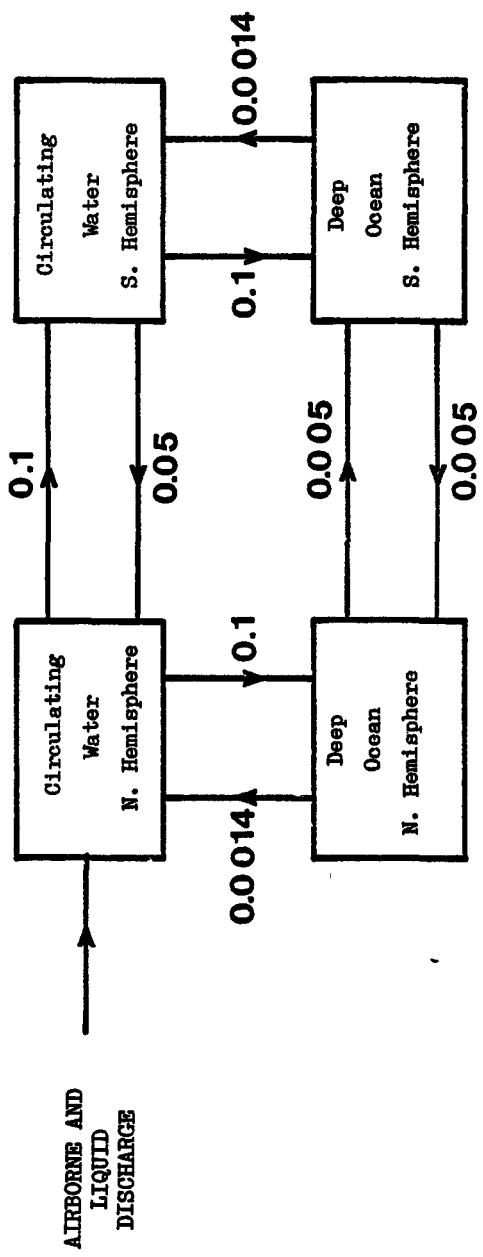
Notes

- (1) The doses are determined solely by γ radiation apart from the skin where the γ contribution is only about 1% of that from β radiation.



Transfer coefficients are given in units of y^{-1}

Figure 5.1 The model used for global circulation of krypton-85



Transfer coefficients are given in units of y^{-1}

Figure 5.2 The model used for global circulation of tritium and iodine-129

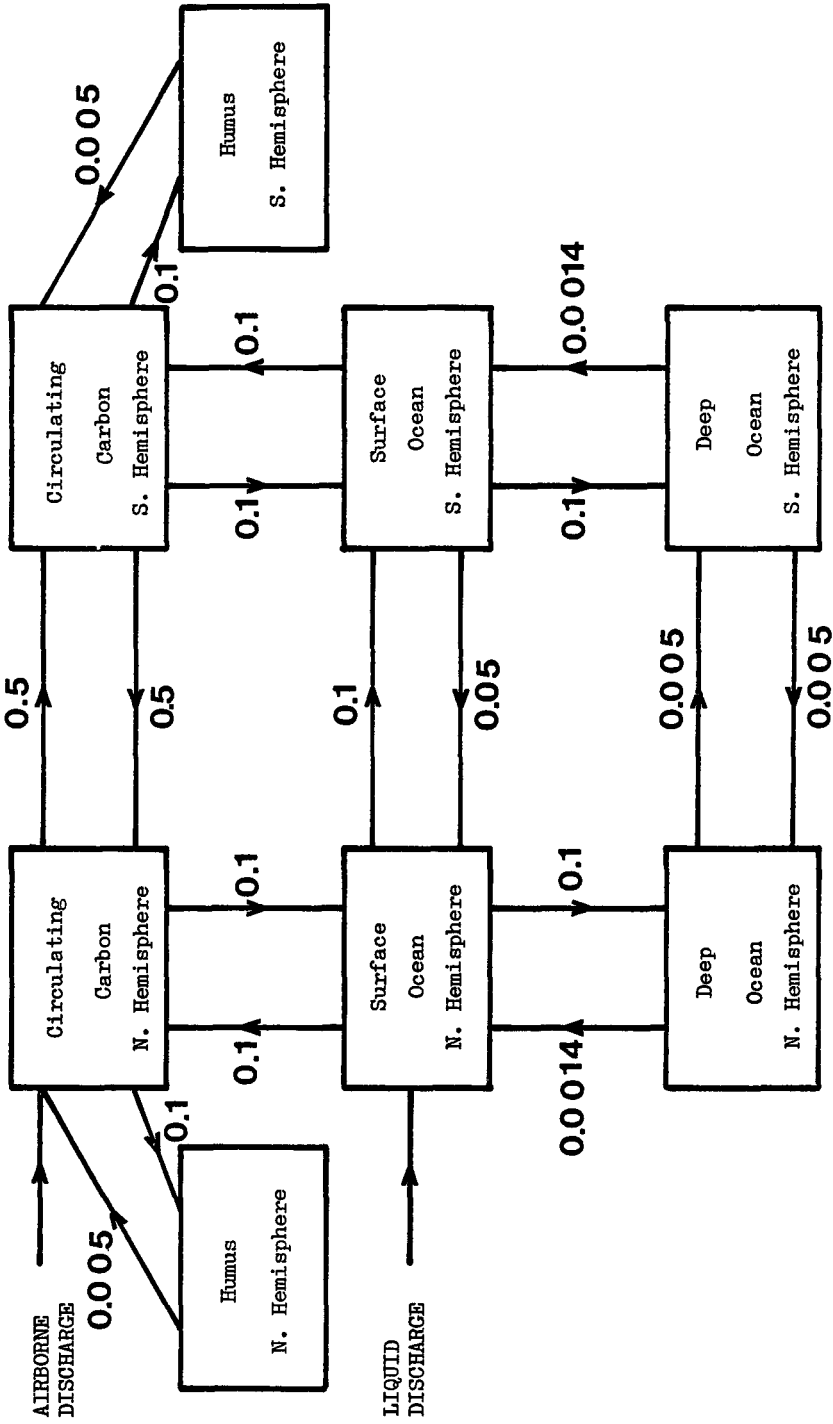


Figure 5.3 Model used for global circulation of carbon-14

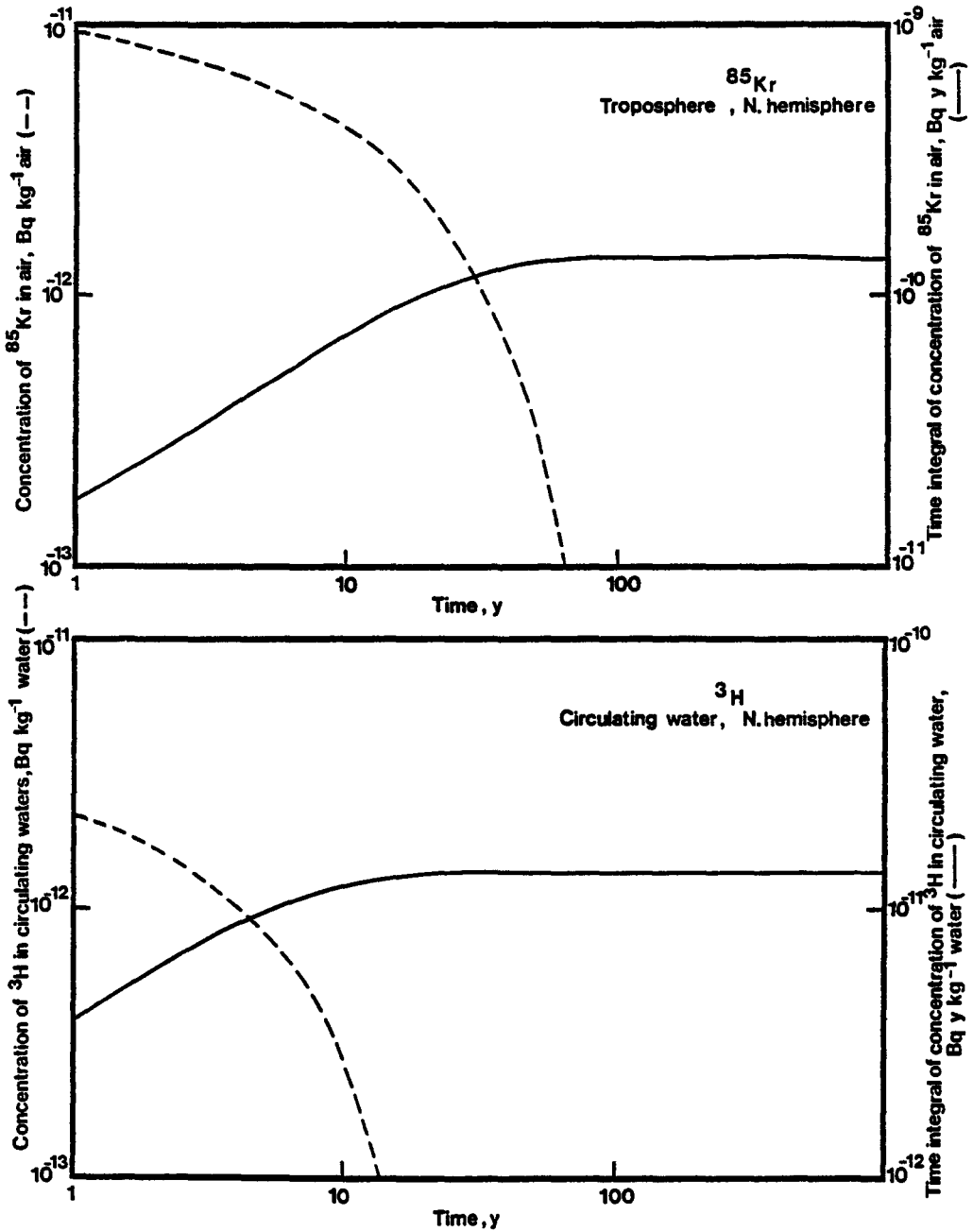


Figure 5.4 The time variation and time integrals of environmental concentrations of krypton-85 and tritium

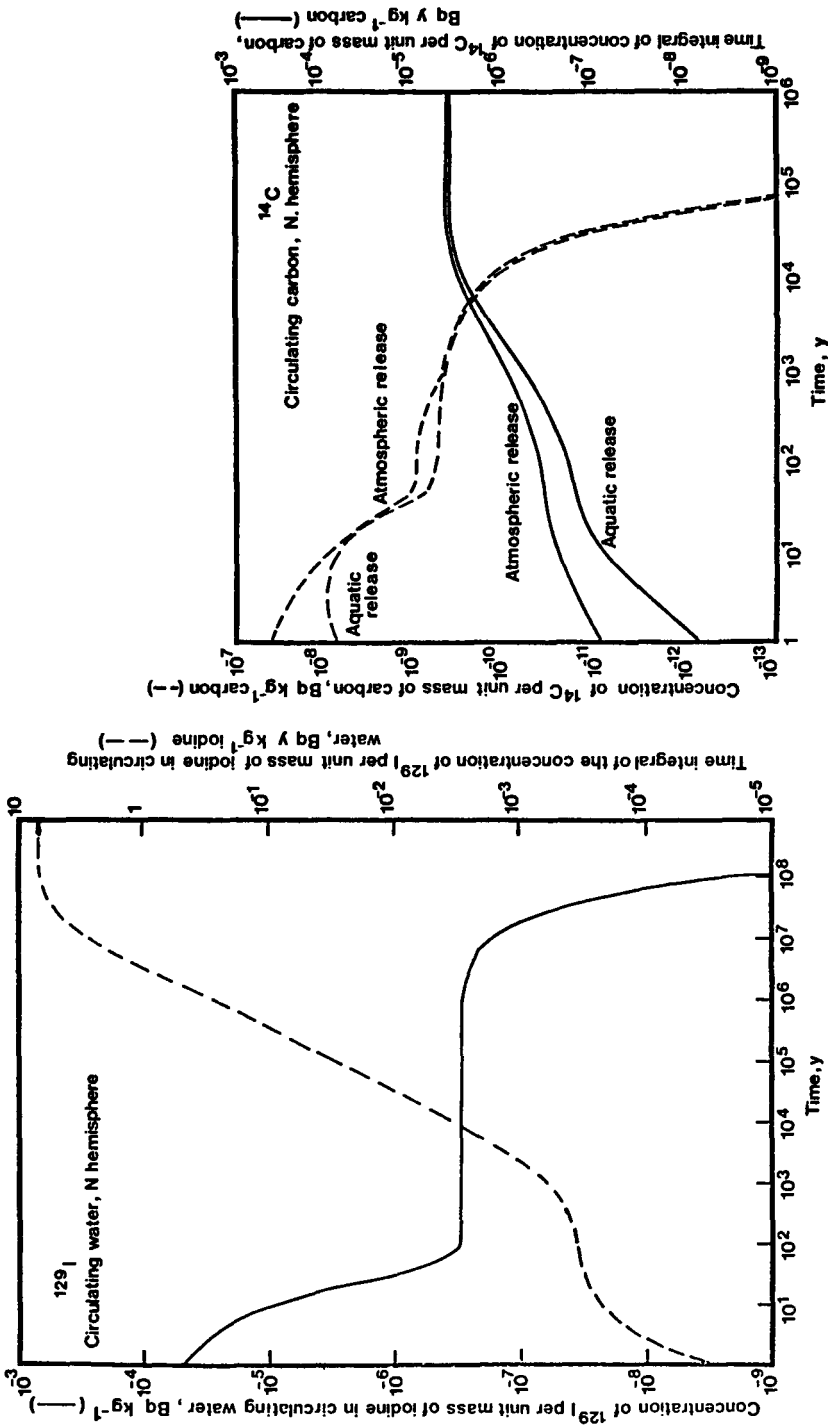


Figure 5.5 The time variation and time integrals of environmental concentration of carbon-14 and iodine-129

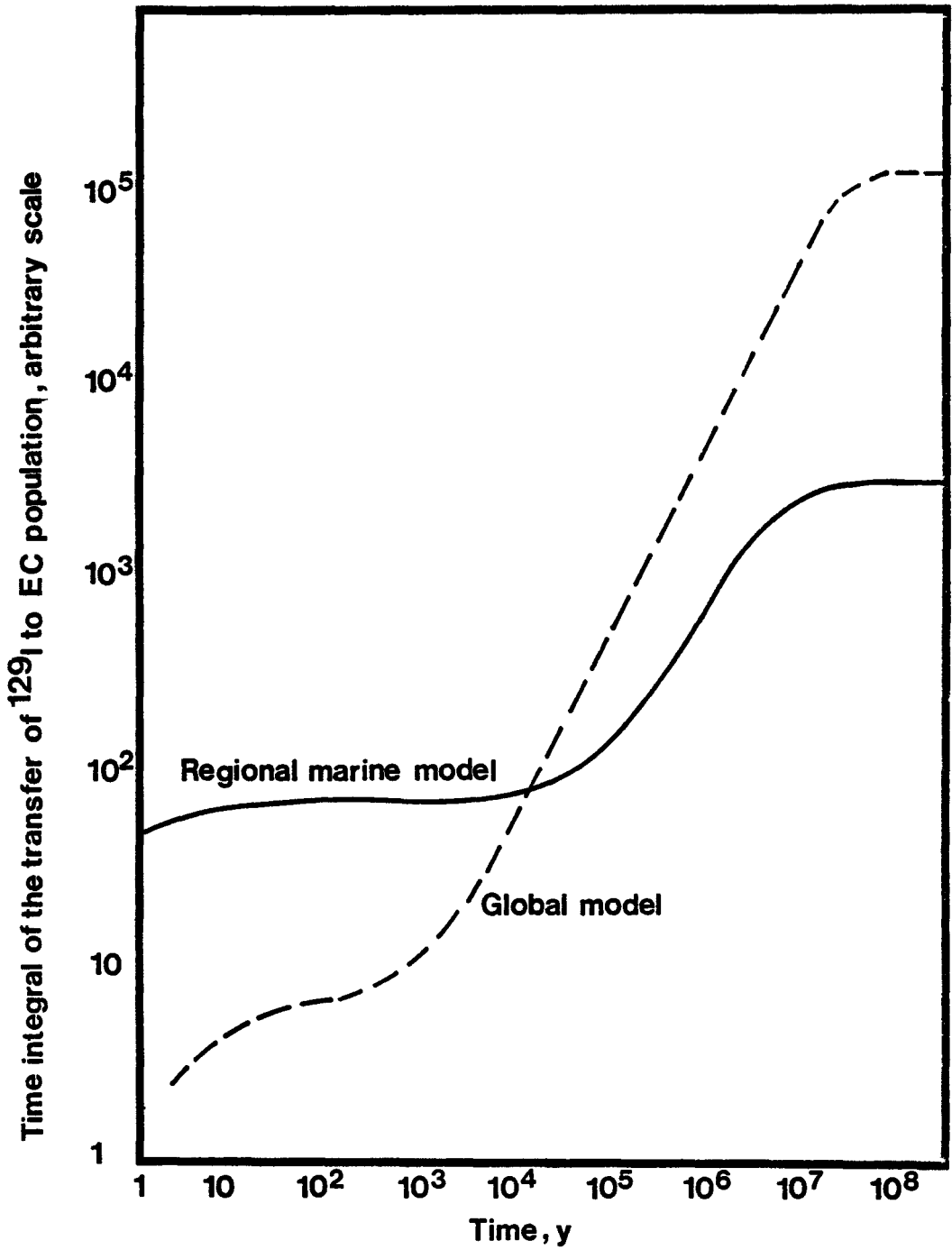


Figure 5.6 The predicted transfer of iodine-129 to the EC population using the regional marine and global models

CHAPTER 6

DOSIMETRIC MODELS

The models used to evaluate the external irradiation of man from the discharge of radionuclides to the atmospheric and to the aquatic environment have been described in Chapters 3 and 4 respectively. In those Chapters the estimation of exposure by internal irradiation was taken only as far as the quantity of activity inhaled or ingested. The irradiation of the body and its various organs from incorporated radionuclides can be evaluated as the product of these intakes and the doses per unit intake for each intake route. The models adopted to determine the dose equivalents per unit intake by inhalation or ingestion of the nuclides of concern are briefly described below. The procedures and data adopted are those described by Adams et al [6.1] which may be consulted for further detail.

6.1 Estimation of dose equivalent in the body from unit intakes of radionuclides by ingestion or inhalation

6.1.1 Introduction

As radioactive material progresses through the body, organs are irradiated both from the radiations resulting from transformations occurring in the organ itself and from those occurring in surrounding organs. Irradiated organs are referred to as target organs and those in which transformations occur are referred to as source organs.

There are four main steps necessary to estimate the dose equivalents delivered in any organ from a given nuclide in a given period of time.

- (i) The computation of the number of nuclear transformations of the inhaled (or ingested) radionuclide in each of the source organs, i.e. those through which the radioactive material passes. A similar computation is necessary for any radioactive daughters formed following intake of the parent nuclide.
- (ii) The preparation of matrices (one for each radionuclide involved) containing the absorbed doses received by the target organs per transformation in the source organs.
- (iii) The conversion of the absorbed doses in the matrices evaluated in (ii) to dose equivalents; quality factors of 1 and 20 are used for low (β, γ) and high (α) LET radiations respectively.
- (iv) The combination of (i) and (iii) to obtain the dose equivalent in each target organ from the inhaled (or ingested) parent and any daughter radionuclides.

Approximately 30 organs are considered as source and/or target organs. In addition to the estimation of dose equivalents in organs the effective dose equivalent is also calculated according to the procedure described in ICRP 26 [6.2] and detailed in Chapter 2.

6.1.2 Procedure adopted

A linear compartment model is used to describe the transport of material from the lung and GI tract to body fluids. The lung is represented by the model of the ICRP Task Group on Lung Dynamics [6.3] and the GI tract by the model of Eve [6.4]. These two models are illustrated in Figures 6.1 and 6.2 respectively, together with the value of the non-element dependent parameters adopted in the models. In the lung model values are given for the three inhalation classes D, W and Y which have clearance times of the order of days, weeks and years, respectively. For ingested material the fraction of each element reaching body fluids is determined by the gut transfer fraction, whilst for inhaled materials it is mainly the inhalation class of the compound and to a lesser extent the gut transfer fraction which is important. The fraction of each element transferred from body fluids to each organ is summarised in Table 6.1 and the retention of the element in these organs is determined by the retention parameters given in Table 6.2.

The number of transformations in a source organ is evaluated from the distribution of each nuclide among the various organs and their retention. Non-penetrating radiations (α, β) emitted in the transformations are assumed to be absorbed in the source organ, apart from those transformations in bone. For bone two radiosensitive tissues, red bone marrow and endosteal cells, are considered. The fraction of the non-penetrating radiations absorbed by these tissues depends on the spatial distribution of transformations in mineral bone. The fraction of energy absorbed in these tissues is evaluated taking into account the relative proportion of transformations in cortical and trabecular bone (characterised by their low and high ratios of surface area to volume, respectively) and whether the nuclide is uniformly distributed throughout the bone volume or preferentially deposited on endosteal surfaces.

For penetrating radiation (γ) only a fraction of the energy emitted by transformation in the source organ is deposited in that organ and further fractions are deposited in other organs. Reference should be made to Adams et al [6.1] for the procedures adopted to determine the energy deposited in source and target organs for transformations in the various source organs leading to the emission of penetrating radiation.

Dose equivalents in each organ are derived from the absorbed doses in each organ using the appropriate quality factor for the radiation considered.

6.1.3 Committed dose equivalents per unit intake

The committed effective dose equivalent and committed dose equivalents in skin, thyroid, and gonads are summarised in Tables 6.3 and 6.4 for unit intake of each nuclide of interest by ingestion and inhalation respectively. The dose equivalent in gonads is taken as the mean of the dose equivalents in the testes and ovaries. The effective

* Within the framework of the CEC programme, "Plutonium Recycle in Light Water Reactors", a study was undertaken on the toxicity of plutonium, americium and curium, (Nenot, J.C. and Stather, J.W. The toxicity of plutonium, americium and curium. EUR 6157 (1979) (Pergamon, Oxford)). The metabolism proposed in that study for plutonium, americium and curium is in general consistent with that adopted in the models used here to calculate committed dose equivalents.

Doses are those given by Adams et al [6.1] and the dose equivalents in individual organs [6.5] are those evaluated by the same authors in the derivation of the effective dose equivalent. Committed dose equivalents are given in Table 6.3 for ingestion and in Table 6.4 for inhalation of the nuclides in various chemical forms or inhalation class respectively. For intake by ingestion gut transfer fractions are assumed for the chemical forms in which the isotopes have been assumed in the environment and are indicated in Table 6.3. The committed dose equivalents from unit intake by inhalation are given for various inhalation classes; the chemical forms of the nuclides associated with the respective inhalation classes are summarised in Table 6.5.

REFERENCES

- [6.1] Adams, N, Hunt, B W, and Reissland, J A, Annual Limits of Intake of Radionuclides for Workers. Harwell, National Radiological Protection Board, NRPB-R82 (1978), (London, HMSO).
- [6.2] ICRP, Recommendations of the International Commission on Radiological Protection. Oxford, Pergamon Press, ICRP Publication 26. Ann. ICRP, 1, no. 3 (1977).
- [6.3] ICRP Task Group on Lung Dynamics. Deposition and retention models for internal dosimetry of the human respiratory tract. Health Phys., 12, 173 (1966).
- [6.4] Eve, I S, A review of the physiology of the gastro-intestinal tract in relation to radiation doses from radioactive materials. Health Phys., 12, 131 (1966).
- [6.5] Reissland, J A, National Radiological Protection Board, Harwell, Private communication, (October, 1978).

Table 6.1 Fraction of material reaching body fluids that is transferred to source tissue

Element	Bone	Liver	Kidneys	Spleen	Testes	Ovaries	Thyroid	Rest of body
Chromium	0.05							0.65
Manganese	0.35	0.25						0.40
Iron		0.08		0.013				0.907
Cobalt		0.05						0.45
Zinc	0.2							0.8
Rubidium	0.25							0.75
Strontium	0.27 ^a							0.73
Yttrium	0.5	0.15						0.1
Zirconium	0.5							0.5
Niobium	0.15	0.3	0.05					0.5
Molybdenum	0.15	0.3	0.018	0.01	0.002		0.02	0.26
Techetium	0.71	0.08	0.01					0.89
Ruthenium								0.85
Silver		0.8						0.2
Antimony		0.14						0.56
Tellurium	0.25						0.3	0.25
Iodine								
Caesium								
Barium	0.6 ^b							1.0
Lanthanum	0.2	0.6		0.05				0.3
Cerium								0.15
Neptunium								
Plutonium								
Americium	0.45	0.45			0.00035	0.00011		
Curium								

Notes

a. 0.14 to cortical bone; 0.13 to trabecular bone b. 0.3 to cortical bone; 0.3 to trabecular bone

Table 6.2
Retention parameters

Element		A ₁	T ₁ (y)	A ₂	T ₂ (y)
Chromium	Bone	1.0	2.7	0.38	2.2 10 ⁻¹
	Rest	0.62	1.6 10 ⁻²		
Manganese	Bone	1.0	1.1 10 ⁻¹	0.6	1.1 10 ⁻¹
	Liver	0.4	1.1 10 ⁻²		
	Rest	0.5	1.1 10 ⁻²		
Iron		1.0	5.5		
Cobalt		0.6	1.6 10 ⁻²	0.2	1.6 10 ⁻¹
Zinc	Bone	1.0	1.1	0.7	1.1
	Rest	0.3	5.5 10 ⁻²		
Rubidium		1.0	1.1 10 ⁻¹		
Strontium	Trab.bone	0.43	1.4 10 ⁻²	0.06	4.7 10 ⁻¹
	Cort.bone	0.36	1.4 10 ⁻²	0.04	4.4 10 ⁻¹
	Rest	0.80	4.9 10 ⁻³	0.15	8.2 10 ⁻²
Yttrium		1.0	∞		
Zirconium	Bone	1.0	2.2 10 ¹		
	Rest	1.0	1.9 10 ⁻²		
Niobium		0.5	1.6 10 ⁻²	0.5	5.5 10 ⁻¹
Molybdenum		0.1	2.7 10 ⁻³	0.9	1.4 10 ⁻¹
Technetium		0.76	4.4 10 ⁻³	0.20	1.0 10 ⁻²
Ruthenium		0.41	2.2 10 ⁻²	0.35	9.6 10 ⁻²
Silver		0.1	9.6 10 ⁻³	0.9	1.4 10 ⁻¹
Antimony		1.0	5.5 10 ⁻²		
Tellurium	Bone	1.0	1.4 10 ¹		
	Rest	1.0	5.5 10 ⁻²		
Iodine	Thyroid	0.25	3.3 10 ⁻¹	0.75	4.9 10 ⁻¹
	Rest	0.11	3.3 10 ⁻²	0.11	4.7 10 ⁻¹
Caesium		0.1	5.5 10 ⁻³	0.9	3.0 10 ⁻¹
Barium	Trab.bone	0.83	5.5 10 ⁻⁵	0.1	9.6 10 ⁻³
	Cort.bone	0.83	5.5 10 ⁻⁵	0.1	9.6 10 ⁻³
	Rest	0.73	2.2 10 ⁻³	0.13	4.9 10 ⁻²
Lanthanum		1.0	9.6		
Cerium					
Neptunium					
Plutonium	Bone	1.0	1 10 ²		
Americium	Liver	1.0	4 10 ¹		
Curium	Gonads	1.0	∞		

Notes The fraction of an element retained in an organ to time, t, is given by $\sum_1 A_1 \exp[-0.693t/T_1]$

Table 6.2 cont.

Element		A ₃	T ₃ (y)	A ₄	T ₄ (y)
Chromium	Bone Rest				
Manganese	Bone Liver Rest				
Iron					
Cobalt		0.2	2.2		
Zinc	Bone Rest				
Rubidium					
Strontium	Trab.bone	0.16	2.5	0.35	6.8
	Cort.bone	0.21	3.0	0.39	2.4 10 ¹
	Rest	0.041	5.5 10 ⁻¹	0.003	4.4
Yttrium					
Zirconium	Bone Rest				
Niobium					
Molybdenum					
Technetium		0.04	6.0 10 ⁻²		
Ruthenium		0.24	2.7		
Silver					
Antimony					
Tellurium	Bone Rest				
Iodine	Thyroid Rest				
Caesium					
Barium	Trab.bone	0.016	1.1	0.047	3.8
	Cort.bone	0.03	2.7	0.047	1.5 10 ¹
	Rest	0.1	3.6 10 ⁻¹	0.017	2.7
Lanthanum					
Cerium					
Neptunium					
Plutonium	Bone				
Americium	Liver				
Curium	Gonads				

Table 6.3

Committed Dose Equivalents per unit
intake by ingestion (Sv per Bq)

Committed Dose Equivalent Sv per Bq						
Nuclide	Form	f_1 (c)	Effective	Gonad	Thyroid	Skin
H-3	H ₂ O	1.0E+00	1.7E-11	1.7E-11	1.7E-11	1.7E-11
C-14	Food(d)	1.0E+00	1.1E-09	1.1E-09	1.1E-09	1.1E-09
Cr-51	Trivalent	1.0E-02	4.0E-11	2.4E-11	4.0E-13	1.6E-12
Cr-51	Hexavalent	1.0E-01	4.0E-11	2.5E-11	3.5E-12	3.9E-12
Mn-54	All	1.0E-01	7.2E-10	5.5E-10	1.1E-10	1.6E-10
Fe-55	All	1.0E-01	1.6E-10	9.9E-11	9.9E-11	9.9E-11
Fe-59	All	1.0E-01	1.8E-09	1.2E-09	5.9E-10	5.1E-10
Co-58	(a)	5.0E-02	7.7E-10	5.8E-10	6.4E-11	8.5E-11
Co-58	(b)	3.0E-01	9.4E-10	7.5E-10	3.7E-10	2.8E-10
Co-60	(a)	5.0E-02	2.7E-09	2.1E-09	7.7E-10	6.9E-10
Co-60	(b)	3.0E-01	7.1E-09	6.3E-09	4.6E-09	3.5E-09
Zn-65	All	5.0E-01	3.9E-09	3.3E-09	3.1E-09	2.3E-09
Rb-86	All	1.0E+00	2.5E-09	2.1E-09	2.1E-09	2.0E-09
Sr-89	Titanate	1.0E-02	2.2E-09	8.2E-12	8.1E-12	8.2E-12
Sr-89	All others	3.0E-01	2.1E-09	2.4E-10	2.4E-10	2.4E-10
Sr-90	Titanate	1.0E-02	3.0E-09	4.4E-11	4.4E-11	4.4E-11
Sr-90	All others	3.0E-01	3.3E-08	1.3E-09	1.3E-09	1.3E-09
Y-90	All	1.0E-04	2.7E-09	1.3E-14	1.3E-14	1.3E-14
Y-91	All	1.0E-04	2.5E-09	1.6E-12	1.3E-13	2.4E-13
Zr-95	All	2.0E-03	9.6E-10	4.8E-10	7.9E-12	4.2E-11
Nb-95	All	1.0E-02	5.9E-10	4.2E-10	1.0E-11	4.4E-11
Mo-99	Sulphide	5.0E-02	1.2E-09	1.3E-10	1.0E-11	1.8E-11
Mo-99	All others	8.0E-01	8.5E-10	2.1E-10	1.7E-10	1.7E-10
Tc-99	All	8.0E-01	2.5E-10	6.6E-11	4.6E-09	6.6E-11
Ru-103	All	5.0E-02	7.3E-10	3.5E-10	6.2E-11	6.9E-11
Ru-106	All	5.0E-02	5.8E-09	1.6E-09	1.4E-09	1.4E-09
Ag-110M	All	5.0E-02	2.9E-09	1.7E-09	1.9E-10	3.8E-10
Sb-125	All	2.0E-01	8.1E-10	4.1E-10	1.7E-10	1.6E-10
Te-127M	All	2.0E-01	2.4E-09	1.0E-10	9.9E-11	9.8E-11
Te-129M	All	2.0E-01	2.6E-09	1.9E-10	1.6E-10	1.5E-10
Te-131M	All	2.0E-01	3.5E-09	3.0E-10	7.2E-08	7.1E-11
Te-132	All	2.0E-01	1.0E-09	2.5E-10	2.0E-08	1.7E-10
I-129	All	1.0E+00	9.9E-08	1.3E-10	3.3E-06	2.4E-10
I-131	All	1.0E+00	1.4E-08	3.4E-11	4.5E-07	7.6E-11
I-132	All	1.0E+00	1.4E-10	2.3E-11	3.4E-09	1.8E-11
I-133	All	1.0E+00	2.5E-09	3.6E-11	8.3E-08	3.7E-11
I-134	All	1.0E+00	5.1E-11	1.0E-11	5.8E-10	8.1E-12
I-135	All	1.0E+00	5.5E-10	3.6E-11	1.8E-08	3.0E-11
Cs-134	All	1.0E+00	2.0E-08	1.9E-08	1.8E-08	1.3E-08
Cs-136	All	1.0E+00	3.1E-09	2.8E-09	2.9E-09	2.0E-09
Cs-137	All	1.0E+00	1.4E-08	1.4E-08	1.3E-08	1.0E-08
Ce-141	All	3.0E-04	7.0E-10	9.1E-12	1.5E-13	3.1E-12
Ce-144	All	3.0E-04	5.3E-09	4.1E-11	5.1E-12	7.3E-12

CONT.

Table 6.3 cont.

Nuclide	Form	f_1 (c)	Effective	Gonad	Thyroid	Skin
Pm-147	All	1.0E-04	2.6E-10	4.4E-16	4.4E-16	4.4E-16
Eu-154	All	1.0E-04	1.9E-09	6.5E-10	9.7E-12	7.0E-11
Eu-155	All	1.0E-04	3.0E-10	5.0E-11	1.3E-13	2.4E-12
Pu-238	O, OH	1.0E-05	1.5E-08	2.3E-09	7.9E-14	7.9E-14
Pu-238	All others	1.0E-04	1.0E-07	2.3E-08	7.9E-13	7.9E-13
Pu-239	O, OH	1.0E-05	1.6E-08	2.6E-09	7.5E-14	7.5E-14
Pu-239	All others	1.0E-04	1.2E-07	2.6E-08	7.5E-13	7.5E-13
Pu-240	O, OH	1.0E-05	1.6E-08	2.6E-09	7.5E-14	7.5E-14
Pu-240	All others	1.0E-04	1.2E-07	2.6E-08	7.5E-13	7.5E-13
Pu-241	O, OH	1.0E-05	2.6E-10	5.7E-11	5.8E-18	5.8E-18
Pu-241	All others	1.0E-04	2.4E-09	5.7E-10	5.8E-17	5.8E-17
Pu-242	O, OH	1.0E-05	1.5E-08	2.5E-09	7.1E-14	7.1E-14
Pu-242	All others	1.0E-04	1.1E-07	2.5E-08	7.1E-13	7.1E-13
Np-239	All	1.0E-02	1.0E-09	8.0E-11	5.6E-13	5.2E-12
Am-241	All	5.0E-04	6.0E-07	1.4E-07	4.0E-12	4.0E-12
Cm-242	All	5.0E-04	1.8E-08	2.6E-09	4.4E-12	4.4E-12
Cm-244	All	5.0E-04	2.9E-07	6.6E-08	4.2E-12	4.2E-12

- (a) Applies to oxides, hydroxides and all other inorganic chromium compounds ingested in tracer quantities.
- (b) Applies to organic complexes and all other inorganic compounds of chromium, except oxides and hydroxides, in the presence of carrier material.
- (c) f_1 is the gut transfer fraction for the nuclide in the chemical form specified.
- (d) The form of ingested carbon is assumed typical of that in diet.

Table 6.4

Committed Dose Equivalents per unit intake by inhalation (Sv per Bq)

Committed Dose Equivalent Sv per Bq						
Nuclide	Inhalation Class(a)	f_1 (b)	Effective	Gonad	Thyroid	Skin
H-3	- { d e f g	-	9.8E-16	6.0E-17	6.0E-17	6.0E-17
H-3		-	1.7E-11	1.7E-11	1.7E-11	1.7E-11
C-14		-	1.1E-12	1.1E-12	1.1E-12	1.1E-12
C-14		-	8.9E-15	2.4E-15	2.4E-15	2.4E-15
C-14		-	9.6E-12	1.8E-12	8.6E-12	1.2E-12
Cr-51	Y	1.0E-01	7.2E-11	1.3E-11	9.8E-12	7.6E-12
Cr-51	D	1.0E-01	3.0E-11	2.2E-11	1.7E-11	1.3E-11
Mn-54	W	1.0E-01	1.7E-09	4.7E-10	7.3E-10	4.9E-10
Mn-54	D	1.0E-01	1.4E-09	7.5E-10	5.6E-10	6.2E-10
Fe-55	W	1.0E-01	3.2E-10	1.7E-10	1.7E-10	1.7E-10
Fe-55	D	1.0E-01	6.7E-10	4.8E-10	4.8E-10	4.8E-10
Fe-59	W	1.0E-01	2.8E-09	1.2E-09	1.1E-09	8.5E-10
Fe-59	D	1.0E-01	4.1E-09	3.3E-09	2.9E-09	2.2E-09
Co-58	Y	5.6E-02	1.9E-09	3.0E-10	9.1E-10	4.9E-10
Co-58	W	5.0E-02	1.2E-09	4.2E-10	5.7E-10	3.3E-10
Co-60	Y	5.0E-02	4.1E-08	3.3E-09	1.6E-08	1.0E-08
Co-60	W	5.0E-02	8.0E-09	3.3E-09	3.7E-09	2.6E-09
Zn-65	Y	5.0E-01	4.8E-09	1.9E-09	3.1E-09	1.9E-09
Zn-65	W	5.0E-01	3.4E-09	2.3E-09	2.6E-09	1.8E-09
Zn-65	D	5.0E-01	4.2E-09	3.5E-09	3.5E-09	2.5E-09
Rb-86	D	1.0E+00	1.7E-09	1.3E-09	1.3E-09	1.3E-09
Rb-88	D	1.0E+00	2.1E-11	1.3E-12	1.3E-12	1.4E-12
Rb-89	D	1.0E+00	9.7E-12	1.4E-12	1.9E-12	1.5E-12
Sr-89	Y	1.0E-02	9.5E-02	8.1E-12	8.2E-12	8.1E-12
Sr-89	D	3.0E-01	1.5E-09	4.2E-10	4.2E-10	4.2E-10
Sr-90	Y	1.0E-02	3.4E-07	2.4E-10	2.4E-10	2.4E-10
Sr-90	D	3.0E-01	5.7E-08	2.3E-09	2.3E-09	2.3E-09
Y-90	Y	1.0E-04	2.2E-09	5.2E-13	5.2E-13	5.2E-13
Y-90	W	1.0E-04	2.0E-09	9.5E-12	9.5E-12	9.5E-12
Y-91	Y	1.0E-04	1.2E-08	7.1E-12	8.3E-12	7.3E-12
Y-91	W	1.0E-04	7.9E-09	1.1E-10	1.1E-10	1.1E-10
Zr-95	Y	2.0E-03	4.9E-09	3.4E-10	1.2E-09	6.3E-10
Zr-95	W	2.0E-03	3.6E-09	5.8E-10	7.6E-10	5.8E-10
Zr-95	D	2.0E-03	5.3E-09	1.5E-09	1.4E-09	1.5E-09
Nb-95	Y	1.0E-02	1.2E-09	2.4E-10	3.7E-10	2.1E-10
Nb-95	W	1.0E-02	8.8E-10	3.5E-10	3.1E-10	2.1E-10
Mo-99	Y	5.0E-02	1.0E-09	5.9E-11	1.6E-11	1.4E-11
Mo-99	D	8.0E-01	5.5E-10	1.3E-10	1.2E-10	1.2E-10
Tc-99	W	8.0E-01	2.0E-09	4.4E-11	3.0E-09	4.4E-11
Tc-99	D	8.0E-01	1.7E-10	5.0E-11	3.5E-09	5.0E-11
Tc-99M	W	8.0E-01	2.0E-12	4.5E-13	2.4E-12	3.4E-13
Tc-99M	D	8.0E-01	3.4E-12	1.1E-12	6.3E-12	6.3E-13
Rh-103M	Y	5.0E-02	1.1E-12	2.0E-15	1.9E-15	1.9E-15
Rh-103M	W	5.0E-02	1.0E-12	2.4E-14	2.4E-14	2.4E-14
Rh-103M	D	5.0E-02	1.2E-12	8.4E-14	8.3E-13	8.2E-12
Ru-103	Y	5.0E-02	2.0E-09	1.9E-10	2.7E-10	1.7E-10

CONT.

Table 6.4 cont.

Nuclide	Inhalation Class(a)	f_1 (b)	Effective	Gonad	Thyroid	Skin
Ru-103	W	5.0E-02	1.3E-09	3.0E-10	2.8E-10	2.0E-10
Ru-103	D	5.0E-02	8.0E-10	7.2E-10	5.9E-10	4.6E-10
Ru-106	Y	5.0E-02	1.3E-07	1.2E-09	1.7E-09	1.4E-09
Ru-106	W	5.0E-02	2.5E-08	4.0E-09	4.0E-09	3.9E-09
Ru-106	D	5.0E-02	1.5E-08	1.4E-08	1.4E-08	1.3E-08
Sb-124	W	2.0E-01	5.6E-09	8.5E-10	9.9E-10	7.8E-10
Sb-124	D	2.0E-01	2.4E-09	1.5E-09	1.2E-09	1.1E-09
Sb-125	W	2.0E-01	2.7E-09	3.4E-10	4.7E-10	3.2E-10
Sb-125	D	2.0E-01	8.0E-10	5.2E-10	4.4E-10	3.7E-10
Te-125M	W	2.0E-01	1.8E-09	6.7E-11	4.1E-11	4.4E-11
Te-125M	D	2.0E-01	1.3E-09	1.2E-10	1.0E-10	9.7E-11
Te-127	W	2.0E-01	8.2E-11	2.0E-12	2.0E-12	1.9E-12
Te-127	D	2.0E-01	6.3E-11	6.9E-12	6.8E-12	6.8E-12
Te-127M	W	2.0E-01	5.8E-09	9.9E-11	1.0E-10	9.9E-11
Te-127M	D	2.0E-01	3.6E-09	2.5E-10	2.5E-10	2.5E-10
Te-129	W	2.0E-01	1.8E-11	4.8E-13	5.1E-13	4.8E-13
Te-129	D	2.0E-01	2.1E-11	1.7E-12	1.6E-12	1.6E-12
Te-129M	W	2.0E-01	5.5E-09	1.5E-10	1.6E-10	1.5E-10
Te-129M	D	2.0E-01	2.2E-09	4.0E-10	3.9E-10	3.8E-10
Te-131M	W	2.0E-01	2.1E-09	1.1E-11	3.5E-08	4.5E-11
Te-131M	D	2.0E-01	1.7E-09	1.9E-10	4.5E-08	9.8E-11
Te-132	W	2.0E-01	7.6E-10	1.5E-10	4.5E-08	8.7E-11
Te-132	D	2.0E-01	1.3E-09	3.1E-10	4.3E-09	2.3E-10
I-129	D	1.0E+00	6.3E-08	8.0E-11	2.1E-06	1.5E-10
I-131	D	1.0E+00	8.3E-09	2.1E-11	2.8E-07	4.9E-11
I-132	D	1.0E+00	8.0E-11	1.0E-11	1.5E-09	9.6E-12
I-133	D	1.0E+00	1.3E-09	2.0E-11	4.4E-08	2.2E-11
I-134	D	1.0E+00	3.0E-11	4.1E-12	2.7E-10	4.2E-12
I-135	D	1.0E+00	3.2E-10	1.7E-11	8.6E-09	1.7E-11
Cs-134	D	1.0E+00	1.3E-08	1.2E-08	1.1E-08	7.9E-09
Cs-135	D	1.0E+00	1.3E-09	1.2E-09	1.2E-09	1.2E-09
Cs-136	D	1.0E+00	2.0E-09	1.7E-09	1.8E-09	1.2E-09
Cs-137	D	1.0E+00	8.8E-09	8.8E-09	7.9E-09	6.6E-09
Cs-138	D	1.0E+00	2.3E-11	3.2E-12	3.6E-12	3.1E-12
Ba-140	D	1.0E-01	9.4E-10	3.6E-10	2.7E-10	2.4E-10
La-140	Y	3.0E-01	1.3E-09	2.8E-10	5.4E-11	6.5E-11
La-140	W	3.0E-04	1.2E-09	2.6E-10	6.7E-11	7.6E-11
Ce-141	Y	3.0E-04	2.2E-09	3.1E-11	2.8E-11	1.7E-11
Ce-141	W	3.0E-04	1.9E-09	5.9E-11	4.7E-11	4.3E-11
Ce-144	Y	3.0E-04	9.5E-08	2.1E-10	2.9E-10	2.6E-10
Ce-144	W	3.0E-04	5.3E-08	1.9E-09	1.9E-09	1.9E-09
Pm-147	Y	1.0E-04	9.3E-09	1.0E-13	1.0E-13	1.0E-13
Pm-147	W	1.0E-04	6.9E-09	5.2E-13	5.2E-13	5.2E-13
Eu-154	Y	1.0E-04	1.1E-07	5.7E-09	1.5E-08	1.1E-08
Eu-154	W	1.0E-04	8.2E-08	1.3E-08	7.4E-09	1.5E-08
Eu-155	Y	1.0E-04	8.3E-09	5.7E-11	2.2E-10	1.5E-10
Eu-155	W	1.0E-04	5.9E-09	1.5E-10	1.3E-10	1.7E-10
Np-239	W	1.0E-02	7.6E-10	5.1E-11	6.9E-12	7.4E-12
Pu-238	Y	1.0E-05	8.2E-05	1.0E-05	3.8E-10	3.8E-10
Pu-238	W	1.0E-04	1.2E-04	2.8E-05	9.5E-10	9.5E-10

CONT.

Table 6.4 cont.

Nuclide	Inhalation Class(a)	f_1 (b)	Effective	Gonad	Thyroid	Skin
Pu-239	Y	1.0E-05	9.0E-05	1.2E-05	3.7E-10	3.7E-10
Pu-239	W	1.0E-04	1.4E-04	3.2E-05	9.0E-10	9.0E-10
Pu-240	Y	1.0E-05	8.9E-05	1.2E-05	3.7E-10	3.7E-10
Pu-240	W	1.0E-04	1.4E-04	3.2E-05	9.0E-10	9.0E-10
Pu-241	Y	1.0E-05	1.6E-06	2.8E-07	2.4E-12	2.4E-12
Pu-241	W	1.0E-04	2.9E-06	6.8E-07	2.2E-13	2.2E-13
Pu-242	Y	1.0E-05	8.5E-05	1.1E-05	3.6E-10	3.6E-10
Pu-242	W	1.0E-04	1.3E-04	3.0E-05	8.5E-10	8.5E-10
Am-241	W	5.0E-04	1.4E-04	3.3E-05	9.6E-10	9.6E-10
Cm-242	W	5.0E-04	4.7E-06	5.7E-07	9.4E-10	9.4E-10
Cm-244	W	5.0E-04	7.0E-05	1.6E-05	1.0E-09	1.0E-09

- (a) The forms of the various nuclides associated with the respective inhalation classes are summarised in Table 6.5.
- (b) f_1 is the gut transfer fraction for the nuclide in the chemical form considered.
- (c) For H-3 inhaled as element.
- (d) For H-3 inhaled as tritiated water.
- (e) For C-14 inhaled as CO₂.
- (f) For C-14 inhaled as CH₄.
- (g) For C-14 inhaled as CO.

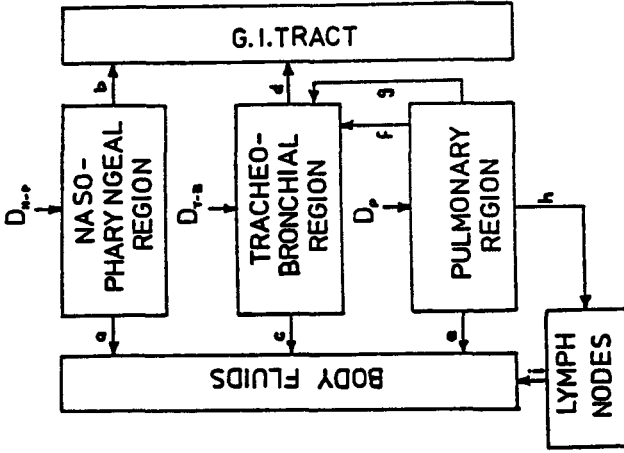
Table 6.5

Inhalation class of the elements in various forms

Element	Inhalation Class		
	D	W	Y
Rb	All		
Sr	All others		Titanate
Y		All others	Oxide Hydroxide
Zr	All others	Oxide Hydroxide Halide Nitrate	Carbide
Nb		All others	Oxide Hydroxide
Mo	All others		Element Sulphide Oxide Hydroxide
Tc	All others	Oxide Hydroxide Halide Nitrate	
Ru	All others	Halide	Oxide Hydroxide
Sb	All others	Oxide Sulphide Hydroxide Halide Nitrate Sulphates Carbonates	
Te	All others	Oxide Hydroxide Nitrates	
I	All		
Cs	All		
Ba	All		
La) Ce)		All others	Oxide Hydroxide Fluoride
Np		All	
Pu		All others	Dioxide
Am		All	
Cm		All	

Region	Pathway	Class							
		D		W		Y			
		T	F	T	F	T	F	T	F
N - P ($D_{N-P} = 0.30$)	a	0.01	0.5	0.01	0.1	0.01	0.1	0.01	0.01
	b	0.01	0.5	0.40	0.9	0.40	0.9	0.40	0.99
T - B ($D_{T-B} = 0.08$)	c	0.01	0.95	0.01	0.5	0.01	0.5	0.01	0.01
	d	0.2	0.05	0.2	0.5	0.2	0.5	0.2	0.99
P ($D_P = 0.25$)	e	0.5	0.8	50	0.15	500	0.05	500	0.05
	f			1.0	0.4	1.0	0.4	1.0	0.4
	g			50	0.4	500	0.4	500	0.4
	h	0.5	0.2	50	0.05	500	0.15	500	0.15
L		0.5	1.0	50	1.0	1000	0.9	1000	0.9
		-	0.0	-	0.0	∞	0.1	∞	0.1

a) Parameters for lung clearance model

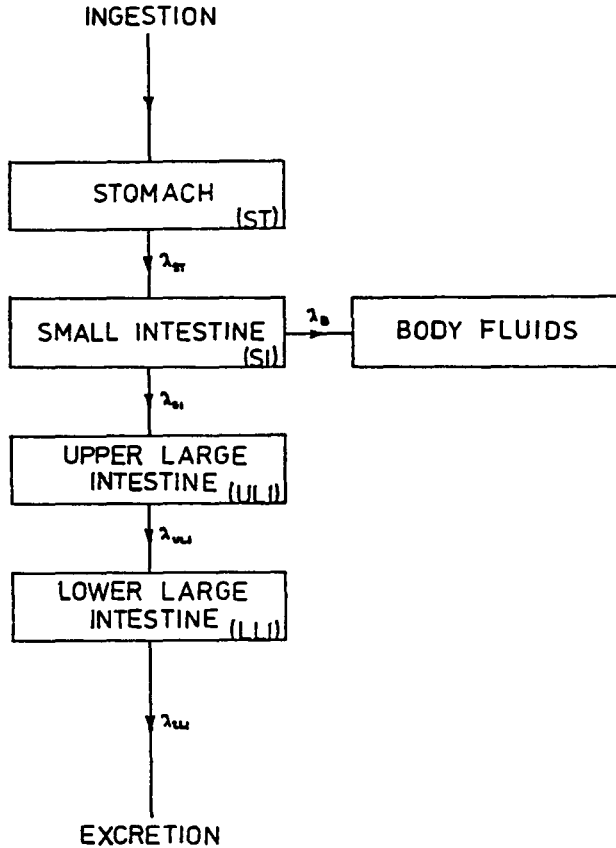


b) Lung clearance model

Figure 6.1 The lung clearance model and values of parameters used in the model.

The removal half-times (T) and compartmental fractions (F) are given for each inhalation class (D, W and Y). The regional depositions D_{N-P} , D_{T-B} and D_P are for an aerosol with AMAD = 1 μ m. Half-times in the table are given in days.

a) Gastrointestinal tract model



b) Values of parameters used in the model

Section of GI tract	Mass of contents (g)	Mean residence time (days)	λ days ⁻¹
Stomach (ST)	250	1/24	24
Small intestine (SI)	400	4/24	6
Upper large intestine (ULI)	220	13/24	1.8
Lower large intestine (LLI)	135	24/24	1

Figure 6.2 The model for the gastrointestinal tract and values of non-element dependent parameters used in the model

CHAPTER 7

APPLICATION OF THE METHODOLOGY TO ESTIMATE COLLECTIVE
AND INDIVIDUAL DOSES

7.1 Introduction

The manner in which the models, described in earlier chapters, can be applied to estimate collective and individual doses is illustrated by means of examples in this chapter.

This study is principally directed towards the evaluation of the health detriment to the population of the European Community following the discharge of effluents to the atmosphere or to the aquatic environment; the appropriate dosimetric quantity for this purpose is the collective dose equivalent commitment (or truncated values of this quantity) resulting from each pathway of exposure. The methodology can equally be applied to the estimation of individual dose equivalents. Additional detailed information is however often required of the habits of the individual if reliable estimates are to be made of such doses; this is contrary to the assessment of collective doses where average habits of the exposed population are in general sufficient.

The examples chosen to demonstrate the application of the methodology have been chosen arbitrarily. The numerical results presented are solely illustrative and must not therefore be considered as having any absolute significance.

7.2 Estimation of doses from atmospheric discharges

7.2.1 General procedure

The estimation of the collective dose equivalent commitment in an exposed population comprises the integration over time and space of the individual dose equivalent rates in that population. In its most general form the collective dose equivalent commitment can be written as

$$\int_d \int_\theta \int_t N(d, \theta, t) \dot{H}(d, \theta, t) dd d\theta dt \dots\dots\dots(7.1)$$

where $N(d, \theta, t)$ is the population at time, t , at a distance, d , and angle, θ , relative to the point of discharge

$\dot{H}(d, \theta, t)$ is the individual dose equivalent rate at d, θ , and t .

Several important modes of irradiation need to be considered in assessing the dose equivalent rate at any particular location following the discharge of radioactive material to the atmosphere; these comprise:

- a) external irradiation (β, γ) from the cloud
- b) inhalation of the cloud
- c) external irradiation (β, γ) from deposited activity
- d) inhalation of resuspended activity
- e) ingestion of contaminated foodstuffs

The irradiation of man by pathways a) - d) is essentially determined by the level of environmental contamination local to the individual, be it the

airborne, or the soil, concentration. Thus the spatial and temporal distributions of the population and activity (and hence dose) can readily be combined in the manner indicated in Equation (7.1) to yield the collective dose equivalent commitments via these pathways of exposure. For irradiation by ingestion of contaminated foodstuffs the same approach cannot be adopted since in general the contamination level local to the individual has in this case only a limited influence in determining the magnitude of exposure; this is a consequence of much of man's diet being obtained far from his local habitat. An alternative procedure is therefore adopted in the estimation of collective dose equivalent commitments via this route. The spatial and temporal distributions of agricultural production are combined with similar distributions of the discharged activity in various foodstuffs to evaluate the total quantity of activity appearing in the diet of the exposed population; the collective effective dose equivalent commitment is then evaluated from knowledge of the dose per unit intake by ingestion of the nuclide of interest. This procedure provides a satisfactory method for estimating the collective dose equivalent commitment but provides no information (other than temporal) on the distribution of the dose among the exposed population. Such information if necessary could be obtained but would necessitate a complex analysis of food distribution practices on a national and possibly international scale. For pathways a) - d) the distribution of the collective dose among the population is on the contrary readily discernible. The general procedures adopted in the estimation of collective dose equivalent commitments via pathways a) - d) and via pathway e) are outlined separately in the following sections.

7.2.1.1 Inhalation and external irradiation pathways (a - d)

To facilitate the numerical evaluation of the collective dose equivalent commitment as represented by equation (7.1) a number of approximations are made; these include a simplified representation of the population and of activity concentrations in various parts of the environment (and hence dose), and adjustments to accommodate the available dosimetric quantities (see Chapter 2). The more important approximations are described.

The spatial distributions of the population and of the radioactive material in various parts of the environment will, in reality, be continuously varying functions of distance, d , and angle θ , relative to the discharge point. These variations have been approximated in the manner indicated in Figure 7.1. The area surrounding the discharge point is divided into a number of annuli of varying radii; these annuli are further subdivided into a number of sectors of width $\Delta \theta$ (see Section 3.4.) If the annular segments are chosen such that the variation in the population density and the activity concentrations in various environmental materials (and hence dose) over the whole segment is small the collective dose equivalent commitment in any segment (d_j, θ_{jj}) can be evaluated as

$$\int_t N(d_j, \theta_{jj}, t) \dot{H}(d_j, \theta_{jj}, t) dt \dots\dots\dots(7.2)$$

where $N(d_j, \theta_{jj}, t)$ is the population in the annular segment (d_j, θ_{jj})

$\dot{H}(d_j, \theta_{jj}, t)$ is the mean dose equivalent rate in the segment (d_j, θ_{jj}) and in general taken as that at the mid point of the segment (\bar{d}_j, θ_{jj})

The spatial component of the integration of the total collective dose equivalent commitment specified in equation (7.1) can thus be reduced to a

summation over the various annular segments. The collective dose equivalent commitment becomes

$$\sum_{(d_j, \theta_{jj})} \int_t N(d_j, \theta_{jj}, t) \dot{H}(d_j, \theta_{jj}, t) dt \dots\dots\dots(7.3)$$

For the purpose of this study it is assumed that the spatial distribution and magnitude of the population remains constant over all time. Equation (7.3) reduces therefore to

$$\sum_{(d_j, \theta_{jj})} N(d, \theta_{jj}) \int_t \dot{H}(d_j, \theta_{jj}, t) dt \dots\dots\dots(7.4)$$

The selection of annular segments is a compromise between minimising computational effort, the availability of appropriate site-specific meteorological data and ensuring that any error introduced into the estimation of the collective dose equivalent commitment on account of the approximations is not significant in comparison with other uncertainties in the overall assessment. The number of sectors depends on the nature and categorisation of the meteorological data available for the discharge location in this report; the number of sectors is either 12 or 18 corresponding to angular width of 30° or 20° respectively. The radii of the annuli adopted in this study are summarised in Table 7.1; they were chosen such that the percentage uncertainty in estimating the collective dose equivalent commitment in each annular segment was comparable. An accurate estimate of the uncertainty in the collective dose equivalent commitment summed over all annular segments is difficult since much depends on the particular population distribution considered; it is considered most unlikely however that an error greater than 20% would ensue from the adoption of this approximate procedure.

A number of points are worthy of note regarding the evaluation of the time integral of the dose equivalent rate and in particular the approximations adopted in order to accommodate available dosimetric quantities. These approximations are reviewed comprehensively in Chapter 2 and are only briefly summarised here; also the detailed procedure adopted in deriving the time integrals of dose equivalent rate are described fully in Chapter 3. For external irradiation from the cloud or from deposited activity the evaluation of the time integral of the dose equivalent rate at a particular location is relatively straight forward. For irradiation from inhaled activity (either from the cloud or from resuspension) the situation is more complex since published data are not available on the variation of the dose equivalent rate following inhalation of activity; moreover account should be taken of the age distribution of the population at exposure. The time integral of the dose equivalent rate can however be conservatively estimated using the committed dose equivalent per unit intake of activity (see Chapter 2 for details) and this procedure is adopted here. For irradiation by inhalation the collective dose equivalent commitment is evaluated as follows using a modified form of equation 7.4.

$$\sum_{(d_j, \theta_{jj})} N(d_j, \theta_{jj}) H_{inh}(i) \int_t \dot{I}(d_j, \theta_{jj}, t) dt \dots\dots\dots(7.5)$$

$$\text{where } \int_t \dot{H}(d_j, \theta_{jj}, t) dt \simeq H_{inh}(i) \int_t \dot{I}(d_j, \theta_{jj}, t) dt \dots\dots\dots(7.6)$$

and $H_{inh}(i)$ is the committed dose equivalent per unit intake of nuclide, i , by inhalation

$\dot{I}(d_j, \theta_{jj}, t)$ is the average individual rate of intake of activity by inhalation in segment (d_j, θ_{jj})

The approximation in equation 7.6 leads to an overestimate in the collective dose equivalent commitments but only for nuclides of long retention time in the body, and even then by not more than a few tens of percent for a population of typical age distribution.

Thus the estimation of collective dose equivalent commitments from the respective pathways of exposure comprises a summation over all annular segments of the product of the population in and time integral of the appropriate dose equivalent rate at the mid-point of the segment (d_j, θ_{jj}) . Collective dose equivalent commitments, or their truncated values, can be evaluated by appropriate choice of the integration period.

7.2.1.2 Irradiation by the ingestion pathway (e)

As discussed earlier the estimation of collective dose equivalent commitments from ingestion of contaminated food products must be evaluated in a different manner. The basis of the estimate is the evaluation of the quantity of activity appearing in agricultural produce which is then assumed to be ingested by the population of the European Community.

In its most general form the collective dose equivalent commitment can be expressed as

$$H_{ing}(i) \sum_k \int_d \int_\theta \int_t PA(d, \theta, t, k) CK(i, d, \theta, t, k) dd d\theta dt \dots\dots\dots(7.7)$$

where $H_{ing}(i)$ is the committed dose equivalent per unit intake of nuclide, i , by ingestion

$PA(d, \theta, t, k)$ is the yield of agricultural product, k , at time, t , at a distance d and angle θ relative to the discharge

$CK(i, d, \theta, t, k)$ is the concentration of nuclide, i , in agricultural product, k , at time, t

The yield and concentration of activity in the various food products will be continuously varying functions of distance d , and angle, θ , relative to the discharge. To facilitate the integration in equation (7.7) these variations have been approximated in the same manner as described for the population distribution in the previous section (see Figure 7.1), that is the creation of annular segments over which the yield and concentration of activity are essentially assumed uniform. The selection of annular segments is identical with that previously described.

The collective dose equivalent commitment from food products can then be expressed as a summation over the annular segments, (d_j, θ_{jj})

$$H_{ing}^{(i)} \sum_k \sum_{(d_j, \theta_{jj})} \int_t PA(d_j, \theta_{jj}, t, k) CK(i, d, \theta_{jj}, t, k) dt \dots\dots\dots(7.8)$$

For the purposes of this study the agricultural practice and yields are assumed constant over all time. Equation (7.8) can therefore be reduced to

$$H_{ing}^{(i)} \sum_k \sum_{(d_j, \theta_{jj})} PA(d_j, \theta_{jj}, k) \int_t CK(i, d, \theta_{jj}, t, k) dt \dots\dots\dots(7.9)$$

The use of the quantity "committed dose equivalent" per unit intake by ingestion in equation (7.9) results in a conservative estimate of the collective dose equivalent commitment for nuclides with long retention times in the body. The reasons for its use are outlined in the previous section where the committed dose equivalent for inhaled activity had to be adopted.

Thus the estimation of the collective dose equivalent commitment from ingestion of each of the food products involves a summation over all annular segments of the product of the yield and time integral of the activity concentration of each foodstuff at the mid point, d_j , of each segment (d_j, θ_{jj}) . This procedure provides no insight into how the collective dose equivalent commitment is distributed in the exposed population; it does however provide information on the spatial distribution of the origin of this dose.

7.2.2 An example of the application of the methodology

To assist in the understanding of the procedures adopted to estimate collective dose equivalent commitments a worked example is presented. Consideration is given primarily to the estimation of the collective effective dose equivalent commitments; the procedure, however, is similar for the evaluation of truncated collective effective dose equivalent commitments after appropriate modification of the integration period and for collective dose equivalent commitments in particular tissues, again by appropriate substitution of the tissue for the effective dose equivalent.

For the purposes of the worked example the collective effective dose equivalent commitment is evaluated in a particular annular segment (d_j, θ_{jj}) for the release of caesium-137 at a rate of 1 Bq s^{-1} continuously for a year. The estimation of the total collective effective dose equivalent commitment from the discharge would necessitate a comparable evaluation for each of the annular segments followed by summation over all segments, but it is not undertaken in this illustrative example. The area surrounding the discharge point is subdivided into 12 sectors of angular width, 30° , in the manner indicated in Figure 7.1. The assumed frequencies with which the wind blows into the sector of interest, θ_{jj} , and in particular meteorological conditions is summarised in Table 7.2^j. The meteorological conditions have been categorised according to the Pasquill scheme (stability classes A-F); in addition categories C and D are considered in two modes in which

precipitation is or is not assumed to be occurring, thus making 8 categories in all. The radial bounds of the annulus are taken as 100 and 200 km, respectively. The population in the annular segment, (\bar{d}_j, θ_{jj}) , is taken as $8 \cdot 10^5$ and the agricultural yields of the products of interest are summarised in Table 7.3.

It must be noted that the values adopted for the various parameters which determine the environmental characteristics of the annular segment considered have been chosen arbitrarily and solely for illustrative purposes. The numerical results evaluated in this section have therefore no absolute significance. Equally no conclusions should be drawn as to the relative importance of the collective effective dose equivalent commitments evaluated for the respective modes of exposure; this would vary considerably with the characteristics of the environment considered (eg, relative magnitude of population and agricultural practice). Judgements on the relative importance of particular modes of exposure should therefore only be made on a case by case basis and after a complete assessment (ie, summation over all annular segments) of a particular discharge.

The evaluation of the collective effective dose equivalent commitment for each of the pathways is outlined.

7.2.2.1 Inhalation of the cloud

Irradiation from the inhalation of activity in the cloud depends on the concentration of activity near ground level. The annual average ground level concentration of nuclide, i , in the atmosphere in the annular segment (\bar{d}_j, θ_{jj}) can be written, from equation (3.25) as

$$C(i, \bar{d}_j, \theta_{jj}) = N Q_o(i) \sum_c X_o(i, c, \bar{d}_j) f(\theta_{jj}, c) \dots\dots\dots(7.10)$$

where N is the number of sectors and is taken as 12

$Q_o(i)$ is the discharge rate of nuclide, i , and is taken as 1 Bq s^{-1} of caesium-137

$X_o(i, c, \bar{d}_j)$ is the concentration in air at \bar{d}_j for unit release rate of caesium-137 in dispersion category, c , and assuming a uniform windrose (Bq m^{-3} per Bq s^{-1})

$f(\theta_{jj}, c)$ is the fraction of the time during which the dispersion category, c , occurs and the wind blows into the sector θ_{jj}

\bar{d}_j is the mid point of the annular segment (\bar{d}_j, θ_{jj}) and is taken as 150 km.

Values of $X_o(i, c, \bar{d}_j)$, evaluated using the models described in Chapter 3, and values assumed for $f(\theta_{jj}, c)$ are summarised in Table 7.2. Substituting these values into equation (7.10) the annual average air concentration in the annular segment (\bar{d}_j, θ_{jj}) is evaluated as $1.96 \cdot 10^{-10} \text{ Bq m}^{-3}$.

The time integral of the activity inhaled by an individual at (\bar{d}_j, θ_{jj}) is

$$I_{inh}(i, \bar{d}_j, \theta_{jj}) = C(i, \bar{d}_j, \theta_{jj}) B \dots\dots\dots(7.11)$$

where B is the annual volume of air inhaled by an adult and is taken to be $8030 \text{ m}^3 \text{ y}^{-1}$

Substituting for $C(i, d_j, \theta_{jj})$ and B in equation (7.11)

$$I_{inh}(i, \bar{d}_j, \theta_{jj}) = 1.96 \cdot 10^{-10} \cdot 8030 = 1.57 \cdot 10^{-6} \quad (\text{Bq})$$

The collective effective dose equivalent commitment in the annular segment (d_j, θ_{jj}) is then, from equation (7.5), given by

$$\begin{aligned} S_E^C(d_j, \theta_{jj}) &= N(d_j, \theta_{jj}) H_{inh}(i) \int_t \dot{I}(i, \bar{d}_j, \theta_{jj}) dt \\ &= N(d_j, \theta_{jj}) H_{inh}(i) I_{inh}(i, \bar{d}_j, \theta_{jj}) \\ &\dots\dots\dots(7.12) \end{aligned}$$

where $H_{inh}(i)$ is the committed effective dose equivalent from unit intake by inhalation of caesium-137 (see Chapter 6) and is equal to $8.8 \cdot 10^{-9} \text{ (Sv Bq}^{-1}\text{)}$.

Substituting for $N(d_j, \theta_{jj})$, $H_{inh}(i)$ and $I_{inh}(i, \bar{d}_j, \theta_{jj})$ in equation (7.12)

$$S_E^C(d_j, \theta_{jj}) = 8 \cdot 10^5 \cdot 8.8 \cdot 10^{-9} \cdot 1.57 \cdot 10^{-6} = 1.1 \cdot 10^{-8} \quad (\text{man Sv})$$

It should be noted that in this calculation it is assumed that the exposed population has been exposed to the same level of air concentration whether they are inside or outside buildings.

7.2.2.2 External irradiation from the cloud

Caesium-137, associated with its very short lived daughter product, barium-137m, is a β/γ emitter. Consideration is given to the evaluation of the collective effective dose equivalent commitment from the photon component and to the collective dose equivalent commitment in skin from the electron component.

Photon component

The average effective dose equivalent rate from cloud γ radiation from a nuclide, i, in the annular segment (d_j, θ_{jj}) can be written, from equation (3.30) as

$$\begin{aligned} \dot{H}_v(i, \bar{d}_j, \theta_{jj}) &= N Q_o(i) \sum_c HG(i, c, \bar{d}_j) f(\theta_{jj}, c) \quad (\text{Sv y}^{-1}) \\ &\dots\dots\dots(7.13) \end{aligned}$$

where $HG(i, c, \bar{d}_j)$ is the cloud γ effective dose equivalent rate for unit release rate (1 Bq s^{-1}) of caesium-137 in dispersion conditions, c, and assuming a uniform windrose and where the other symbols have the meaning as previously indicated

Values of $HG(i, c, \bar{d}_j)$, evaluated using the models described in Chapter 3, and values assumed for $f(\theta_{jj}, c)$ are summarised in Table 7.2. Substituting these values in equation (7.13) the average effective dose equivalent rate in the annular segment (\bar{d}_j, θ_{jj}) is $1.5 \cdot 10^{-16} \text{ Sv y}^{-1}$. For a discharge continuous at 1 Bq s^{-1} for a year the time integral of the average effective dose equivalent rate is $1.5 \cdot 10^{-16} \text{ Sv}$.

From equation (7.4) the collective effective dose equivalent commitment from external ν radiation from the cloud is

$$\begin{aligned} S_E^C(d_j, \theta_{jj}) &= N(d_j, \theta_{jj}) \int_t \dot{H}_\nu(i, \bar{d}_j, \theta_{jj}) dt \\ &= 8 \cdot 10^5 \cdot 1.5 \cdot 10^{-16} = 1.2 \cdot 10^{-10} \quad (\text{man Sv}) \end{aligned} \quad \dots\dots\dots(7.14)$$

This estimate makes no allowance for shielding of the exposed population by building structures; it will therefore be an overestimate of the actual collective effective dose equivalent commitment by a factor which will vary according to the habits of and type of building structure utilised by the population in question.

Electron component

The average dose equivalent rate in skin from cloud β irradiation from nuclide, i , in the annular segment (\bar{d}_j, θ_{jj}) can be written from equation (3.31) as

$$\begin{aligned} \dot{H}_\beta(i, \bar{d}_j, \theta_{jj}) &= N Q_o(i) \sum_c HB(i, c, \bar{d}_j) f(\theta_{jj}, c) \quad (\text{Sv y}^{-1}) \\ &\dots\dots\dots(7.15) \end{aligned}$$

where $HB(i, c, \bar{d}_j)$ is the cloud β dose equivalent rate in skin for unit release rate of caesium-137 (1 Bq s^{-1}) in dispersion category, c , and assuming a uniform windrose and where the other symbols have the meaning previously defined.

$$HB(i, c, \bar{d}_j) = HBT(i) X_o(i, c, \bar{d}_j) \quad \dots\dots\dots(7.16)$$

where $HBT(i)$ is the dose equivalent rate in skin per unit air concentration of nuclide, i , (Sv y^{-1} per Bq m^{-3}). For caesium-137 in equilibrium with its daughter product the value is $4.44 \cdot 10^{-7} \text{ Sv y}^{-1}$ per Bq m^{-3} .

Substituting for $HB(i, c, \bar{d}_j)$ from equation (7.16) into equation (7.15) and further substituting from equation (7.10) the expression for $H(i, \bar{d}_j, \theta_{jj})$ can be reduced to

$$H_\beta(i, \bar{d}_j, \theta_{jj}) = HBT(i) C(i, \bar{d}_j, \theta_{jj}) \quad \dots\dots\dots(7.17)$$

Substituting for HBT(i) and C(i, \bar{d}_j, θ_{jj}) in equation (7.17)

$$H_{\beta}(i, \bar{d}_j, \theta_{jj}) = 4.44 \cdot 10^{-7} \cdot 1.96 \cdot 10^{-10} = 8.7 \cdot 10^{-17} \quad (\text{Sv } y^{-1})$$

For a discharge continuous for 1 year the time integral of the average dose equivalent in skin is $8.7 \cdot 10^{-17}$ Sv.

From equation (7.4) the collective dose equivalent in skin in segment (d_j, θ_{jj}) from cloud β irradiation is

$$\begin{aligned} S_E^C(d_j, \theta_{jj}) &= N(d_j, \theta_{jj}) \int_t H_{\beta}(i, \bar{d}_j, \theta_{jj}) dt \\ &= 8 \cdot 10^5 \cdot 8.7 \cdot 10^{-17} = 7 \cdot 10^{-11} \quad (\text{man Sv}) \end{aligned}$$

The estimate assumes that the air concentration is identical inside and outside buildings and moreover assumes no shielding due to clothing or position of the body in relation to other structures which may provide further shielding; the value quoted is therefore an overestimate.

7.2.2.3 External radiation from deposited activity

As for external radiation from the cloud, consideration is given separately to photon and electron components from deposited activity.

Photon component

The time integral of the effective dose equivalent rate from photon irradiation in segment (d_j, θ_{jj}) from deposited activity can be written from equation 3.40 as

$$HD_{\nu}(i, \bar{d}_j, \theta_{jj}, t) = \omega(i, \bar{d}_j, \theta_{jj}) F_{\nu}(i, t) \quad (\text{Sv})$$

.....(7.18)

where $F_{\nu}(i, t)$ is the integral to time, t, of the effective dose equivalent rate received by a person continuously exposed to external ν radiation from radionuclide, i, deposited at a rate of $1 \text{ Bq m}^{-2} \text{ s}^{-1}$ continuously for 1 year on undisturbed pasture

and $\omega(i, \bar{d}_j, \theta_{jj})$ is the average deposition rate at \bar{d}_j, θ_{jj}

and is given from equation (3.29), as

$$\omega(i, \bar{d}_j, \theta_{jj}) = N Q_0(i) \sum_c G(i, c, \bar{d}_j) f(\theta_{jj}, c) \quad (\text{Bq m}^{-2} \text{ s}^{-1})$$

where $G(i, c, \bar{d}_j)$ is the deposition rate at \bar{d}_j in dispersion category, c, for unit discharge rate of nuclide, i, and assuming a uniform windrose.

The time integral of the effective dose equivalent rate for the continuous deposition of caesium-137 at a rate of $1 \text{ Bq m}^{-2} \text{ s}^{-1}$ for a year, $F_{\nu}(i, t)$ is given as a function of time in Table 3.23; the infinite time integral is

$1.6 \cdot 10^1$ Sv per Bq $m^{-2} s^{-1}$ for a year. Values of $G(i, c, \bar{d}_j)$, evaluated using the models in Chapter 3, and $f(\theta_{jj}, c)$ are summarised in Table 7.2. Substituting for the various parameters into equation (7.19) and then (7.18) the infinite time integral of the effective dose equivalent rate at \bar{d}_j, θ_{jj} is

$$HD_{\nu}(i, \bar{d}_j, \theta_{jj}, \infty) = 1.04 \cdot 10^{-12} \cdot 1.6 \cdot 10^1 = 1.7 \cdot 10^{-11} \quad (\text{Sv})$$

From equation (7.4) the collective effective dose equivalent commitment from ν radiation from deposited activity following a continuous release of caesium-137 at a rate of 1 Bq s^{-1} for 1 year is

$$\begin{aligned} S_E^C(d_j, \theta_{jj}) &= N(d_j, \theta_{jj}) \cdot HD_{\nu}(i, \bar{d}_j, \theta_{jj}, \infty) \\ &= 8 \cdot 10^5 \cdot 1.7 \cdot 10^{-11} = 1.4 \cdot 10^{-5} \quad (\text{man Sv}) \end{aligned}$$

The collective effective dose equivalent commitment evaluated above assumes the exposed population to be outdoors continuously. If the fraction of time spent outdoors is f_2 , and the ratio of the dose indoors to that outdoors is f_3 , then the collective effective dose equivalent commitment as evaluated as above for a population continuously outdoors must be reduced by the following factor

$$f_2 + (1 - f_2) f_3$$

Assuming the fraction of time spent outdoors to be 0.2 and the ratio of the dose indoors to that outdoors to be 0.2 [7.1] then the collective effective dose equivalent commitment becomes

$$1.4 \cdot 10^{-5} (0.2 + 0.8 \cdot 0.2) = 5.10^{-6} \quad (\text{man Sv})$$

Electron component

The time integral of the dose equivalent rate in skin from β irradiation from deposited activity can be expressed from equation 3.41 as

$$HD_{\beta}(i, \bar{d}_j, \theta_{jj}, t) = \omega(i, \bar{d}_j, \theta_{jj}) F_{\beta}(i, t) \quad (\text{Sv})$$

.....(7.20)

where $F_{\beta}(i, t)$ is the integral to time, t , of the dose equivalent rate in skin received by a person continuously exposed to external β radiation from radionuclide, i , deposited at a rate of $1 \text{ Bq m}^{-2} \text{ s}^{-1}$ continuously for 1 year on undisturbed pasture

$$\omega(i, \bar{d}_j, \theta_{jj}) \text{ is defined in equation (7.19)}$$

The infinite time integral of the dose equivalent rate in skin, $F_{\beta}(i, \infty)$, is $2.2 \cdot 10^{-8}$ Sv per $\text{Bq m}^{-2} \text{ s}^{-1}$ of caesium-137 for 1 y and substituting into equation (7.20)

$$HD_{\beta}(i, \bar{d}_j, \theta_{jj}, \infty) = 1.04 \cdot 10^{-12} \cdot 2.2 \cdot 10^{-8} = 2.3 \cdot 10^{-20} \quad (\text{Sv})$$

From equation (7.4) the collective dose equivalent commitment in skin from β irradiation from deposited activity following the continuous discharge of caesium-137 at a rate of 1 Bq s^{-1} for a year becomes:-

$$\begin{aligned} S_E^C(d_j, \theta_{jj}) &= N(d_j, \theta_{jj}) HD_{\beta}(i, \bar{d}_j, \theta_{jj}, \infty) \\ &= 8 \cdot 10^5 \cdot 2.3 \cdot 10^{-20} = 1.8 \cdot 10^{-14} \quad (\text{man Sv}) \end{aligned}$$

Again this value assumes the population to be continuously outdoors. Assuming as above that the fraction of time spent outdoors is 0.2 and that the dose indoors is zero owing to building structures affording essentially total shielding from β radiation the collective dose equivalent commitment in skin becomes

$$0.2 \cdot 1.8 \cdot 10^{-14} = 3.6 \cdot 10^{-15} \quad (\text{man Sv})$$

7.2.2.4 Inhalation of resuspended activity

The time integral of the individual inhalation rate of resuspended activity at \bar{d}_j, θ_{jj} can be written from equation (3.42) as

$$IRS(i, \bar{d}_j, \theta_{jj}, t) = \frac{1}{3.15 \cdot 10^7} \omega(i, \bar{d}_j, \theta_{jj}) I_R(i, t) B \quad (\text{Bq})$$

.....(7.21)

where $I_R(i, t)$ is the time integral of the resuspended air concentration following deposition of nuclide, i , at a rate of $1 \text{ Bq m}^{-2} \text{ s}^{-1}$ continuously for 1 year

and $\omega(i, \bar{d}_j, \theta_{jj})$ is as defined in equation (7.19)

The time integral of the resuspended air concentration following unit deposition of caesium-137 at a rate of $1 \text{ Bq m}^{-2} \text{ s}^{-1}$ for a year is illustrated in Figure 3.5; the infinite time integral is $2.2 \cdot 10^9 \text{ Bq s m}^{-3}$ per $\text{Bq m}^{-2} \text{ s}^{-1}$ for one year. The value of $\omega(i, \bar{d}_j, \theta_{jj})$ is a function of the frequency distribution of dispersion conditions assumed for the sector θ ; it is evaluated in Section 7.1.2.3 as $1.04 \cdot 10^{-12} \text{ Bq m}^{-2} \text{ s}^{-1}$ at \bar{d}_j for a discharge rate of 1 Bq s^{-1} of caesium-137.

Substituting into equation (7.21) the infinite time integral of the individual inhalation rate of resuspended activity at \bar{d}_j, θ_{jj} is

$$\begin{aligned} IRS(i, \bar{d}_j, \theta_{jj}, \infty) &= \frac{1.04 \cdot 10^{-12} \cdot 2.2 \cdot 10^9 \cdot 8030}{3.15 \cdot 10^7} \quad (\text{Bq}) \\ &= 5.8 \cdot 10^{-7} \quad (\text{Bq}) \end{aligned}$$

The collective effective dose equivalent commitment in the annular segment (\bar{d}_j, θ_{jj}) is then, from equation (7.5) given by

$$\begin{aligned}
 S_E^C(d_j, \theta_{jj}) &= N(d_j, \theta_{jj}) H_{inh}(i) \int_t I(i, d_j, \theta_{jj}) dt \\
 &= N(d_j, \theta_{jj}) H_{inh}(i) IRS(i, d_j, \theta_{jj}, \infty)
 \end{aligned}
 \dots\dots\dots(7.22)$$

where $H_{inh}(i)$ is the committed effective dose equivalent from unit intake by inhalation of caesium-137 (see Chapter 6) and is equal to $8.8 \cdot 10^{-9}$ Sv Bq⁻¹

Substituting in equation (7.22)

$$S_E^C(d_j, \theta_{jj}) = 8 \cdot 10^5 \cdot 8.8 \cdot 10^{-9} \cdot 5.8 \cdot 10^{-7} = 4.1 \cdot 10^{-9} \quad (\text{man Sv})$$

7.2.2.5 Ingestion of contamination foodstuffs

The time integral, from the beginning of the release to time t, of the quantity of nuclide, i, in foodstuff, k, derived from an annular segment d_j, θ_{jj} can be written from equation (3.44) as

$$CCP(i, d_j, \theta_{jj}, k, t) = \omega(i, \bar{d}_j, \theta_{jj}) CP(i, k, t) PA(d_j, \theta_{jj}, k) TD(i, k) \quad (\text{Bq})
 \dots\dots\dots(7.23)$$

where $CP(i, k, t)$ is the time integrated concentration of nuclide, i, in unit mass of foodstuff, k, following the deposition of nuclide, i, at a continuous rate of $1 \text{ Bq m}^{-2} \text{ s}^{-1}$ for 1 year

$PA(d_j, \theta_{jj}, k)$ is the annual yield of foodstuff, k, in the segment d_j, θ_{jj}

$TD(i, k) = \exp - \lambda_i \tau_k$ where λ_i is the radioactive decay constant and τ_k is the delay between harvest (or animal slaughter) and consumption

and $\omega(i, \bar{d}_j, \theta_{jj})$ is the deposition rate of nuclide, i, at d_j, θ_{jj} and is defined in equation (7.19)

The deposition rate, $\omega(i, \bar{d}_j, \theta_{jj})$ for unit discharge rate of caesium-137 is evaluated in section 7.1.2.3 for the frequency distribution of dispersion conditions given in Table 7.2 and which were selected to characterise the sector θ_{jj} ; the value of ω is estimated as $1.04 \cdot 10^{-12} \text{ Bq m}^{-2} \text{ s}^{-1}$ per Bq s^{-1} . The infinite time integrals of the concentration, $(CP(i, k, \infty))$ s of caesium-137 in unit mass of each foodstuff are summarised in Table 7.3 for a deposition rate of $1 \text{ Bq m}^{-2} \text{ s}^{-1}$ continuous for a year and were evaluated using the models described in Chapter 3. The assumed annual yields of each foodstuff in the sector (d_j, θ_{jj}) are also summarised in Table 7.3, together with the mean delay periods, τ_k , assumed between harvest of a crop (or slaughter of an animal) and consumption of the food product.

Substituting the various values in equation (7.23) and summing over the food products listed in Table 7.3 the infinite time integral for the quantity of caesium-137 in foodstuffs at the time of consumption obtained from the segment d_j, θ_{jj} is 79 Bq. The collective effective dose equivalent commitment from foodstuffs derived from the segment (d_j, θ_{jj}) can from equation (7.9) be written as

$$\begin{aligned}
 S_E^C(d_j, \theta_{jj}) &= H_{ing}(i) \sum_k PA(\bar{d}_j, \theta_{jj}, k) \int_0^{\infty} CK(i, \bar{d}_j, \theta_{jj}, t, k) dt \\
 &= H_{ing}(i) \sum_k CCP(i, \bar{d}_j, \theta_{jj}, k, \infty)
 \end{aligned}
 \dots\dots\dots(7.24)$$

The committed effective dose equivalent per unit intake of caesium-137 by ingestion is evaluated in Chapter 6 as $1.4 \cdot 10^{-8}$ Sv Bq⁻¹. Substituting in equation (7.24)

$$\begin{aligned}
 S_E^C(d_j, \theta_{jj}) &= 1.4 \cdot 10^{-8} \cdot 79 && (\text{man Sv}) \\
 &= 1.1 \cdot 10^{-6} && (\text{man Sv})
 \end{aligned}$$

It should finally be noted that the above collective effective dose equivalent commitment is not received by the population in the segment (d_j, θ_{jj}) but by the population consuming the food products derived from this segment.

7.2.2.6 Summary of the collective dose equivalent commitments from the atmospheric discharge of caesium-137

The collective effective dose equivalent commitments (and selected doses in skin) via the respective pathways are summarised in Table 7.4. The values refer to the doses delivered to the population in a single annular segment or to the doses resulting from foodstuffs derived from that segment. The environmental characteristics assumed for the segment were chosen arbitrarily and therefore the numerical results in Table 7.4 have no absolute or relative significance; the numerical values are particular to the assumptions made. The evaluation of the total collective effective dose equivalent commitment entails a comparable evaluation over each annular segment and summation over all segments.

It should finally be noted that the example presented took account only of doses arising during the first pass of activity after discharge. Some nuclides (eg, krypton-85, iodine-129, carbon-14 and tritium) because of their mobility and long half-lives may become globally dispersed and account must be taken of this additional contribution to the exposure of the population.

7.2.3 Indicative individual exposure

The methodology can equally be applied to the estimation of individual as well as collective exposure, although reliable estimates of the former require fairly detailed habits data. The procedures described in Sections 7.2.1 and 7.2.2 for the assessment of collective dose equivalent commitments from external irradiation and inhalation pathways have their origins in the estimation of individual dose rates at particular locations, for example in annular segments (\bar{d}_j, θ_{jj}) .

The estimates are however subject to the assumption of individuals with habits representative of the average in the population; this is sufficient for the estimation of collective doses.

The estimation of individual dose equivalents is particularly relevant in the context of comparisons with dose equivalent limits. The manner in which the methodology can be applied to evaluate indicative individual dose equivalents for this purpose is summarised. The magnitude of annual individual dose equivalents is, for long lived nuclides, and particularly for those with long retention times in the body, a function of the duration of the discharge practice. For the purpose of illustration the discharge is assumed to continue for a period of 50 years and annual dose equivalents are evaluated in the last year of the practice; in general this corresponds to the maximum annual dose equivalent. Other periods of duration of the practice could equally be chosen, as appropriate.

For external irradiation from the cloud the dose is delivered only during the period of the discharge and does not vary from year to year. The annual dose equivalent at \bar{d}_j, θ_{jj} is then obtained from equation (7.13) as

$$N Q_o(i) \sum_c HG(i, c, \bar{d}_j) f(\theta_{jj}, c) \quad (\text{Sv } y^{-1})$$

.....(7.25)

Inhalation of activity from the cloud continues during the discharge practice; the dose however, particularly for long lived nuclides, may continue to be delivered well beyond this period. The annual dose equivalent in the 50th year of discharge can be equated to the committed dose equivalent from the intake during the first year of discharge (or more generally the annual dose in the nth year of discharge can be equated with the time integral to n years of the dose equivalent rate from intake in the first year). Thus the annual dose equivalent from inhalation of the cloud at \bar{d}_j, θ_{jj} in the 50th year of discharge can be derived from equation (7.10) as

$$B H_{inh}(i) N Q_o(i) \sum_c X_o(i, c, \bar{d}_j) f(\theta_{jj}, c) \quad (\text{Sv } y^{-1})$$

.....(7.26)

The annual dose equivalents from external radiation and the inhalation of resuspended activity resulting from activity deposited on land surfaces will increase during the discharge period and may or may not reach an equilibrium depending on the radioactive half life and environmental behaviour of the nuclide considered. For external irradiation, be it β or γ , the annual dose equivalent in the 50th year of discharge can be equated to the time integral to 50 years of the dose equivalent rate from the deposition in the first year (or again more generally the annual dose equivalent in the nth year can be equated to the time integral to the nth year of the dose equivalent rate from deposition in the first year). Thus the annual dose equivalent at \bar{d}_j, θ_{jj} in the 50th year can be written from equations (7.18) and (7.19) as

$$N Q_o(i) \sum_c G(i, c, \bar{d}_j) f(\theta_{jj}, c) F_v(i, 50) \quad (\text{Sv } y^{-1})$$

.....(7.27)

In the case of inhalation of resuspended activity the annual dose equivalent in the 50th year cannot in general be equated in the same way to the committed dose equivalent from intakes in the first year; this is a consequence of the intake of activity by this route increasing for some nuclides as the discharge continues. The annual dose equivalent in the 50th year can however be conservatively estimated by equating it to the committed dose equivalent from intakes by this route in the 50th year of the practice. The resulting over-estimate may be as much as a factor of 2 but in general will be considerably smaller. The annual dose equivalent from inhalation of resuspended activity, from equation (7.21) is at \bar{d}_j, θ_{jj}

$$B H_{inh}(i) \frac{1}{3.15 \cdot 10^7} \omega(i, \bar{d}_j, \theta_{jj}) I_R(i, 50) \quad (Sv \text{ y}^{-1})$$

.....(7.28)

For ingestion of contaminated foodstuffs it is not possible to estimate individual doses unless some assumption is made regarding the source of the individual's dietary intake. As an extreme hypothesis the individual is assumed to derive his total diet from his local habitat; average annual individual dietary intakes, $P(k)$, of the various food products are summarised in Table 7.3 [7.27].

In a similar manner to the intake by inhalation of resuspended activity the intake of activity by ingestion may increase during the practice owing to the accumulation of long lived nuclides in the environment. The equality between the annual dose equivalent in the nth year of practice and the time integral to n of the dose equivalent rate from intakes in the first year, which holds for a continuous rate of intake, cannot be adopted. As for resuspension the annual dose equivalent in the 50th year can be conservatively assessed by equating it with the committed dose equivalent from intakes in the 50th year; the same caveats as outlined above apply to the degree of conservatism in this estimate. The annual dose equivalent in the 50th year from a dietary intake derived solely at \bar{d}_j, θ_{jj} can, from equation (7.23) be written as

$$\sum_k H_{ing}(i) \omega(i, \bar{d}_j, \theta_{jj}) CP(i, k, 50) P(k) TD(i, k) \quad (Sv \text{ y}^{-1})$$

.....(7.29)

Thus from equations (7.25) to (7.29) indicative individual annual dose equivalents can be derived that are typical of the maximum likely to be received at \bar{d}_j, θ_{jj} during the duration of a discharge practice. Estimates of critical group doses can thus be made subject to specification of its habits (eg. its spatial distribution for most routes of exposure and its source of diet for ingestion). For example, assuming the population within 5 km of the discharge to be representative of the most exposed group, an indicative annual dose equivalent to a critical group could be derived as the average annual dose in the annular segments of 5 km radius surrounding the discharge point. Other equally plausible assumptions could be adopted in the estimation of indicative doses to the most exposed group of individuals.

7.3 Estimation of doses from discharges to the aquatic environment

7.3.1 General procedure

The general procedure adopted in the estimation of collective dose equivalent commitments from discharges to the aquatic environment is in principle similar to that for atmospheric discharges. The various aquatic environments modelled in Chapter 4 are subdivided into various compartments or sections. For each compartment the collective dose equivalent commitment (and/or its truncated values) is evaluated for each route of exposure and the collective dose equivalent commitment in the whole population is evaluated by summation over all compartments. (eg. the model which represents the Northern European system of waters comprises some 17 individual compartments.)

To assist in the understanding of the procedure an example is given in the following section of the estimation of the collective effective dose equivalent commitment in a particular section of a river and in a particular compartment of the marine environment.

7.3.2 An example of the application of the methodology

As an illustrative example it is assumed that caesium-137 is discharged into a river at a rate of 1 Bq s^{-1} for a period of 1 year and that this river flows into the Mediterranean. Consideration is given to the collective effective dose equivalent commitment arising from one section of the river and one compartment of the Mediterranean.

The pathways of exposure considered (see Diagram 4.1) are:

- for the river section

- ingestion of drinking water
- ingestion of fish
- ingestion of irrigated food crops
- external irradiation from sediments

The river section is assumed to commence at the point of discharge and is 25 km long (Section 7 in Table 4.3)

- for the marine environment

- ingestion of fish, crustacea and molluscs

The marine compartment considered is the western Mediterranean (see Figure 4.12).

7.3.2.1 River environment

The doses by the various pathways are determined by the activity concentration in the river water and sediments in the section of interest. The activity concentration of caesium-137 in filtered water (used for the evaluation of the activity ingested from drinking water and fish) is estimated during the discharge as $2.0 \cdot 10^{-4} \text{ Bq m}^{-3}$ (see equation (4.4)) while the concentration in untreated water (which is used for irrigation) is estimated as $4.4 \cdot 10^{-4} \text{ Bq m}^{-3}$ (see equation (4.3)). These concentrations are assumed constant at these values over the duration of the discharge and to be zero afterwards. The concentration however in the sediments (which

is used to determine external γ irradiation) in the section of river of interest varies with time. The quantity used to assess the collective effective dose equivalent commitment is the infinite time integral of the activity concentration.

Each route of exposure is considered in turn.

Ingestion of drinking water

It is assumed that the total population of the communities bordering the section of river considered derives its drinking water from the river or its aquifer (which is assumed to be contaminated at the same concentration as the river water). Assuming an average individual water intake of 1.2 litres per day by $1.3 \cdot 10^5$ people comprising these communities yields a collective intake by ingestion of 11 Bq (see Table 4.5). The collective effective dose equivalent commitment can be evaluated as the product of this intake and the committed effective dose per unit intake of caesium-137 by ingestion ($1.4 \cdot 10^{-8}$ Sv Bq $^{-1}$ - see Chapter 6) and is equal to $1.5 \cdot 10^{-7}$ man Sv.

The time delay which occurs between the extraction of water from the river or its aquifer and its consumption is variable. In this study a value of 7 days is assumed which, for caesium-137 owing to its long half-life, does not lead to a significant reduction in the dose.

Ingestion of fish

The collective intake of activity by ingestion of fish is the product of the concentration in the filtered water, the concentration factor between fish and filtered water, the annual yield of fish in the river section considered and the edible fraction of fish and is given by:-

$$2 \cdot 10^{-4} \text{ (Bq m}^{-3}\text{)} \cdot 10^3 \text{ (m}^3 \text{ t}^{-1}\text{)} \cdot 50 \text{ (t)} \cdot 0.5 \\ = 5 \text{ (Bq)} \text{ (see Table 4.5)}$$

The collective effective dose equivalent commitment can be derived as the product of this collective intake and the committed effective dose per unit intake, and is $7 \cdot 10^{-8}$ man Sv. The delay between the catch and consumption of fish is taken as one day, which is insignificant in so far as the dose from caesium-137 is concerned.

Ingestion of irrigated food products

The quantities of agricultural products irrigated by the river section of interest are given in Table 4.7. For example, the annual yields of green vegetables and root vegetables are $2.2 \cdot 10^8$ and $1.4 \cdot 10^8$ kg y $^{-1}$, respectively. The integrated concentration of caesium-137 in the green vegetables is derived as the product of the concentration in the untreated water ($4.4 \cdot 10^{-4}$ Bq m $^{-3}$), the rate of irrigation ($6.38 \cdot 10^{-9}$ m 3 s $^{-1}$ per m 2 of ground) and the appropriate transfer factor between the activity in the green vegetables per unit deposition rate during irrigation ($1.1 \cdot 10^5$ Bq y kg $^{-1}$ per Bq m $^{-2}$ s $^{-1}$ during a year). The infinite time integral of caesium-137 in green vegetables is thus $3.1 \cdot 10^{-7}$ Bq y kg $^{-1}$ and corresponds to a collective effective dose equivalent commitment of $9.5 \cdot 10^{-7}$ man Sv. For root vegetables, the transfer factor between the deposition rate during irrigation and the integrated activity in those food products is taken as $1.2 \cdot 10^4$ Bq y kg $^{-1}$ per Bq m $^{-2}$ s $^{-1}$

during a year (Table 7.3). The corresponding infinite time integral of caesium-137 in root vegetables is thus $3.4 \cdot 10^{-8} \text{ Bq y kg}^{-1}$, which, associated with a production of $2.2 \cdot 10^8 \text{ kg y}^{-1}$, leads to a collective effective dose equivalent commitment of $6.7 \cdot 10^{-8} \text{ man Sv}$. The time delay, assumed between harvest and consumption is 7 days for green vegetables and 6 months for root vegetables. In the case of caesium-137, these time delays do not significantly affect the doses obtained.

External Irradiation

The external irradiation of fishermen (who are assumed to number 20 per km of river and to spend 200 hours per year on the river banks) is estimated from the integrated concentration of activity on the sediments.

The evaluation is given in Section 4.2.3.3.

From these occupancy data and the infinite time integral of the external γ dose from deposited caesium-137 the collective effective dose equivalent commitment is estimated to be $9.5 \cdot 10^{-10} \text{ man Sv}$.

7.3.2.2 Marine environment

The collective effective dose equivalent commitment from ingestion of sea foods is obtained as the sum over each foodstuff of the product of the infinite time integral of the collective intake of caesium-137 in that foodstuff and the committed effective dose equivalent per unit intake by ingestion. The infinite time integral of the collective intake of caesium-137 in each foodstuff is derived as the product of the annual yield of the edible fraction of the sea food, the infinite time integral of the concentration of caesium-137 in sea water, and the concentration factor between the foodstuff and sea water for caesium. The yields of fish, crustacea, and molluscs in the marine compartment considered are $1.13 \cdot 10^5 \text{ t y}^{-1}$, $2.4 \cdot 10^3 \text{ t y}^{-1}$ and $2.7 \cdot 10^4 \text{ t y}^{-1}$ respectively (see Table 4.18). Using these yields and for a discharge into a river of 1 Bq s^{-1} for a year which flows into this marine compartment a collective effective dose equivalent commitment of $3.1 \cdot 10^{-9} \text{ man Sv}$ has been evaluated.

The delay between the catch and consumption of the various sea foods is assumed to be 7 days; this again is too short to have any significant influence on the dose from caesium-137.

7.3.2.3 Summary of the collective dose equivalent commitments from discharges of caesium-137 to the aquatic environment

The collective effective dose equivalent commitments from the various pathways are summarised in Table 7.5 for the assumed river section and marine compartment. Comparable estimates would need to be made for each section or compartment of the river and marine environment in order to estimate the total collective effective dose equivalent commitment from the discharge considered.

It must be stressed that the numerical values given in Table 7.5 are particular to the section of river and sea considered and to their assumed environmental characteristics.

Moreover the values refer to only one section of the respective environments and no conclusions should therefore be drawn as to the relative importance of the various pathways of exposure. Such conclusions can only be drawn following a complete evaluation of the collective dose equivalent commitments from the total aquatic system.

REFERENCES

- [7.1] United Nations Sources and Effects of Ionizing Radiation. United Nations Scientific Committee on the Effects of Atomic Radiation 1977 Report to the General Assembly, with Annexes. New York, 1977.
- [7.2] OECD, Food Consumption Statistics 1955 - 1973. Paris. 1975.

Table 7.1: Radii used to specify annular bands used to characterise the spatial distribution of the population, agricultural production and activity concentration

Radial limits of annulus, km	Radial distance to mid-point of annulus, km
0 - 1	0.5
1 - 2	1.5
2 - 3	2.5
3 - 5	4
5 - 7	6
7 - 10	8.5
10 - 15	12.5
15 - 20	17.5
20 - 35	27.5
35 - 50	42.5
50 - 70	60
70 - 100	85
100 - 200	150
200 - 300	250
300 - 450	375
450 - 700	575
700 - 1100	900
1100 - 1600	1350
1600 - 2000	1800
2000 - 2400	2200
2400 - 3000	2700

Table 7.2: Frequency distribution of dispersion categories assumed for the sector θ_{jj} and airborne concentration, deposition rate and cloud γ dose at a distance of 150 km for 1 Bq s^{-1} continuous discharge of caesium-137

Pasquill dispersion category	Probability of occurrence of dispersion category, c in direction θ $f(\theta_{jj}, c)$	Atmospheric concentration ¹⁾ Bq m^{-3} per Bq s^{-1} $X_o(i, c, d)$	Deposition rate ¹⁾ $\text{Bq m}^{-2} \text{ s}^{-1}$ per Bq s^{-1} $G(i, c, d)$	Cloud γ effective dose equivalent rate ¹⁾ Sv y^{-1} per Bq s^{-1} $\text{HG}(i, c, d)$	
Dry Weather	A	0.00083	$3.3 \cdot 10^{-10}$	$1.62 \cdot 10^{-12}$	$2.63 \cdot 10^{-16}$
	B	0.00417	$2.05 \cdot 10^{-10}$	$1.02 \cdot 10^{-12}$	$1.63 \cdot 10^{-16}$
	C	0.0083	$1.75 \cdot 10^{-10}$	$8.7 \cdot 10^{-13}$	$1.38 \cdot 10^{-16}$
	D	0.04750	$2.0 \cdot 10^{-10}$	$9.9 \cdot 10^{-13}$	$1.55 \cdot 10^{-16}$
	E	0.00583	$4.85 \cdot 10^{-10}$	$2.44 \cdot 10^{-12}$	$3.4 \cdot 10^{-16}$
	F	0.00583	$1.5 \cdot 10^{-10}$	$7.2 \cdot 10^{-13}$	$9.7 \cdot 10^{-17}$
Precipitations	C	0.00167	$7.7 \cdot 10^{-12}$	$7.8 \cdot 10^{-13}$	$6.0 \cdot 10^{-18}$
	D	0.00667	$8.3 \cdot 10^{-13}$	$7.3 \cdot 10^{-13}$	$7.0 \cdot 10^{-18}$
		Weighted values according to frequency of dispersion conditions in direction θ			
		$C(i, d, \theta)$	$\omega(i, d, \theta)$	$H_\gamma(i, d, \theta)$	
		$1.96 \cdot 10^{-10}$	$1.04 \cdot 10^{-12}$	$1.5 \cdot 10^{-16}$	

Notes

- 1) Evaluated for a discharge rate of 1 Bq s^{-1} assuming a uniform wind rose and continuous persistence of the dispersion category, c.

Table 7.3: Infinite time integral of the concentration of caesium-137 in the various food products, assumed annual yields in the chosen annular segment, mean delay periods between harvest and consumption, and individual consumption rates

Food product	Infinite time integral of concentration CP (Bq y kg ⁻¹ per Bq m ⁻² s ⁻¹)	Annual production in the segment considered PA (kg y ⁻¹)	Mean delay between harvest and consumption τ_k	Indicative individual consumption rate P(k) ₁ kg y ⁻¹
Fresh milk	3.9 10 ⁵	2.4 10 ⁷	2 days	104.6
Milk products	3.9 10 ⁵	3.2 10 ⁷	3 months	21.1
Cow meat	1.5 10 ⁶	6.1 10 ⁶	7 days	27.9
Cow liver	1.6 10 ⁶	1.5 10 ⁵	7 days	0.71
Sheep meat	4.8 10 ⁶	4.2 10 ⁶	7 days	3.2
Sheep liver	2.8 10 ⁶	1.0 10 ⁵	7 days	0.13
Green vegetables	2.0 10 ⁵	1.3 10 ⁷	7 days	144.1
Root vegetables	1.1 10 ⁴	2.3 10 ⁷	6 months	114.0
Cereals	4.1 10 ⁵	5.2 10 ⁷	11 months	81.4

Table 7.4 Summary of the collective dose equivalent commitments in (or from) an annular segment due to an atmospheric discharge of 1 Bq s^{-1} caesium-137 for a year¹⁾)

Pathway	Collective effective dose equivalent commitment (man Sv)	Pathway	Collective dose equivalent commitment in skin (man Sv)
<u>During passage of cloud:-</u>		<u>During passage of cloud:-</u>	
External photon irradiation	$1.2 \cdot 10^{-10}$	External electron irradiation	$7.0 \cdot 10^{-11}$
Inhalation	$1.0 \cdot 10^{-8}$		
<u>From deposited activity:-</u>		<u>From deposited activity:-</u>	
External photon irradiation	$5.0 \cdot 10^{-6}$	External electron irradiation	$4.0 \cdot 10^{-15}$
Inhalation	$4.0 \cdot 10^{-9}$		
Ingestion	$1.1 \cdot 10^{-6}$		
Total	$6.1 \cdot 10^{-6}$		$7.0 \cdot 10^{-11}$

Note

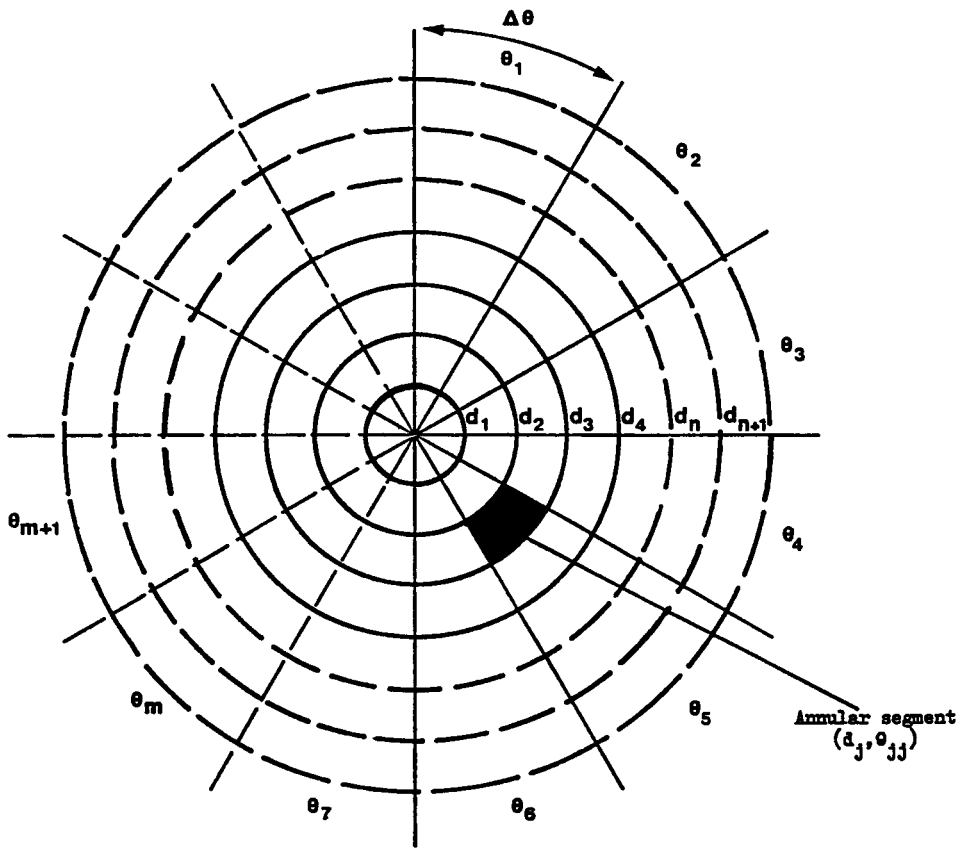
- 1) The numerical values of the collective dose equivalent commitments are particular to the environmental characteristics of the annular segment which were chosen arbitrarily for illustration. They have therefore no absolute or relative significance and no attempt should be made to draw conclusions from the values presented.

Table 7.5: Collective effective dose equivalent commitment for discharges to the aquatic environment¹⁾

Aquatic environment	Method of irradiation		Collective effective dose equivalent commitment man Sv
Marine compartment	INGESTION	Fish	$3 \cdot 10^{-9}$
		Crustacea	$3 \cdot 10^{-11}$
		Molluscs	$4 \cdot 10^{-10}$
River section	INGESTION	Drinking water	$1 \cdot 10^{-7}$
		Freshwater fish	$7 \cdot 10^{-8}$
		Irrigated green vegetables (and fruit)	$1 \cdot 10^{-6}$
		Irrigated root vegetables	$7 \cdot 10^{-8}$
	EXTERNAL γ IRRADIATION	Sediments	$1 \cdot 10^{-9}$

Note

- 1) The numerical values of the collective dose equivalent commitments are particular to the environmental characteristics of the river and marine compartments which were chosen for illustration. They have therefore no absolute or relative significance and no attempt should be made to draw conclusions from the values presented.



$$\Delta\theta = \frac{360^\circ}{N}$$
 where N is the number of sectors

Figure 7.1 Illustration of the scheme of annular segments adopted to represent the spatial distribution of population and activity in various parts of the environment

CHAPTER 8

THE ESTIMATION OF HEALTH EFFECTS IN AN EXPOSED

POPULATION

8.1 Introduction

Exposure of a population to radiation may lead to the incidence of stochastic and non-stochastic health effects (somatic effects) and stochastic effects in its descendants (hereditary effects). Non-stochastic effects occur only if particular threshold levels of dose are exceeded; these levels are far in excess of doses typically encountered from the discharges of effluents during the normal operation of the nuclear fuel cycle and non-stochastic effects can, therefore, be disregarded in the present context. The important stochastic effects are carcinogenesis in the exposed population and hereditary effects in its descendants. The probability of occurrence of stochastic effects is assumed proportional to dose, without threshold.

The appearance of stochastic effects, and thus the expression of the risk following irradiation is not immediate but extends over a considerable period which may be as large as several tens of years. Age at exposure has therefore a considerable influence on the probability that a particular dose equivalent will induce a given health effect; the probability will decrease when life expectancy at the time of irradiation becomes comparable with or smaller than the median time taken for the appearance of the effect (assuming the radiosensitivity of tissue to be independent of age). A rigorous evaluation of the incidence of stochastic effects in an exposed population must, therefore, take account of the age distribution of the population since for each age at exposure or intake, the temporal distribution of dose equivalent will affect the probability of appearance of the effect. The latter is particularly important for internally incorporated radionuclides with long effective half-lives in the body when exposure continues over an extended period. The inclusion of such factors leads to a relatively complex procedure for the estimation of health effects and for the purpose of this study a simpler, but conservative approach is adopted. This simplification is considered justified in the context of the low levels of exposure typically encountered from effluent discharges (and consequently the small numbers of health effects) and the inherent uncertainties in the risk coefficients adopted to convert dose equivalent to health effects; nevertheless its conservatism should be recognised.

8.2 Estimation of the numbers of health effects

8.2.1 Fatal cancers and hereditary effects in the first two generations

The use of the quantity, collective effective dose equivalent commitment (together with values truncated at particular times) as a measure of health detriment is adopted in this report. Assuming linearity between dose equivalent and effect, the relationship between these two quantities given by ICRP in Publication 26 [8.1] can be used to estimate the incidence of particular health effects. ICRP has recommended a risk coefficient of $1.65 \times 10^{-2} \text{ Sv}^{-1}$ to be applied to the effective dose

equivalent for estimation of the incidence of radiation induced fatal cancers (other than in skin) and hereditary effects in the first two generations. The coefficient was derived in the context of occupational exposures; as has been explained it is assumed here to be equally applicable to exposure of the general public within the uncertainty introduced by other approximations in this assessment. The product of collective effective dose equivalent commitment (and/or its truncated values) and a risk coefficient of $1.65 \cdot 10^{-2} \text{ Sv}^{-1}$ yields the incidence of the health effects of the types specified above; the estimation of other important health effects (e.g. fatal cancers in skin, non-fatal cancers, and hereditary effects in subsequent generations) is considered later. The number of health effects evaluated in the above manner will be an overestimate for several reasons, principally

- the collective effective dose equivalent commitment evaluated in this report is an overestimate of the actual dose equivalent received by the population (see Chapter 2).
- no account is taken of the age distribution of the population nor of the temporal distributions of dose equivalent, and consequent risk, within it.

But it underestimates the total health detriment because it does not include all subsequent hereditary effects, fatal skin cancers nor the non-fatal cancers.

It is difficult to generalise on the degree of approximation since much depends on the age distribution of the exposed population and the nature of the exposure (e.g. duration, radionuclide, etc.). However, for a population of age distribution typical of the European Community, the overestimate on account of the above considerations is unlikely to be high; much greater factors could ensue if consideration were limited to irradiation of particular age groups in the population.

An additional, and perhaps more important, consideration is the degree of conservatism in the assumption of linearity between dose equivalent and effect. The ICRP [8.2] has stated that the risk coefficients given in Publication 26 are intended to be realistic estimates of the effects of irradiation at low annual dose equivalents (up to the Commission's recommended dose equivalent limits). Notwithstanding this, there remains a considerable body of scientific opinion that regards these risk coefficients as overestimates of the true risk at the levels of annual dose equivalent typical of those contributing significantly to the collective dose equivalent to the general public from most operations in the nuclear fuel cycle (e.g. typically annual dose equivalents much lower than $1 \mu\text{Sv}$). This aspect is the subject of continuing debate and is unlikely to be resolved quickly; for the purposes of this study linearity between dose equivalent and effect at all levels of dose equivalent is assumed while recognising the possible conservatism of this approach.

8.2.2 Other health effects

Fatal cancers in skin, non-fatal cancers and hereditary effects in subsequent generations are further radiation induced health effects which need consideration; depending on the nature of the irradiation, these may contribute significantly to the total number of health effects. To allow for fatal skin cancers the ICRP has now recommended [8.2] that in the

assessment of detriment a weighting factor, w_T , of 0.01 be used for the dose equivalent in the skin. This implies a risk coefficient for fatal skin cancer of $1.65 \cdot 10^{-4} \text{ Sv}^{-1}$ which has been approximated to $2 \cdot 10^{-4} \text{ Sv}^{-1}$ in this study.

For most organs the incidence of a radiation induced cancer can be considered to lead to fatality; the principal exceptions comprise the skin, breast and thyroid. In the case of radioactive effluent releases it is not clear that the breast would be irradiated exclusively and, therefore, any incidence of non-fatal cancer may not add significantly to the total health detriment. There may be a significant incidence of non-fatal cancers following irradiation of the thyroid and skin, but the ICRP has given no guidance as to their incidence per unit dose. We have, therefore, not proposed any non-fatal cancer incidence in this methodology. We have estimated organ doses (Chapter 6) so that if risk coefficients become available, the health effects could be calculated.

The risk of serious hereditary ill-health within the first two generations following the irradiation of the gonads of either parent is taken by ICRP in Publication 26 8.17 as about 0.01 Sv^{-1} ; the additional damage in all subsequent generations is considered to be of the same magnitude. For uniform irradiation of a population (of age distribution typical to the European Community), the total incidence of hereditary effects per unit collective dose equivalent in gonads can be estimated as about $8 \cdot 10^{-3} \text{ Sv}^{-1}$ in gonads after making appropriate corrections for the genetically significant component of the dose equivalent. A risk coefficient of $4 \cdot 10^{-3}$ per unit of collective gonad dose of the exposed population is implicit in the procedure outlined in Section 8.2.1. to estimate the incidence of fatal cancers and hereditary effects in the first two generations from the collective effective dose equivalent; the incidence of hereditary effects in subsequent generations can, therefore, be assessed using a risk coefficient of $4 \cdot 10^{-3}$ per unit collective gonad dose.

8.2.3 Procedure

The risk coefficients specified above are sufficient to estimate the incidence of fatal cancer in the exposed population and the hereditary effects in its descendants. There is some merit however in adjusting the manner in which these coefficients are applied with the objective of achieving a more appropriate grouping of the like effects. For example application in their present form would result in the estimation of fatal cancers (not in skin) plus hereditary effects in the first two generations without any means of determining their relative magnitudes.

The scheme for applying the various coefficients to enable the separate estimation of fatal cancers and hereditary effects is summarised in Table 8.1*. The incidence of fatal cancer is estimated from the

*Within the framework of the CEC programme - Plutonium Recycle in Light Water Reactors - a study was undertaken on the toxicity of plutonium, americium and curium (Nenot, J.C. and Stather, J.W. The toxicity of plutonium, americium and curium. EUR 6157 (1979) (Pergamon, Oxford)). The risk coefficients proposed in that study are consistent with those recommended in ICRP Publication 26 and which have been adopted in this study.

collective effective dose equivalent with appropriate provision made for the extraction of hereditary effects and the addition of fatal skin cancers. The total incidence of hereditary effects is evaluated although the fraction appearing in the first two generations can be readily estimated as one half of the total.

The use of the scheme outlined in Table 8.1 in conjunction with the collective dose equivalent commitments (or truncated values) as evaluated in this study enables the incidence of the respective health effects to be evaluated. It must be noted, however, that the procedure advocated, for simplicity, in this study leads to an approximation to the total number of health effects in the exposed population.

REFERENCES

- [8.1] ICRP, Recommendations of the International Commission on Radiological Protection. Oxford, Pergamon Press, ICRP Publication 26. Ann. ICRP, 1, no 3 (1977).
- [8.2] ICRP, Statement from the 1978 Stockholm Meeting of the International Commission on Radiological Protection. Ann. ICRP, 2, no 1 (1978).

Table 8.1 Application of risk coefficients to evaluate fatal cancers, and hereditary effects

Health Effect	Number of Effects ¹⁾
Fatal Cancers	$1.65 \cdot 10^{-2} S_E + 2 \cdot 10^{-4} S_S - 4 \cdot 10^{-3} S_G$
Hereditary Effects ²⁾	$8 \cdot 10^{-3} S_G$

Notes

- (1) S_E , S_S , and S_G are the collective effective dose equivalent and collective dose equivalents in skin and gonads respectively.
- (2) The total number of hereditary effects appearing over all generations is quoted; those appearing in the first two generations is half the quoted value.

CHAPTER 9

CONCLUSIONS

This report provides the description of a comprehensive methodology for the assessment of the health detriment to the population of the European Community from radioactive effluents discharged within the area of the Community. The health detriment provides a quantitative measure of the radiological impact of a release of radioactivity to the environment and is also an important input to the procedure of optimisation for the management of radioactive wastes.

In order to estimate the health detriment mathematical models have had to be developed which represent the transfer of a wide range of radionuclides through atmospheric, terrestrial and aquatic pathways.

The models enable the spatial and temporal distribution of radioactivity through the environment to be predicted and are thus more extensive than those which have been used in the past for calculation of doses to critical groups.

As a result of developing these models an effluent release to the atmospheric or aquatic environment for essentially any location in the European Community can be taken and the resulting collective dose to the population predicted as a function of time.

This report is concerned with a methodology which may be applied to assess the radiological consequences of radioactive effluents. It has therefore been necessary to choose representative values of parameters which necessarily reflect a compromise within their range of variability. Thus when particular releases from specific sites are considered, it may be necessary to choose alternative values for parameters to reflect the conditions of interest.

One of the more important advantages of having developed the models is that sensitivity analysis may be undertaken to identify those parameters where uncertainty in their value has a significant effect on the overall result. The use of such analysis gives an indication as to those areas where research effort should be concentrated to improve the overall accuracy of the assessment. These studies should form one of the next stages in assessing the radiological impact of effluent releases.

A number of conservative assumptions have been adopted in the estimation of the health detriment and it must be recognised that in some applications, particularly optimisation studies, there may be a need for the use of more realistic estimates of the number and types of different health effects. However, the methodology developed here represents the first attempt to assess total health detriment and provides a basis on which to build in future.

GLOSSARY

ABSORBED DOSE

- is a measure of the energy deposited in matter by ionising radiation. The absorbed dose D is defined as:-

$$D = \frac{d\bar{E}}{dm}$$

where $d\bar{E}$ is the mean energy imparted by ionising radiation to the matter in a volume element and dm is the mass of the matter in that volume element. The special SI unit of absorbed dose is the "gray"

$$1 \text{ gray (Gy)} = 100 \text{ rad} = 1 \text{ J kg}^{-1}$$

STOCHASTIC EFFECTS

- are those for which the probability of an effect occurring, rather than its severity, is regarded as a function of dose, without threshold.

NON-STOCHASTIC EFFECTS

- are those for which the severity of the effect varies with dose and for which a threshold may therefore occur.

ACTIVITY

- of a quantity of radioactive material, is the number of nuclear transformations which occur in this quantity in unit time. The SI unit of activity is the "becquerel" 1 becquerel (Bq) = 1 nuclear transformation per second.

DOSE EQUIVALENT

- is a quantity which correlates better with the deleterious effects of exposure to ionising radiation, more particularly with the delayed stochastic effects, than does absorbed dose. The dose equivalent H is defined as:-

$$H = DQN$$

where D is the absorbed dose, Q is the quality factor which allows for the different biological effectiveness of various types of radiation, and N is the product of all other modifying factors. A value of unity has been assigned to N by ICRP. For most practical purposes the following approximate values of Q can be used for both external and internal irradiation.

X-rays, γ rays and electrons	1
Neutrons, protons etc of unknown energy	10
α particles and other multiply-charged particles of unknown energy	20

Thermal neutrons

2.3

These values of Q and hence values of H are intended only for use in radiation protection applications and then only in the context of the system of dose limitation. They are not necessarily appropriate for assessing the consequences of severe accidental exposures in man.

The special SI unit of dose equivalent is the "sievert"
1 sievert (Sv) = 100 rem = 1 J kg⁻¹

EFFECTIVE DOSE EQUIVALENT

- H_E, is defined as:-

$$H_E = \sum_T w_T H_T$$

Where H_T is the dose equivalent in tissue T and w_T is a weighting factor representing the proportion of the stochastic risk resulting from irradiation of tissue T to the total risk when the body is irradiated uniformly. The expression thus acts as an indicator of the stochastic risk assumed to result from any irradiation, whether uniform or non-uniform. The values of w_T recommended by the ICRP are tabulated in ICRP Publication 26.

COMMITTED DOSE EQUIVALENT

- is the time integral over 50 y of the dose equivalent rate which will be received by an individual following an intake of radioactive material into the body. The integration time of 50 years following the intake represents a working life. Committed dose equivalent, H₅₀, is defined as:-

$$H_{50} = \int_{t_0}^{t_0 + 50 \text{ y}} \dot{H}(t) dt$$

where $\dot{H}(t)$ is the dose equivalent rate in the organ or tissue at time t following a single intake of radioactivity at time t₀.

COMMITTED EFFECTIVE DOSE EQUIVALENT

- H_{50,E} is obtained by replacing dose equivalent rate by effective dose equivalent rate in the above expression.

- COLLECTIVE DOSE EQUIVALENT - is a quantity introduced to provide a measure of the health detriment in an exposed population. The collective dose equivalent S is given by:

$$S = \int_0^{\infty} H N(H) dH$$

where $N(H)$ is the number of individuals receiving a dose equivalent in the whole body or any specified organ or tissue in the range H to $H + dH$. The unit of collective dose equivalent is the "man sievert".

- COLLECTIVE EFFECTIVE DOSE EQUIVALENT - S_E , is obtained by replacing dose equivalent by effective dose equivalent in the above expression.

- DOSE EQUIVALENT COMMITMENT - from a given practice is the infinite time integral of the per caput dose equivalent rate $\bar{H}(t)$, in a given organ or tissue for a specified population. Dose equivalent commitment H^C is defined as:-

$$H^C = \int_0^{\infty} \bar{H}(t) dt$$

where $\bar{H}(t)$ is the per caput dose equivalent rate as a function of time t .

- EFFECTIVE DOSE EQUIVALENT COMMITMENT - H_E^C is obtained by replacing dose equivalent rate by effective dose equivalent rate in the above expression.

- TRUNCATED DOSE EQUIVALENT COMMITMENT - The dose equivalent commitment becomes the truncated dose equivalent commitment if the period of integration is reduced to a value less than infinity.

- COLLECTIVE EFFECTIVE DOSE EQUIVALENT COMMITMENT - S_E^C , is defined as:-

$$S_E^C = \int_0^{\infty} \dot{S}_E(t) dt$$

where $\dot{S}_E(t)$ is the collective effective dose equivalent rate.

COLLECTIVE INTAKE

- the collective intake of a radionuclide by the population under consideration is obtained as:-

$$IC = \int_0^{\infty} I N(I) dI$$

where I is the intake and N(I) is the number of people with intakes between I and I + dI.

